

GEOLOGICA ULTRAIECTINA

Mededelingen van de
Faculteit Aardwetenschappen
Universiteit Utrecht

No 200

Reconstruction and modelling of Holocene coastal
evolution of the western Netherlands

Jelmer Cleveringa

ISBN: 90-5744-057-1

Cover illustration (Figure 4.8, Chapter 4): Hypothetical coast-perpendicular cross section through a prograded coastal system. Thin lines indicate the coastal profile at different time steps. The coastal profile is kept similar for all time steps. The spacing of the profile decreases, which can be regarded as a decrease in the rate of coastal progradation. A number of cores (arrows) with randomly distributed samples (dots) is indicated. The dots from different cores that are found on the same coastal profile are of equal age. The dots of equal age are connected to form isochrons (the thick lines). The isochrons display a clear steepening trend in the seaward direction. As the geometry of the coastal profiles does not change, the trend in the isochrons is an ‘apparent steepening’. Compare the isochrons in the hypothetical cross section to those in the Haarlem cross section (Figure 4.1).

The illustration is an excellent example of a model simulation that helps to explain an observed pattern.

Illustratie op de omslag (Figuur 4.8, Hoofdstuk 4): Hypothetische dwarsdoorsnede door de afzettingen van een uitbouwende kust. De dunne lijntjes zijn kustprofielen van opeenvolgende ouderdom, die elke steeds dezelfde vorm hebben. De profielen liggen steeds dicht op elkaar, omdat de snelheid waarmee de kust uitbouwt, afneemt. In het profiel is een aantal boringen aangegeven (pijltjes), met daarin willekeurig verdeelde monsterpunten (stippen). De monsters uit verschillende kernen die op hetzelfde kustprofiel liggen worden verbonden en vormen dan tijdlijnen (de dikke lijnen). De tijdlijnen lopen steeds steiler dicht naar de kust toe. Omdat de versteiling van de tijdlijnen niet veroorzaakt wordt door een versteiling van de kustprofielen spreken we hier van een “schijnbare versteiling”. De tijdlijnen uit dit model kunnen vergeleken worden met de daadwerkelijk verkregen tijdlijnen in de dwarsdoorsnede bij Haarlem (Figuur 4.1).

Deze illustratie is een goed voorbeeld van de toepassing van een model om geobserveerde patronen te kunnen verklaren.

Reconstruction and modelling of Holocene coastal evolution of the western Netherlands

Reconstructie en modellering van de Holocene kustontwikkeling van westelijk Nederland

(met een samenvatting in het Nederlands)

Proefschrift

ter verkrijging van de graad van doctor
aan de Universiteit Utrecht
op gezag van de Rector Magnificus, Prof. Dr H.O. Voorma
ingevolge het besluit van het college voor promoties
in het openbaar te verdedigen op
woensdag 6 december 2000 des ochtends te 10.30 uur

door

JELMER CLEVERINGA

Geboren op 20 augustus 1972, te Coevorden

Promotor: Prof. Dr P.L. de Boer
Faculteit Aardwetenschappen, Universiteit Utrecht

Co-promotor: Dr A.J.F. van der Spek
TNO-NITG, Utrecht

Het onderzoek, dat aan dit proefschrift ten grondslag heeft gelegen, is gefinancierd door de Europese Unie, in het kader van het MAST III PACE project (MAS3-CT95-0002) en door het Instituut voor Paleomilieu en Paleoklimaat Utrecht (IPPU). Het werk aan hoofdstuk 6 en 7 is grotendeels uitgevoerd tijdens een bezoek aan de Coastal Studies Unit van de Faculty of Geosciences, Sydney University, Australië. Dit werkbezoek werd mogelijk gemaakt door een reisbeurs van NWO.

Voor Sas

Contents

Authors	9
Chapter 1: Introduction	11
Chapter 2: Deposition and erosion during final transgression and initial progradation; Holocene coastal deposits at Ypenburg (Rijswijk, The Netherlands)	25
Chapter 3: Holocene coastal evolution in the Western Netherlands (I): Facies	57
Chapter 4: Holocene coastal evolution in the Western Netherlands(II): Chronostratigraphy based on high-resolution AMS ¹⁴ C dating of shells	83
Chapter 5: A model for shoreface deposition of Holocene prograded coastal deposits (Haarlem, The Netherlands), based on grain-size distributions and sedimentary structures	113
Chapter 6: Modelling the decrease in wave-height over the shoreface due to slope-induced changes in bottom friction	133
Chapter 7: Simulations of Holocene coastal stratigraphy from the western Netherlands with the Shoreface Translation Model	145
Chapter 8: Summary and conclusions	169
Samenvatting in het Nederlands (summary in Dutch)	175
References	185
Dankwoord (Acknowledgements)	195
Curriculum Vitae	197

Authors

Chapter 2: Deposition and erosion during final transgression and initial progradation; Holocene coastal deposits at Ypenburg (Rijswijk, The Netherlands)

Co-author: Ad. J.F van der Spek¹

Chapter 3: Holocene coastal evolution in the Western Netherlands (I): Facies

Co-author: Ad. J.F van der Spek¹

Chapter 4: Holocene coastal evolution in the Western Netherlands(II): Chronostratigraphy based on high-resolution AMS ¹⁴C dating of shells

Co-author: Ad. J.F van der Spek¹

Chapter 5: A model for shoreface deposition of Holocene prograded coastal deposits (Haarlem, The Netherlands), based on grain-size distributions and sedimentary structures.

Co-author: Bart Schrijver

Chapter 6: Modelling the decrease in wave-height over the shoreface due to slope-induced changes in bottom friction.

Co-author: Peter. J Cowell²

Chapter 7: Simulations of Holocene coastal stratigraphy from the western Netherlands with the Shoreface Translation Model.

Co-authors: Peter J. Cowell² and Peter S. Roy³

1: Nederlands Instituut voor Toegepaste Geowetenschappen TNO, Utrecht.

2: Coastal Studies Unit, Faculty of Geosciences, Sydney University, Australia.

3: Geological Survey of New South Wales, Department of Mineral Resources & Coastal Studies Unit, Faculty of Geosciences, Sydney University, Australia.

Chapter 1: Introduction.

1.1 Introduction

The coast of the western Netherlands is an important environment for the Netherlands and its inhabitants. Along the coast dunes and sea dikes act as coastal defences against flooding, harbours have an important economic function, the dune areas are used for groundwater extraction and beaches are widely used for recreation. The shifting position of the coastline has determined the locus of inhabitation in historic and prehistoric times. This thesis focuses on Holocene coastal deposits in the western Netherlands and on the modelling of large-scale and long-term coastal evolution. Knowledge of the long-term coastal evolution has applications in the research of the subsurface (geology, hydrology and archaeology), in studies of year-to-year coastal behaviour, and especially in the prediction of long-term trends. Natural long-term trends and responses to large-scale interventions have important implications for the management of the coastal zone. A good understanding of the processes of long-term coastal evolution is thus of utmost importance for the western Netherlands.



Figure 1.1 : The Netherlands, with the topographic names used in this thesis. Shading indicates study area.

In this Introduction a short historical framework of research on Holocene coastal deposits in the Netherlands is sketched, followed by a description of the deposits, their depositional environments and the controls on Holocene coastal evolution. The Introduction is concluded with the aims and scientific methods of the research, and a note on numerical modelling of coastal evolution.

1.2 Historical framework

19th century

The study of coastal deposits in The Netherlands has a long history, which is intertwined with the history of flood protection. Ever since the low-lying parts of the Netherlands have been inhabited, flooding has been a threat for the people. Floods have been recognised as the principle agent for the formation of the coastal plain from the beginning of the study of earth history (Van der Woud, 1998). Early geological investigations started in Groningen, in the Northern Netherlands (Acker Stratingh, 1837). Subsidence of the coastal area was an important aspect of these studies (Venema, 1854). The systematic study of the geology of the Holocene ('Alluvium') began with the first geological mapping of the Netherlands by Staring (1856). Staring presented a comprehensive interpretation of coastal deposits, in terms of modern-day processes of waves and tides. Based on observations of the sediment supply from the large rivers (Rhine and Meuse) and from the English Channel area ('Nauw van Calais', 'de Hoofden') Staring suggested that most of the Holocene coastal sediments in the western Netherlands originated from reworking of older deposits ('diliuvium') from the North Sea floor. Staring rejected suggestions of subsidence of the Netherlands (i.e., sea-level rise and subsidence), and attributed changes in level to compaction of sediments. The work and viewpoints of Staring dominated thinking on Holocene deposition until the end of the 19th century.

20th century to World War II

Evidence for subsidence of the western Netherlands was presented by a large number of authors (cf. Steenhuis, 1917). Dubois (1910) used the height increase from the eastern to the western beach deposits in a dune cross section near Haarlem in conjunction with an observed rate of subsidence to obtain a remarkably accurate estimate for the age of certain Holocene beach deposits of 3000 to 4000 years before present. Tesch (1922, 1935) suggested that the subsidence should be regarded as the result of a uniform rise of sea level, rather than as tectonic subsidence. The main argument he used was the common occurrence of peat at the base of the Holocene deposits from depths of -20 m NAP¹ up, which he coupled to flooding of the landscape.

Lorié (1890) suggested that the dunes of the western Netherlands developed on a large spit bar that extended from Calais (in Northern France) to Texel. In the beginning of the 20th century E. Dubois (1910, 1911) suggested that the origin of dune sand of the western Netherlands must have been the Channel area, rather than the North Sea floor. Investigations of the Holocene coastal deposits in Northern France and Belgium supported these notions (G. Dubois, 1924). These viewpoints were shared by Tesch, who discussed the origin of the coastal deposits in the western Netherlands in 13 papers ('Duinstudiën'), which were iterated in a book (Tesch, 1935). The work of Tesch was related to a new geological map that was to be produced by the newly established geological survey of The Netherlands (of which Tesch was the director).

¹ NAP: Nieuw Amsterdams Peil, the Dutch Ordnance Level, roughly similar to the modern mean sea level.

The palaeo-reconstructions of the coastal developments of Tesch (1927) give a comprehensive overview of the ideas at that time. Tesch stated that initial deposition during the Holocene consisted of tidal deposits, similar to the deposits in the modern Wadden Sea. The zone of deposition extended into the modern North Sea. These deposits predated the formation of the spit bar from Calais to Texel ('Oud Holoceen', sea level below -5 m NAP). As the Channel area breached, sediment supply from the south started and the spit bar was formed. A lagoon developed behind the spit bar and marine clay was deposited in the lagoon. The spit bar was interrupted by a number of fluvial outlets. Eventually peat formed in the lagoon behind the spit bar. During the Middle Ages the spit bar would have been breached from the sea and marine clay was deposited on top of the peat.

Research of Van Veen (1937b, 1937a), conducted in the 1930's in relation with questions about coastal defence suggested very limited sediment transport from the Channel area to the Netherlands in the modern situation. Based on extensive morphological, historical and geological research Van Veen concluded that such sediment transport had been limited throughout the Holocene. He also presented evidence against a sudden breach of the Channel area in Holocene times. Although the outcome of Van Veen's research was debated by Tesch (Tesch 1937, Van Veen 1937), the ideas on the origin of a spitbar that developed from the south were abandoned. Timmermans (1935, 1939) presented support for a North Sea origin of a spit bar, based on scaled models of beach evolution.

20th century after World War II

After the Second World War the study of Holocene deposits in the Netherlands expanded rapidly. The study of Holocene pollen had already started prior to the Second World War (Polak, 1929), and had led, in conjunction with the recognition of climate-induced vegetation changes in Scandinavia, to a stratigraphic subdivision of the Holocene. The stratigraphic subdivision enabled correlation of peat layers. In addition, the development of radiocarbon dating presented the first means of absolute dating of Holocene coastal deposits (De Vries and Barendsen, 1954). The production of a detailed soil map of the Netherlands was an important factor in the collection of information (Edelman, 1950). In 1953 the flooding of large parts of the provinces of Zeeland and Zuid-Holland speeded up plans for improved coastal defence of these areas. The plans required a good knowledge of the subsurface, and initiated the production of a new, more detailed geological map.

Already in 1939 a national congress was held on the subject of sea-level rise during the Holocene. A second congress on the subject was held in 1954 and resulted in a series of publications on the subject (Anonymous, 1954, amongst others: Bennema, 1954, Van Straaten, 1954). Eventually this culminated in the publication of the sea-level curve of the Netherlands by Jelgersma (1960, 1961), based on radiocarbon dates of basal peat. The importance of the topography of the Pleistocene substrate on Holocene coastal evolution had also been recognised, and a number of maps of the Pleistocene topography was published (Faber, 1942, 1947, Pannekoek, 1956, Pons and Bennema, 1958, Pons and Wiggers, 1958). The Velzen excavation (a large construction pit for a tunnel) allowed investigation of the entire Holocene sequence in the western Netherlands and of the Pleistocene substrate (Van Straaten, 1957a).

All research efforts on Holocene coastal deposits culminated in the proceedings of the Jubilee Convention of the K.N.G.M.G. (the Royal Geological and Mining Society of the Netherlands) in The Hague (Anonymous, 1963). Pons *et al.* (1963) published a new and extensive set of palaeo-geographic maps. Van Straaten (1963) presented a description of the Holocene deposits and their genesis.

The palaeo-geographic reconstructions of Pons *et al.* (1963) start with the gradual flooding of the North Sea basin during the Early Holocene (after Jelgersma, 1961). Initial

coastal deposition in the western Netherlands consisted of fresh to brackish lagoonal deposits. With ongoing sea-level rise tidal deposition occurred, in conjunction with the formation of coastal barriers. As the rate of sea-level rise decreased, the extent of tidal deposition decreased and more coastal barriers started to form. Inlets were continuously present, but their position changed. Following this period of tidal deposition, the marine influences behind the barrier ceased completely and peat was formed. The coastal barriers started to prograde. The coastal barriers remained intersected by three fluvial outlets. After the phase of progradation several marine incursions occurred and the extruding parts of the coastal barriers were eroded.

Modern sedimentological research and the ‘Coastal Genesis’ project

The work of Van Straaten (1965) on a number of cores from the vicinity of The Hague is regarded the first sedimentological study of prograded beach and shoreface deposits in the Netherlands. Based on palynological and lithological correlations (Zagwijn, 1965), Van Straaten (1965) envisaged a complicated evolution of transgressive back-barrier deposits, transgressive offshore deposits and prograded shoreface and beach deposits. Van Straaten (1965) suggested, but with antipathy, that cross-shore transport has added substantially to coastal progradation, at least more than he originally envisaged (Van Straaten, 1961).

The International Geological Correlation Project 61 on Holocene sea-level movements that started in 1974 was another impulse to the study of coastal deposits and resulted in the publication of a more detailed peat-based sea-level curve for the western Netherlands in 1982 (Van de Plassche, 1982a, 1982b). A sea-level curve for Holland, based on sedimentological high- and low-water indicators was published by Roep and Beets (1988). This study was part of extensive studies in the Alkmaar region in North Holland (amongst others Beets *et al.*, 1981, De Mulder and Bosch, 1982, Roep, 1984, Westerhoff *et al.*, 1987, Westerhoff and Cleveringa, 1990, Beets *et al.*, 1996b).

In 1985 the Coastal Genesis (‘Kustgenese’) project started and combined geological and historical data with observations and modelling of modern sediment fluxes and sediment-transport processes. The aim of the project was to increase the insight into factors and conditions causing coastal change (Stive, 1987). In an important paper Beets *et al.* (1992) recognised the importance of sediment supply and accommodation space, with sea-level rise and the Pleistocene subsurface as the main controls on large-scale coastal evolution. More geological results of the Coastal Genesis project were published in Beets *et al.* (1996a), and in PhD theses of Sha (1990), Van der Valk (1992), Pool (1993), Van der Spek (1994), Van der Meene (1994), and Oost (1995). One of the Coastal Genesis projects was the construction of a coast-perpendicular cross section near Haarlem, and ¹⁴C dating of shells from prograded shoreface and beach deposits to reconstruct the large-scale profile evolution (Van der Valk, 1992, 1996). This profile reconstruction provided a base for model reconstructions of Holocene coastal evolution of the western Netherlands (Stive and De Vriend, 1995, Cowell *et al.*, 1999).

1.3 Holocene deposition in the western Netherlands

Transgression

In map view, Pleistocene or older deposits at or near the surface dominate the southern and eastern parts of The Netherlands (Figure 1.2). These deposits have an elevation above modern mean sea level. In the western and northern Netherlands Holocene deposits border the modern North Sea coast. In the northwestern part of the Netherlands some Pleistocene ice-pushed glacial deposits are found at or near the surface. Transgressive back-barrier deposits and peat dominate the remainder of the western and Northern Netherlands. The lowermost and hence oldest sequence of Holocene deposits consists of peat, overlain by clay (Figure 1.3), either with a high organic content and roots or with traces of bioturbation and shells (dominated by

Hydrobia shells : Van Straaten, 1957b). The depositional environment of the clay varied from freshwater lacustrine (Van der Woude, 1984) to marine (Van Straaten, 1957b). In the southern half of the coastal plain peat layers occur within the organic-rich clay (Van Staalduinen, 1979, De Mulder *et al.*, 1983). From the clay upward, the shell assemblage becomes dominated by shells from tidal-flat systems (*Cerastoderma edule* and *C. glaucum*, *Mytilus edule*, and *Scrobicularia plana*), associated with an increase in the sand content of the deposits (Van Straaten, 1963).

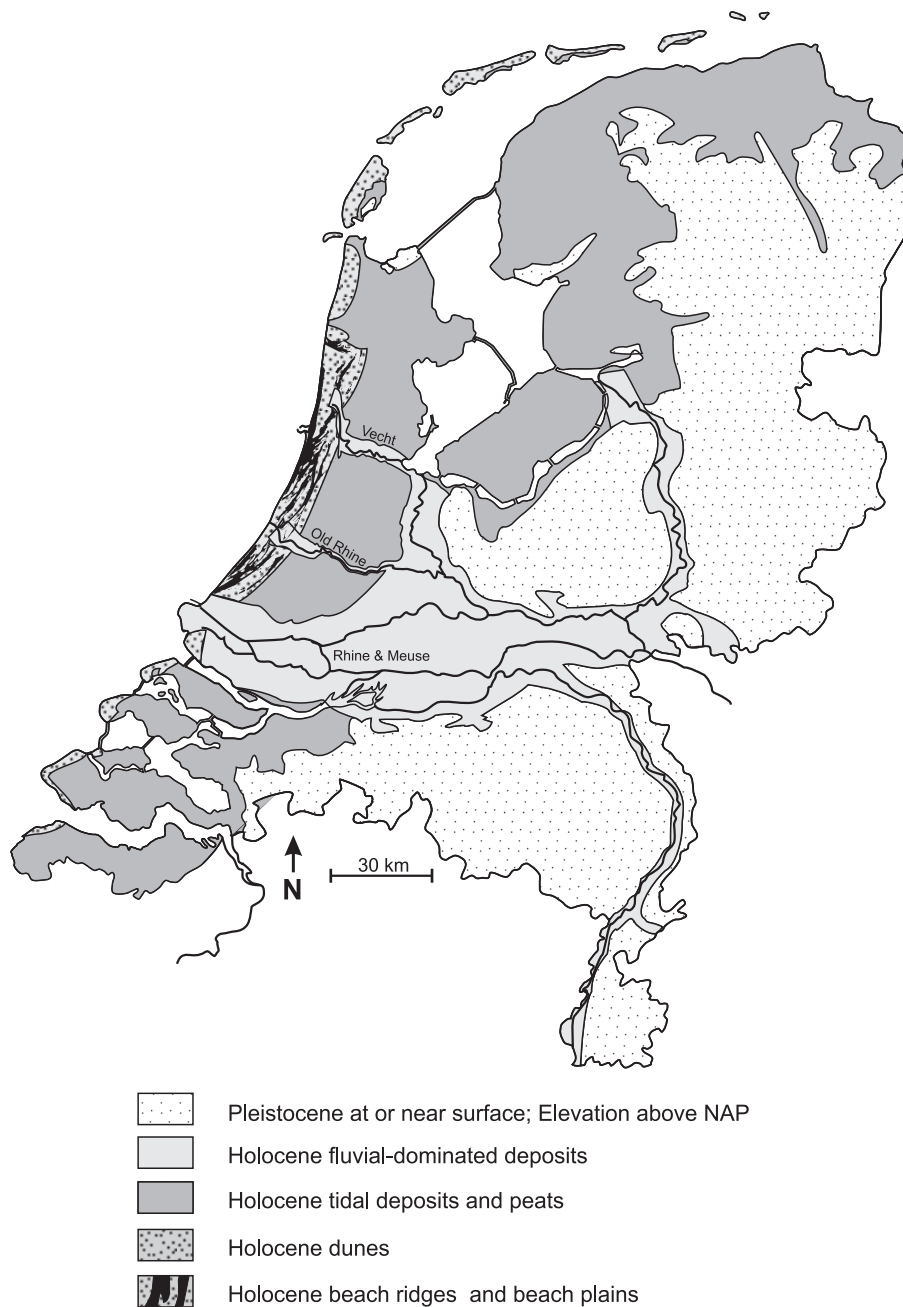


Figure 1.2 : Simplified map of the Holocene geology of The Netherlands (after Van Staalduinen and Van Veen, 1975; Beets and Van der Spek, 2000).

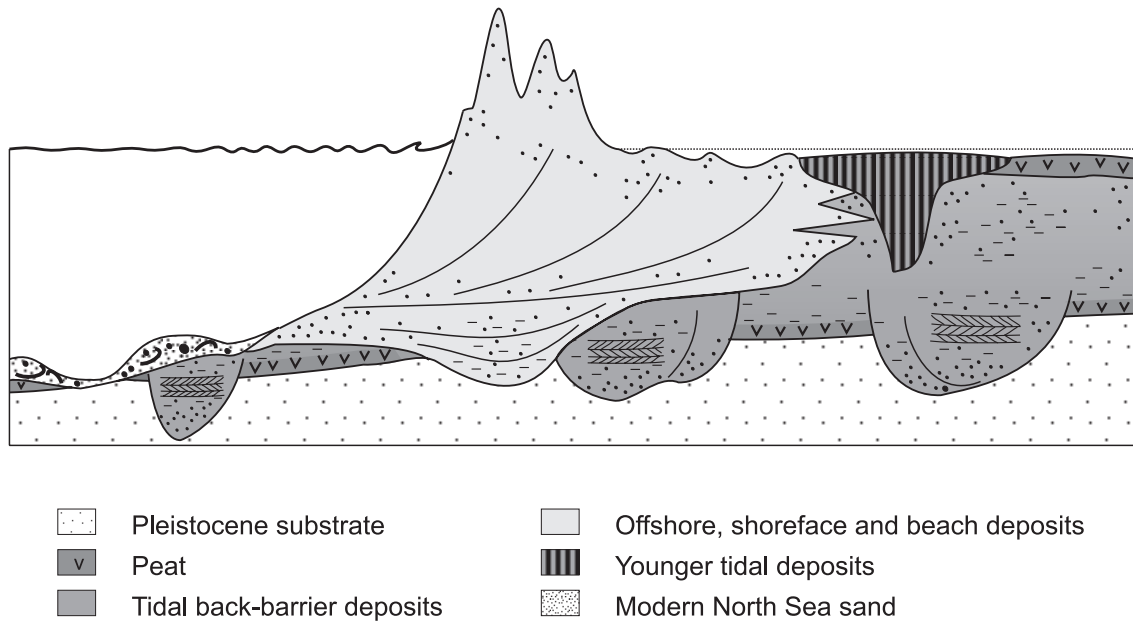


Figure 1.3 : Schematic coast-perpendicular cross section from the western Netherlands.

Holocene deposition started with the formation of peat, as a result of the changing climate conditions and a rise in groundwater level (Jelgersma and Pannekoek, 1960, Jelgersma, 1961). The peat formed on the Pleistocene substrate (Figure 1.4), which dips westward with a slope that varies between 0.014° and 0.019° (De Gans *et al.*, 1993). Sea level (Figure 1.5) controlled the groundwater level, so the onset of peat growth marked the rising sea level in the coastal plain (Jelgersma and Pannekoek, 1960, Jelgersma, 1961, 1979, Van de Plassche, 1986). The deposition of the clay in lacustrine and tide-influenced lagoonal and estuarine settings started when the ongoing sea-level rise resulted in the drowning and subsequent flooding of the peat. The clay was deposited in the landward parts of back-barrier basins, where tides influenced the depositional environment. Both basal-peat formation and mud deposition occurred diachronously. The locus of formation and deposition shifted landward with the rise of sea level.

In the more seaward parts of the back-barrier basins, tidal flats and tidal channels developed. At least nine tidal-inlets and associated tidal channel systems can be recognised in the subsurface of the western Netherlands. Tidal-channel deposits are found in varying abundance. The deepest tidal-channel incisions are found in the western half of the coastal plain (De Gans *et al.*, 1993). The width and depth of the tidal-channel incisions increases from the south to the north of the coastal plain. Deep tidal-channel incisions usually cut into the Pleistocene and have eroded most of the basal peat (De Gans *et al.*, 1993). The sequence of seaward back-barrier deposits overlying landward back-barrier deposits indicates transgression. Eventually the shoreline passed the location of the modern shoreline and moved to its most landward location during the Holocene, at 5500 BP in the south and from 4500 to 3700 in the north. The nature of the seaward part of the transgressive coast, i.e., the shoreline and the shoreface, is not known.

Progradation

In the western Netherlands the transgression was followed by a stage of coastal progradation. A thin rim of about ten kilometres of prograded shoreface, beach and dune deposits flanks the modern North Sea (figure 1.2). The prograded coastal barrier consisted of shoreface, beach and low foredunes deposits. Tidal inlets were closed by the prograding coastal barrier. In the

former tidal back-barrier basins the marine influences vanished. In the basins freshwater conditions prevailed and eventually the formation of a new layer of peat began. The nature of the transition stage from transgression to progradation is not well known. This stage has only been studied in the Alkmaar/Bergen area (Westerhoff and Cleveringa, 1990, Beets *et al.*, 1996b). Offshore deposits from the transition stage have not been found. The start of progradation occurred around 5500 BP in the south, and from 4400 to about 3500 BP in the north (Beets *et al.*, 1992). Beach-ridge development alternated with beach-plain deposition (Figure 1.2). Near Rotterdam, Leiden and north of Haarlem fluvial outlets interrupted the beach-plain and beach-ridge pattern (Figure 1.2). At the fluvial outlet of the Oude Rijn near Leiden, the beach-ridge and beach-plain pattern diverges seaward, leaving the morphological imprint of a wave-influenced delta (cf. Galloway, 1975). The end of coastal progradation was diachronous, it ended early in the south, after 3500 BP near Wassenaar, and much later in the north, after 1900 BP near Haarlem (Van der Spek *et al.*, 1999).

The shoreface deposits overlie the earlier described transgressive back-barrier deposits (Figure 1.3). The basal part of the shoreface deposits consists of facies that deviate from modern shoreface deposits (Van Straaten, 1965, Van der Valk, 1992, 1996). These deposits were attributed to the transgressive shoreface by Van Straaten, However, Van der Valk presumed that these deposits were of a prograded origin. In the coast-perpendicular cross section the depth of the base of the shoreface deposits increases westward (Figure 1.3). The top height of the beach deposits increases westward as well (Figure 1.3), following the rise of sea level during progradation. The shoreface, breaker bar and beach deposits thus form a westward thickening wedge (Figure 1.3). This pattern is observed along the entire coast. The cover of high dunes (Figure 1.3), the so-called Younger Dunes, is restricted to the westernmost 5 to 8 kilometres along the modern shoreline (Jelgersma *et al.*, 1970). The thickness of the shoreface deposits decreases seaward from the modern shoreline on (Beets *et al.*, 1995).

After progradation ended some coastal erosion occurred. The amount of coastal erosion varied strongly alongshore. The pattern of truncated beach ridges at the modern shoreline suggests that erosion was strongest south of The Hague and near the former Oude Rijn outlet at Katwijk (Beets *et al.*, 1992). The end of coastal progradation coincided with the formation of high dunes on top of the westernmost rim of shoreface, beach and low foredune deposits (Umbgrove, 1947, Zagwijn, 1969, Jelgersma *et al.*, 1970). After and during progradation several marine incursions occurred through the fluvial outlets, and young tidal sediments were deposited behind the coastal barrier. (figure 1.3, see for instance Van Staalduinen, 1979, Westerhoff *et al.*, 1987, De Gans *et al.*, 1998).

1.4 Controls on large-scale coastal evolution

Transgression

The transgressive coastal evolution was controlled by the balance between the accommodation space for sediment in the tidal back-barrier basins, which was created by the rise in sea level, and the supply of sediment, both alongshore and cross-shore (following Curray, 1964, Nichols, 1989, Beets *et al.*, 1992, 1994, Beets and Van der Spek, 2000). The Pleistocene relief (Figure 1.4) controlled the geometry and size of the tidal back-barrier basins and thus influenced their accommodation space. The top of the Pleistocene is well known from borings (De Gans *et al.*, 1993, De Gans and Van Gijssel, 1996, simplified in figure 1.4). The Pleistocene landscape can be broadly subdivided in two long and wide funnel-shaped basins, the Southern Rhine/Meuse valley and the Northern Vecht (and IJssel) valley. The area in between (from west of Utrecht to west of Amsterdam) is relatively high and separates the basins.

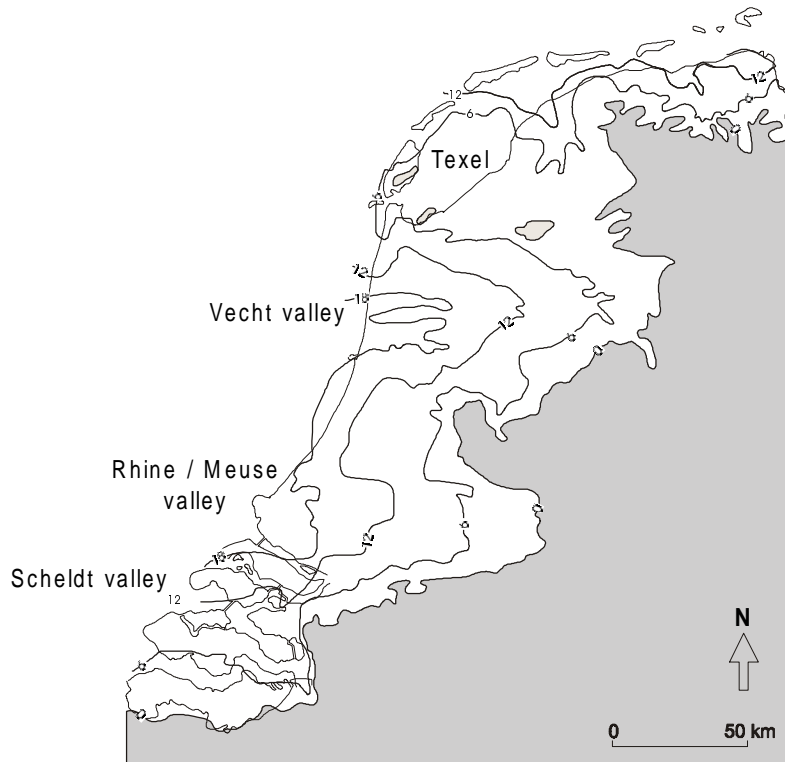


Figure 1.4: Simplified map of the top height of the Pleistocene, after Beets et al. (2000).

The sea-level curve of the western Netherlands is based on dating of the base of the basal peat from the back-barrier basins (Jelgersma, 1961, 1979, figure 1.5). The sea-level curve represents the rise in groundwater in the back-barrier that was induced by the rise in sea level. The trend of the curve has been confirmed by reconstructions of sea level with sedimentary structures and ages of shells and overlying peat (Roep and Beets, 1988, Van de Plassche and Roep, 1989). Slight variations in the rate of sea-level change may have occurred (Van de Plassche, 1986).

The initial rapid rise in sea level (> 0.8 m/100 year, prior to 7000 BP, figure 1.5), and the gentle dip of the Pleistocene substrate resulted in the development of large tidal back-barrier basins. The rapid rise of sea level created a vast amount of accommodation space in the tidal back-barrier basins, which resulted in a large sediment demand. The input of fluvial sediment into the back-barrier basins and into the entire coastal system was limited. The sediment demand thus resulted in the import of sediment from offshore, which resulted in coastal retreat, i.e., barrier rollover. Coastal retreat continued as long as the increase in accommodation space exceeded the rate of deposition in the back-barrier basins.

The rate of sea-level rise slowed down progressively during the Holocene (0.15 m/100year from 5000 to 3000 BP). During the last 2000 years the overall rate of sea-level rise has been about 0.05 m/100year. The decrease in the rate of sea-level rise resulted in a decrease in the rate at which accommodation space was created. Eventually the sediment supply from the offshore filled in the accommodation space, and tidal back-barrier basins silted up completely.

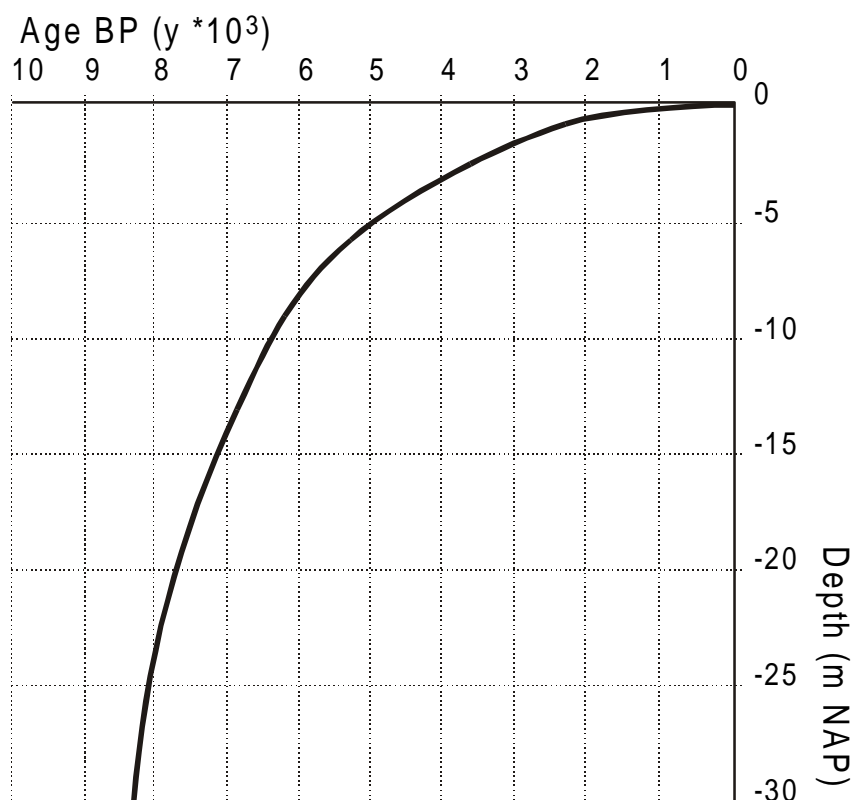


Figure 1.5: Holocene sea-level curve of the western Netherlands, after Jelgersma (1979).

Changes in the wave climate and tides during the Holocene seem to have been limited. Reconstructions of waves and tides are based on geological observations of storm, high- and low-water markers in coastal deposits or on model calculations. Observations of high-water and low-water markers in beach deposits suggest that limited changes in the tidal range occurred from 5500 BP to present (Roep and Beets, 1988). Observations suggest an increase in the height up to which storm deposits were formed during the last 4500 years, which is related to climate variations and changes in the shoreface profile (Jelgersma *et al.*, 1995). Model reconstructions of palaeo-tide levels also show little changes in the tidal range after 6000 BP (Franken, 1987, Hulsén, 1994, 1995, Gerritsen and Berentsen, 1998). Model reconstructions of the direction of sediment transport along the Holland coast demonstrate a clear change in the direction of the residual tidal transport from cross-shore to alongshore after 5000 BP (Gerritsen and Berentsen, 1998, Van der Molen, Submitted). Calculations of the palaeo-wave action also demonstrate little changes after 6000 BP (Stive, 1987). The influences of the changes in the wave and tide conditions on large-scale coastal evolution, at least after 6000 BP, seem to have been limited (Beets *et al.*, 1992).

The volume of sediments stored in the Holocene deposits gives an indication of the sediment supply. The volume of Holocene coastal sediments in The Netherlands has been calculated by Beets *et al.* (1994, 'bijlage 2'), and Beets and Van der Spek (2000). The coastal deposits in the western Netherlands ('Holland', from The Hague to Alkmaar/Bergen) consist of $44 \cdot 10^9$ m³ of sand (59 %), of $27 \cdot 10^9$ m³ of mud (36 %) and of $4 \cdot 10^9$ m³ (5 %) of peat. An estimate of the period during which net deposition of the sediments occurred shows that 60 % of the sediments was deposited up to 5000 BP, prior to the closure of the tidal inlets, 30 % was deposited from 5000 to 2700 BP, and 10 % was deposited during the last 2700 years BP (Beets and Van der Spek, 2000).

Three sources of sediment have contributed to the development of the western Netherlands: 1) fluvial sources, 2) older transgressive Holocene deposits on the North Sea floor, and 3) erosion of the Pleistocene basement (Beets and Van der Spek, 2000). Based on a conservative estimate of the fluvial contributions, 10 % of the coastal deposits in The Netherlands is supposed to originate from fluvial sources directly (Beets and Van der Spek, 2000). In contrast to the modern incised-valley systems, as for instance on the US East Coast (Dalrymple *et al.*, 1994) and the French Atlantic coast (Allen and Posamentier, 1993), and for instance the coastal systems of southeastern Australia (Thom, 1983, Roy, 1994, Roy and Boyd, 1996), the coast of the western Netherlands is not incised in and bound by bedrock. Both the basement and the lateral boundaries consist of sand, locally with gravel, silt, clay and peat. Furthermore, the Southern Bight of the North Sea, west of The Netherlands, is relatively shallow and subject to tidal and storm-wave reworking. Therefore North Sea floor sediments are easily available and can be entrained by waves and tidal currents, and the deposits on the North Sea floor thus formed a viable source of sediments for the western Netherlands. Erosion of the protruding Pleistocene basement at the Texel High (Figure 1.4) contributed as well.

Progradation

The end of transgression and hence the start of coastal progradation was controlled by the silting up of the tidal back-barrier basins (*Nichols, 1989, Beets *et al.*, 1992, Beets *et al.*, 1994, Beets and Van der Spek, 2000). The silting up of the tidal back-barrier basins also resulted in the diminishing of the tidal-inlet channels, and eventually resulted in their complete closure. Alongshore variations in the timing of the end of transgression, and hence in the beginning of progradation, can be attributed to differences in the size of the transgressive back-barrier basins. Small tidal basins silted up earlier than large ones and therefore ended the transgression earlier for the small basins. As soon as the tidal back-barrier basins had silted up, the sediment that was previously directed into the back-barrier basins became available for the shoreface and beach. This initiated coastal progradation.

Progradation continued until the sediment supply diminished and other sediments sinks became active, for instance the western Wadden Sea and the aeolian dunes.

The majority of the sediments in the western Netherlands was deposited during coastal transgression. During the stage of transgression the onshore-directed cross-shore sediment transport from the North Sea floor into the tidal back-barrier basins was an effective sediment-transport mechanism. Incision of tidal channels into the Pleistocene basement contributed sediments to the transgressive deposition. The closure of the tidal inlets with the start of coastal progradation put an end to cross-shore-sediment transport via tidal inlet channels. The relative importance of longshore sediment sources versus cross-shore sediment transport for coastal progradation has been debated since these deposits have been studied. It is important to notice that the volume of prograded deposits is relatively small compared to the volume of transgressive deposits. The total sediment transport towards the prograding coastal system thus was more limited than during transgression (Beets *et al.*, 1992). However, as the back-barrier basins did not provide accommodation space anymore and rate of sea-level rise was limited, the relatively small sediment supply was sufficient to result in coastal progradation.

1.5 Scope of the thesis

A number of aspects of the large-scale coastal evolution of the western Netherlands is not well understood. Focus of the thesis is on the stretch of prograded deposits, its landward boundary, and its seaward extension. The morphology and geology of the transgressive shoreline and shoreface are not well constrained and neither are the morphology and geology

of the transition stage from transgression to progradation. Furthermore, the timing and duration of the stage of transition is not well known. Although the amount of data from the prograded shoreface deposits is relatively large, there still is a number of ambiguities, especially regarding the deviating facies at the base of the shoreface sequence. Finally, the relative contribution of cross-shore versus longshore sediment transport to coastal progradation remains a point of debate.

The aims of this thesis are related to the underexposed points mentioned above. The first aim is to analyse the nature of the transgressive shoreline and shoreface. The second aim is to investigate the nature, timing and duration of the stage of transition from transgression to progradation. The third aim is to increase the knowledge of the timing, duration and depositional environments of the coastal progradation, in order to assess the relative contributions of longshore and cross-shore sediment transport.

The research area stretches from The Hague to Haarlem (Figure 1.1). Traditional sedimentological techniques, i.e., facies models: environmental reconstructions based on lithology, sedimentary structures and other environmental indicators like diatoms, pollen and shells, are used to study changes in the depositional environment. The age of the deposits and estimates of sedimentation and progradation rates are based on detailed AMS ^{14}C dating of shells. The wave-height reduction due to bottom friction is calculated with a simple model to reconstruct the effect of a changing shoreface profile during coastal evolution. A computer model of large-scale coastal evolution (the Shoreface Translation Model of Cowell *et al.*, 1995) is applied to reconstruct various scenarios of coastal change during the Holocene. The combined results of reconstructions and modelling improve the knowledge of large-scale coastal evolution.

1.6 A note on the use of models for large-scale coastal evolution

The application of numerical models in the geological research of coastal deposits has two purposes. Firstly, models can constrain palaeo-conditions. For instance, models are used to quantify wave climate (Stive, 1987), tides (Franken, 1987, Hulsen, 1994, 1995, Gerritsen and Berentsen, 1998, Van der Molen, Submitted) and sediment transport (Zitman, 1987) over short time spans in the past. Secondly, stratigraphic models are used to mimic the geological evolution and the resulting stratigraphy over long time spans. The aim of numerical models in geological research has been clearly expressed by Oreskes (1994): ‘models are representations, useful for guiding further study, but not susceptible to proof’. One application of numerical models is to reduce the number of likely scenarios of coastal evolution. This goes hand in hand with more traditional research, which can provide the means to verify (aspects of) the model outcome. In addition, models may reveal interdependencies and feedback mechanisms in the depositional system that were previously unnoticed (Cross and Harbaugh, 1990), which is especially true for stratigraphic models.

Ideally, palaeo-condition models and stratigraphic models would consist of the same building blocks, i.e., stratigraphic models would be palaeo-condition models run for longer time spans to reveal the stratigraphic evolution. Our inadequate understanding of numerous geological processes (Cross and Harbaugh, 1990) and the inherent complexities in morphodynamic processes (amongst others: positive and negative feedback mechanisms, thresholds, and self-organisation :Cowell and Thom, 1994) hinders the up-scaling of short time-scale palaeo-conditions models to longer time spans. Therefore, alternative approaches are used to model stratigraphic evolution, with geometric-equilibrium profiles or diffusion equations ruling long-term evolution (Carey *et al.*, 1999). Unfortunately, there are no independent checks on the applied rules for long-term evolution. The –usually not quantitative- comparison between model outcome and stratigraphy is the only way to verify

the applicability of the rules. There is no unambiguous method to distinguish between differences that result from local stratigraphic deviations, processes not represented in the model, model flaws, and limitations of the underlying model rules. Hence, for models of long-term geological processes the notion that the model outcome is one representation (out of many) of the evolution (cf. Oreskes *et al.*, 1994), rather than reality, is extra true. However, the added value of model simulations, in particular the exposure of previously unnoticed patterns, make simulations a valuable tool in the study of coastal evolution.

Chapter 2: Deposition and erosion during final transgression and initial coastal progradation; Holocene coastal deposits at Ypenburg (Rijswijk, The Netherlands).

Abstract

The preservation potential of the seaward parts of transgressive coasts is limited, because these parts are continuously being eroded. Only when a transgression changes towards coastal progradation, the transgressive deposits at the seaward edge of the coastal system may be preserved. The Ypenburg area (east of The Hague, The Netherlands) is located at the boundary between Holocene transgressive back-barrier deposits and prograded shoreface deposits. In the area the transition from transgression to progradation is preserved. In this study the deposits from the transition are described and the local coastal evolution is reconstructed.

The base of the Holocene sequence is formed by peat and organic-rich clay deposited in a fluvio-lacustrine and estuarine swamp. Towards the top of this interval marine influences increase, because the coastline shifted eastward to the area. In the southwestern half of the study area, these deposits are truncated by an erosion surface, which is overlain by deposits of small tidal channels. These are in turn overlain by washover deposits. This sequence of deposits reflects ongoing coastal retreat. Carbon dates in the washover deposits indicate mainly aggradation occurred. The washover deposits represent the stage of aggradation, when the coastal behaviour shifts from transgression to progradation. On top of the washover deposits beach-ridge, beach-plain, marsh and dune deposits mark the onset of coastal progradation.

The northeastern half of the study area is dominated by tidal channel deposits and spit-like elongate sand bodies. The wide erosion of the tidal channel resulted from coastal retreat, and the development of the area as the tidal-inlet channel. The abundance of mud in the channel deposits indicates that the importance of the tidal flow through the inlet rapidly diminished. The elongate sand-bodies mark the final closure of the remnant of the tidal inlet. Small tidal channels remained active during storms in between the elongate sand-bodies. The closure of the inlet occurred from south to north. Deposition of the elongate sand-bodies started after the beginning of coastal progradation in the southwestern half of the area

2.1 Introduction

The morphology of transgressive coastal systems depends on the relative magnitude of waves and tides, and on the morphology of the substrate (Boyd *et al.*, 1992). In tide-dominated settings coastal systems consist of tidal flats separated by inlet channels, or -in incised valley systems- of tide-dominated estuaries. Tidal-channel and tidal-flat deposits dominate the depositional sequence of these systems. In wave-dominated settings the coastal system consist of a coastal barrier with abundant washovers behind them in strand-plain or lagoon, or -in incised-valley systems- of wave-dominated estuaries. The depositional sequences of these systems consist of lagoonal sediments overlain by washover deposits. In general, the preservation potential of transgressive deposits from the seaward edge of the coastal system is very limited, because this part is constantly being eroded in the course of coastal retreat. Deposits from the landward part of the coastal system may escape erosion during transgression, and can be found in the shoreface and shelf sequence (Nummedal and Swift, 1987). Prograded coastal sequences are abundant on many modern coasts and consist of tidal flats, deltas and strand-plain systems, depending on the relative contribution of tides, fluvial input and waves (Boyd *et al.*, 1992). The preservation potential of prograded coastal deposits is high compared to that of transgressive coastal systems.

Shifts from transgression to progradation have been recognised in many Holocene coastal sequences around the world. A shift from transgression to progradation may result in the preservation of some transgressive deposits on the seaward side of the coastal system. This preservation presents a unique opportunity to study these transgressive deposits, and may shed some light on the morphology of the seaward part of the transgressive coastal system.

In many cases the shift from transgression to progradation is associated with a shift from tide- to wave-dominated deposition (Davis and Clifton, 1987, Davis and Clifton, 1994). The shift from tide- to wave-dominated deposition is related to changes in the morphology of the coastal system, e.g. to the closure of the tidal inlets. In the Western Netherlands studies from the Alkmaar region (Figure 1.1 and 1.2) include the transition from transgression to progradation. In this area the progressive fill of the tidal back-barrier basins leads to a decrease of tidal influences, and hence an increase in the wave influences (Westerhoff *et al.*, 1987, Beets *et al.*, 1996b).

The aim of this chapter is to present the characteristics of the coastal deposits in the Ypenburg area, east of The Hague (The Netherlands) and to reconstruct the coastal evolution of the area. The Ypenburg area is situated on the boundary between the tidal back-barrier deposits of the transgressive coastal system and the beach-plain and beach-ridge deposits of the subsequent prograded coastal system (Figure 1.2 and 1.3). In the subsurface of the Ypenburg area the remnants of the transition from the transgressive coastal system to the prograding coastal system are preserved. The development of the Ypenburg area into building location provided abundant subsurface data of Holocene coastal deposits. Furthermore, Neolithic finds, including a well preserved graveyard, triggered extensive archeological research, which provided additional subsurface data and facilitated geological research.

2.2 Geological setting

The study area is located (south)east of The Hague, and borders the suburbs of Rijswijk and Voorburg (Figure 1.1). The area has been in use as a military airbase and until recently it was inaccessible for geological research. The airbase was closed in the 90's and the area is now being developed as a suburb of The Hague.

Southeast of Ypenburg back-barrier sediments consist of sandy tidal-channel deposits with adjacent mud-flat deposits. The tidal channel system stretches eastward for about 12 km

(Van der Valk, 1996b, De Gans *et al.*, 1998). The back-barrier deposits from part of the transgressive coastal system.

Northwest of Ypenburg the coastal stretch consists of a westward-thickening wedge of prograded coastal-barrier deposits (Van Straaten, 1965, De Mulder *et al.*, 1983, Roep *et al.*, 1983, De Gans *et al.*, 1998). The surface morphology of this area is dominated by a series of beach ridges and beach plains. Directly northwest of Ypenburg the oldest and most eastern beach ridge is found, separated from the more westward ridges by a broad beach plain. The ridges consist of low dunes, while the plains form lows which have subsequently been covered with peat. The most western part of the beach-ridge and beach-plain area is covered with high and relatively young dunes. The beach-ridge pattern can be traced 12 km to the northeast, up to the former mouth of the Old Rhine near Katwijk and Leiden (De Gans *et al.*, 1998, figure 1.3). This branch of the Rhine was the main Rhine outlet from approximately 4300 BP until about 2900 à 2600 BP, when the Vecht became the active branch of the Rhine (Törnqvist, 1993).

Southwest of The Hague the beach-ridge pattern converges and curves westwards, towards the recent coastline. The recent coastline erosively crosscuts the prograded beach ridges in the vicinity of Monster (Figure 1.1 and 1.2). The most eastward beach ridges are very difficult to trace to the southwest. Beneath Voorburg and Rijswijk these ridges are clearly connected, but further to the southeast only small dune and ridge patches are present (these patches are more or less aligned parallel to the beach ridges, see De Mulder *et al.*, 1983, De Gans *et al.*, 1998). Further to the southwest fluvial and estuarine deposits of the Rhine and Meuse rivers are found (Van Staalduinen, 1979). After and during the progradation of the coast, the area was flooded from the Meuse outlet in the south (near Rotterdam, figure 1.1, Van Staalduinen, 1979). Tidal deposits that originate from this flooding are found in the northwestern part of Ypenburg (De Gans *et al.*, 1998), where they incise and overlie the older coastal deposits (Figure 2.1 B).

The deposits at Ypenburg can successfully be correlated with the succession found in a construction pit one kilometre south of Ypenburg that has been described by Van der Valk (1996b). The pit was deeper (down to -8 m NAP) than any of the trenches in the Ypenburg area. The small dunes on top of sandy coastal deposits in the construction pit are the equivalent of the sandy deposits in the northwestern part of Ypenburg.

2.3 Methods

Data on the subsurface of the Ypenburg area are derived from four undisturbed cores, numerous hand drillings, sections from trenches and pits, and a large number of cone penetration tests (CPT's). Cone penetration tests measure the resistance of the subsurface to vertical stress (cone resistance, in figure 2.3 and 2.4) and torque stress. The ratio between vertical stress and torque stress gives a friction parameter. The combination of cone resistance and the friction parameter is a measure of the lithology (Amorosi and Marchi, 1999, and references therein). The inferred lithology from the CPT's can be correlated with the lithology of the undisturbed cores and sections from trenches. In this way CPT's can be used for stratigraphic correlations and sedimentological interpretations (Westerhoff *et al.*, 1987, Beets *et al.*, 1996b, Amorosi and Marchi, 1999)). The characteristics of the shallow deposits are primarily taken from sections in trenches.

Nineteen shell samples and one fossil tree leaf were collected from cores and trenches to determine the time of deposition with AMS ¹⁴C dating (Appendix 2.A). Where possible, *in-situ* doublets of *Scrobicularia plana* were collected. Otherwise, doublets or undamaged single shells with remnants of the periostracum were taken. The doublets of *Scrobicularia* were found in living position within the sediment, this position was some 15 cm under the palaeo

surface. Their age is thus slightly less than that of the surrounding sediments. All other shells were transported to their final resting-place, so their age is higher than the age of the site of deposition. The tree leaf was found within a clay layer among numerous other leaves and plant remains. The perfect condition of the leaves suggests that they have not been transported over a long distance and that their age is similar to the age of the sediment in which they were buried. All 14C dates on shells were corrected for the marine reservoir effect (marine corrected in Appendix A, (m) BP in text) and these ages are used throughout the text. Calendar ages have been obtained by calibrating the marine-corrected ages (Calib 4, Stuiver and Reimer, 1993, calibrated age in Appendix A).

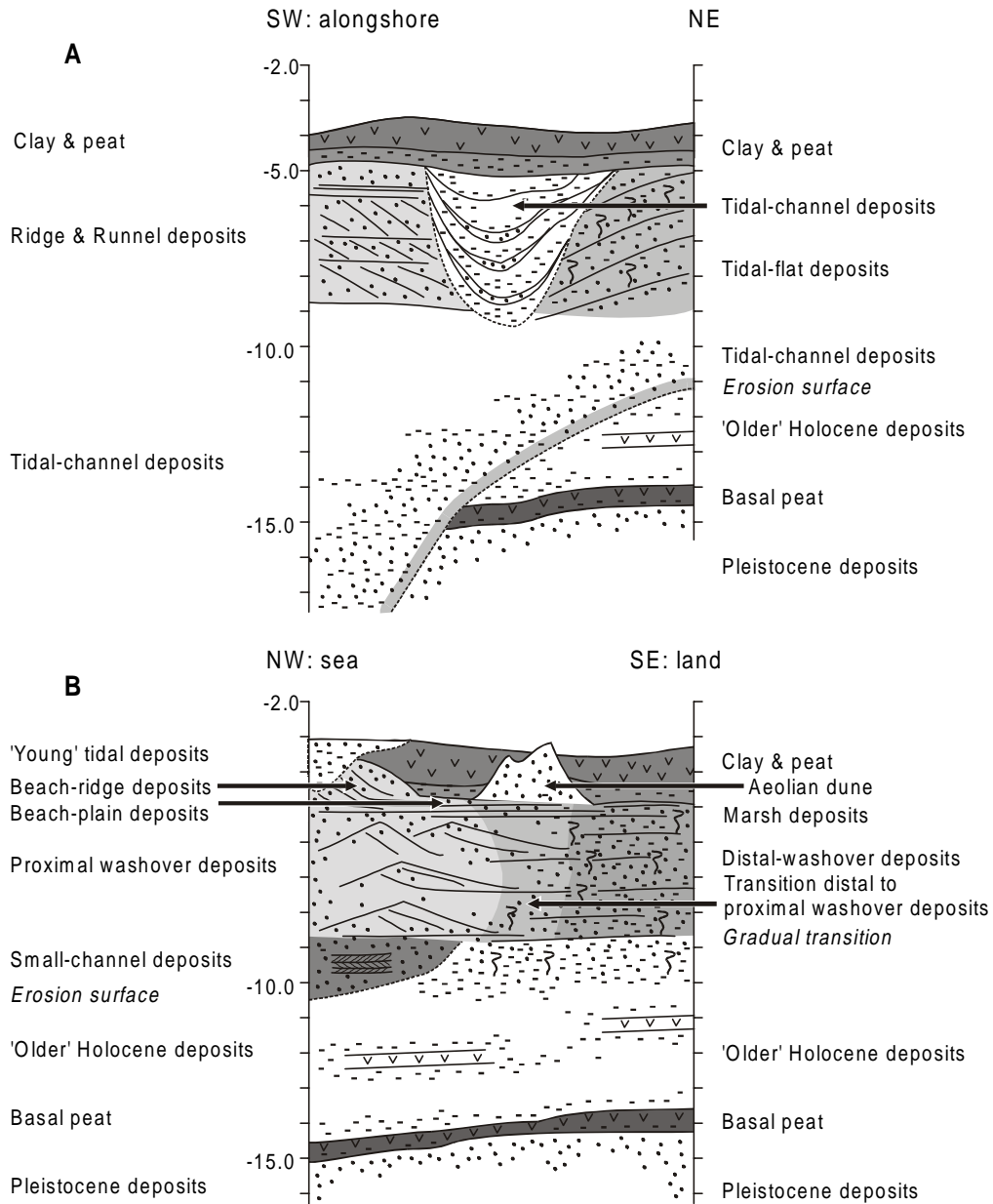


Figure 2.1: Schematic stratigraphic sequences of the Ypenburg area. Figure 2 A: Stratigraphic sequence in the northeastern half of the area. Figure 2 B: stratigraphic sequences in the southwest.

2.4 The depositional sequence at Ypenburg

The sequence of the deposits is given in two stratigraphic columns (Figure 2.1). The facies models of the deposits are presented and discussed below. The facies distribution is presented in a map (Figure 2.2), and in two cross sections (Figure 2.3 and 2.4). The results of the AMS ^{14}C dates are presented in appendix 2.A, and the dates are indicated in figures 2.2 and 2.3.

The Ypenburg area can roughly be divided in a northern half that is dominated by tidal channel deposits (Figure 2.1A), and a southern half that is dominated by washover deposits (Figure 2.1B). The most striking morphological features of the northern half are elongated sand bodies amidst tidal channel deposits (Figure 2.2). The southern half is characterised by the transition of proximal to distal washover deposits from northwest to southeast (Figure 2.4). Small channels are found in the uppermost 3 m throughout the entire Ypenburg area; some of these channels are too small to incorporate in the map of Figure 2.2.

2.4.1 Sequence in the southwestern half of Ypenburg

Pleistocene sands form the base of the Holocene deposition (Figure 2.1 A and B). The basal part of the Holocene sequence consists of Basal peat and Older Holocene deposits. The deposits above -10 m NAP are very diverse. In the southeastern half (Figure 2.1 B and cross section D-D', Figure 2.3) a gradual transition from the clay of the Older Holocene deposits into more sand-rich bioturbated deposits is observed. Towards the top of sequence the trend continued as the amount of roots increases. In the southwestern half (Figure 2.1 B and cross section D-D', Figure 2.3) the transition from Older Holocene deposits into overlying deposits is abrupt. The overlying deposits are sandy and rich in shells, and have distinct cross-bedding. Towards the top of the sequence the cross-bedding vanishes and horizontal sand mud laminations are found, with an isolated occurrence of cross-bedding on the southwestern boundary of the area. Aeolian dune deposits with traces of Neolithic inhabitation are found on top of the sequence in the centre of the area. In the entire area a clay layer overlies the deposits, with a peat layer on top. In the southwestern half of the area sand-mud laminations cap the sequence (Figure 2.1 B).

Pleistocene and Older Holocene deposits.

Holocene deposits overly sandy fluvial deposits from the last ice age (De Mulder *et al.*, 1983, De Groot and De Gans, 1996). They start with an organic-rich clay-to-peat bed of 40 cm (Figure 2.1). Above the peat, laminated and root-bearing organic-rich clays are found, intercalated with thin (up to 30 cm) peat beds (Figures 2.5 and 2.6) The interval has a thickness of about 4 m. The top of the organic-rich laminated clay shows a gradual increase in sand content. With the increase of the sand fraction, brackish (*Hydrobia ulvae*) and marine (*Scrobicularia plana*) shells and marine bioturbation traces (*Hydrobia* layers, attributed to the lugworm *Arenicola marina*, Van Straaten, 1964) are found (Figure 2.5). In the southern half of Ypenburg an interval of 5 m of alternating high and low cone-resistance values is found in several CPT's, from -17 m to -13 m. The interval is interpreted as an alternation of sand and mud layers.

The depth of the basal peat (-15 m) with respect to the sea-level curve of Jelgersma (1979) suggest peat formation started around 7200 BP. Correlation with comparable deposits from the vicinity (Van Staalduinen, 1979, De Mulder *et al.*, 1983, Van der Valk, 1992, De Gans *et al.*, 1998) also suggests that the deposits are of Early to Middle Holocene age. The high organic content, roots and peat indicates deposition under fresh-water conditions. The deposits originate from fluvial, swamp, lacustrine and estuarine environments (Van Staalduinen, 1979, De Mulder *et al.*, 1983, Van der Woude, 1984). These environments dominated the landward side of the transgressive back-barrier basin, due to the dominance of

freshwater influxes at that side of the basin. The local occurrence of alternating high- and low-cone resistance in the CPT's probably represents sand-mud bedding from a small tide-influenced channel. The upward increase in sand content and the upward occurrence of brackish and marine shells point to a shift to more marine depositional conditions. The bioturbation and the shell content point to deposition on a tidal flat. Shells from the top of the interval have been dated at 5925 ± 44 (m) BP (YP 2-13) and 5862 ± 37 (m) BP (YP 3-9, figure 2.3).

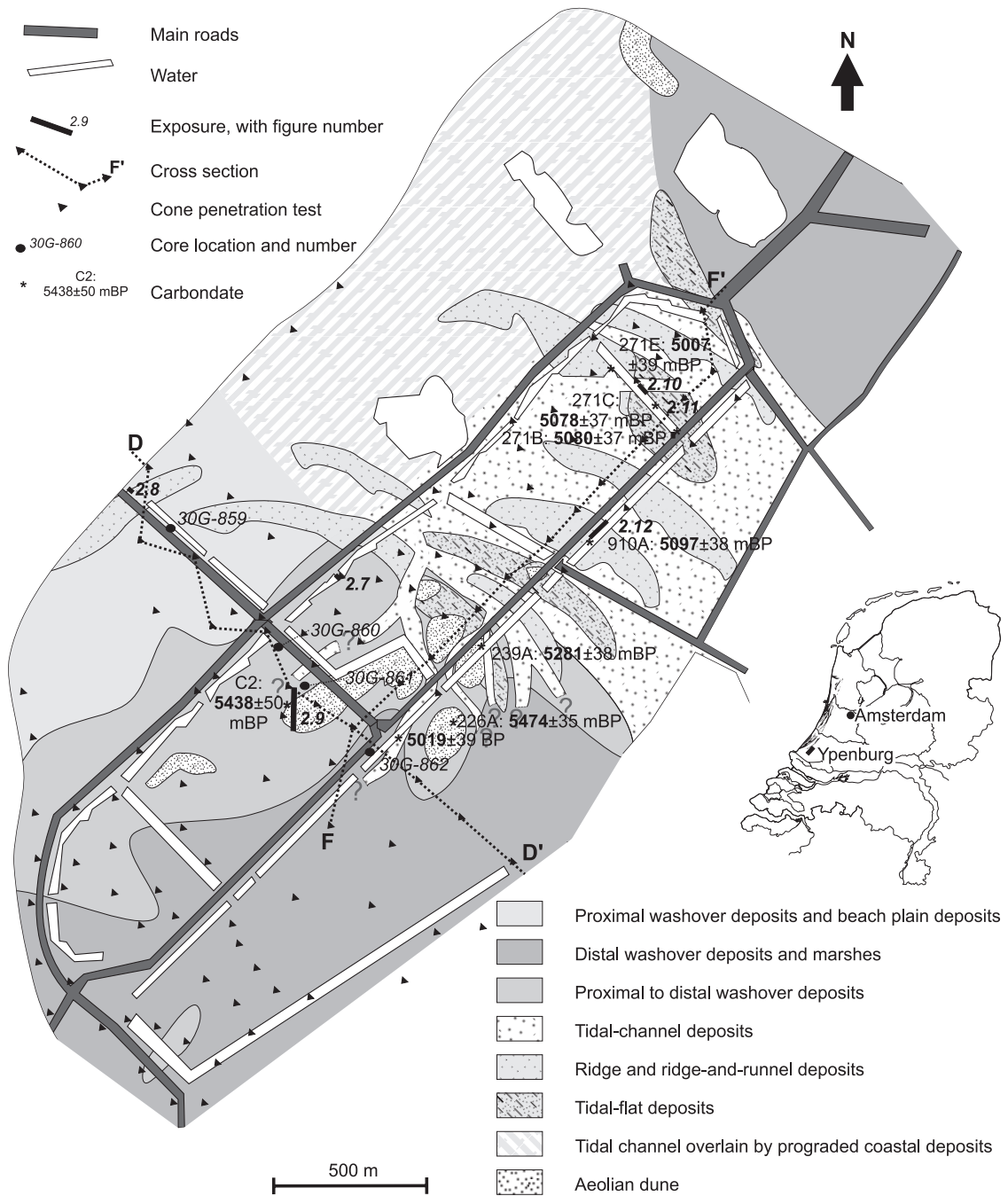


Figure 2.2: Detailed geological map of the Ypenburg area, based on hand borings, cored borings, CPT's and exposures along trenches. The ^{14}C dates on shells from trenches and pits are indicated.

Small-channel deposits

In the southwestern half, sandy deposits abruptly truncate the Older Holocene organic-rich laminated clays (Figure 2.6). The abrupt transition is an erosion surface. The surface is characterised by a basal shell lag, and is overlain by 1 to 2 m of cross-laminated sand with some mud flasers and thin shell layers (Figure 2.6). The basal lag and sedimentary characteristics point to deposition in small tidal channels. The local incision of small channels has generated the erosion surface. Transported shells (full grown, single valves, all shells originate from tidal environments; part of the shells are covered with Bryozoa, indicating prolonged presence on the channel floor) from just above the erosion surface give ages of 5803 ± 47 (m) BP (YP 3-2) and 5602 ± 44 (m) BP (YP 1-1, figure 2.3).

Proximal washover deposits

In the southwestern half of Ypenburg (Figure 2.1 B and 2.3) sands with high- and low-angle cross-bedding, with partly preserved top sets, erosion planes, some mud flasers and layers, and thick chaotic shell beds are found. Individual beds are 5 to 10 cm thick. The cross beds with preserved top sets form mounds of about 1 m high and up to 10 m long (Figure 2.7). The direction of progradation varies between the southwest and the southeast. Foresets show alternations between high and low angles, and generally become progressively more gentle in the direction of progradation. The mounds often overlie deposits from small channel (up to 3 m wide). In some cases the small channels are filled with thick clay beds (Figure 2.7), but sandy-channel fills with cross lamination, (wave) ripple lamination, flasers and clay laminae are found as well. Towards the top of the sequence low-angle cross-bedding becomes more abundant and mud layers become rare. In the CPT's a repetition of peaks in cone resistance represent these deposits (Figure 2.3).

The preservation of top sets in the mounds indicates that progradation was associated with aggradation. All of the deposits have been preserved, including the clay layers that are associated with the deposits. This indicates that the depositional environment was not regularly reworked and points to deposition during events. The presence of flasers, mud layers and erosion planes within the deposits, point to quiet periods during formation, alternating with reactivation and deposition. The chaotic shell beds point to rapid settling from suspension. The aggradation and progradation of the deposits, as well as the chaotic shell beds point to deposition on washover fans during storms. The signs of reactivation indicate variation in the storm activity and are likely related to variations in the water level. These variations may be in part tide-influenced.

Washover deposition takes place when storm-driven set-up overtops and erodes a coastal barrier and sediment is entrained in the flow. As the sediment-loaded water enters the back-barrier area, the flow expands and the flow velocity decreases rapidly, resulting in very rapid sedimentation on a washover fan (Schwartz, 1982). The high-angle cross beds point to sub-aqueous deposition (Schwartz, 1982), as does the presence of the mud layers. Similar mud layers were observed in washover fans in Miocene deposits in the German Bight (Boersma, 1991). The transition towards more low-angle deposits and the absence of clay layers to the top of the sequence point to more sub-aerial deposition. The small channels that are found with the washover fans are probably washover channels, formed by the washover currents and by the return flow of the storm-driven set up.

The deposits miss the regular reactivation surfaces and mud drapes of tidal bars (cf. DeMowbray and Visser, 1984), and do not have the levelled top and regular character of wave-built bars (Davis *et al.*, 1972). In these environments the more regular character of the reworking would not have permitted the preservation of the mud layers and the top sets.

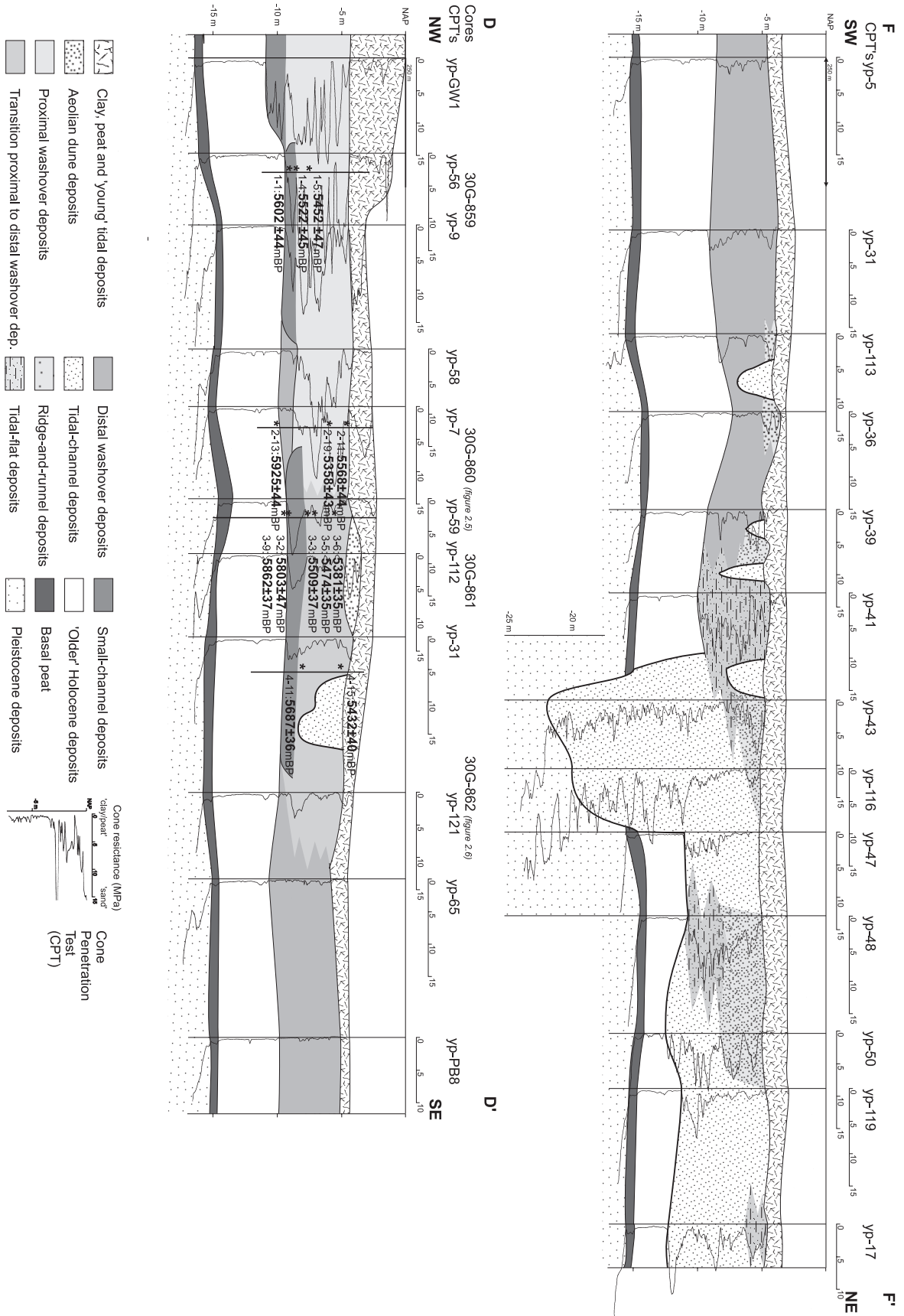


Figure 2.3 (left) and Figure 2.4 (right): caption continued on following page.

In the cores the transition from the small-channel deposits into the overlying washover deposits is gradual. The transition is associated with an increase in grain size and shell content, distinct parallel and cross-bedding and thick mud layers. The sequence of proximal washover deposits is 5 m thick. In the vicinity of the dunes (sample location C2, figure 2.2), deposits with high-angle foresets and abundant shells are found on the northeastern flank of a small tidal channel. Other contacts between tidal channel deposits and washover deposits have not been observed. The washover deposits adjacent to the channel probably originated from the tidal channel, and may be regarded as a transition to levee deposits.

The dates from the proximal washover deposits range from 5522 ± 45 (m) BP (YP 1-4) to 5358 ± 43 (m) BP (YP 2-19). The washover that was found adjacent to a tidal channel gave an age of 5281 ± 38 (m) BP (YPT 239A). One out-of-sequence date (older age overlying younger age sample) was found in core YP2 (30G-860)). This is probably due to the reworking of older shell material.

Distal washover deposits

In the southeastern half of the Ypenburg area, bioturbated muddy sand beds of several cm to dm thick with remnants of even lamination are found (Figure 2.6). These deposits are the lateral equivalent of the proximal washover deposits in the west and are found between 10 m to 6 m below NAP. Within the deposits *Scrobicularia plana* doublets are common, both *in-situ* and concentrated in washed-out layers. Roots are increasingly abundant to the top of the interval. There is a gradual transition from the underlying small-channel deposits and from Older Holocene organic-rich laminated clays to these bioturbated beds.

The bioturbated sand beds are probably the distal toes of the washover fans. The transition of the proximal to the distal washover deposits has not been exposed. The most likely transition seems to be a gradual one, with the toes of the fans thinning into sand beds, which later were bioturbated. The area was probably inter-tidal considering the degree of bioturbation and the abundance of *Scrobicularia* shells. The increase of roots towards the top of the interval indicates that the area developed into a supra-tidal marsh. The layers of washed out *Scrobicularia* shells point to large-scale erosive events that may have resulted from storms.

The seven dates from the distal washover deposits range from 5687 ± 36 (m) BP (YP 4-11) to 5381 ± 35 (m) BP (YP 3-6, figure 2.3). Proximal washover deposits from the same depth have slightly younger ages (50 to 100 years, figure 2.3), indicating a slightly seaward dipping palaeo surface.

Ridge deposits.

A narrow bar at the western boundary of the area (location 2.8 in figure 2.2) consists of low-angle cross-bedded sets, up to 30 cm high, with marked variations in the dip of the laminae. The sets dip to the southeast. Relatively steep sets are found alternating with relative gentle sets, stretching over about 1 m (Figure 2.8). The laminae continue into horizontal bioturbated sand-mud laminations. On the cross-bedded sets some shells are found and mud is absent. These deposits overly proximal washover deposits. In contrast to the washover deposits, the deposits lack mud layers and chaotic shell beds.

Figure 2.3 (previous page, left): NW-SE cross section from the southwestern half of the Ypenburg area, based on CPT's and four cores. This cross section is orientated perpendicular to the palaeo-shoreline. The ^{14}C dates on shells from the borings are given.

Figure 2.4 (previous page, right): NE-SW cross section of the Ypenburg area, based on CPT's and exposures along a trench. The cross section is oriented parallel to the palaeo-shoreline and crosscuts the tidal channel in the northern part of the area.

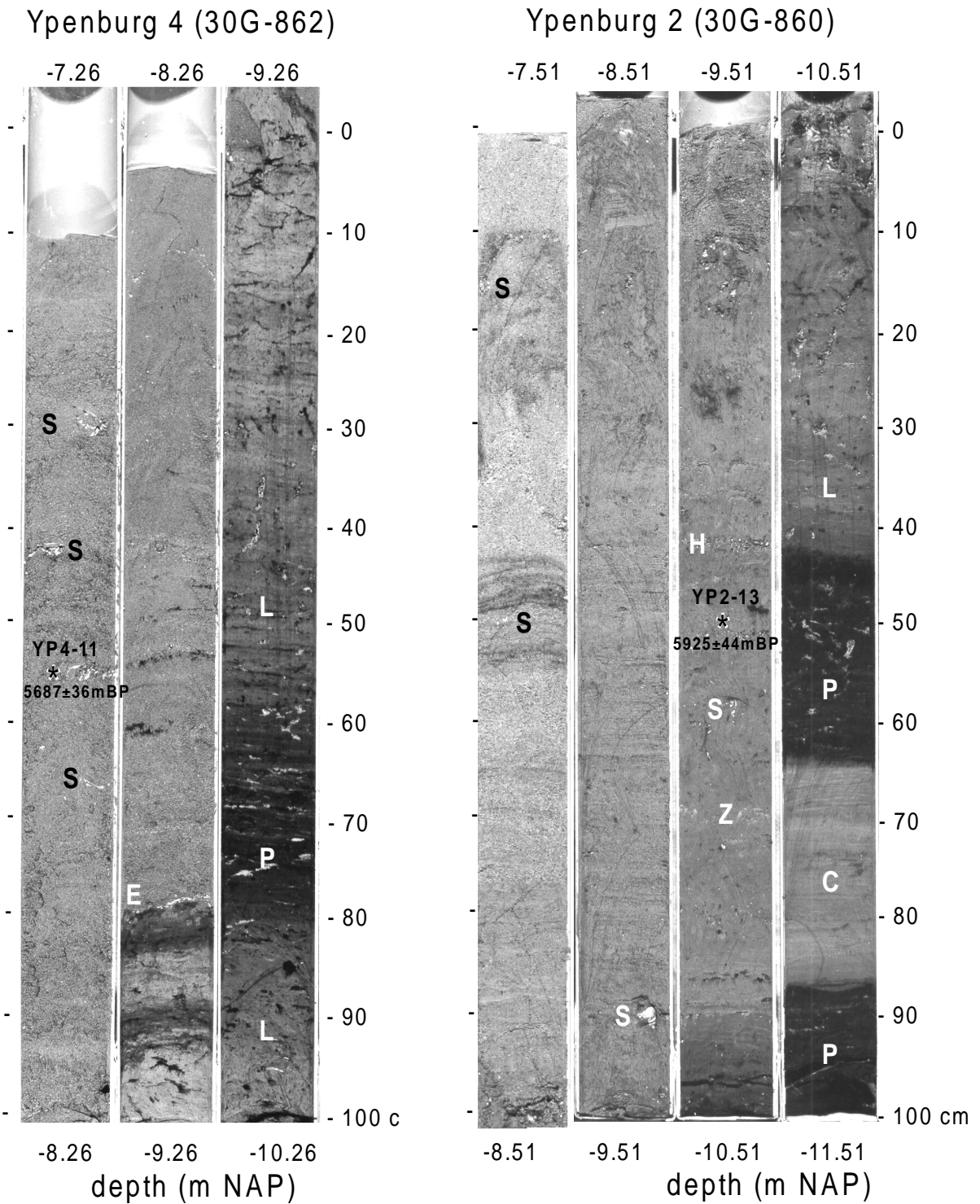


Figure 2.5 (left): Photograph of core Ypenburg 2 (30G-860), -11.51 to -7.51 m NAP. The basal 55 cm of the sequence consists of peat (P), with an intercalated clay layer of 20 cm thick (C). The intercalated clay layer likely develop below a floating-peat bed in a tide-influenced back-barrier setting. The overlying even-laminated clay has a high organic content and contains roots (L). These are the ‘Older Holocene deposits’. From -10.41 m NAP upwards the sand content increases, small patches of bioturbated sand are visible (Z) and several *Hydrobia* layers (H) and *Scrobicularia* shells (S) occur. The increase in sand content continues in the overlying two metres, and eventually results in muddy sand beds, with remnants of even lamination. These beds are thought to represent distal wash-over deposits.

This bar on the western edge of the area was likely deposited as a wave-built beach bar. The variation in dip was caused by the shift in water level due to tides, by changes in the wave intensity (cf. Beets *et al.*, 1981).

Dates from the ridge deposits are not available, but the observation that the toes of the ridges continue into horizontal bioturbated-sand-mud laminations suggest the age of the ridge is equal to the age of these deposits, i.e., younger than 5358 ± 43 (m) BP (YP 2-19), see below.

Beach-plain deposits

A repetition of horizontal sand and clay layers is found in the southwestern half of the area, from the western boundary to the small dunes in the centre of the area (Figure 2.2). The deposits consist of even horizontal sand-mud laminations, with an increase in sand content from base to top, associated with a decrease in bioturbation (Figure 2.9, base of B, C and D). Locally cross lamination, low-angle cross beds and beds with shells and shell fragments are found. The toes of the sets of the low-angle cross beds of the western ridge continue into sand-mud lamination. To the east the deposits grade into root-bearing sand-mud laminations. The beach-plain deposits overlie proximal washover deposits. The thickness of the interval is about 1.5 m. The deposits are absent in the small channels that dissect the area. In contrast to the distal washover deposits the amount of mud in the deposited is limited, the bioturbation is less intense, shells are rare, and roots are hardly present in the deposits

The even sand-clay laminations were deposited on a tidal flat. The upward decrease in bioturbation, associated with the upward increase in sand content, probably represent a change from inter- to supra-tidal setting. The cross beds, shells and shells fragments represent spring-tide and storm-surge deposition. The tidal flat deposits originate from the lee side of the ridge at the western boundary of the area (Figure 2.2 and 2.3). An inter- to supra-tidal flat behind a beach ridge is usually referred to as a beach-plain, and hence, the evens and-mud laminations are interpreted to be beach-plain deposits.

The beach-plain deposits are younger than the underlying proximal and distal washover deposits ($< \text{than } 5358 \pm 43$ (m) BP, YP 2-19).

Marshes

The southwestern half of Ypenburg, from small dunes in the middle of the area to the eastern edge (Figure 2.2) consists of root-bearing sand-mud laminations (Figure 2.9 D). The sand layers have a crinkled appearance and are up to 1 cm thick. The intermittent mud laminae have similar thickness. Shells are absent. The top of the interval undulates 50 cm over distances of 25 to 50 m, and the higher lying parts are somewhat sandier than the lower ones. The root-bearing sand-mud laminations overly distal washover deposits. The transition from distal washover deposits into marsh deposits is gradual, the thickness of the sand beds decreases and the root abundance increases. The thickness of the marsh deposits is about 1.5 m. Locally deposits from small creeks dissect the sand-mud laminations.

Figure 2.6 (previous page, right): Photograph of core Ypenburg 4 (30G-862) from -10.26 to -7.26 m NAP. The lower half of the section (from -10.26 to -9.06 m NAP) consists of even-laminated root-bearing clay (L) with a high organic content and a peat layer (P). These are the ‘Older Holocene deposits’, deposited in a fresh-water environment. The upper half of the section from -9.06 to -7.26 m NAP consists of fine sand with bi-directional cross lamination. Some small shell-layers occur in this interval, the shells are mainly from *Hydrobia ulvae*. A shell layer separates the sandy deposits from the clays below (E). The fine sands have been deposited in small tidal channels, the shell layer is a channel lag. *Scrobicularia* shells (S) are abundant at the top of the interval.

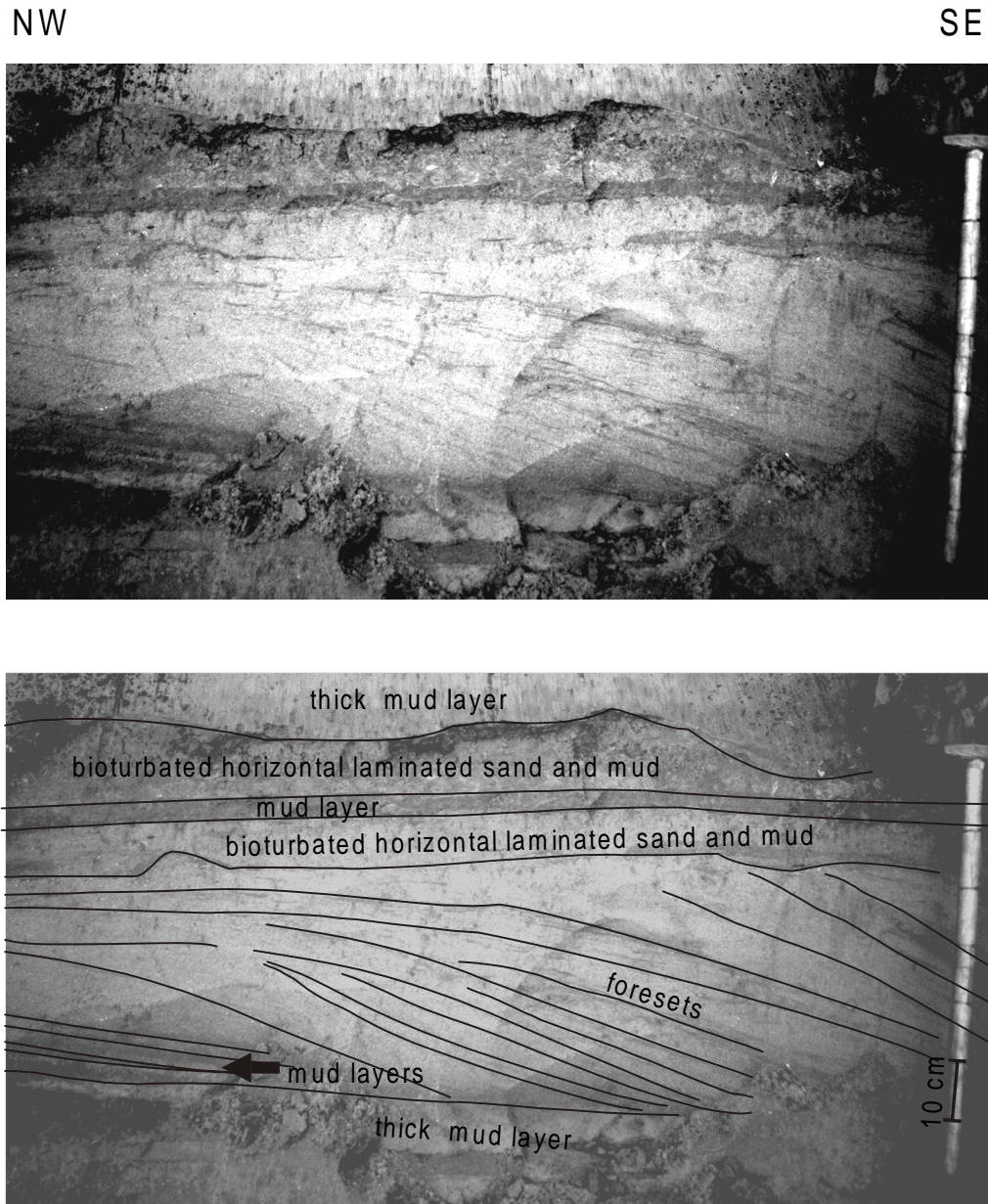


Figure 2.7 (wash-over lobe): Photograph of section in trench, view direction is to the north-east. Markers on the spade handle indicate 10 cm intervals. The washover lobes are characterised high-angle convex up crossbeds, often with distinct aggrading and prograding sets with partly preserved topsets, by limited sorting, and by thick shell layers on the toes of the sets. The occurrence of massive clay layers indicates that deposition took place under sub-aqueous conditions.

The abundance of roots and the absence of shells point to deposition in a supra-tidal vegetated environment, i.e., a salt marsh. The undulations were probably inherited from the underlying washover deposits.

In the area of root-bearing sand-mud laminations an elongated sand body of about 300 m long and 100 wide occurs (location of sample 226A, figure 2.2). The height of the top of the sand body decreases towards the south, from about -3.0 m to -4.0 m NAP, along with an increase in width. A similar elongated sand body is found in the southernmost corner of the

area. The lower part of the sand body is characterised by low-angle cross-bedding, with shells and shell fragments. The sets dip to the east. The highest parts are capped with aeolian deposits. These elongated sand-bodies were probably deposited as washover sand bodies within the marsh environment.

A date from the marsh deposits gives an age of 5432 ± 40 (m) BP (YP 4-15, figure 2.3). The age of a shell from the elongated sand body within the marsh deposits is 5474 ± 35 (m) BP (YPT 226A, figure 2.2).

Dunes

The transition of tidal sand flat to marsh deposits is delineated by a number of small aeolian dunes (Figure 2.2 and 2.9). In the upper northern corner of the study area another small dune is found. The dunes consist of well-sorted yellow sand with soils and occasionally clear swaley cross-bedding and erosion surfaces. The toes of the dunes contain mud lamination and flasers (Figure 2.9A). All dunes contain mud layers that are continuous throughout the dune, with small channel-like incisions (Figure 2.9). Traces of Neolithic inhabitation are found in some dunes and range from a burial site with well preserved skeletons to waterholes and shaft marks. The largest of the dunes has a length of about 1 km and a width of 150 m. The other dunes are much smaller (up to 250 m long). Some dunes overlie beach-plain and marsh deposits (Figure 2.9), while others were deposited directly on top of proximal washover deposits.

The well sorted sand, the distinct yellow colour, the soils and the swaley cross-bedding all point to deposition as aeolian dunes, above the mean high-water level. The abundance of traces of human inhabitation supports a position above the mean high-water level. The mud flasers and layers at the toe of the dunes suggest that the dune toes were flooded regularly. The mud layers that are found throughout the dunes suggest that the whole dune was occasionally flooded, probably during extreme storms. The south-dipping orientation of the mud layers indicates the dunes prograded to the south.

Small (10 to 25 m wide) tidal channels separate the dunes (Figure 2.2). The limited size of the channels hinders (precise) mapping and the lateral continuation of the channels from their position in the trenches is not well known. The small channels have similar characteristics as the tidal channels outlined below. The channels continue into marsh deposits, but their lateral extent is not known. Within the marsh deposits small creek incisions (up to 2 m wide, 0.5 m deep) are found, but a connection to the small tidal channels has not been observed.

Ages of underlying washover, marsh and beach-plain deposits suggest that dune formation started after 5358 ± 43 (m) BP (YP 2-19).

2.4.2 Sequence in the northeastern half of Ypenburg

The base of the sequence in the northeastern half of Ypenburg is similar to the base in the southwestern half and consists of Pleistocene and Older Holocene deposits (Figure 2.1 A). Incised into and on top of these basal deposits a complex pattern of deposits is found (Figure 2.1 A and 2.4). The top 3 meters of this sequence was exposed in trenches and consisted of a lateral alternation of channel fills of up to 200 m wide, with intermittent sandy deposits that displayed cross-bedding or horizontal-laminated bedding, also of about 200 m wide. In at least one case a channel incised and cross cut these sandy deposits. In map view the deposits presents a pattern of elongated sand bodies with intermittent lows that consist of channel fills (Figure 2.2).

SE

NW

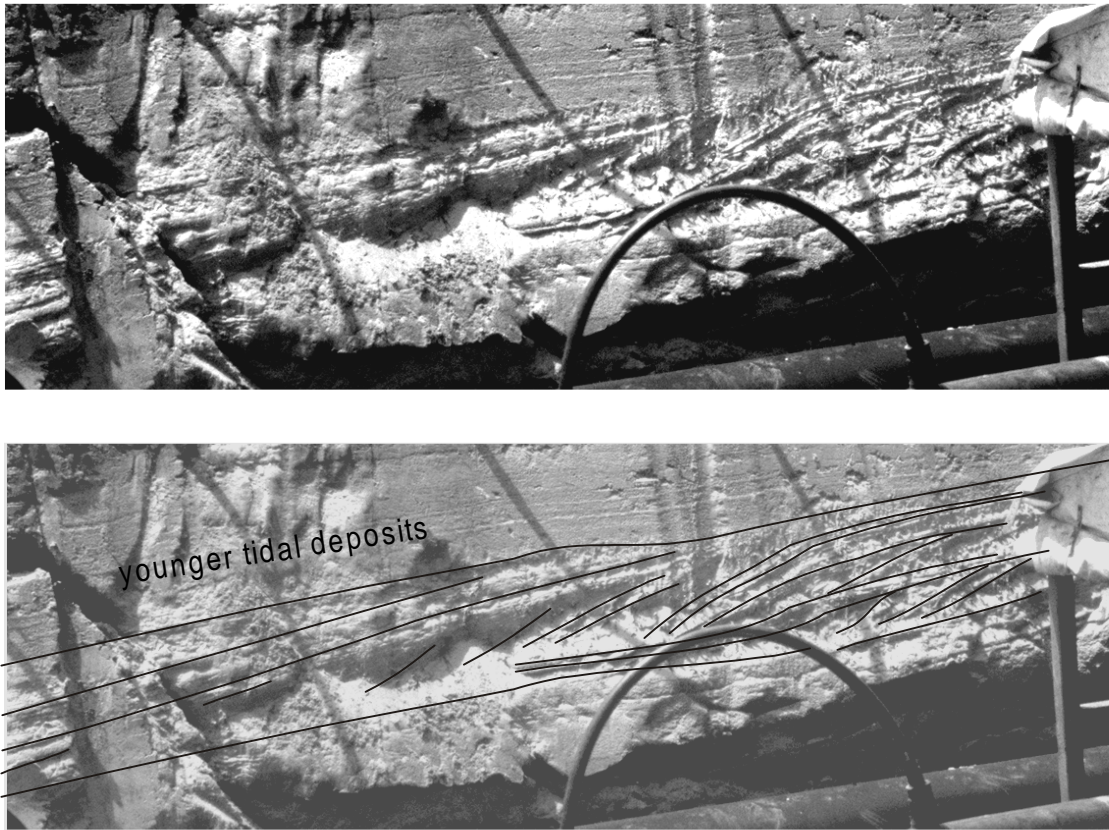


Figure 2.8 (ridge, in beach plain area): Shallow section in trench in the southwestern half of the area. View direction is to the southwest. Low-angle cross bedding, with varying dip angles and plane beds. Height of the cross-bedded interval is about 40 cm.

Tidal-channel deposits

Alternating sand-mud bedding in channel incisions is found throughout the Ypenburg area. The widest extent and thickest accumulation of the sand-mud laminations is found in the northeastern half of the area (Figure 2.2). In the CPT's sand-mud alternations are represented by rapidly alternating high and low values of cone resistance (see for example CPT's yp 43 and yp 116 in figure 2.4) and friction parameter. The maximum values of the cone resistance decrease upward, indicating a fining upward in grain size and thinning upward of sand beds. The basal depth of these deposits goes down to -25 m NAP in a small west-east trending stretch, but usually it varies around -12 m NAP.

In the upper 5 m of the subsurface sand-mud bedding is found in small channel incisions (Figure 2.10). The small channels have a distinct divergent fill, the bedding wedges out to both flanks of the channel (Figure 2.10). The thickness of the mud beds (up to 20 cm) is generally much greater than the thickness of the sand beds (up to 4 cm). Peat boulders, peat detritus and organic debris are locally abundant at the base of the channels. In one channel perfectly preserved tree leaves were found buried below a mud layer. In a few occasions sandy point-bar deposits, with intercalated clay layers of limited thickness are found within the small channel incisions.

The alternating sand-mud bedding likely originates from deposition in tidal channels. The wide extent of the deposits in the northern half (Figure 2.2) and the deep incision (Figure

2.4) represent a large tidal channel. The channel can be traced eastward from the Ypenburg area for some 12 kilometres (Van der Valk, 1995, Van der Valk, 1996b, De Gans *et al.*, 1998). In the study area small dunes mark the southern and the northern margin of the large tidal channel. The decrease in the maximum cone-resistance values from base to top likely represents the usual fining-upward trend of channel deposits.

The sand-mud alternations, from the small channel incisions in the upper 5 m of the area also point to tide-influenced deposition. The divergent channel-wide deposition is very unlikely in tidal channels that develop under conditions of normal daily-tidal currents. The divergent fill suggests that channel incision occurred during abnormal conditions, and that under normal conditions the cross-sectional area was much too wide for its tidal volume (cf. Eysink, 1979, Eysink, 1990, for equilibrium between tidal volume and cross section of channels in the modern Wadden Sea). Storm conditions with a strong water-level set-up are the most likely candidates for channel incision. The incision resulted directly from the storm set-up or from the return flow when storm-conditions ceased. The sandy point-bar deposits in some of the channels suggest that some of the small channels developed under normal semi-daily tidal conditions.

No dates are available from the deeply incised tidal channel. It is not unlikely that the deep incision silted up before the widespread incision down to -12 m NAP started. The age of the wide tidal channel incision and deposition down to around -12 m is also not dated. The depth of -12 m NAP of the base of the channels corresponds to the sea level around 6800 BP. The deposits originate from a subtidal environment, so the tidal channel is younger than 6800 BP. The base of the incised tidal channel must at least be as old as the age of the elongated sand bodies that overly it. Dates from the elongated sand bodies range from 5281 ± 38 (m) BP (YPT 239A) to 5007 ± 39 (m) BP (YPT 271E, figure 2.2). After the wide tidal channel incision started to silt up and deposition of the elongated sand bodies began, small tidal channels remained between the sand bodies. In addition new small tidal channels incised and filled up. The age of the small tidal channels is available from one date on a tree leaf (5019 ± 39 BP, YPT19A, figure 2.2). One small channel, with an age of the 5007 ± 39 (m) BP (YPT 271E, figure 2.2), crosscuts an elongated sand body.

Tidal-flat deposits

Bioturbated horizontal-laminated sandy to muddy deposits are found associated with the tidal-channel deposits in the northeastern half of the area (Figure 2.2 and 2.4). The deposits occur in at least three elongated bodies that border and overly tidal-channel deposits. The beds are slightly inclined to the northwest and change from sandy to muddy. The sandy deposits contain thin mud layers that are partly bioturbated (Figure 2.11). The muddy deposits have been bioturbated completely and contain *Scrobicularia plana* doublets in living position. The lower part of the sequence consists of cross-laminated sand with abundant flasers and mud layers.

The sandy to muddy bioturbated deposits have all characteristics of tidal-flat deposits, repeated deposition alternated with quiet periods. The presence of *Scrobicularia* shells also indicates a tidal-flat environment. Deposition occurred on shoals, situated along and within the tidal channel. The sandy deposits originate from exposed channel banks and the muddy deposits from more sheltered intertidal flats. The cross-lamination originates from deposition by tidal currents on tidal flats or in small channels. The absence of wave-formed structures (wave-ripple lamination, ridge and runnel systems) suggests that the area of deposition was sheltered from intense wave action.

Two in-situ *Scrobicularia plana* doublets have been dated, one from the muddy deposits (5078 ± 37 (m) BP, YPT-271C) and one from the sandy deposits (5080 ± 37 BP, YPT-271B).

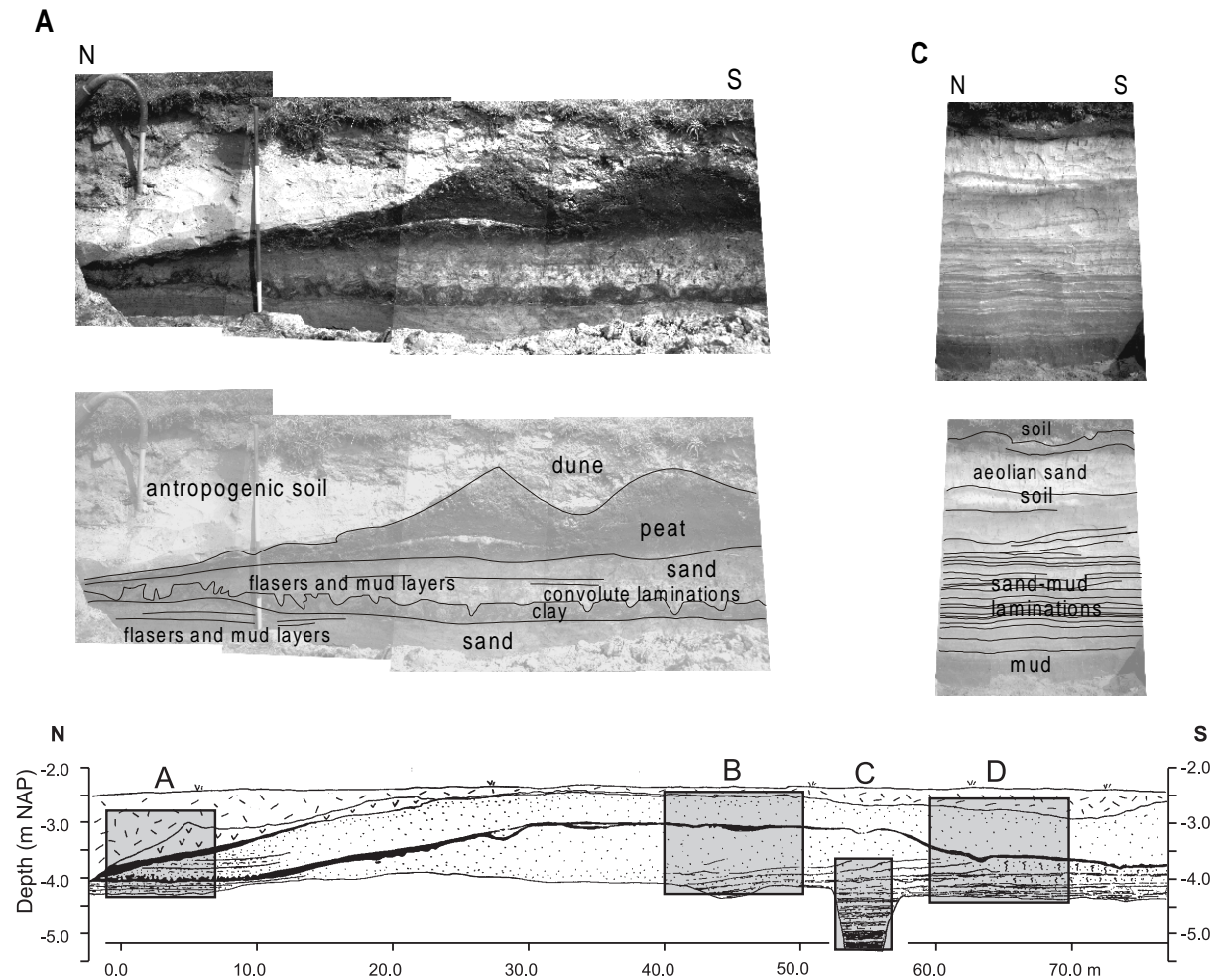


Figure 2.9 (beach plain and aeolian dune): Continued on following page.

Ridge and runnel deposits.

Cross-bedded sand with few mud layers and shells are found in elongated sand bodies bordering and overlying the tidal channel deposits in the northeastern half of the area (Figure 2.2 and 2.4). These elongated sand bodies are found amidst the elongated sand bodies that consist of bioturbated horizontal-laminated sandy to muddy deposits (Figure 2.2 and 2.4). The sand bodies form slight elevations in the landscape, due to differences in compaction with respect to the surrounding clayey channel deposits. The elongated sand bodies consist of a series of high-angle cross beds, with some troughs (Figure 2.12). The foresets dip predominantly to the southeast and southwest. The cross beds continue for 10 to 20 m, and are overlain by even sand-mud lamination with distinct burrowed levels (Figure 2.12). Wave-ripple lamination, mud flasers and mud layers are locally abundant on sets of the cross beds and in the troughs. Shells are found in stable position (convex-up) on the sets of the cross beds. One trough contains a basal 10 to 20 cm thick bed of wood and peat fragments (Figure 2.12).

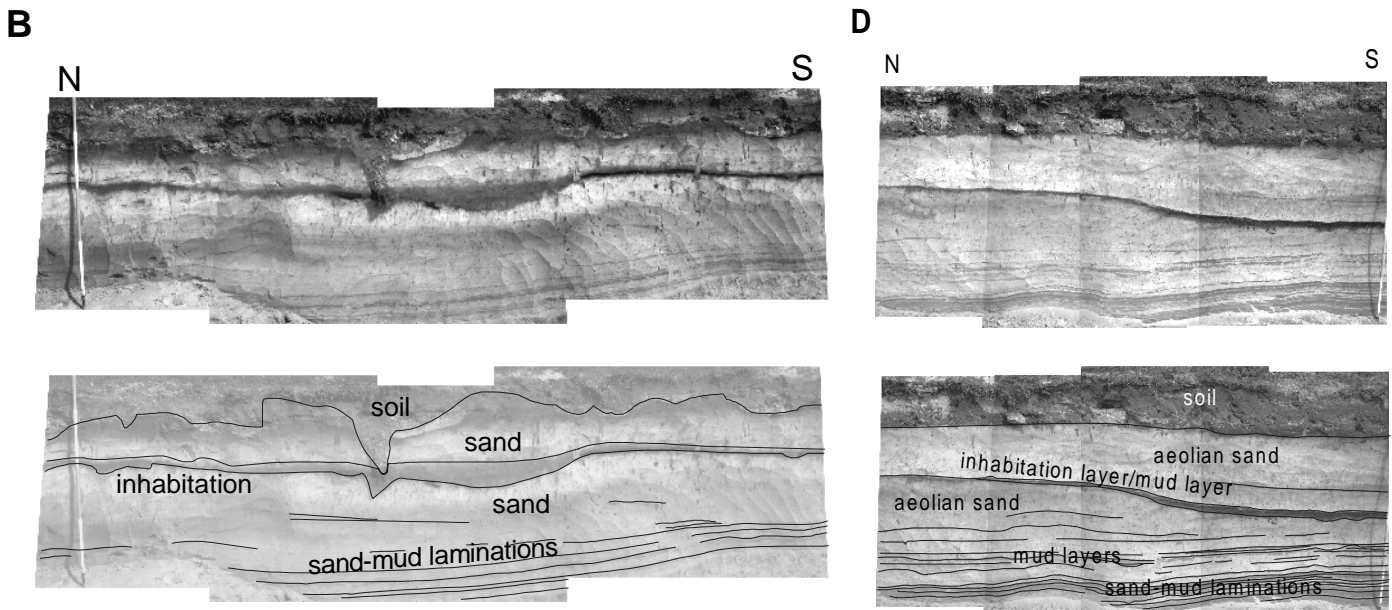


Figure 2.9 (beach plain and aeolian dune): Photo mosaic and sketch of section through the dune. View direction is to the east, the markers at the rods indicates 50 cm intervals. The base of the deposits consists of sand-clay lamination with distinct bioturbation levels. The laminations are more sandy to the top. Occasionally layers with shell fragments and cross lamination occur, which are interpreted as overwash. In the southern part two root-bearing intervals occur, which indicate deposition took place in a supratidal environment. The toes of the dune deposits contain abundant flasers and clay laminations, which indicate the toe was flooded regularly. The black to grey clay layer indicates the dune prograded to the south. In this layer traces of Neolithic inhabitation have been found, ranging from flint arrowheads to waterholes. The top of the dune represents another inhabitation layer.

The deposits deviate from the proximal washover deposits from the southwestern half of the Ypenburg area. The chaotic shells layers and preserved top sets of the proximal washovers are absent in the ridge-and-runnel deposits. The wave ripple lamination, the shells in stable position on the sets and the regular and continuous nature of the cross beds characterise the ridge-and-runnel deposits.

The cross beds in elongated sand bodies were probably deposited as wave-built ridges and the troughs were formed as runnels. The orientation of the foresets indicates that the waves predominantly came from the northwest. The even sand-mud lamination at the top was likely deposited on a sandy intertidal-flat or beach-plain. Such a sequence of cross-bedded sands overlain by even lamination was also observed in the Alkmaar region by Beets and Roep (1981). Despite differences in appearance, the ridge deposits in the southwestern half of Ypenburg (Figure 2.8, see description above, figure 2.2 and 2.3 for location) and the ridge and runnel deposits described here are thought to be of similar wave-built origin. The prevalence of low-angle cross-bedding and the absence of troughs in the ridge deposits (Figure 2.8) is probably related to its development on proximal washover deposits.

Two of the ridge and runnel sand bodies have been dated: one in the middle of the tidal channel area gives an age of 5097 ± 38 (m) BP (YPT-910A), one more to the north gives an age of 5007 ± 39 (m) BP (YPT-271E).

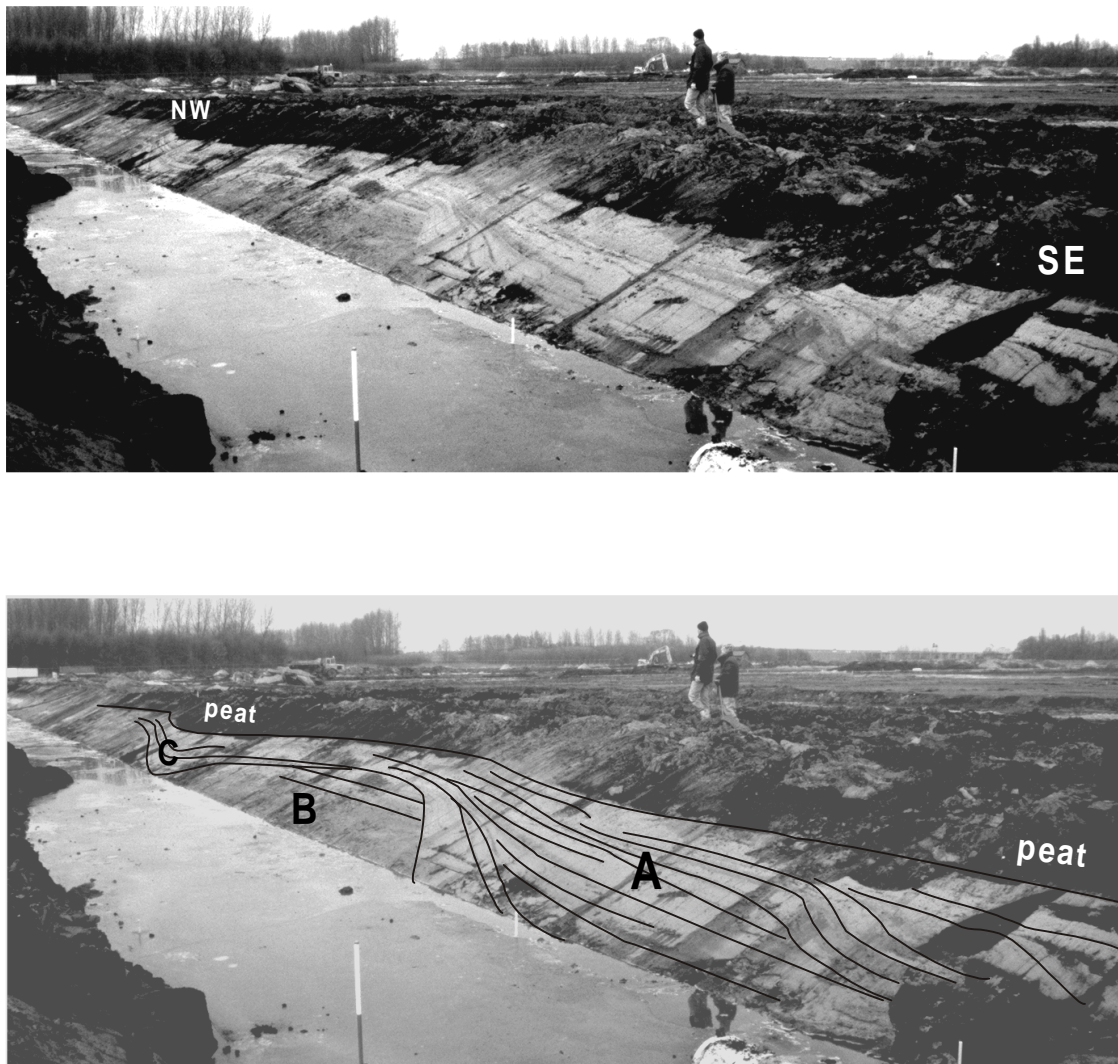


Figure 2.10 (small tidal channels): Photograph of section in trench. View direction is to the north, marker at rod indicates 50 cm interval. Channels (A and C), with an erosive base and a divergent fill of mud-sand bedding. These channels are found in the north-eastern half of the area and crosscut ridge-and-runnel deposits and tidal-flat deposits (B). Channels with similar sizes and characteristics are found throughout the area (figure 2.1). The channels were probably formed during storms. Under normal conditions tidal flow in the channels was limited allowing deposition of mud and hindering its subsequent erosion. The presence of smaller incised channels within the tidal channels (visible in the direct foreground) suggests repeated erosion during storms.

2.4.3 Cover

Younger clay and peat

A clay layer, overlain by a peat layer, is found on top of the older deposits (see for instance figure 2.10 and 2.12) and covers the undulating dune and ridge topography. The clay layer is up to 40 cm thick in the deepest parts of this topography (tidal channels, beach plain and marsh areas) and thin or absent on the higher ridges and dunes. The overlying peat has not been preserved in the entire area. Below an old dike in the southern edge of the area the

thickness of the peat reaches up to 2 m, in the rest of the area it is up to several dm thick at most. The peat contains large tree trunks and abundant roots, especially at the base of the sequence.

Analyses of the diatom content of the clay cover near the Rijswijk A4 pit revealed that initially the depositional environment was marine and gradually changed into brackish to fresh water (De Wolf, 1986b). Eventually peat formation occurred under fresh-water conditions. The change to freshwater condition was induced by increased freshwater input from the posterior peat swamp. The clay originated from ongoing marine incursions. The base of the peat from the vicinity of Ypenburg give ages of 4670 ± 65 to 4400 ± 40 BP (Zagwijn, 1965, De Mulder *et al.*, 1983, in Van der Valk, 1996b).

Younger tidal deposits

The southwestern part of Ypenburg is covered with a meter-thick sequence of horizontal sand-clay laminations. The sand-clay laminations consists of cm-thick sand layers with intercalated mm-thick mud laminae, and are bioturbated and root bearing throughout. The base of this sequence is erosive, part or all of the peat and some of the underlying coastal deposits were removed prior to deposition. At the basal surface brackish water shells (*Cerastoderma glaucum* and *Hydrobia ulvae*) are abundant.

All characteristics point to deposition in a brackish tidal environment. The basal incision points to a channel origin, and the bioturbation and roots point to intertidal flat to supratidal marsh deposition of the sand-mud lamination. The deposits can be traced underneath Rijswijk and Delft and are part of a tidal back-barrier system that developed in response to a marine incursion via the Meuse outlet, near Rotterdam. The age of similar deposits south of the Ypenburg area ranges from 2645 ± 65 to 1725 ± 65 BP (Van Staaldin, 1979).

2.5 Evolution of the Ypenburg area

The basal Holocene sequence is similar in the southwestern and northeastern halves of the area (Figure 2.1) and consists of basal peat overlain by organic-rich laminated clays with peat intervals (Figure 2.5). The sequence is similar to deposits from the vicinity of Delft and has been interpreted as fluvio-lacustrine swamp and estuarine deposits that aggraded in response to sea-level rise (Van Staaldin, 1979). Small tide-influenced channels were part of the depositional system (Figure 2.13A). The deep tidal channel incision in the northeastern half (Figure 2.4) originated as such a small channel. The coastal barrier was located somewhere west of the area.

The shift to marine conditions that is indicated by the increased sand-content and the occurrence of marine shells (Figure 2.5) is the result of the eastward shift of the coastal system with the rising sea level (Figure 2.13B). The transition to more marine conditions occurred around 5900 BP, as indicated by the age of the uppermost Older Holocene deposits and the age of erosion surface at the base of the small-channels deposits. The wide incision of the tidal channel in the northeastern half of Ypenburg probably corresponded with the increase in marine conditions. With the eastward shift of the coastal system, the size of the tidal channel increased, due to the more proximal position of the area to the shoreline, where tidal channels are larger than in the distal reaches of the tidal back-barrier basins. Eventually the shoreline was located at the Ypenburg area, where it reached its most landward position. With the shoreline in the Ypenburg the tidal channel should be regarded as a tidal inlet. The associated tidal-channel system extended eastward for about 12 km (Van der Valk, 1992, 1996b, De Gans *et al.* 1998).

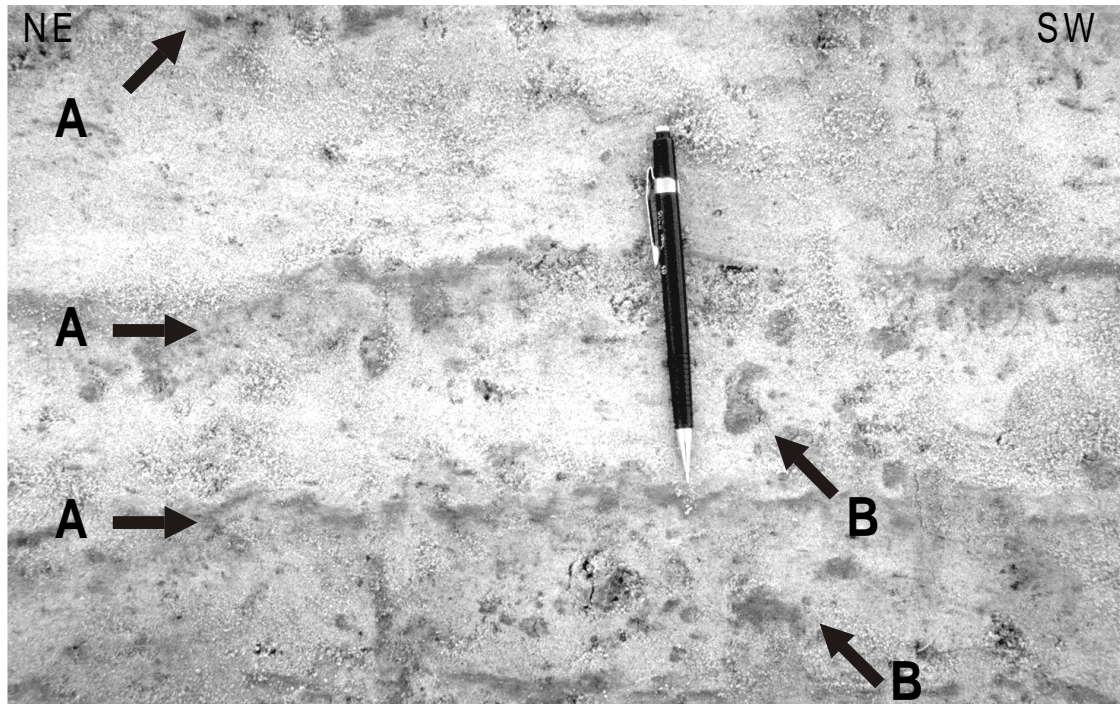


Figure 2.11 (sandy tidal flats): Detail of tidal-sand flat deposits in the northwestern half of the area (pencil is 14 cm). Dark layers (A) are bioturbated mud layers, within predominantly sandy deposits. Individual burrows are found within the sand beds (B).

With the shift to marine conditions, the differentiation of the depositional environments started. The eastward shift of the coastal system in response to the rise in sea level ended when the rate of sea-level rise decreased and the tidal back-barrier basin silted up (Beets *et al.*, 1992, 1994, Beets and Van der Spek, 2000). The silting up of the back-barrier basins also resulted in a decrease of the tidal inlet dimensions. The developments in the northeastern half of Ypenburg are related to the decrease of the inlet dimensions. In the southwestern half of Ypenburg the local developments are related to the coastal retreat, the halt of coastal retreat and the onset of progradation. The developments in the two areas will be discussed separately, followed by a discussion of the relation between the two areas.

2.5.1 Southwestern area

Small channels and erosion

Small-channel deposits (Figure 2.6) erosively overlie the Older Holocene deposits. The age of the Older Holocene deposits (~5900 BP) and the age of the shells at the erosion surface (5800 BP and 5600 BP) suggest that the erosion occurred shortly after deposition of the Older Holocene deposits. Although the age of the erosion surface itself may be younger than the age of the transported shells suggests, the age of overlying washover deposits (~ 5500 BP) demonstrates that the erosion period cannot represent more than 400 years. The sea level of 5800 BP to 5500 BP ranged from about -7 m to -6 m NAP. The base of the small channel deposits ranges from -9 to -8 m NAP, suggesting deposition in very shallow channels. Wave influence is not observed in the channel deposits. A sheltered position behind a barrier is thus envisaged. The abundance of small channels decreases in eastward direction (Figure 2.3).

The small channels were part of the transgressive barrier morphology (Figure 2.13B), and likely evolved in response to local flooding via washovers during storms. The decrease in abundance to the east supports an origin associated with the transgressive coastal barrier west of the area. The absence of subsurface information west of Ypenburg hinders a more detailed reconstruction of barrier location and morphology.

Washover deposition

The washover deposits become more distal to the southeast. The proximal washovers were deposited directly at the back of the barrier (as their name suggests: ‘washed over the barrier’, and breached through the barrier). The foresets indicate deposition from the west, northwest and north, so from the North Sea and from the remnant of the tidal inlet. The proximal washovers are stacked, and the presence of small-incised channels indicates repeated erosion, followed by deposition.

With respect to the underlying small-channel deposits and Older Holocene deposits, the proximal-washovers deposits represent a more seaward depositional environment. The transition to washover sequence is thus transgressive (Figure 2.13C). The age of the uppermost washover deposits is high in the southeast and is relatively low in the northwest. The age decrease to the northwest demonstrates progradation of the washover deposits. In other words, the basal transition to the washover deposits represents transgression, the uppermost part of the washover sequence shows coastal progradation had started, and hence, the sequence of washover deposits represents the stage of transition. The thickness of the washover deposits (about 5 m, figure 2.3) shows that during the stage of transition the coastal system aggraded (Figure 2.13C and D).

Washover deposition continued from at least 5500 BP to at least 5360 BP. As the top of the westernmost proximal washover deposits has not been dated, it can not be excluded that deposition continued longer. If we assume that deposition lasted from 5500 BP to 5200 BP, the sedimentation rate of the proximal washover deposits (with a thickness of about 5 m, figure 2.3) was about 2.5 m/100 years. The deposition rate of the distal washover deposits was slightly lower: 3 m deposited from 5700 BP to 5450 BP (in YP4, 30G-862) gives a sedimentation rate of 1.2 m/100 years. The rate of sedimentation clearly outpaced the rate of sea-level rise during the period of deposition (0.6 m/100y).

Initial washover deposition was sub-aqueous, i.e., storm set up resulted in an elevated water level in the area behind the coastal barrier. The aggradation of the washover deposits resulted in a progressively higher substrate for washover deposition and hence, water depth during deposition was increasingly lower, until sub-aerial deposition occurred (Figure 2.13C and D).

The sediments for washover deposition originated from the palaeo-North Sea and the remnant of the tidal inlet. The nature of the barrier over which washover deposition occurred is not known. The barrier likely formed by the combination of daily wave action and washover deposition. Limited surface knowledge of the area directly west of Ypenburg hinders the recognition of such a barrier, but no surface elevations that may mark such a barrier (like the younger beach ridges) have been observed. Alternatively, all traces of such a barrier may have been eroded altogether during in the course of coastal evolution.

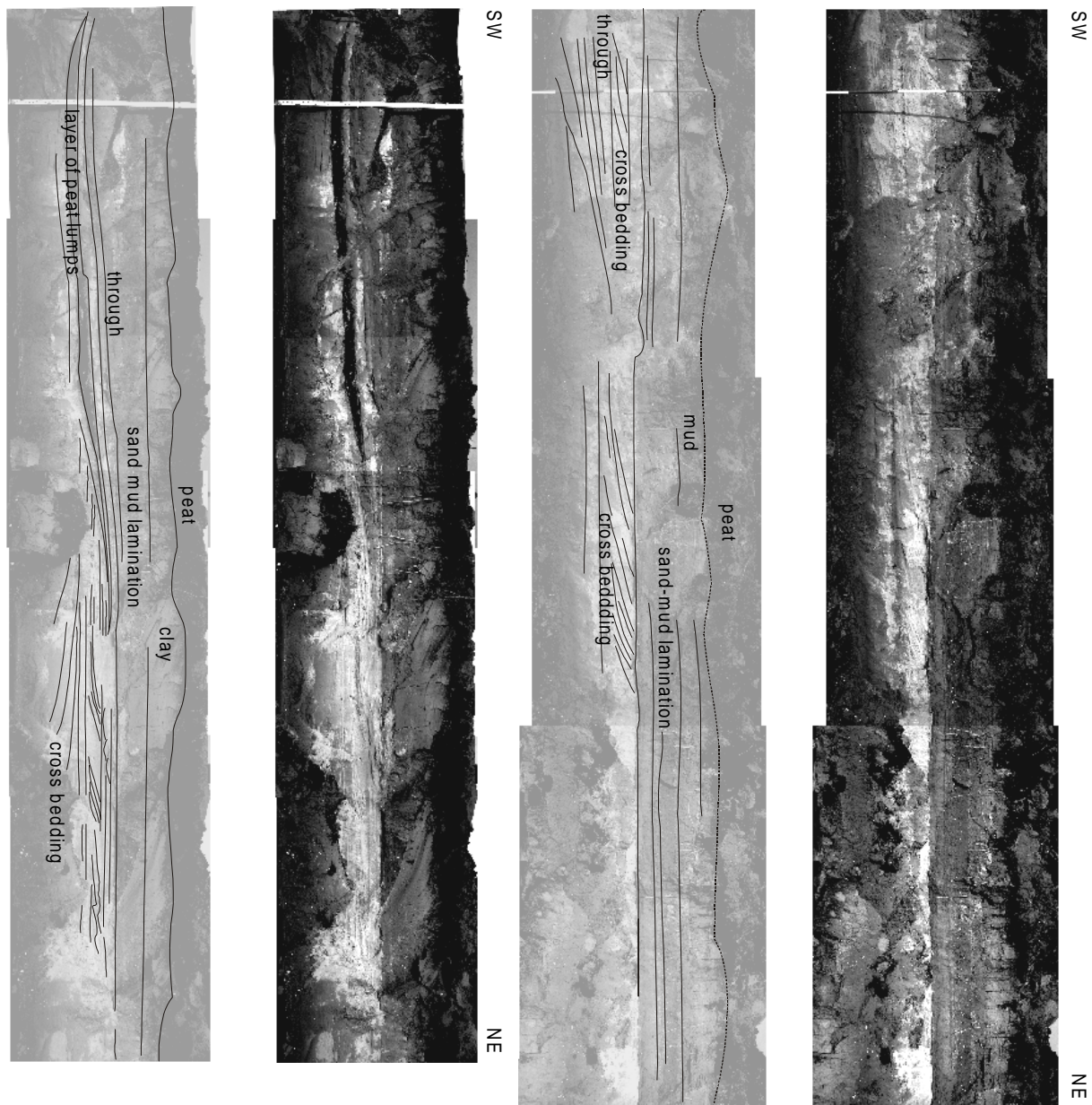


Figure 2.12 (ridge and runnel, the left panel is a continuation of the right panel): Section in trench, in the northern half of the area, view direction is to the northwest. Markers at rod indicate 50 cm intervals. Clear high- and low-angle cross bedding, wave-ripple lamination, and small erosive channels, with to the top even lamination with clay layers and bioturbated intervals. All shells are found in a convex-up position on the sets. All characteristics of the deposits point to up building by wave action in ridges and runnels. The ridge-and-runnel deposits form a spit-like bar along the tidal-channel flank.

Beach ridge, beach plain marsh and dunes.

The deposits overlying the washover deposits have the largest spatial variability (Figure 2.1B). The proximal to distal trend of the underlying washover deposits can be recognised in the distribution of the facies: marsh deposits overly distal washover deposits, ridge deposits and dunes overly proximal washover deposits, and beach-plain deposits are found in between (Figure 2.1B). The ridge deposits continue landward into beach-plain deposits of similar age.

The marsh deposits are found laterally continuous of the beach-plain deposits and are therefore of similar age (Figure 2.9). The dunes overlie beach-plain and marsh deposits and thus are younger. The channels that dissect the beach plain and separate the dunes have a fill of 5019 ± 35 BP (YPT-19A, figure 2.2) and are younger than the beach-plain deposits.

The beach-plain deposits originate from an intertidal to supratidal flat on which deposition occurred during spring flood and storms. In a sense, this can be regarded as distal washover deposition as well. However, the sand-mud-lamination is more regularly spaced, indicating a more frequent and structured depositional environment. The depositional environment misses the pulsated supply of large amount of sediment followed by relatively long quiet periods. Overall, the transition of washover deposition to the overlying deposits represents a change from chaotic high-energy storm deposition to more tranquil and structured deposition. Storms still resulted in high water levels and higher rates of deposition, but signs of high-energy wave reworking are only visible in the ridge deposits on the southwestern boundary of the area (location 2.8 in figure 2.2, figure 2.8). The ridge sheltered the beach plain from direct wave influences (Figure 2.13E).

The western location of the beach ridge can be interpreted as a continuation of coastal progradation, with respect to the underlying washover deposits. Dune formation initiated on slightly elevated parts of the beach plain, the elevation resulting from underlying washover lobes (Figure 2.13E). The beach plain and beach ridge favoured dune formation because it acted as a source of sand. The channels that intersected the beach-plain deposits limited the spatial extent of dunes and prevented the formation of a continuous dune ridge.

Summarising the development in the southwestern half of Ypenburg: in the top of the Older-Holocene deposits marine influences mark the eastward retreat of the coastal barrier to the area. This is followed by erosion by small tidal channels, which were part of the transgressive coastal barrier. This was followed by deposition of washovers from a more seaward position behind the coastal barrier. So far, the sequence of deposition represents transgression. Deposition of the washovers was chaotic, with the repeated incision by small washover channels. Deposition the washovers resulted in a phase of coastal aggradation, which outpaced the rise of sea level, and resulted in the shift from sub-aqueous to sub-aerial washover deposition. The ages of the uppermost washover deposits show a westward shift of deposition, marking the onset of coastal progradation. After the chaotic deposition of the washovers a more structured coastal morphology developed, similar to younger prograded coastal deposits from the western Netherlands, with beach-ridge, beach-plain and marsh. Eventually dune formation commenced on the slight elevations formed by washover lobes.

2.5.2 Northeastern area

In the development of the southwestern area we may infer three stages of channel evolution. The first stage is related to the deep channel incision. It is likely that the ancestor of this channel was present as a tide-influenced channel from the onset of deposition of the Older Holocene deposits (Figure 2.13A). The small tide-influenced channel present within Older Holocene deposits in the southeastern half of the area shows that such channels existed during early stages of Holocene deposition. The second stage of the channel evolution is related to the channel incision throughout the northeastern half of the area down to about -12 m NAP (Figure 2.4). The final stage of the evolution of the northeastern area is related to the deposition of the elongated sand bodies in the remnant of the tidal channel, and the development of small tidal channels in between and cross cutting them (Figure 2.13F).

The second stage of channel evolution, the wide erosion down to -12 m, determines the widespread occurrence of channel deposits. This stage is not well dated, its depth

precludes deposition prior to 6800 BP. The stage likely represents the retreat of the coastal barrier to its most landward position, as a consequence of sea-level rise. With the retreat of the coastal barrier the tidal inlet shifted landward to the Ypenburg area. The tidal channels associated with the tidal inlet extended some 12 km to the east (Van der Valk, 1992, 1996b, De Gans *et al.* 1998). Please notice that the palaeo water depth of the tidal channel during this stage was about up to -7.5 m at most (assuming an age up to 5000 (m) BP). This is very limited compared to other Holocene tidal-channel incisions (see amongst others: Westerhoff *et al.*, 1987, and Chapter 3, Van der Valk, 1996a), and it also small compared to modern Wadden Sea inlets (see for instance Eysink, 1990).

The lack of age control on the tidal channel incision makes it difficult to correlate this stage of channel evolution to the deposition in the southwestern half. As it is likely that this stage of channel expansion was associated with coastal retreat, channel widening probably was concurrent with the transgressive deposition. So, channel widening occurred along with the increase in sand and marine shells in the Older Holocene deposits, along with erosion by and deposition in small channels, or along with the first deposition of washovers (Figure 2.13 B,C and D). The age of the ridge-and-runnel and tidal flat deposits overlying the tidal channel suggest that at least a remnant of the tidal inlet was still (temporarily) exposed to waves after washover deposition had occurred.

The final stage of the channel evolution is related to the deposition of the elongated sand bodies with intermittent small tidal channels. In map view the elongate sand bodies appear like re-curved spits (Figure 2.2), although it is unclear whether or how the sand bodies are connected to the landward margins of the channel. The deposits that make up the sand bodies differ distinctly. The tidal-flat deposits (Figure 2.11) originate from a sheltered tidal environment, and the ridge-and-runnel deposits (Figure 2.12) originate from a wave-influenced environment. The predominantly southeast to southwest dip of the sets in the ridge deposits (Figure 2.12) indicates that the waves approached the ridges from the north. The age of the tidal-flat and ridge-and-runnel deposits is similar and the deposits must have evolved adjacent to each other. A likely scenario is that the ridge-and-runnel deposits have sheltered the area at their back from direct wave influences. In the sheltered area tidal-flat deposition occurred. On top of the ridge-and-runnel deposits sand-mud laminations, identical to the beach-plain deposits are present (Figure 2.12). These deposits likely represent the stage where the ridge-runnel sand body is not exposed to direct wave-influences anymore, probably because a new sand body has evolved seaward of it.

The dates from the northeastern area are younger to the northeast, from 5300 BP at the channel margin to 5000 BP for the most northeastern ridge-and-runnel sand body (see dates in figure 2.2.). The ridge-and-runnel deposits developed as spits from the southwestern margin of the tidal-channel area and protected the area behind them. The spits evolved as series of separate units, with small tidal channels in the lows in between. In the protected channel area behind the spits tidal flats evolved (Figure 2.13 E and F). The morphology is comparable to barrier spits described by Hine (1979), although the intermittent lows did not develop as marshes but kept their tidal-channel characteristics. Crosscutting of the ridges by small tidal channels indicates that during extreme storm conditions the set-up resulted in severe erosion. The abundance of mud in the channels (Figure 2.10) suggest that quiet conditions prevailed. Tidal currents in the channels were never sufficiently strong to erode the mud. Only during storms erosion within the channels and of new channels occurred.

The likely scenario for the development of the elongated sand bodies with the intermittent small tidal channels is that the area, which had evolved into a relatively wide tidal inlet gradual decreased in cross-sectional area and eventually closed. The abundance of mud deposition in the tidal channels (Figure 2.10), indicates that the tidal-inlet was not subject to

strong tidal currents anymore. The abundance of mud is also apparent from the decrease of the cone-resistance values in cross section F-F', which indicating a fining upward of the tidal-channel deposits (Figure 2.4, for instance YP 116, YP 47 and YP 119). It is likely that prior to the deposition of the elongated sand bodies the tidal-inlet already was reduced in importance. The northeastern half of Ypenburg therefore was a remnant tidal inlet during the final stages of deposition in the area. The deposition of the re-curved spits progressively filled in the remnant of the inlet. The abundance of sediment just south of the inlet, evident from thick stack of washover deposits, further enhanced deposition of the elongated sand bodies, by longshore sediment transport.

Alternatively, the channel has migrated laterally to the north, associated with the continuous deposition of elongated sand bodies. The location of the channel has changed, but the channel-cross section has remained largely similar. Although this type of evolution can not be ruled out on basis of the ages of the deposits, it is not very likely, given our understanding of the regional large-scale coastal evolution. It is especially hard to correlate such a constant tidal channel size with the complete end of tidal-channel deposition when progradation of the Rijswijk-Voorburg beach ridge started. Also, the abundance of mud in the tidal channel deposits suggest that the tidal currents had a limited strength, which is difficult to associate with channel migration

2.5.3 Relation between the northeastern and southwestern areas

The transgressive sequence in the southwestern half is likely related to the incision of the tidal channel in the northeastern half. The ages from the elongated sand bodies all post-date the ages of the washover deposits. In other words, during the stage of transition from transgression to progradation, closure of the tidal-inlet channel had not yet begun. However, the fining upward inferred from the CPT's suggests increasingly quieter depositional conditions during the evolution of the inlet. The evolution of the elongated sand bodies must have occurred synchronous with the deposition of the beach-ridge, beach-plain and marshes. The similarity in appearance of the beach-ridge deposits from the southwestern boundary of Ypenburg (location 2.8 in figure 2.2 and figure 2.8) and the ridge-and-runnel deposits from the northeastern half (Figure 2.2 and 2.12) suggest deposition under similar conditions. This also holds for the occurrence of sand-mud laminations in the beach-plain deposits, on top of the ridge-and-runnel deposits in the tidal-sand flat deposits. So, the end of the exposure of the remnant of the tidal-inlet channel to waves took from 5300 until at least 5000 BP. The end of exposure to waves started only after progradation had already begun around 5400 BP in the southwestern half of the area. The remnant of the tidal inlet must have been closed of completely for waves and storm surges when the Rijswijk-Voorburg beach ridge formed over the entire coastal stretch fronting the Ypenburg area, around 5000 to 4750 BP (Roep *et al.*, 1983).

The similarity in age of the small tidal channels in the southwestern half of the area (~5000 BP, YPT-19A) with the ridge-and-runnel deposits in the upper northeast (~5000 BP, YPT-271E) demonstrates deposition in small tidal channels occurred in the entire area at that time (Figure 2.13F). The formation of the small tidal channels in the northeastern part of Ypenburg was probably enhanced by the low-lying nature of that stretch. The activity in the small tidal channels was storm induced and did not represent frequent tidal action, as is evident from the clay-rich divergent fills (Figure 2.10). Probably storm set-up resulted in a temporarily larger tidal volume in the remnant of the tidal back-barrier basin.

Eventually the entire area of the former tidal channel was cut off from tidal and storm influences, with the deposition of sand in front of the entire area (tidal-channel deposits overlain by prograded coastal deposits in the northern corner of the area, figure 2.2). The

deposition of this sand marked the onset of progradation in this area. We have no dates from these deposits. Hereafter progradation continued over the entire northwestern boundary of Ypenburg and led to the development of the Rijswijk-Voorburg beach ridge, between 5000 and 4750 BP (Roep *et al.*, 1983).

2.5.4 Cover

The deposition of clay over all but the highest points of the area indicates that eventually quiet conditions prevailed. The quiet conditions resulted from the development of the Rijswijk-Voorburg beach ridge, which sheltered the beach-plain area behind it, including the area Ypenburg. Flooding of the Ypenburg area, and with it the delivery of the clay, occurred over the prograded beach-plain and beach ridge deposits and from the fluvial outlets of the Old Rhine River to the north and the Meuse River to the south.

The change to freshwater conditions was probably related to stagnant conditions and freshwater runoff from the peat east of the area. Eventually a vegetation cover developed, which resulted in the formation of a thick peat layer (at least 3 m). The younger tidal deposits in the southwestern edge of the area can be traced from underneath the cities of Rijswijk and Delft to the former outlet of the Rhine and Meuse (Figure 1.2). The tidal-channel system (“The Gantel”) evolved as a consequence of ingressions through Meuse and Rhine Outlet, south of Ypenburg.

Figure 2.13 (Following page): Reconstruction of depositional environments at Ypenburg. The visible boundaries of the two large reconstructions A and F have similar orientations as cross sections E-E’ (the short side) and F-F’ (the long side).

Figure 2.13 A (Basal deposition): During the Early and Middle Holocene sedimentation of organic-rich clays and the formation of peat occurred in a fluvio-lacustrine to estuarine environment. The deeply incised part of the tidal in the northeastern half of the area was probably active as a tidally influenced channel. Reconstruction after Van der Woude (1981).

Figure 2.13 B (Basal erosion and small channels): Small-channel deposits erode into the Older Holocene deposits in the southwestern half of the area. More to the east erosion by the small channels was restricted and localised. Adjacent to the channels bioturbated sandy mud was deposited on tidal flats. Our knowledge of the evolution of the tidal channel during this period is limited, hence the limited display of the northeastern half in the reconstruction.

The evolution from the fluvio-lacustrine environment of the Early and Middle Holocene to the tidal flat environment resulted from the transgression of the coastal barrier towards the Ypenburg area. The erosion by the small channels represents a further stage in the transgression, with a position of the shoreline close to the area.

Figure 2.13 C (Washover deposition): On top of the small channels washovers were deposited. Under storm conditions, proximal washovers were deposited in the western half of the area, and distal washovers are deposited to the east. The proximal washovers, i.e., the washover fans or lobes were deposited sub-aqueous, due to the storm set-up of the water level. With respect to previous reconstruction the washovers represent deposition directly behind the shoreline, and therefore represents further transgression.

Figure 2.13 D (Washover deposition): A stack of proximal washover fans was deposited in the northwestern half of the area. Because the sedimentation rate exceeded the rate of sea-level rise, deposition resulted in aggradation above MSL. The sedimentation rate of the distal washover deposits was much lower and little changed in the southeastern half of the area.

Figure 2.13 E (Beach ridge, beach plain, marsh and ridge-and-runnel deposition): After deposition of the washover a more organised depositional system evolved, with a beach-ridge in the west, a beach-plain and marshes in the east. The small channels that dissect the beach-plain are remainders of the underlying deposits, as are slight undulations in the surface that covers the washover lobes. The undulations form the cores for dune formation. Along the tidal channel an elongated sand body with a re-curved spit-like appearance evolved, by deposition of ridges and runnels.

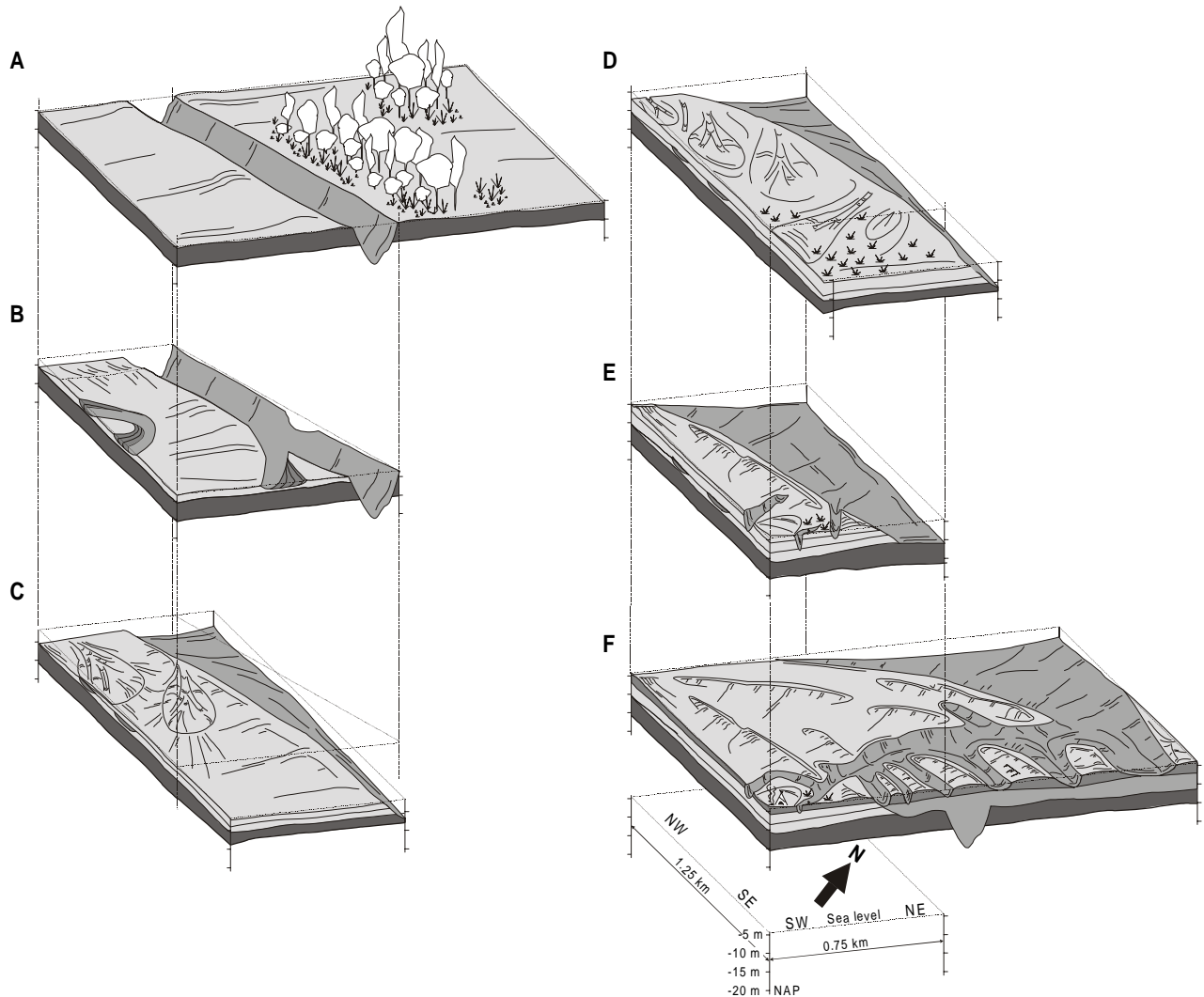


Figure 2.13 F (Beach ridge, beach plain, marsh and ridge-and-runnel deposition): After deposition of the oldest spit-like ridge-and-runnel system a number of re-curved elongated sand bodies with similar characteristics evolved. In the areas between the sand-bodies small tidal channels remained active and deposition on tidal flats occurred. During storms small channels breached the ridges. Eventually the development of the sand bodies completely closed the tidal channel and channel activity ended. During the evolution of the spits, little happened in the southwestern half of the area.

2.6 Discussion

The transition from transgression to progradation occurred around 5400 BP. The prograded deposits at Ypenburg are older than early prograded deposits at Haarlem (Van der Valk, 1996a) and Alkmaar (De Mulder and Bosch, 1982, Westerhoff *et al.*, 1987, Beets *et al.*, 1996b). Thus, they are the oldest prograded coastal deposits in the Western Netherlands. In addition to the differences in age there are differences in depositional sequences. Certain facies are only recognised in the Ypenburg area (washover deposits, tidal channels with divergent fills), while certain facies do occur in other areas as well, but with a different morphology (e.g. small patch-like dunes).

2.6.1 Facies

Washovers

Washover deposits make up a large part of the sequence at Ypenburg. Distal washover deposits, consisting of parallel beds of up to 30 cm thick, sometimes with abundant shells fragments, have been found within beach-plain sequences of prograded deposits in the Western Netherlands (Roep *et al.*, 1983, Van Someren, 1988, Van der Valk, 1996a). A single large washover fan from the transgressive coastal deposits near Haarlem is presented in a palaeo reconstruction of the area (Van der Valk, 1996a). Descriptions of proximal washovers lobes from transgressive deposits of the Western Netherlands have not been found. The limited recognition of Holocene washover deposits is striking, considering observations of modern transgressive coasts, where overwash during storms plays an important role in coastal deposition (Schwartz, 1982, Reinson, 1984, Elliot, 1986, Dean, 1991, Reinson, 1992). Although washovers may be a common feature of modern transgressive coastal systems, the preservation potential of washovers in a transgressive setting is limited. During storms the shoreface and beach are eroded and sediment is funnelled into the back barrier. During following storms the washovers that have previously been deposited and make up the barrier, are cannibalised: the sediment is re-used to form new washovers in a more landward position. The chances of preservation of washover deposits on a retreating coast thus are limited. The preservation potential is much larger when transgression stops, and progradation starts, as occurred in the Ypenburg area.

In addition to the limited preservation potential that limits the abundance of proximal washover deposits, these deposits may not have been recognised as such. Van der Valk (1996b, figure 12 and 13), in his study of coastal deposits in the Rijswijk excavation, presents two figures of ridge-and-runnel deposits where we suggest a washover origin. The convex-up foresets, the delta-like aggradation and progradation, the abundance of very chaotic shell layers at the toe sets and the limited number of reactivation and erosion surfaces are all comparable to the proximal washover deposits in the Ypenburg area. The exposure studied by Van der Valk (1996b) was located about one kilometre south of Ypenburg, and the deposits are found in a similar height interval as the washover deposits. The recognition of washover deposits in cores is difficult because the deposits may easily be confused with other marine facies.

Tidal channels with divergent fills

Tidal channels with divergent fills i.e., layers that thin towards both channel flanks (Figure 2.10), are common throughout the whole Ypenburg area. The channels border and intersect ridge-and-runnel and tidal-flat deposits, and are found within beach-plain deposits, where they separate the small dunes. The channels have been active up to a late stage in the evolution of the area, when most activity in the tidal channel area had already ceased. The channel deposits are very clayey, with clay layers up to 20 cm thick. Occasionally new incisions of smaller, slightly younger channels are observed, which in turn have a divergent fill (in foreground of figure 2.10). To our knowledge such deposits have not been described from Western Netherlands coastal deposits. The genesis of these channels is probably storm-related, with incision of the channels during storm set-up, or during the return flow after storm set-up in the back barrier. The former tidal channel may have funnelled much of the storm set-up into the area. This could explain why these channels have not been observed in the nearby Rijswijk A4 pit (Van der Valk, 1996b).

The patchy distribution of small dunes

The dunes in the area are small, both in height and in extent. This dune morphology deviates from the linear and continuous dunes on top of younger prograded deposits to the west. The

limited lateral extent of the Ypenburg dunes is related to their initiation points and to the confinement by small tidal channels. The initiation points for dune formation were small elevations, formed by previously deposited washover lobes. The dunes inherited the confined geometry of the washover lobes. The abundance of small tidal channels in the area of dune formation limited dune growth to the stretches in between the channels. Dunes on younger prograded deposits developed on beach ridges with an elongated alongshore geometry (similar to the ridge deposits, figure 2.8) and were not hindered by the presence of tidal channels.

2.6.2 The transgressive barrier

One kilometre south of the Ypenburg area along the direction of the palaeo shoreline (indicated by the beach ridge of Rijswijk-Voorburg) the lateral equivalent of the Ypenburg sequence has been exposed in a large construction pit (the Rijswijk-A4 temporary exposure Van der Valk, 1996b). The age of the shells from the deposits range from 5350 ± 80 to 5610 ± 70 (Van der Valk, 1996b). These ages are not corrected for $\delta^{13}\text{C}$ and marine reservoir effect, but since these effects even out ages are comparable to our (m) BP ages (cf. Mook, 1991). The ages of the deposits are comparable to the ages of the washover deposits in the Ypenburg area. Above we have already discussed the nature of cross-bedded sands from the Rijswijk A4 pit, which are best interpreted as washover fans. On basis of the similarity in age and sedimentary characteristics can be concluded that the transitional stage of washover deposition stretch at least one kilometre south of Ypenburg. Limited subsurface data further south of the Rijswijk-A4 pit hinders the reconstruction of the extent of this type of deposition.

The deep excavation of the Rijswijk-A4 pit allowed a more extensive study of the deposits below the stack of washovers. In the Ypenburg area these deposits (the small channels deposits) have only been observed in cores. In the Rijswijk A4 pit the deposits from the similar height interval (from -7 to -9 m NAP) consist of plane beds, low angle to through cross-bedded sands, some with escape structures of *Macoma balthica*, flasers, and minor bioturbation (figures 7 and 9 in Van der Valk, 1996b). Through-cross-bedding, escape structures and plane bedding point to strong wave influences during deposition. The sedimentary structures are well comparable to those observed in sub-tidal pools and lower tidal flats of the Hudson Bay, Canada (Martini, 1991). In the Hudson Bay, the deposits have a wave-dominated character, despite their macro-tidal setting. A similar situation is envisaged for the Rijswijk A4 deposits: deposition took place on a strongly wave-influenced sub-tidal flat. Indications for the presence of small tidal channels, as is evident from the basal shell lag and the bi-directional cross lamination in the cores from Ypenburg, are absent in the deposits of the Rijswijk A4 pit.

The basal deposits from the Rijswijk-A4 pit and the Ypenburg thus suggest that during the final stage of transgression, the coastal morphology consisted of a strongly wave-influenced sub-tidal flat, with adjacent small tidal channels that were sheltered from direct wave-influences. The nature of the shoreface morphology can only be guessed at.

With the end of transgression the deposition of washovers started. The deposition of the washover is only possible with a coastal barrier over which storm-driven set up is funnelled. As discussed above, the barrier itself probably consisted of washover deposits, which were remoulded by fair-weather waves. The barrier was easily overtopped, as is evident from the stack of washover lobes and washover channels, and probably was of limited height and extent. The size and morphology of this proto-barrier should not be compared to the beach-ridge deposits (with foredunes) of the younger prograded coast.

The change from chaotic washover deposition to a more 'normal' structured coastal environment is partly related to morphological changes of the shoreface, more seaward of the

area. Changes in shoreface geometry alter the direction and impact of wave and storm action. The shoreface was located west of Ypenburg, and its nature must be hypothesised, as subsurface data from that area is absent and it is likely that its evolution was (at least in part) erosive. It is likely that a decrease in the rate of coastal retreat allows for more reworking on the shoreface and a complete halt of transgression gives an even larger period for reworking. So, the effect of the transition to progradation is probably reworking and deepening of the shoreface. Any irregularities on the shoreface, which resulted in wave refraction, will have been smoothed out in the course of reworking.

2.7 Conclusions

The location of the study area, at the boundary of transgressive back-barrier deposits and prograded shoreface and beach deposits enables the study of deposits from the final stages of transgression, and the initial stages of coastal progradation.

In the southwestern half of the study area washover, beach-plain, dune and marsh deposits are found. The deposits from the area are dominated by proximal to distal trends to the southeast. The northeastern half of the study area is dominated by wide erosion by a tidal channel, overlain by tidal-channel, ridge-and-runnel and tidal flat deposits. In mapview the west-east orientation of the ridge-and-runnel and tidal flat deposits in elongate sand bodies is distinct. The orientation is parallel to the orientation of the tidal channel.

The transgressive sequence consists of progressively marine-influenced intertidal-flat deposits, deposits from small tidal channels, associated with an erosion surface, and washover deposits. The end of coastal retreat resulted in a stack of washover deposits. The washovers aggraded, and evolved from sub-aqueous to sub-aerial, because their sedimentation rate outpaced the rate of sea-level rise. While transgression and aggradation dominated the southwestern half of the area, a small tidal inlet formed in the northeastern half.

As progradation continued a more 'normal' coastal system evolved, that consisted of a beach-ridge, beach-plain and marsh. This was associated with the development of small aeolian dunes. During this stage activity in the tidal-inlet channel ceased and eventually the tidal-inlet channel was progressively sheltered from wave action, by the deposition of elongate sand bodies. Part of these sand bodies evolved as re-curved spits from the southwest. Small tidal channels remained present between the elongate sand bodies, and new small channels were eroded during storms.

Eventually deposition in remnant of the tidal inlet ceased, and deposition in the small tidal channels ended. Progradation started over the entire stretch northwest of Ypenburg and led to the deposition of the continuous Rijswijk-Voorburg beach ridge. In the Ypenburg area itself clay was deposited. Finally the area developed into a swamp where peat formation started

Appendix A (following page): AMS ¹⁴C-dates from the Ypenburg area.

Sample	trenches	depth	shell species	shell position	Age	Age (marine corrected)	Calibrated age	C14 lab	
	date	(m) NAP							Carbon years BP
YPT271B	27-jan-98	-5,70	<i>Scrobicularia plana</i>	in situ, doublet	periostracum, ligament	5482 ± 37 BP	5080 ± 37 BP	5900 - 5846 BP	9903
YPT271C	27-jan-98	-6,40	<i>Scrobicularia plana</i>	in situ, doublet	periostracum, ligament	5480 ± 37 BP	5078 ± 37 BP	5899 - 5844 BP	9904
YPT271E	27-jan-98	-5,70	<i>Spisula subtruncata</i>	transported, single	leached, some periostracum	5409 ± 39 BP	5007 ± 39 BP	5851 - 5720 BP	9905
YpenburgC2	19-mei-98	-5,59	<i>Scrobicularia plana</i>	in situ, doublet	periostracum	5840 ± 50 BP	5438 ± 50 BP	6290 - 6197 BP	7638
YPT19A	1-sep-98	-5,50	<i>Plant leave</i>	transported	birch, oak, maple, ash	5019 ± 39 BP	5019 ± 39 BP	5882-5827 & 5752-5711 & 5668-5663 BP	9907
YPT239A	23-sep-98	-5,00	<i>Spisula subtruncata</i>	transported, doublet	periostracum, ligament	5683 ± 38 BP	5281 ± 38 BP	6161 - 5997 BP	9902
YPT910A	9-okt-98	-4,40	<i>Scrobicularia plana</i>	doublet, niet in situ	fragmenten ,periostracum	5499 ± 38 BP	5097 ± 38 BP	5909 - 5860 BP	9901
YPT226A	22-jun-99	-4,20	<i>Scrobicularia plana</i>	transported, single, leached		5876 ± 35 BP	5474 ± 35 BP	6303 - 6265 BP	9906
	core number								
YP1-1	30G-859	-8,95	<i>Macoma balthica</i>	transported, single	some periostracum, ligament	6004 ± 44 BP	5602 ± 44 BP	6456 - 6374 BP	9888
YP1-4	30G-859	-8,28	<i>Macoma balthica</i>	transported, single	some perisotrarium	5924 ± 45 BP	5522 ± 45 BP	6387 - 6282 BP	9889
YP1-5	30G-859	-7,58	<i>Macoma balthica, juv</i>	transported, single	fragments, blue	5854 ± 47 BP	5452 ± 47 BP	6296 - 6232 BP	9890
YP2-11	30G-860	-4,50	<i>Macoma balthica, juv</i>	transported, single		5970 ± 44 BP	5568 ± 44 BP	6416 - 6310 BP	9891
YP2-13	30G-860	-10,00	<i>Scrobicularia plana</i>	in situ, doublet	periostracum, ligament	6327 ± 44 BP	5925 ± 44 BP	6841 - 6722 BP	9892
YP2-19	30G-860	-6,24	<i>Macoma balthica, juv</i>	transported, single		5760 ± 43 BP	5358 ± 43 BP	6233 - 6156 BP	9893
YP3-2	30G-861	-9,35	<i>Scrobicularia plana</i>	transported, single	periostracum, ligament	6205 ± 47 BP	5803 ± 47 BP	6706 - 6601 BP	9894
YP3-3	30G-861	-7,96	<i>Scrobicularia plana</i>	in situ, doublet	periostracum, ligament	5911 ± 37 BP	5509 ± 37 BP	6351 - 6280 BP	9895
YP3-5	30G-861	-7,16	<i>Scrobicularia plana</i>	in situ, doublet	periostracum, ligament	5876 ± 35 BP	5474 ± 35 BP	6303 - 6265 BP	9896
YP3-6	30G-861	-5,95	<i>Scrobicularia plana</i>	in situ, doublet	periostracum	5783 ± 35 BP	5381 ± 35 BP	6255 - 6169 BP	9897
YP3-9	30G-861	-9,45	<i>Scrobicularia plana</i>	in burrow, doublet	perisostracum	6264 ± 37 BP	5862 ± 37 BP	6742 - 6660 BP	9898
YP4-11	30G-862	-7,79	<i>Scrobicularia plana</i>	transported, doublet	periostracum, ligament	6089 ± 36 BP	5687 ± 36 BP	6552 - 6454 BP	9899
YP4-15	30G-862	-5,06	<i>Scrobicularia plana, juv.</i>	transported, doublet	periostracum, ligament	5834 ± 40 BP	5432 ± 40 BP	6282 - 6201 BP	9900

Chapter 3: Holocene coastal evolution in the Western Netherlands (I): Facies.

Abstract

The characteristics and distribution of coastal deposits in two coast-perpendicular cross sections, near Haarlem and Wassenaar, were investigated. The cross sections stretch from the hindmost prograded beach ridge and beach plain onto the modern shoreface. The two cross sections consist of basal Pleistocene deposits and Holocene back-barrier deposits of the transgressive coastal system (Unit 1), overlain by offshore deposits of the transgressive coastal system (Unit 2), followed by deposits of the prograded coastal system (Unit 3).

The lithologic and sedimentary characteristics of coastal deposits in the Haarlem and Wassenaar cross sections are well comparable. Unit 1 consists of Pleistocene sands, remnants of Holocene basal peat and clay and Holocene tidal deposits. The Holocene deposits of Unit 1 are back-barrier sediments formed during transgression. The deposits of Unit 2 overly Unit 1 and are the offshore equivalent of the Holocene transgressive deposits. The transgressive deposits consist of shoreface sands, coarse-grained offshore deposits, and sand-mud laminations. At the landward end of the cross sections the tidal deposits of Unit 1 gradually change into shoreface, breaker bar and beach deposits of Unit 2. The change marks the decrease of tidal influences at the end of the transgression. Unit 3 was formed by the progradation of beach and breaker-bar deposits over shoreface sands. During the beginning of progradation non-deposition dominated the shelf and lowermost shoreface. On the lower shoreface distal storm layers were deposited and from the middle and upper shoreface upward thick proximal storm beds were deposited. During later stages of progradation the deposition of proximal storm layers replaced distal storm layers on the lower shoreface.

3.1 Introduction

Transgressive depositional sequences consist of back-barrier (lagoonal, tidal) deposits overlain by offshore deposits (deposits formed seaward of the shoreline: beach, shoreface, shelf, cf. Kraft and John, 1979, figure 6.10A of Galloway and Hobday, 1983). Holocene transgressive coastal deposits are found on numerous locations around the world, where modern coastlines recede or have been receding. The archetype for prograded coastal deposits is Galveston Island (Gulf of Mexico, Texas, USA: Bernard *et al.*, 1962). The surface morphology of Galveston Island shows a series of parallel beach ridges, separated by lows. In the subsurface Holocene beach and upper shoreface sand is found on top of Holocene lower shoreface silt and mud (Bernard *et al.*, 1962). In other words shallow-water deposits overlie deeper-water deposits, due to progradation of shallow-water over deeper-water environments. ^{14}C dates on shells from the deposits confirm progradation. Combinations of transgressive coastal deposits overlain by prograded coastal deposits are also common in Holocene coastal systems, including examples as the Costa Nayarit (Curry *et al.*, 1969), several barriers in Southeast Australia (Thom, 1983, Roy, 1994, Roy *et al.*, 1994) and the Western Netherlands (Van Straaten, 1965, Roep *et al.*, 1991, Van der Valk, 1992, 1996a).

Van Straaten (1965) presented a cross section through the beach ridges and beach plains in the Western Netherlands near The Hague. In this cross section he recognised a prograded coastal sequence of lower shoreface deposits overlain by upper-shoreface and beach deposits. Dating of peat from the beach plains confirmed coastal progradation (Zagwijn, 1965). Van Straaten (1965) found coarse-grained deposits from an offshore environment below the prograded sequence. He attributed the coarse-grained deposits to shoreface-connected ridges from the previous transgressive coastal system. Underneath the offshore deposits tidal-channel and lacustrine deposits and basal peat were found, which were regarded as transgressive back-barrier deposits.

Van der Valk (1992, 1996a) meticulously described deposits from a coast-perpendicular cross section south of Haarlem. 24 shell samples were carbon dated, and the dates were used to reconstruct shoreface profiles of the prograded coastal system. The sequence of deposits in the Haarlem cross section is comparable to the sequence of the The Hague cross section; tidal-channel deposits at the base, overlain by coarse-grained shoreface deposits, in turn overlain by shoreface and beach deposits. Similar to the interpretation of Van Straaten (1965), Van der Valk (1992, 1996a) attributed the tidal deposits to the transgressive coastal system. He attributed all overlying deposits to the prograded coastal system, and did not recognise transgressive shoreface deposits.

A coast-perpendicular cross section near Wassenaar was described and interpreted in a Ms. thesis (Van Someren, 1988). Reconstructed shoreface profiles based on carbon dates from the Wassenaar cross section were presented by Roep *et al.* (1991). The sequence of deposits and the pattern of reconstructed shoreface profiles is comparable to that of the Haarlem cross section. The age of the deposits is slightly higher in the Wassenaar cross section.

The sequence below the modern shoreface was described and interpreted by Beets *et al.* (1995). It consists of Pleistocene sand, overlain by basal peat or tidal back-barrier deposits, in turn overlain by shoreface deposits with a layer of modern North Sea sand on top. The basal peat and tidal back-barrier deposits originate from the transgressive coastal system, and the overlying shoreface deposits are part of the prograded coastal system. The North Sea sand on top of the sequence resulted from modern reworking and winnowing of fine sediments on the North Sea floor.

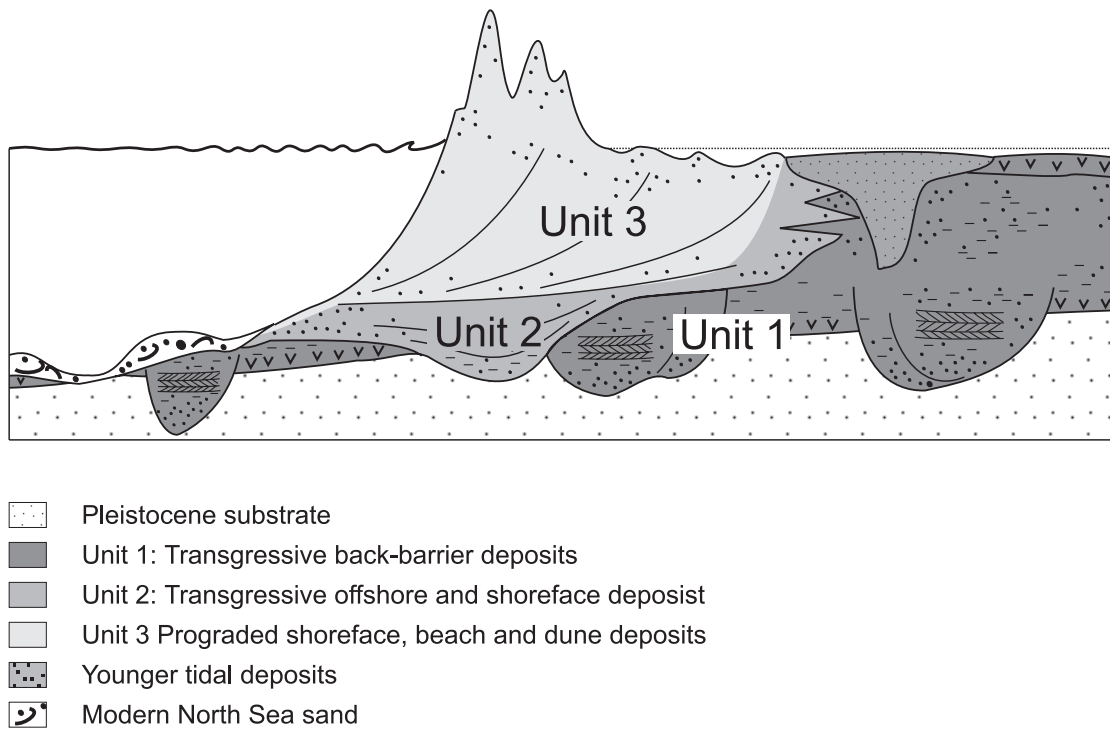


Figure 3.1: Schematic coast-perpendicular cross section, with the Pleistocene basement and the transgressive back-barrier deposits (Unit 1), transgressive offshore deposits (Unit 2) and prograded-shoreface and beach deposits (Unit 3).

The aim of this chapter is to present a comprehensive facies description and model of the coastal barrier and the underlying deposits in the Western Netherlands, in order to refine the model for coastal evolution of the area. The Haarlem and Wassenaar cross sections are reinterpreted, and the cross sections are extended onto the modern lower shoreface. We follow the interpretation of Van Straaten (1965), and distinguish a basal Holocene Unit 1, which consists of tidal back-barrier deposits, an overlying Unit 2, which consists of transgressive shoreface deposits, and a top Unit 3, with prograded shoreface and beach deposits (Figure 3.1). Overlying dune and peat deposits and North Sea sands are not discussed in this study. Unit 1 can be recognised on basis of its sedimentary characteristics and shell content alone. In a part of the cross sections Unit 2 and 3 have different sediment characteristics, while otherwise the distinction is made on basis of the age of the deposits. The age of deposits, based on ^{14}C dates of single shells, is presented and discussed in the next chapter.

3.2 Research Area

In the Western Netherlands, from Monster to Bergen aan Zee (Figure 1.1) Holocene shoreface and beach deposits are found directly landward of the modern coast (Figure 1.2 and 3.2). In map view the deposits are represented by a series of beach ridges and beach plains that extend up to 10 km east of the coastline. The deposits originate from the phases of coastal progradation in the area, that started around 5500 BP in the south near Monster and around 4500 BP in the north near Bergen. The phase of progradation ended around 2000 (earlier in the south Beets *et al.*, 1992). Landward of and underneath the prograded beach and shoreface deposits Holocene tidal deposits are found. The tidal deposits pre-date the prograded deposits and originate from the transgressive coastal system that preceded coastal progradation (Beets *et al.*, 1992, see also Chapter 1). Underneath the modern shoreface, a relative thin sequence of shoreface deposits is found on top of Holocene tidal deposits or on the Pleistocene basement (Beets *et al.*, 1995).

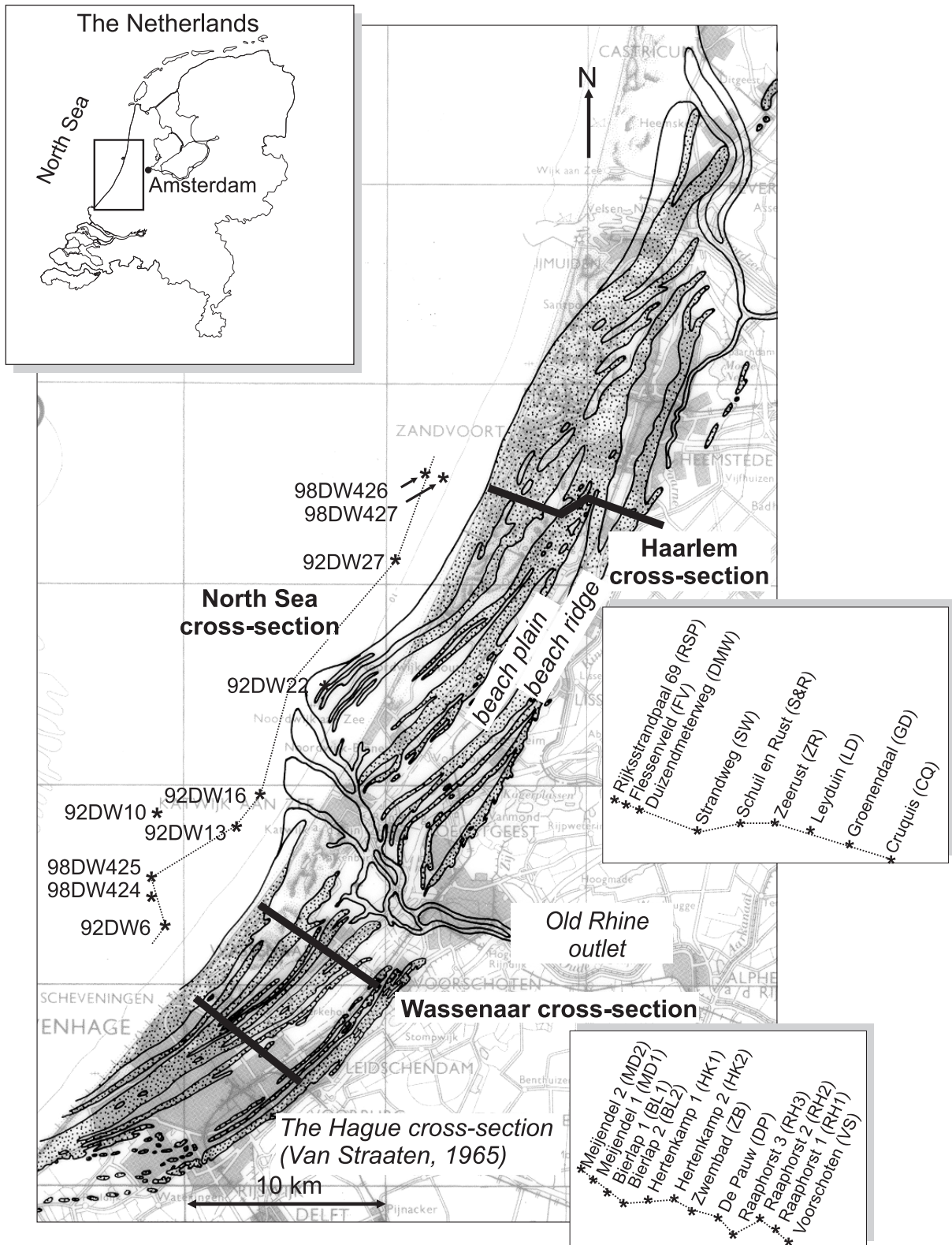


Figure 3.2: Location map, the pattern of beach ridges and beach plains is indicated, as well as the location of the former Rhine Outlet. The reconstructed beach-ridge and beach-plain pattern that extended west of the modern coastline is indicated as well. The Haarlem and Wassaenaar cross sections are indicated (thick lines), as is the The Hague cross section (Van Straaten, 1965), and the offshore cores and cross section (stippled line, see next Chapter). A. Pruijssers compiled the map with the beach-ridge and beach-plain pattern.

The Wassenaar (Van Someren, 1988) and Haarlem (Van der Valk, 1992, 1996a) cross sections are oriented perpendicular to the coast. The Haarlem cross section stretches from the landward edge of the prograded deposits to the shoreline and further onto the modern shoreface (Van der Valk, 1992, 1996a). New vibrocores were collected from the shoreface (Van der Spek *et al.*, 1999). The Wassenaar cross section originally stretched from the most landward prograded deposits to 2 kilometres east of the shoreline (Van Someren, 1988). Between the seaward end of the Wassenaar cross section and the beach two additional cores were collected (Van der Spek *et al.*, 1999). The cross section was further extended to the modern shoreface with three vibracores (Beets *et al.*, 1995, Van der Spek *et al.*, 1999).

The land-based borings consist of series of 1 m long undisturbed cores. The lateral spacing was 0.5 km in the Wassenaar cross section and 1 km in the Haarlem cross section. The offshore cores consist of continuous vibrocores, which are up to 5 m long. Abbreviations of core names are used throughout the text (see figures 2.1, 3.1 and 3.2). Lacquer peels and photographs were used to describe the facies. The shell content and facies of the Wassenaar cross section were described earlier by Van Someren (1988). Van der Valk (1992, Van der Valk, 1996a) presented descriptions of facies, grain size, shell, pollen, diatom and foraminifer content of the Haarlem cross section.

3.3 Units and Facies

3.3.1 Unit 1

Pleistocene sands form the basement for Holocene deposition. The Holocene back-barrier deposits originate from the transgressive coastal system and consist of Basal Peat and Clay and of tidal deposits. The Holocene deposits of Unit 1 are found at depths from -27 to -12 m NAP below. East of the cross sections tidal-channel deposits of Unit 1 are found up to the modern ground surface, at a level of -3 m NAP.

Pleistocene sand

The Pleistocene deposits consist of middle to coarse sand with a distinct light yellow colour and mica flakes. Sedimentary structures consist of low- to high-angle cross-bedding and plane bedding, with abundant reworked shells and shell fragments on the laminae (shells are reworked Eemian and Weichselien species). Some of the top intervals of the Pleistocene deposits are composed of cross-laminated fine sand to silt, in some occasions with peat detritus on the laminae. The cross-bedding, and the absence of mud layers and flasers point to deposition by rivers. These fluvial deposits are of Weichselian age (Doppert *et al.*, 1975).

Basal Peat and Clay

In two cores of the Wassenaar cross section a clayey peat layer overlies the Pleistocene sands. Deposits of this type are absent near Haarlem. The peat is dark-brown to black. It gradually converges upward into laminated and root-bearing clay with a high organic carbon content. The peat and clay form the earliest Holocene deposits, that originated from a gradually drowning landscape (Jelgersma and Pannekoek, 1960, Jelgersma, 1961, Van Straaten, 1965, Beets *et al.*, 1995). The main agent for the drowning was the rising groundwater table, induced by the Holocene rise in sea level. For extensive overviews of Basal Peat characteristics see Jelgersma (1961, 1979) and Van der Plassche (1986).

Tidal deposits

Tidal deposits are characterised by a *Cerastoderma*-shell assemblage that consist of *Cerastoderma edule*, *C. Glaucum*, *Scrobicularia plana*, *Macoma balthica*, *Hydrobia ulvae*, and *Littorina littorae*. The base of the tidal deposits is always erosive. Three types of tidal deposits were recognised on basis of their mud and organic content, bioturbation and

sedimentary structures. The tidal deposits originate from tidal channels (Van Straaten, 1965, Van der Valk, 1992, 1996, Beets *et al.*, 1995) and tidal flats.

Muddy channel deposits

The deposits consist of sand-mud laminations, with crinkle sand laminae. The mud is dark-brown when freshly exposed, owing to its very high organic content. The sand laminae are seldom continuous and are at most some mm thick. Bioturbated intervals with a thickness of at most 40 cm are found, with the remnants of the sand laminae still visible. Deposits of this type are restricted the Wassenaar cross section.

The sand-mud laminations were deposited in a quiet and restricted environment with occasional sand influxes. The sand-mud alternations likely resulted from recurring tidal currents. The *Cerastoderma*-shell assemblage indicates deposition in a tidal back-barrier environment, probably in an estuarine channel. Similar sand-mud laminations have been found near Delft (Van Staaldin, 1979, De Wolf, 1986a) and Leidschendam (Törnqvist *et al.*, in press).

Bioturbated grey sand

Grey sand mixed with mud, with varying traces of bioturbation and remnants of horizontal parallel beds (up to 10 cm thick). Some clusters of tidal shells are attributed to the burrowing activity of the lugwurm, *Arenicola arenaria* (Van Straaten, 1954a, 1964).

The shell content, mud admixture and bioturbation point to deposition in a tidal environment. The thick horizontal parallel beds points to upper-stage plane bed conditions during deposition, while the bioturbation points to relatively quiet periods with intense reworking. Deposition probably occurred in a sub- or inter-tidal flat setting.

Sandy channel deposits

The deposits consist of grey coarse to middle sand with clay layers, clay flakes and flasers (Figure 3.3). Bi-directional cross lamination, cross-bedding and parallel bedding are abundant and bioturbation is absent. The base of the interval is an erosion surface, which is, in some cases, marked by a shell lag or peat boulders. In some cores thick shell layers are abundant. In some cores the tidal-channel deposits are characterised by a distinct fining-upward sequence, while in others the top of the deposits is coarser than the lower parts.

The occurrence of bi-directional cross-bedding, flasers and clay layers, as well as the shell assemblage all point to deposition in large tidal channels (Van Straaten, 1965, Van der Valk, 1992, 1996, Beets *et al.*, 1995). The tidal channels incised deep into the underlying Pleistocene deposits.

3.3.2 Unit 2

The deposits of Unit 2 were formed seaward of the shoreline. Most deposits of Unit 2 originate from the North Sea shelf and from the shoreface. Only in the most landward cores (core GD in the Haarlem cross section and VS and in the Wassenaar cross section) breaker-bar and beach deposits are found. The characteristics of the breaker bar and beach deposits are described together with Unit 3, where the majority of such deposits is found. Unit 2 was deposited as part of the transgressive coastal system. The deposits in the most landward cores GD and VS represent the transition to coastal progradation. Unit 2 is found at depths from -20 m NAP up to the modern ground surface. The depth of occurrence and the thickness of Unit 2 decreases landward.

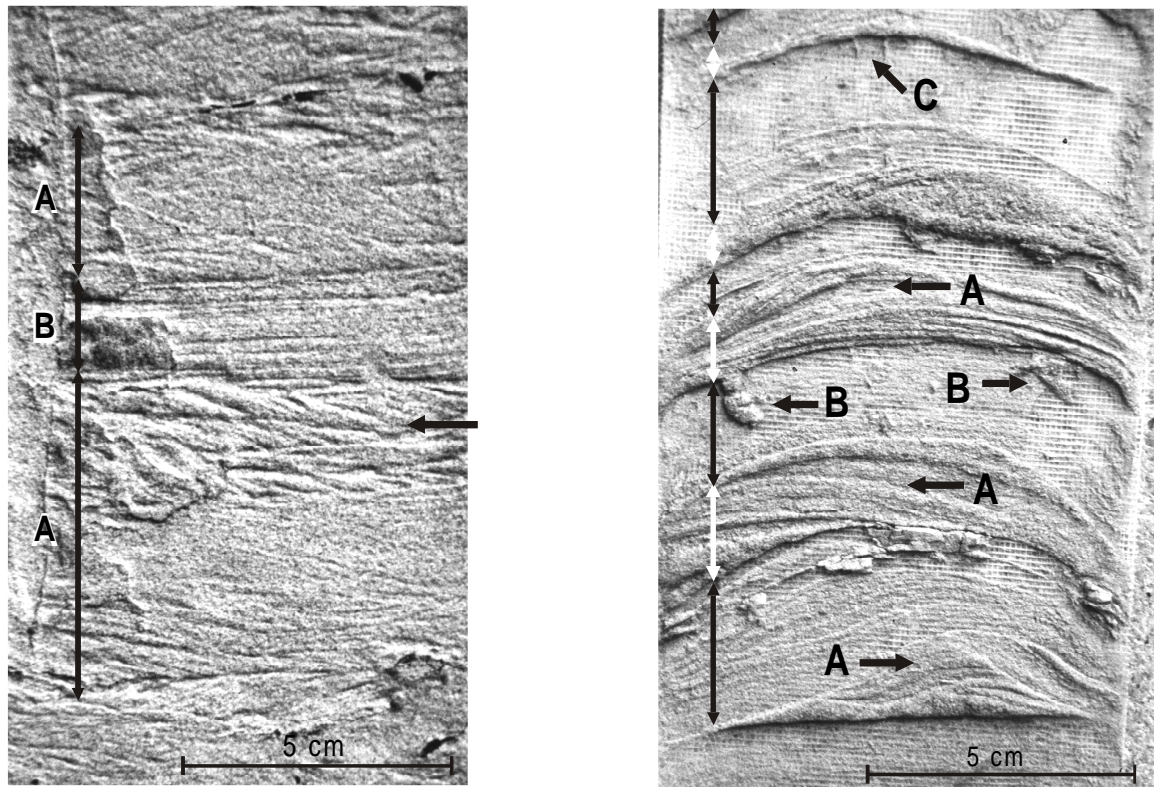


Figure 3.3 (left): Tidal-channel deposits of Unit 1 in core SW in the Haarlem cross section with ripple lamination (A) and horizontal lamination (B) (SW: -17.90 to -17.72 m NAP).

Figure 3.4 (right): Sand-mud laminations from Unit 2 in the core SW of the Haarlem cross section. Sand layers (white intervals) with wave-ripple lamination (A) intercalated with mud layers (black intervals). Small burrows (B and C) penetrate the mud layers from the sand layers above. (SW: -17.01 to 16.91 m NAP).

Sand-Mud laminations

Sand-mud laminations in ZR, SR and LD and in the Wassenaar cores consist of thin (up to 1 cm thick) silt to fine-grained sand laminae with inter-bedded clay laminae of similar thickness. Within some coarse-grained laminae faint wave-ripple lamination is visible, and some of the bounding surfaces of the laminae have a wavy geometry (wavelength up to 10 cm). A very limited amount of shells and shell fragments is found. The most abundant species is *Spisula subtruncata*. The sand-mud laminations in FV, DMW, and SW consist of fine- to middle-sand layers, up to 5 cm thick, alternating with mud intervals of similar thickness (Figure 3.4). Within the sand layers, parallel bedding and wave-ripple lamination is clearly visible. Shells and shell fragments are abundant (mainly juvenile *Spisula subtruncata*, some doublets) and are usually found in convex-up position on the laminae. Furthermore rubble shell beds without preferred orientations of the shells occur. All cores display a distinct coarsening-upward trend, the sand layers thicken and the mud layers thin to the top.

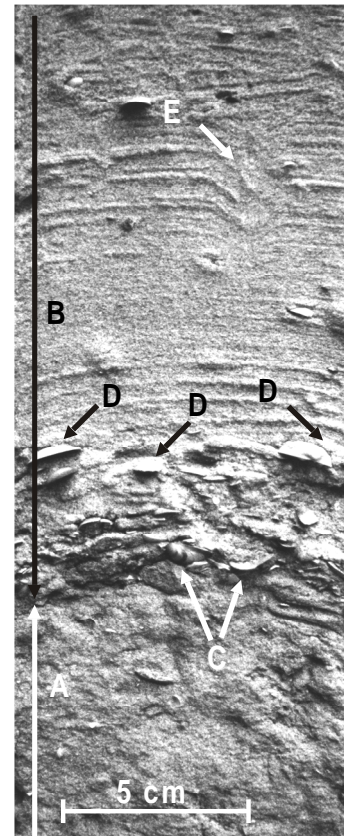
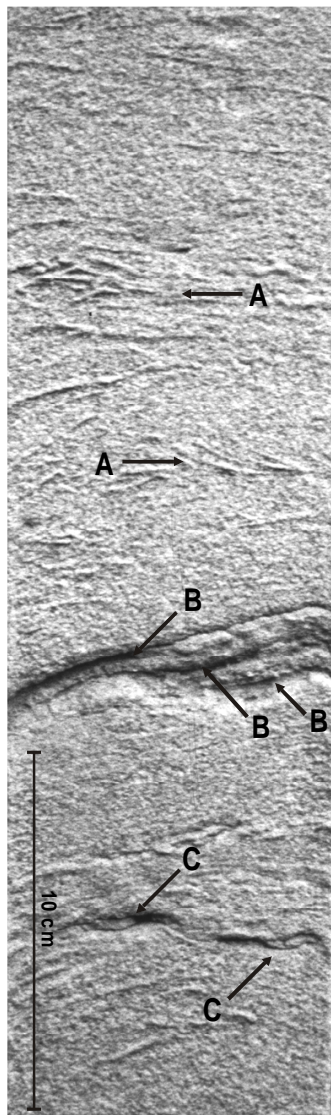


Figure 3.5 (left): Coarse-grained offshore deposits of Unit 2 in core ZR of the Haarlem cross section. Sand with some remnants of cross bedding and cross lamination (A), and with mud layers (B) and mud pebbles (C). (ZR: -13.37 to -13.16 m NAP).

Figure 3.6 (right, continued on following page, left): Examples of shoreface sands from Unit 3 in two cores. Figure 3.6A: Shoreface sands in core DMW of the Haarlem cross section with the bioturbated top of a storm bed (A), overlain by a storm bed (B) with a shell layer at the base (C), and some convex-up shells at basal laminae (D). In the top of the storm bed an individual burrow disturbs the horizontal even lamination (E). (DMW: -8.85 to -8.62 m NAP). Figure 3.6B: Shoreface sands in core HK2 from the Wassenaar cross section with a storm bed with some dispersed shells (for instance indicated at B) on perfectly even horizontal lamination. The storm bed overlies (A indicates basal erosion surface) a fine-grained interval (mud and silt) at the top of another storm bed. (HK2: -8.64 to -8.39 m NAP).

Figure 3.7 (following page, right): Cross-bedded interval within the cross-bedded shoreface sands from unit 1 in core RH2 of the Wassenaar cross section. A denotes the basal erosion surface. At the top of the photograph the cross-bedded interval is truncated (B) and another cross bed starts on top. (RH2: -6.27 to -6.09 m NAP).

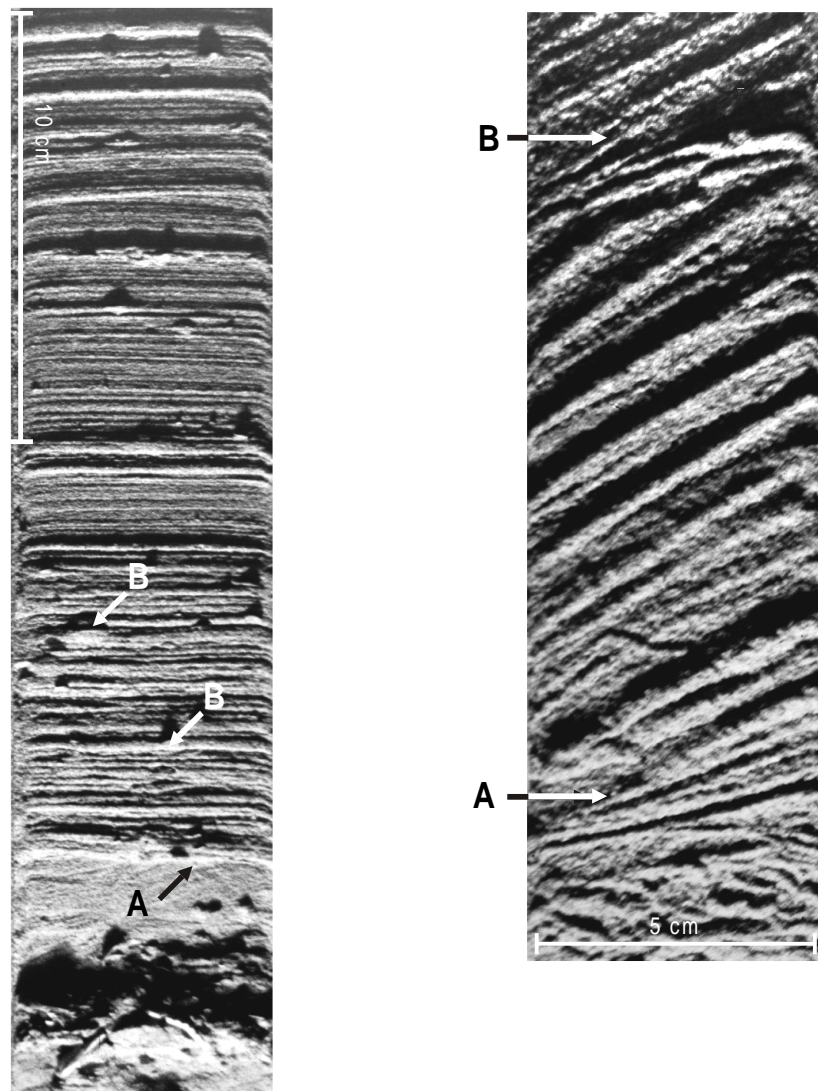


Figure 3.6 B (left) and Figure 3.7 (right): Captions on previous page.

The presence of *Spisula subtruncata* points to deposition in a marine environment seaward of the shoreline (Van Straaten, 1965, Eisma, 1966, Van der Valk, 1992, 1996a). The deposition of mud could only occur under calm conditions, without severe reworking by waves and currents. The sand layers mark occasional influxes of sand, and the wave-ripple lamination demonstrates that these influxes were associated with wave action. Wave action was very restricted, i.e., not severe enough to erode the mud, but sufficient to produce wave-ripple lamination. The limited bioturbation points to restricted conditions during deposition. A combination of rapid sedimentation, induced by the large amounts of mud, and low oxygenation is the most likely candidate for the restricted conditions. Deposition of the sand laminae likely occurred as storm layers (cf. Aigner, 1985), similar to the deposition of sand layers in the 'Bergen Clay' (Westerhoff *et al.*, 1987, Westerhoff and Cleveringa, 1990, Beets *et al.*, 1996b). Occasionally direct wave action resulted in the formation of wave-ripples. The overall coarsening upward of the interval originated from an increasingly shallower environment and hence from an increase of wave influence. The thick sand layers and larger grain size in DMW, FV and SW probably resulted from a more proximal location to the source of the sand than the ZR, SR and LD and Wassenaar cores.

Coarse-grained offshore deposits

The coarse-grained offshore deposits consist of low- to high-angle bi-directional cross-bedding and some parallel beds (Figure 3.5), although in many cases the sedimentary structures are hardly visible. Some of the cross beds display a slight convex fanning of the sets. Shells, mainly *Spisula subtruncata*, are found on the laminae in stable, convex-up position. The coarse-grained deposits in core SR consist of cross beds with abundant clay flakes and clay layers. In core ZR three 10 to 30 cm thick graded sand beds with shells are associated with the coarse-grained deposits. One underlies and two overlie the coarse-grained interval. The underlying tidal-channel deposits and coarse-grained deposits differ in their the shell content, with the *Cerastoderma*-assemblage dominating the tidal deposits, and *Spisula subtruncata* dominating the coarse-grained deposits.

The *Spisula subtruncata* shells are evidence of an offshore environment. The cross-bedding of the coarse-grained deposits indicates deposition by currents, while the fanning of the sets and the stable position of the shells point to wave influences. A combination of currents and waves (combined flow, Arnott and Southard, 1990, Van der Meene *et al.*, 1996) is thought to have been acting during deposition. The restricted abundance of clay layers, and the relative scarcity of shells is in contrast with the characteristic of modern combined-flow deposits from the North Sea (Van der Meene *et al.*, 1996). The depositional environment will be discussed below.

Shoreface sands

The shoreface sands consist of an amalgamation of graded beds, usually with shells at the base (Figure 3.6A) and a transition to silt and mud at the top (Figure 3.6B). The grain size varies strongly, from the base to the top of the sequence, between cores and within the individual graded beds. The individual beds are 10 to 40 cm thick and display a fining upward. The overall trend in the sequence is coarsening upward. In the westernmost halves of the cross section a fining upward trend is present in the basal few metre of the sequence. The graded beds have distinct and neat parallel bedding (Figure 3.6), in some cases with a slight dip (to 5°). Occasionally wave-ripple laminated beds and low-angle divergent cross beds (“micro-HCS”) are found. The shells (mainly *Spisula subtruncata*) are concentrated in shell layers and are also dispersed over the laminae in stable, convex-up position (Figure 3.6A). Shell layers are usually found at the base of the beds, with the shells chaotically distributed or in stable convex-up position. Parts of the deposits are bioturbated, specifically the lowermost part of the sequence. The base of each graded bed is an erosion surface. The transition of fine sand to silt and mud at the top of the beds is often absent, due to subsequent erosion (Figure 3.6B).

Kumar and Sanders (1976) describe storm deposits near Fire Island (US East Coast). The storm deposits consist of a basal lag of gravel, with an overlying sand interval and a wave-rippled or bioturbated interval at the top. The individual storm beds are up to 1 m thick. The overall sequence in the storm beds of Kumar and Sanders (1976) and in the graded beds of the western Netherlands is comparable. The shell layers at the base compare to their basal gravel lag and the finely laminated sand resembles their sand interval. Instead of their bioturbated or wave-ripple laminated top interval we find a silt to mud layer at the top of the beds. Differences are the thickness of the beds (up to 1 m, compared to 30 cm), and the grain size of the basal lag (pebbles versus coarse sand and shells at most). As Van der Valk (1996a) already pointed out, the stack of graded beds resembles the amalgamated shoreface sands which Howard and Reineck (1981) described for the California shelf and Aigner and Reineck (1982) and Aigner (1985) for the German Bight. These deposits consist of beds with basal shell layers, overlain by laminated sands and a top with wave-ripple lamination, and in some cases a mud layer. The only difference between these amalgamated shoreface sands and our

graded beds seems to be the grading. Only the proximal storm layers of Aigner and Reineck are locally “weakly graded”.

The similarity between the graded beds in the Haarlem and Wassenaar cross sections and the storm deposits in the literature (Kumar and Sanders, 1976, Howard and Reineck, 1981, Aigner and Reineck, 1982, Aigner, 1985) suggests a similar mode of formation. Kumar and Sanders (1976) interpret their shoreface beds as the result of storm reworking and re-deposition. The basal pebble layers are lag deposits and represent the peak of the storm, while the parallel beds were deposited during the waning storm phase. The tops of beds were deposited under fair-weather conditions. The amalgamated beds of Howard and Reineck (1981), Aigner and Reineck (1982) and Aigner (1985) are interpreted as stacks of storm beds. The shell beds are lags, the parallel lamination represents the waning of the storm and the wave-ripple lamination represents the final stages of the storm, while mud layers may be deposited under fair-weather conditions. The common wave-reworking of shallow parts of the shoreface profile versus infrequent reworking of the deeper parts causes the overall coarsening upward trend of the shoreface deposits (Clifton *et al.*, 1971, Howard *et al.*, 1972, Reineck and Singh, 1972, Davidson-Arnott and Greenwood, 1974, Reineck and Singh, 1975, Davidson-Arnott and Greenwood, 1976, Hunter, 1979, Howard and Reineck, 1981, compiled in figure 7.11 of Elliot, 1986).

3.3.3 Unit 3

Unit 3 is found on top of Unit 2. The deposits were formed seaward of the coastal barrier and were deposited as part of the prograding coastal system. A major part of Unit 3 consists of shoreface sands, and a small part consists of sand-mud laminations. The description and interpretation of these facies is presented above, with Unit 2. In the landward halves of the cross sections a gradual transition of Unit 2 to 3 is observed, within the interval of sand-mud laminations. In the middle parts of the cross sections a distinct facies transition, from coarse-grained offshore deposits or sand-mud laminations into shoreface sands marks the transition of Unit 2 to 3. In the offshore cores of the cross sections the transition of Unit 2 to 3 occurs within shoreface sands. The depth of the transition from 2 to 3 increases seaward. The top height of the beach deposits also increases seaward, and Unit 3 thus forms a seaward thickening wedge.

Cross-bedded shoreface sands

The cross-bedded shoreface sands are characterised by middle sand with distinct cross-bedding and cross lamination and with a very limited amount of shells and mud layers (Figure 3.7). The majority of the shells is *Spisula subtruncata*.

The cross-bedded shoreface sands originate from a depth at which wave reworking must have been severe, as is evident from adjacent cores that contain graded storm beds at similar depths. Direct evidence of wave reworking within the cross-bedded intervals is absent. However, the absence of mud layers and flasers presents indirect evidence of wave action. The cross-bedding resembles the bedding of large-scale bed forms.

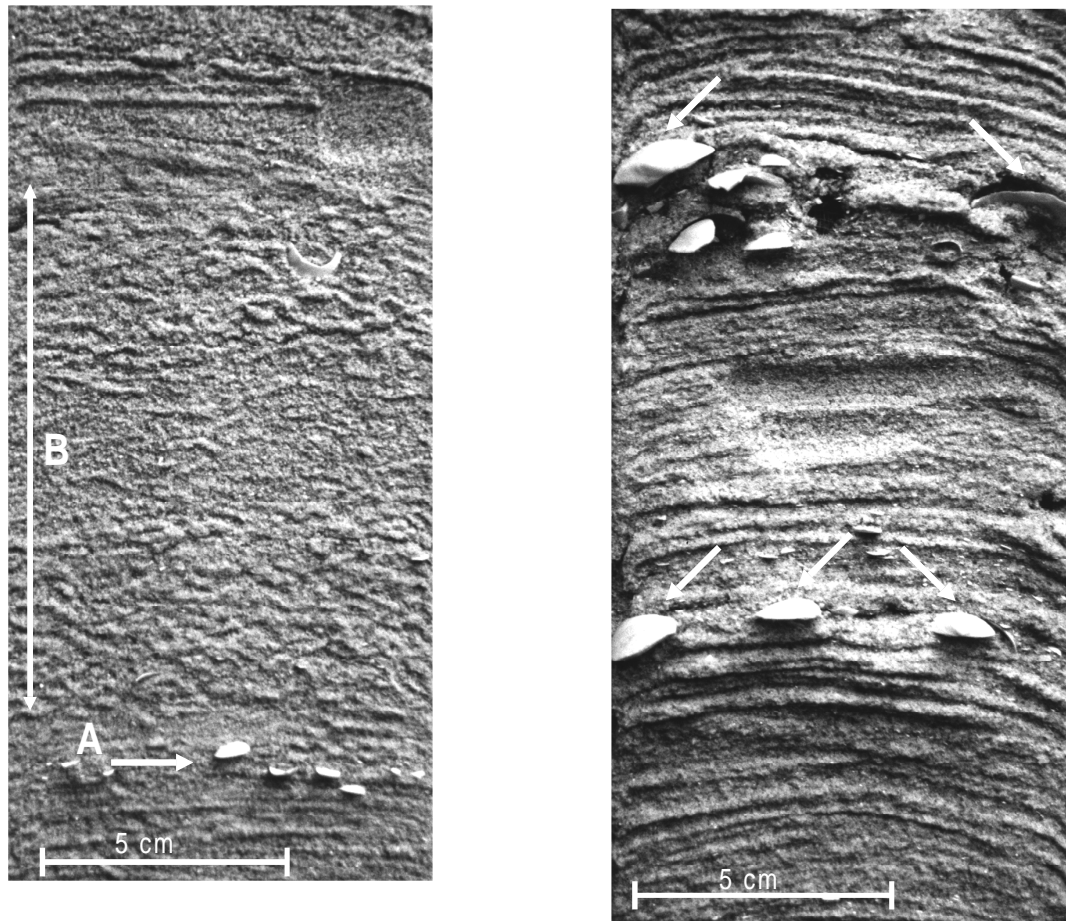


Figure 3.8: Examples of beach deposits from Unit 3 from two cores.

Figure 3.8 A (left): Beach sands in Unit 3 of core SW from the Haarlem cross section, displaying an interval with pockmarked sand without lamination (B). The intervals that underly and overly the pockmarked interval display even horizontal lamination. A shell layer is present just below the interval (A). The interval likely originated from bubble sands in the inter-tidal zone (cf. De Boer, 1979) or from liquefaction of a sand layer. (SW: -2.38 to -2.20 m NAP).

Figure 3.8 B (right): Two shell layers in beach sands of Unit 3 from core DMW in the Haarlem cross section. All shells are in convex-up position (at arrows). At the top shell layer a truncation of the even lamination is visible. (DMW: 0.20 to 0.38 m NAP).

Beets *et al.* (1981) observed cross-bedding in beach-plain sequences near Alkmaar, which they related to preserved wave-built ridges. Deposition in wave-built ridges is likely for the cross-bedded shoreface deposits in the upper metres of the sequence. Deeper lying parts of the cross-bedded shoreface sands may originate from mega-ripple migration in tidal channels. Such channels may have been present behind rapidly prograding beach ridges, and at the heads of spit platforms (cf. Kumar and Sanders, 1974).

Breaker-bar and beach sands

The breaker-bar and beach deposits consist predominantly of parallel-laminated medium sand with slightly inclined sets, occasionally with cross-bedding and cross lamination. Some thick chaotic shell beds, crinkle-sand laminae and pockmarked sand beds (Figure 3.8 A) are found as well. In the upper part of the interval thin shell layers with shells in convex-up position occur (Figure 3.8 B). The amount of shells and cross-bedding varies. In the Haarlem section the amount of shells increases seaward. Thick high-angle cross beds are restricted to the cores DMW and RSP in the Haarlem cross section. The base of the interval is taken at the lowermost cross bed, and the top boundary is taken at the highest shell layer, highest detritus layer or highest cross lamination.

The parallel-laminated sand was deposited under conditions of breaking waves, swash and backwash. The cross-bedded intervals result from bedform migration. The thick chaotic shell beds may also have been formed by bed-form migration, as this process results in the overturning of the shells from their stable position (Clifton and Boggs, 1970). Breaker bars and superimposed megaripples generated the cross-bedding. The deposits reflect the highly variable conditions on the upper shoreface, breaker bar and beach. The transition into the overlying dune sands is gradual. Storm-high-water marks are present in the form of convex-up shell layers, ripple beds and adhesion ripple marks (crinkle sand laminae and pockmarked sand) (Roep and Beets, 1988).

Beach-plain deposits

Deposits of bioturbated sand and mud layers of several centimetres (Figure 3.9 A and B) are found at similar levels as beach deposits in adjacent cores. Bioturbation decreases to the top of the deposits. Occasionally (up to 30 cm) thick beds with dispersed chaotic shells are found, while in other cores thick mud layers occur. Usually a peat layer overlies the beach-plain deposits. The ratio of sand to mud varies within the deposits and between the cores. The beach-plain deposits are associated with several types of underlying deposits, but do not occur on top of beach and breaker bar sand.

The general characteristic of these deposits is the absence of direct wave influence. The bioturbated sand-mud bedding resembles inter- or sub-tidal flat deposition. The thick sand and shell beds resemble distal washover deposits and mud layers indicate deposition under tranquil conditions. Such deposits that have been produced under very variable conditions are found in beach-plains of prograded coastal deposits (Beets *et al.*, 1981, Roep *et al.*, 1983, Roep and Beets, 1988). The beach plain is an area behind a low beach ridge that is regularly flooded during spring tide and storms. Its deep position relative to the beach ridges and the groundwater pressure from surrounding dunes result in wet conditions, which hinder the formation of aeolian dunes. The wet conditions enhance the growth of vegetation and the formation of peat (Jelgersma *et al.*, 1970).

3.3.4 North Sea sand and Dunes

On top of Unit 3 North Sea sand is found in the offshore cores, and dune sand in the land-based cores.

North Sea sand

Cross-bedded yellow to brown coarse sands (grain size 300 μ and larger) with abundant shells, shell fragments and small pebbles. The shells resemble the modern North Sea fauna (Eisma, 1966, De Bruyne and Van der Valk, 1991), but do locally consist of a *Cerastoderma*-shell assemblage.

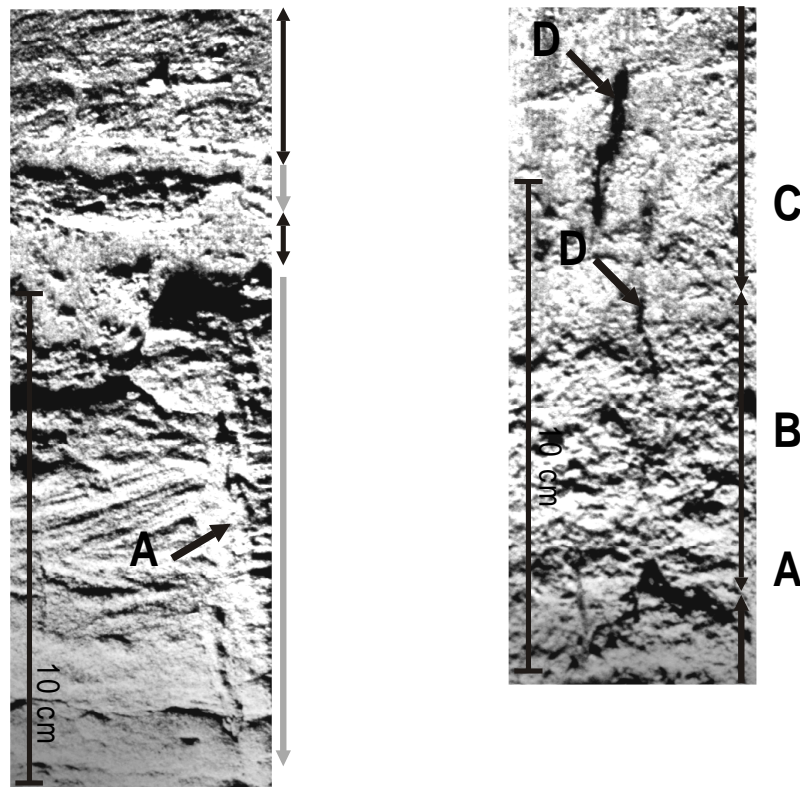


Figure 3.9: Examples of beach-plain deposits in Unit 3 from core RH1 in the Wassenaar cross section.

Figure 3.9 A (left): Bioturbated sandy interval with some remnants of lamination (basal white interval), overlain by a muddy interval. At A a large burrow is visible that penetrates the sand. In the muddy interval a bioturbated remnant of another sand layer is visible (top white interval). (RH1: -3.88 to -3.73).

Figure 3.9 B (right): Bioturbated sandy interval (A) overlain by a bioturbated sandy-mud interval (B), in turn overlain by a muddy interval (C), with dark remnants of roots (D). The roots penetrate the mud from an overlying peat layer. Sedimentary structures are completely obliterated by the bioturbation. (RH1: -2.91 to -2.77).

Following Van Straaten (1961, 1965) and Beets *et al.* (1995) we interpret the North Sea sand deposits as an erosive lag, from which fines have been removed. The cross-bedding results from megaripples that are commonly found on the North Sea floor (Houbolt, 1968, Van Alphen, 1989). The megaripple fields form due to strong tidal currents. Megaripple migration is probably an important process for the removal of fines, as is occasional storm reworking. The local occurrence of the *Cerastoderma*-shell assemblage probably results from the erosion of older tidal deposits (Beets *et al.*, 1995, Flessa, 1998). The abundance of shells results from concentration due to winnowing of fine sand, and from the ongoing shell production on the North Sea floor.

Dune sand

Blond to brown fine sand with parallel laminations, low-angle cross beds and low-angle truncation planes. In some parts, especially at the top of the interval, sections without any structures are found. These intervals are usually associated with overlying brownish soil horizons. Occasionally organic-rich horizons and even peat beds are found. Roots penetrate from the soil horizons, and from organic-rich horizons and peat beds into the underlying sand. The transition from the underlying beach deposits into this interval is gradual. Aeolian sands are found in between cross-laminated beach sands.

The blond to brown fine sand is aeolian dune sand. Soils and organic-rich horizons result from (local) wet conditions and vegetation. Soil formation has led to the loss of the original sedimentary structures. For an extensive description and interpretation see Jelgersma *et al.* (1970). The alternation of beach and dune sands resulted from short-term changes in water level due to tides and storm set up.

3.4 Cross sections

Above a description and interpretation of the deposits is presented. The distribution of the facies within the Wassenaar and Haarlem cross sections (Figures 3.10 and 3.11) is presented below. The age range of deposition is indicated as well. For a more elaborate discussion of the age of the deposits see the next chapter (Chapter 4).

3.4.1 Wassenaar cross section

Unit 1

The Holocene deposits of Unit 1 have been deposited prior to 5900 BP. The Basal Peat in the cross section is found around -15 m NAP (Figure 3.10), implying that formation occurred around 7400 BP (Jelgersma, 1979). The boundary between Pleistocene sand and the Holocene tidal deposits is erosive, and ranges from -23.5 to -15 m (Figure 3.10). This height range is due to variations in depth of the incisions of the tidal channels.

The Holocene deposits of Unit 1 originate from tidal back-barrier basins of the transgressive coastal system. The remnants of basal peat and clay are the oldest Holocene deposits, from the landward side of the back-barrier basin. The tidal channels originated from a more seaward position in the back-barrier basins. The sequence of basal peat, erosively overlain by tidal channel deposits, is transgressive.

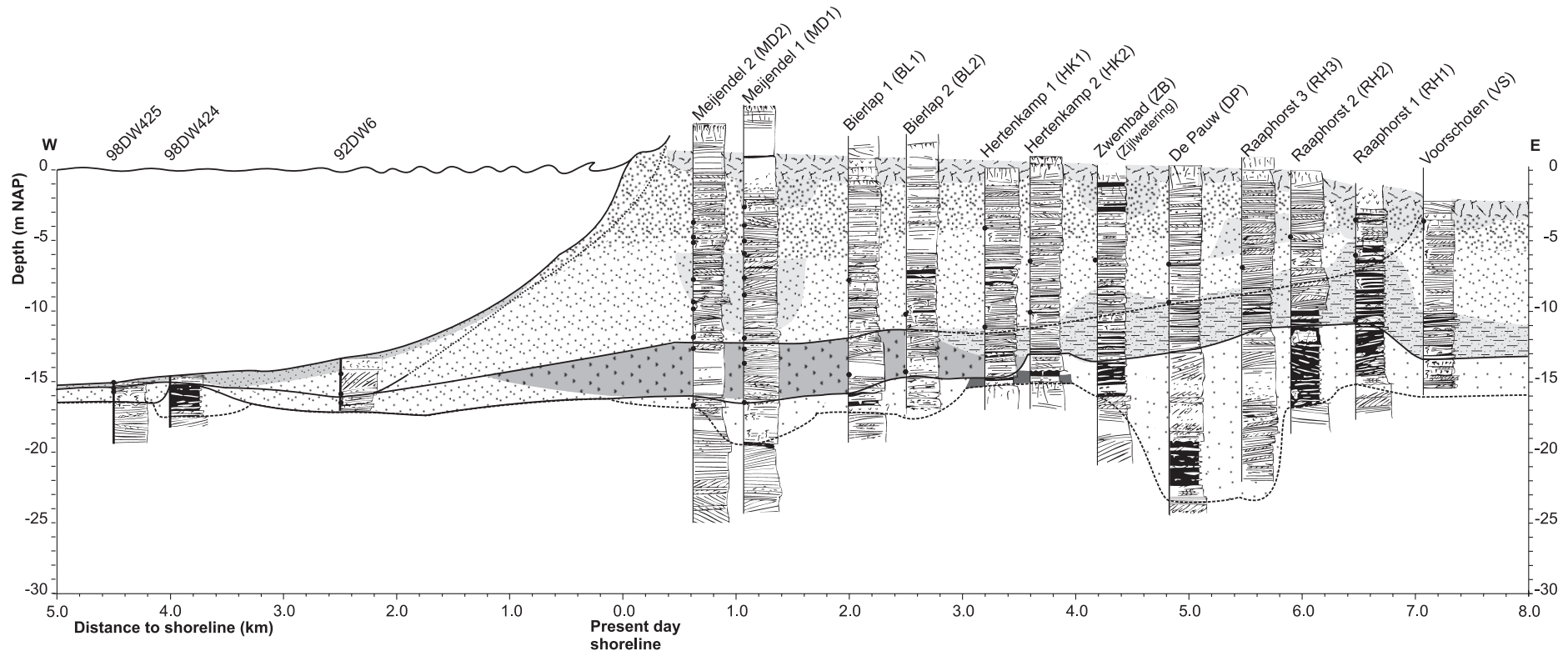
Unit 2

The transition from Unit 1 to Unit 2 is marked by a distinct change in facies, from tidal channel deposits to various types of offshore deposits (Figure 3.10). The facies change is accompanied by a change in shell fauna, from a *Cerastoderma*-shell assemblage to a *Spisula*-shell assemblage. The sequence of tidal back-barrier deposits in Unit 1, overlain by offshore deposits of Unit 2, is transgressive.

The cross-shore variation in the deposits is large, with shoreface sands in the offshore cores, coarse-grained offshore deposits in cores MD2 to BL 1 and sand-mud laminations further east (Figure 3.10). In core VS shoreface and beach deposits are present. The age of Unit 2 ranges from 5900 BP to 4500 BP. The deposits of Unit 2 are older than the overlying prograded coastal deposits of Unit 3, and were part of the transgressive coastal system.

The large cross-shore variation in the deposits indicates that the transgressive shoreface was a complex depositional environment. The shoreface sands at the seaward side indicate that wave action was severe enough to produce storm beds. More landward wave action was restricted, allowing the deposition of mud. The origin of the coarse-grained offshore deposits is discussed below. The shoreface and beach deposits at the landward edge of the cross section in core VS mark the palaeo-shoreline. The deposition of shoreface and beach sands occurred after the tidal flow of the transgressive coast diminished. The deposits in core VS thus mark the transition of a transgressive to prograding coast.

Wassenaar cross-section



- | | | | |
|--|--------------------------------|--|----------------------------------|
| | Dune sand, peat and soils | | Sand-mud laminations |
| | North Sea sand | | Coarse-grained offshore deposits |
| | Beach-plain deposits | | Tidal deposits |
| | Breaker-bar and beach deposits | | Basal peat and clay |
| | Cross-bedded shoreface sands | | Pleistocene sand |
| | Shoreface sands | | |

-
- Peat
 - Roots
 - Shells, shell layer
 - Parallel bedding
 - Bioturbation
 - Cross bedding
 - Wave-ripple lamination
 - Sand-mud layers (black = mud)
 - Cross lamination
 - Erosion surface

Figure 3.10: Caption on following page.

Unit 3

The age of Unit 3 ranges from 4500 BP to 3500 BP, and the seaward decrease of ages clearly demonstrates coastal progradation. Progradation rates of the interval are very high (at least 5 km in 1000 years: 5 m/year Van der Spek *et al.*, 1999, see also Chapter 4). During progradation in the landward half of the cross section, non-deposition and erosion dominated the lowermost shoreface and shelf in the seaward half (Figure 3.12). The deposits of Unit 3 are highly variable, with shoreface sands, cross-bedded shoreface sands, breaker bar and beach sands and beach-plain deposits (Figure 3.10). In the cores west of RH2, shoreface sands and cross-bedded shoreface sands are found in the interval of –12 up to –5 m (Figure 3.10). Breaker-bar and beach deposits or beach-plain deposits overlie the shoreface sand and cross-bedded shoreface sands (Figure 3.10).

Cross-bedded sands seem to preferably overlie by beach-plain deposits. A complex relation is envisaged between the sand-mud laminations in core RH1 and the cross-bedded shoreface sands in core RH2 (Figure 3.10). The cross-bedded sand likely originated from a spit-like bar that sheltered the area behind from most wave reworking. In the sheltered area the sand-mud laminations were deposited (Figure 3.12 A). Later a small tidal channel developed in the sheltered area, which was later on followed by deposition on a beach plain. A similar development was envisaged by Van Straaten (1965) for the lateral equivalent of RH1 and RH2 near The Hague. We use the term spit-like bar, because a spit-bar extends from a headland or beach, which is not necessarily true here. The bar may have evolved from long-shore transport (as a spit), or as an emerging bar from cross-shore transport.

The prograded deposits in the Wassenaar cross section developed as part of the wave-dominated delta of the Old Rhine at Katwijk. The abundance of cross-bedded shoreface deposits and beach-plain deposits was part of this development.

3.4.2 Haarlem cross section

Unit 1

The Holocene deposits of Unit 2 were formed prior to 5100 BP. Basal Peat and Clay are absent in the Haarlem cross section. These have been formed and deposited, but removed during subsequent erosion by the tidal channels. The boundary between Pleistocene and tidal channel deposits ranges from –27 to –18 m NAP (Figure 3.11), due to differences in the incision depth of the tidal channels.

The Holocene deposits of Unit 1 originate from tidal channels of the transgressive coastal system. The large variation in the top height of Unit 1 results from the fact that the tidal channels were not completely filled in with channel deposits. This left a depression from the abandoned inlet channel on the transgressive shoreface and shelf.

Figure 3.10: Cross section with sedimentary logs of cores of the Wassenaar cross section. The distribution of facies is indicated, as well as the boundaries of units 1 to 3. Basal deposits of Unit 1 consist of Pleistocene sand and Holocene transgressive back-barrier deposits. Basal Peat and Clay is found in cores BL1, HK and HK2. Deeply incised tidal channels with thick tidal-channel deposits in cores DP and RH3. Unit 2 consists of transgressive offshore deposits: shoreface sand in the marine cores, coarse-grained offshore deposits from MD 2 to HK1, and sand-mud laminations more landward. In core VS a transition of tidal channel deposits into shoreface sands and beach deposits is observed. Unit 3 consists of prograded shoreface deposits, overlain by beach deposits. Cross-bedded shoreface sands are present in several cores, as are beach-plain deposits. The top height of Unit 2 increases seaward, which resulted from the rise of the sea level during progradation.

Haarlem cross-section

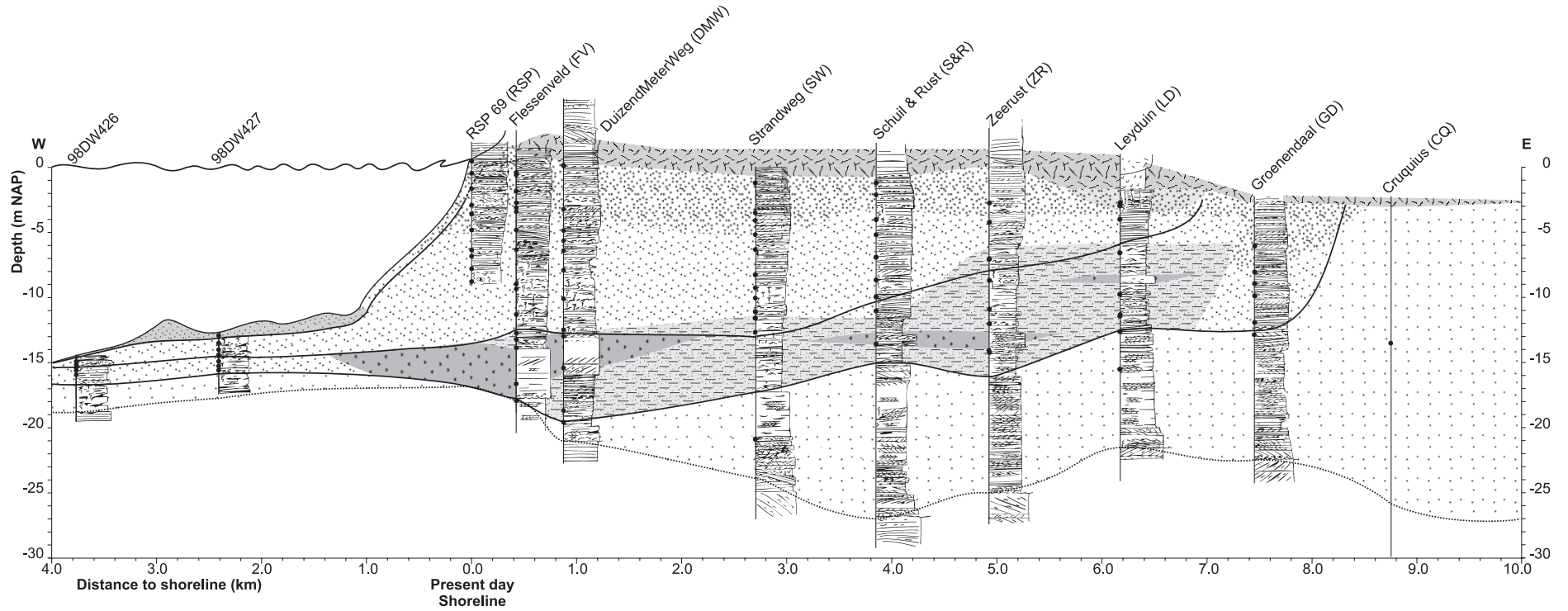


Figure 3.11: Caption on following page.

Unit 2

The transition from the underlying tidal deposits into the offshore deposits of Unit 2 is distinct. Similar to the Wassenaar cross section, this is a classic transgressive sequence. In core GD at the landward end of the cross section a gradual change from tidal-channel deposits into shoreface sands is observed (Figure 3.11). The deposits in core GD mark the gradual transition of the transgressive tidal deposits to shoreface and beach deposition of the prograded coast. As such it may be regarded a transition stage from transgression to progradation.

The age of Unit 2 ranges from 5100 to 4200 BP. The deposits in Unit 2 are older than the deposits in Unit 3, and originate from the transgressive coastal system. The variation in facies in Unit 2 is distinct. Shoreface sands are found in the offshore cores. Coarse-grained offshore deposits are particularly abundant in cores FV and DMW, with a thickness up to 4 m. In the more landward cores sand-mud laminations are abundant (Figure 3.11). In the landward half of the cross section sand-mud laminations envelop coarse-grained deposits (Figure 3.12 B). In core DMW the sand-mud laminations filled the depression left by the abandoned transgressive tidal channel.

Unit 3

The age of Unit 3 ranges from 4200 to 400 BP, and decreases seaward. Unit 3 was deposited by the prograding coastal system. Progradation rates were much lower than in the Wassenaar cross section, and decrease seaward (Van der Spek *et al.*, 1999, see also Chapter 4). During progradation, non-deposition and erosion dominated the lowermost shoreface and shelf in the seaward half of the cross section (Figure 3.12 C and D). In Unit 3 beach and breaker-bar deposits overlie shoreface sands and sand-mud laminations (Figure 3.11). Beach-plain deposits are found only in core LD, at the eastern edge of Unit 3. Cross-bedded shoreface sands are absent in the Haarlem cross section. The boundary between Unit 3 and the overlying dune sand increases in height from east to west, from -2 m NAP +2 m NAP (the +2 m NAP boundary equals the modern beach surface in RSP). From east to west a number of distinct trends is recognised in this Unit (Figure 3.11). The base of the shoreface sands deepens from -6 m in LD down to -15 m in the marine cores. Sand-mud laminations display a seaward decrease in abundance. Shells become increasingly more abundant in the seaward direction, and the grain size of shoreface sands and beach and breaker-bar deposits increases seaward as well. In addition, the thickness of the beach and breaker-bar deposits increases seaward, not only because the upper boundary increases in height, but also because the lower boundary increases in depth from -2.5 m in FV to -5 m in RSP.

Figure 3.11: Cross section with sedimentary logs of cores of the Haarlem cross section. The facies are indicated, as well as the boundaries of units 1 to 3. For legend see figure 3.10. Unit 1 consists of Pleistocene sand and Holocene tidal-channel deposits. The tidal channels have incised down to -27 m in core S&R. The abundance of tidal-channel deposits increases landward. The overlying deposits of Unit 2 are transgressive offshore deposits, consisting of shoreface sands in the marine cores, of coarse-grained offshore deposits in the cores FV and DMW, and mainly of sand-mud laminations in the other cores. In core GD a gradual transition of tidal-channel deposits of Unit 1 into shoreface sands and beach deposits of Unit 2 is observed. Unit 3 consists of shoreface sand and breaker-bar and beach deposits. Only in core LD beach-plain deposits are found. The top height of Unit 3 increases seaward, which resulted from the rise of sea level during progradation. The base of the breaker-bar and beach deposits is found increasingly deeper seaward, thus indicating that the breaker-bar zone increased in vertical extent during progradation.

The shoreface and beach deposits of the initial prograding coastal barrier differ from those of the following stages of progradation. Initially, sand-mud laminations were deposited in deeper water, overlain by shoreface deposits and breaker-bar and beach sands (Figure 3.12 C). This sequence resembles the distal-to-proximal trends in the nearshore storm deposits of Aigner and Reineck (1982). During later stages of progradation sand-mud laminations were not deposited anymore, and amalgamated storm beds of the shoreface sand extended over the entire shoreface profile (Figure 3.12 D). Distal storm deposits as described by Aigner and Reineck (1982) are entirely absent in this depositional sequence. The seaward height increase of the breaker-bar and beach intervals is due to the rise in sea level during progradation. The entire prograded sequence was deposited under relatively low-energy conditions during initially progradation, while the following progradation occurred under progressively higher energetic conditions.

3.5 Large-scale coastal evolution

3.5.1 Unit 1

A major part of the transgressive back-barrier deposits consists of tidal-channel deposits. The transgressive coastal system consisted of tidal back-barrier systems, with fully developed tidal inlets and tidal-channel systems (Beets *et al.*, 1992). The transgressive sequence of tidal-channel deposits is similar to the tidal-inlet migration model of Hoyt and Henry (1967) and to the basal part of the barrier-inlet model of Reinson (1984, 1992). The thickness of the tidal-channel deposits is related to the dimensions of the tidal back-barrier basins of the transgressive coastal system (Beets *et al.* 1992, 1994, 2000). The depth of the tidal-channel incisions in Unit 1 is deep in the Haarlem cross section, as compared to its depth in the Wassenaar cross section. The large depth of the tidal channel incisions in the Haarlem cross section resulted from the larger tidal back-barrier basin. As a consequence of the limited incision depth in the Wassenaar cross section, some Basal Peat and Clay has escaped erosion.

3.5.2 Unit 2

The sequence offshore deposits of Unit 2 on top of tidal back-barrier deposits in Unit 1 is a classic transgressive sequence. Transgression resulted from the ongoing sediment import from seaward of the barrier into the tidal back-barrier basins (Beets *et al.*, 1992, 1994, Beets and Van der Spek, 2000). The end of the transgression resulted from the in-fill of all accommodation space in the tidal back-barrier basins. With this in-fill the tidal prisms of the tidal basins decreased and the tidal channels silted up. Hence, the diminishing and closure of the tidal inlets accompanied the end of transgression. This is visible in the transition of the tidal deposition into shoreface and beach deposition at the landward sides of the cross sections (cores VS and GD).

The tidal-inlet channel of the transgressive coastal system was largest and most deeply incised at the seaward edge of the back-barrier basin. This location of maximum incision coincides with the location where later coastal progradation started. Hence, the basis for offshore deposition consists of tidal-channel deposits and remnant tidal-channel incisions. The direct consequence of the larger and deeper tidal channels near Haarlem is that the base of Unit 2 lies deeper in the Haarlem cross section. The deep depression left by the abandoned tidal inlet was largely filled up with sand-mud laminations.

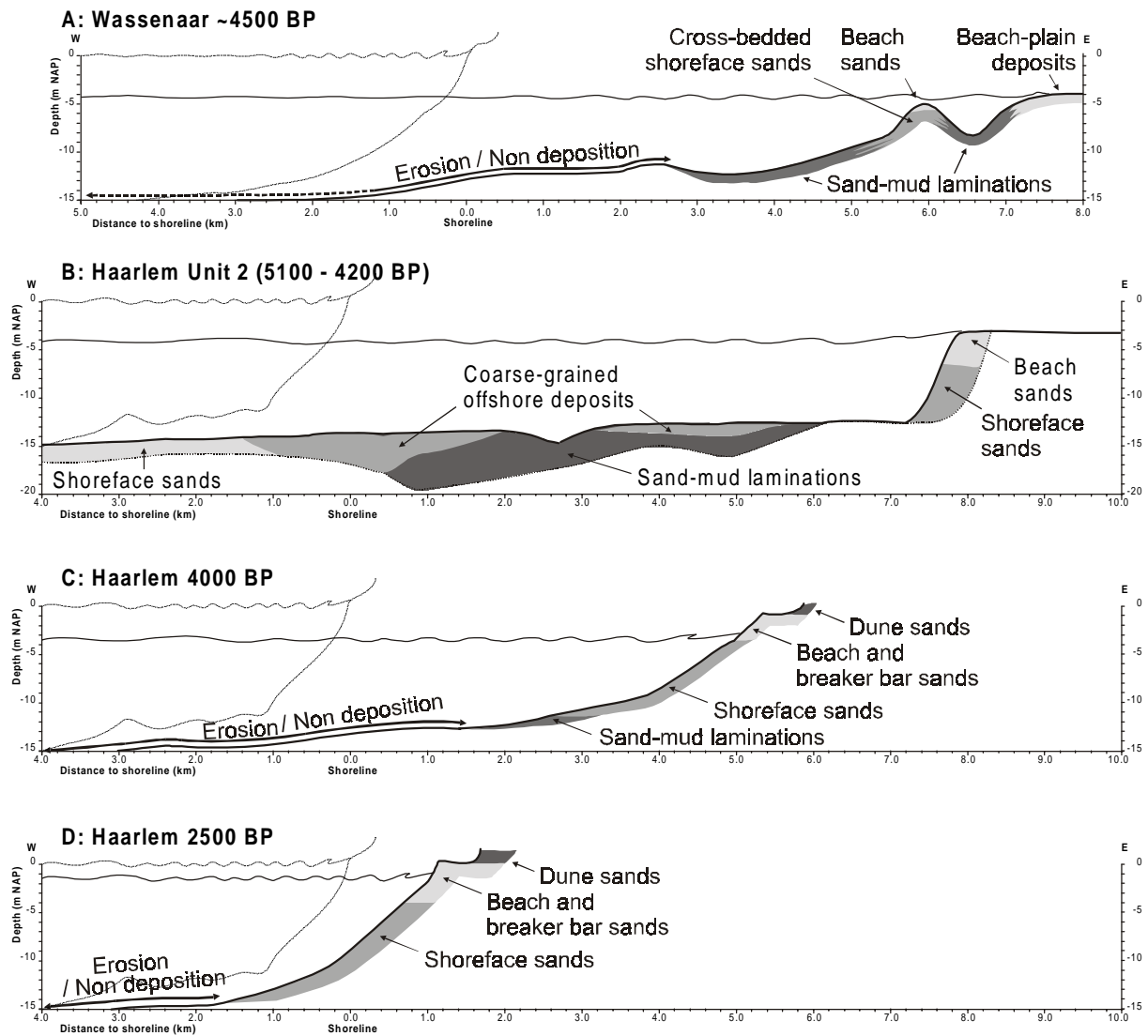


Figure 3.12: Cartoon with depositional environments and facies distribution during different stages of coastal evolution. The modern sea level and coastal profile are indicated as a reference.

Figure 3.12 A: Deposition during the initial stage of coastal progradation at Wassenaar (about 4500 BP). Deposition was restricted to the landward half of the cross section. At the seaward half erosion or non-deposition occurred.

Figure 3.12 B: Deposition of Unit 2 in the Haarlem cross section (from 5100 to 4200 BP) during the transgressive stage of coastal evolution. On the seaward side of the profile deposition of shoreface sands occurred. In the landward edge of the cross section shoreface sands are deposited on top of tidal-channel deposits.

Figure 3.12 C: The Haarlem cross section at one-third of its progradation, at 4000 BP. At the lowermost shoreface in the western half of the profile erosion or non-deposition occurred.

Figure 3.12 D: Deposition during the last stage of coastal progradation at the Haarlem cross section at 2500 BP. Erosion or non-deposition occurred on the lower-most shoreface. Notice the differences with the previous reconstruction. During progradation the overall shoreface profile becomes steeper. Deposition of sand-mud laminations was absent on the lower shoreface during final progradation. The depth at which breaker-bar and beach deposition occurred became larger.

The complexity of the depositional environments in Unit 2 is likely related to the transgressive nature of the coast, or more specifically to the onshore directed cross-shore sediment transport induced by the tidal inlets (Beets *et al.*, 1992). The relatively shallow substrate (10 to –12 m waterdepth, apart from the local deeper depressions), and the gentle slope of the shelf and shoreface may have contributed as well. There is no unambiguous interpretation of the conditions that have led to the formation of the coarse-grained offshore deposits (see discussion below).

3.5.3 Unit 3

The deposits in Unit 3 consist of a prograding sequence of coastal deposits. During progradation non-deposition or erosion occurred on the lower shoreface and shelf, due to reworking by tidal currents. The diversity of facies in Unit 3 in the Wassenaar cross section contrasts with the limited variation in the Haarlem cross section. The development of the wave-dominated delta of the Old Rhine near Leiden, of which the deposition at Wassenaar was a part, was the likely agent in the diversity of the facies. The formation of the delta enhanced progradation rates and changed the local coastal configuration (hence, the seaward curvature of the beach-ridges around Katwijk, figure 3.2). It is unclear whether the formation of the wave-dominated delta influenced the depositional conditions directly, or that the high progradation rates increased the preservation potential of the deposits (see discussion below).

Coarse sand grains are entirely absent in the middle part of the shoreface sequence in the western half of the cross sections (also observed in the The Hague cross section: Van Straaten, 1965). The fining-upward trend overlain by a coarsening-upward trend in the shoreface deposits suggests that little cross-shore transport of coarse sand grains occurred. In the Haarlem cross section distinct seaward trends in the facies (increase in grain-size, shell content and thickness of the breaker bar interval) are present, related to the seaward decrease in progradation rate. Such features are absent in the Wassenaar cross section.

3.6 Discussion

3.6.1 2D-3D

Both cross sections are oriented perpendicular to the coast, and therefore there is a strong tendency to regard coastal developments as cross-shore phenomena. This is not realistic, because most coastal morphological patterns are clearly 3-dimensional. Similarly, most processes have cross-shore and longshore components. For instance, the distribution of the beach plains and beach ridges is not uniform alongshore. Near fluvial outlets the pattern of beach ridges and beach plains curves seaward, and near former tidal inlets the pattern curves landward. Two examples of spatial variability that may be misinterpreted if only the cross-shore aspects are considered.

The base of the tidal channel deposits varies strongly within the two cross sections. This is best explained by the arbitrary cross cutting of a (slightly) meandering channel by a straight cross section. In some places the cross section will cut through the deepest channel incision, while in other places the shallower flanks of the channel are intersected. Conclusions on the depth of incision can therefore not be based on the cross sections alone. However, based on the average depth of the base of the tidal-channel deposits, it is clear that the tidal channels near Haarlem have incised deeper and hence that the tidal channel was larger than at Wassenaar.

The deposits at core GD show a gradual transition of sandy tidal-channel deposits into shoreface, breaker bar and beach. The deposition in GD likely represents the diminishing of tidal action with an associated increase in wave action at that location. After deposition in GD

around 5050 (m) BP, deposition in the area halted, and restarted after 4200 (m) BP more seaward in core LD. In other words, there is a hiatus between core GD and core LD. The hiatus is not necessarily continuous alongshore. It is more likely that in the period in between 5050 and 4200 (m) BP deposition continued somewhere north or south of the cross section. The origin of the alongshore shift of deposition is likely related to the gradual closure of the tidal inlet near Haarlem.

3.6.2 Unit 2

The occurrence of coarse-grained offshore deposits is restricted to the transgressive offshore deposits of Unit 2. Sand-mud laminations are found in Unit 3 as well, but their relation with the coarse-grained deposits (underlying, overlying and enveloping, figure 3.10 and 3.11) obliges a discussion of the two in conjunction.

The mud in the sand-mud laminations has been deposited under relative quiet conditions on the shoreface. The depression formed by the top of the tidal-channel deposits (mainly in DMW) was sheltered from direct wave influences, and acted as a quiet sink for material that was brought in suspension elsewhere. Sand-mud laminations at higher levels in cores (in ZR and LD for instance) were deposited on the palaeo-shoreface. This implies that the conditions on the shoreface were relatively quiet.

Van Straaten (1965) suggested that coarse-grained offshore deposits originated as shoreface-connected ridges on the shelf which translated landward. Similar ridges on modern shelves and shorefaces are usually restricted to transgressive coasts (Swift *et al.*, 1978), but they are also found along the relatively stable modern Dutch coast, from Wassenaar to Bergen aan Zee (Van der Meene, 1994, 1996). Geostrophic storm flows and tidal currents generate the ridges (Stahl *et al.*, 1974, Swift and Field, 1981, Antia, 1994, Snedden *et al.*, 1994, Van der Meene, 1994). Transgression may enhance ridge formation because remnants of older coastal deposits may act as initiation points for ridge development (Swift and Field, 1981). In addition there was a strong onshore-directed sediment transport through the tidal inlets during transgression (Beets *et al.*, 1992), which may have enhanced ridge formation.

The cross-bedding in the coarse-grained offshore deposits is evidence of currents as the main agents of sediment transport. Sand-mud laminations envelop the coarse-grained deposits, demonstrating that these currents were not continuously present on the middle and lower shoreface. Continuous or frequent current action would have prohibited the deposition of the fine-grained sediments. The currents likely originated as storm- and wave-driven currents. This is supported by the presence of one thick storm layer below and two above the coarse grained deposits in SR, which demonstrate that storm were of influenced when coarse-grained deposition occurred.

Although coarse-grained offshore deposits are regularly described as reworked palimpsest sediments on modern shoreface-shelf systems (Swift *et al.*, 1978, Snedden and Dalrymple, 1999), they have, to our knowledge, not been described from Holocene coastal sequences. The abundance of this type of deposits in the Western Netherlands coastal deposits suggests that it may be a normal type of deposit in transgressive offshore sequences. Regular recognition of coarse-grained offshore deposits in various fossil sequences (Bergman and Snedden, 1999, and references in here) indeed suggests such deposits to be a normal part of coastal sequences.

3.6.3 Progradation rates and preservation

In the prograded coastal deposits in the Alkmaar area a correspondence between fast progradation and beach-plain deposition and slow progradation and beach-ridge development was observed (Beets *et al.*, 1981, Roep, 1984). The authors also envisaged a relation between

gentle shoreface slopes, high progradation rates and beach-plain deposition, and steeper shoreface slopes and beach-ridge development. The beach-plain deposits are underlain by high- and low-angle cross beds (Beets *et al.*, 1981). Van den Berg (1977) pointed to the relation between the progradation rate and the preservation of structures on two modern beaches. Low progradation rates result in the preservation of storm related structures only, because all other structures are erased during high-energy reworking. High progradation rates result in the preservation of various types of structures, which form under every-day conditions. During storms only parts of the every-day structures are eroded, the remainder is buried during progradation and stays out of reach of storm reworking. Van Straaten (1965) envisaged a similar relation between sedimentation rates and the abundance of mud layers in shoreface sediments. A high sedimentation rate results in the burial of the mud layers that are therefore less accessible for reworking (Van Straaten, 1965).

The overall rate of progradation of the Wassenaar cross section is higher than the progradation rate in the Haarlem cross section. Beach-plain deposits and cross-bedded shoreface sands are consequently more abundant in the Wassenaar cross section. The amount of mud layers in the shoreface sands of the Wassenaar cross section is also higher. A relation between progradation rates and the preservation of structures similar to that proposed by Beets *et al.* (1981) and Roep (1984) is envisaged. Slow progradation facilitates storm reworking of the majority of the deposits and results in the deposition of shoreface storm beds only. Fast progradation hinders storm reworking of all of the deposits and cross-bedded shoreface and beach-plain deposits, as well as mud layers, can be preserved. A gentler shoreface slope during initial progradation (see Chapters 4 and 6) may also have facilitated the formation and preservation of cross-bedded shoreface and beach-plain deposits.

In the Haarlem cross section the progradation rate decreases seaward (Van der Spek *et al.*, 1999), and there is a seaward increase of average grain-size and shell content. The decrease of the progradation rate (and thus of the sedimentation rate) results from a drop in the net supply of sand. The shell production on the shoreface was probably not affected by the diminishing of the progradation rate. Hence, the sedimentation rate of the sand decreased and the sedimentation rate of the shells remained constant, leading to an relative increase of shells. With the decrease of the progradation rate the relative intensity of wave reworking increased. The sediment was buried less fast and hence it took longer before it was out of reach of storm reworking. The more frequent reworking of the deposits means that more fine-grained sediments can be winnowed from the deposits. In other words, the increase in shell content and the increase in grain size are related to the decrease of the rate of progradation.

3.7 Conclusions

Pleistocene sands form the basis for Holocene coastal evolution. The Holocene transgressive back-barrier deposits consist mainly of tidal channel deposits. Locally remains of older transgressive deposits, i.e., Basal Peat and Clay have escaped erosion by tidal channels.

Transgressive offshore deposits are found in both cross sections, and consist of shoreface sand, coarse-grained offshore deposits and sand-mud laminations. The transgressive offshore deposits are more divers than the prograded offshore deposits. The transgressive offshore coarse-grained deposits are attributed to the formation of shoreface-connected ridges. Formation of these deposits was probably facilitated by the onshore sediment transport via tidal inlets. The deposition of sand-mud laminations was facilitated by depressions on the sea floor, left by the tidal-channel incisions, and by the overall quieter depositional conditions on the shoreface.

At the landward end of the cross sections a gradual transition is found of tidal-channel deposits of Unit 1 into to shoreface sands and beach deposits of Unit 2. These deposits mark the decrease in the influence of the tidal inlets during the end of transgression.

Prograded deposits consist of shoreface sands, breaker-bar and beach deposits. Beach-plain deposits and cross-bedded shoreface sands are abundant in Unit 3 in the Wassenaar cross section. The abundance of these deposits in the Wassenaar cross section is attributed to high progradation rates, which increase their preservation potential. In the Haarlem cross section beach-plain deposits are restricted to the landward side. A seaward increase in shell content and grain size is observed in the Haarlem cross section, which is related to the decrease of the rate of progradation. The decrease in progradation rate led to a relative increase in the input of shells, and allowed more time for the winnowing and removal of fine-grained sediment.

Chapter 4: Holocene coastal evolution in the Western Netherlands (II): Chronostratigraphy based on high-resolution AMS ¹⁴C dating of single shells.

Abstract

The chronostratigraphic framework of the Holocene coastal deposits in the western Netherlands has been refined with AMS radiocarbon dates of single shells. Selecting pristine juvenile shells from cores gives consistent dates, despite the fact that all shell material has been reworked prior to deposition. The sequence of Holocene coastal deposits consists of transgressive tidal deposits, overlain by transgressive offshore deposits, in turn overlain by prograded shoreface and beach deposits. The presence of transgressive shoreface deposits shows that the shoreface was already subject to intense wave reworking and thus that the presence of transgressive remnants in the North Sea was limited. Hence, transgressive remnants from the North Sea floor have contributed little to coastal progradation. Longshore sediment transport has played a dominant role in coastal progradation. The high progradation rates near Wassenaar are related to its proximity to the major sediment source in the South and to the proximity of an active Rhine branch. The lower progradation rates near Haarlem result from the reduction of the curvature of the shoreline and the resulting decrease in the imbalance of the longshore sediment transport. The steeper slope of successively younger isochrons in the Haarlem cross section is an artefact of the method.

4.1 Introduction

From Monster to Camperduin the shoreward edge of the western Netherlands coastal plain consists of transgressive deposits overlain by prograded shoreface and beach deposits. In chapter 2 we have described the facies development during the transition of transgression to coastal progradation near Ypenburg. In the previous chapter (Chapter 3) the deposits from the transgressive and prograded sequence in two coast-perpendicular cross sections near Wassenaar and Haarlem were portrayed. Previously, descriptions and interpretations of these deposits have been presented by Van Straaten (1965) for a cross section near The Hague and by Van der Valk (1992, 1996a) for a cross section near Haarlem. Basal Holocene deposits consist of peat and organic-rich clays and of tidal-flat and tidal channel deposits. These deposits originate from transgressive tidal back-barrier basins. The overlying deposits were formed seaward of the coastal barrier and on the beach. Directly on top of the tidal deposits coarse-grained offshore deposits and sand-mud laminations are found. Van Straaten (1965) suggested that these deposits were part of the transgressive coastal system. These deposits are in turn overlain by shoreface and beach deposits, which form part of the prograded coastal system.

From the 1950's onward ^{14}C dates have been used to date Holocene deposits. Initially the prograded nature of the shoreface and beach deposits from the western Netherlands was demonstrated with ^{14}C dates of peat from beach plains (Zagwijn, 1965). Van der Valk (1992, 1996a) presented the first ^{14}C dates of shell samples from transgressive and prograded deposits in a coast-perpendicular cross section south of Haarlem. He used conventional ^{14}C dating, which required shell samples of about 30 grams, and selected pristine shells of a single species from shell-rich intervals. The ^{14}C dates supported the prograded origin of the shoreface and beach deposits and enabled the reconstruction of palaeo-shoreface profiles. The reconstructed profiles of the palaeo-shoreface are increasingly steeper in the direction of progradation. The rates of progradation varied through time. A similar coast-perpendicular cross section with ^{14}C dates was constructed near Wassenaar (Roep *et al.*, 1991). The ^{14}C dates of the Wassenaar cross section indicate higher rates of coastal progradation than near Haarlem.

In this chapter we present the results of the AMS ^{14}C dating of single shells. The purpose of this chapter is threefold: 1) discuss the applicability of single-shell dating of shoreface and beach deposits ; 2) present a more detailed timeframe of deposition and erosion of the transgressive and prograded coastal deposits; and 3) demonstrate the implications of the detailed timeframe for the large-scale coastal evolution of the western Netherlands. The AMS ^{14}C dating technique allows to date carbonate samples of 10 mg, like for instance a single juvenile shell. The restriction to shell-rich intervals, that was imposed by the sample requirements of the conventional ^{14}C dating technique, is absent in the AMS ^{14}C dating technique. The detail in the timeframe is improved by dating of dense vertical-spaced shells samples from cores from the Haarlem cross section. The detailed timeframe was extended to series of cores from the modern shoreface. The Wassenaar cross section was continued seaward. Existing data from the cross sections were compiled and are presented together with the new data.

4.2 Shell dating.

Marine shells are commonly used for the dating of beach and shoreface deposits. Shells from these environments are seldomly found articulated and are even rarer found in situ, i.e., articulated and in living position. Most shells are found concentrated in shell layers, or concentrated on the basal laminae of storm layers (Kidwell, 1991a). Shell concentrations usually consist of a large percentage of shell fragments and worn shells (Kidwell, 1991a,

Kidwell, 1991b). All shell concentrations from beach and shoreface consist of shell material that is a mixture of fresh, recently deceased and older reworked material (Kidwell, 1991b, Roy, 1991). The ratio between fresh and old reworked material depends on the rate at which new shells are added and old shell material is being removed (by abrasion and wearing and by permanent deposition). This ratio influences the ages obtained from the dating of reworked shell material, which was demonstrated by the dating of shell mixtures (shells hash) from the Australian shelf (Roy, 1991).

Dating of shell mixtures with fresh and reworked material can demonstrate trends in deposition (cf. Roy, 1991), but will always render ages that are noteworthy older than the hosting deposits. This problem can be partly surpassed by selecting and dating small and fragile juvenile shells, if possible with the periostracum (thin organic cover on the outside of the shell) still in place. Shells with signs of wear (cracks, worn slot, or etched top surface) should be excluded. One may assume that such pristine and fragile shells have had a limited history of reworking and are only slightly older than the surrounding deposits (Van der Valk, 1996b, 1996a). The problem with conventional ^{14}C dating is the relatively large amount of fragile shells that is required. The AMS ^{14}C dating technique requires only 10 mg of carbonate for dating and thus allows dating of single juvenile shells. The dating of single shells has the advantage of picking a 'good looking' shell, permitting the exclusion of material that most certainly has been reworked. In addition, the small sample size permits the sampling of intervals with a limited shell content, allowing a higher sampling density. The disadvantage is that occasionally shells are selected that have miraculously survived reworking, without displaying signs of that history. Despite their good looks such shells are seriously older than the hosting sediment and thus render an age that is 'too' old.

The ideal shell species for the dating of shoreface and beach deposits prefer these habitats and are absent in others. On the modern Dutch coast *Spisula subtruncata* is found in abundance on the shoreface and on the seaward side of ebb-tidal deltas (Van Straaten, 1965, Eisma, 1966, De Bruyne and Van der Valk, 1991). The species is also abundant in Holocene shoreface and beach deposits. It does not prefer tidal back-barrier environments, and is almost absent in Holocene tidal deposits (Van Straaten, 1965, Van der Valk, 1996a). The abundance of *Spisula subtruncata* shells and its preference for shoreface and beach environments make it very suitable for dating. In some shoreface and beach deposits *Macoma balthica* shells are found in abundance (Van Straaten, 1965, Van Someren, 1988). Preferentially *Macoma balthica* inhabits tidal environments, but it may be found on the shoreface as well. If *Spisula* shells of sufficient quality were present these were preferred over *Macoma* shells.

4.3 Methods

Area & Sampling

In this study we focus on two coast-perpendicular cross sections, one at Wassenaar, just south of Leiden, and one near Haarlem, about 25 km to the North (Figure 3.2). In addition shoreface deposits from offshore cores in a coast-parallel cross section were dated. The coast-parallel cross section connects the two coast-perpendicular cross sections. The offshore cores were collected by Beets (1995) and Van der Spek (1999) using a vibracorer with a penetration depth up to 5.0 m. For abbreviations of core names see figures 2.1, 4.1 and 4.2.

Van der Valk (1992, 1996a) used shells from bailer samples for conventional ^{14}C dating. New shell samples for AMS ^{14}C dating were collected from all Haarlem cores and from the MD1 and MD2 cores near Wassenaar. The Wassenaar cores were not available for sampling. Sampling was based on the study of lacquer peels and photographs, to incorporate all possible shells. On average 4 samples were collected per meter, sample thickness varied from 2 to 10 cm. The sample thickness of core DMW is about 30 cm.

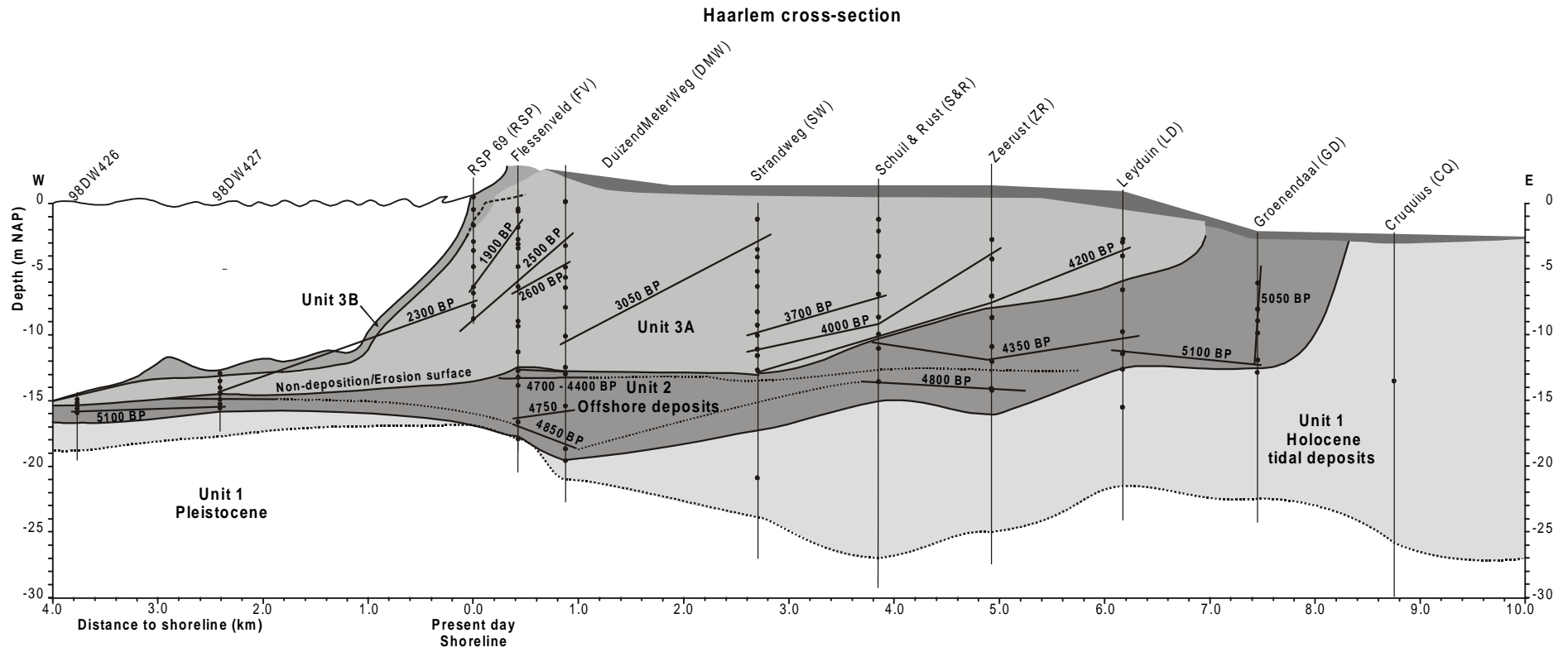


Figure 4.1 : Caption on following page.

The samples were sieved over a 2 mm mesh to separate shells from the sediment. Whenever possible, juvenile *Spisula subtruncata* with periostracum and without signs of damage or leaching were selected for dating. Articulated shells are considered to be the least transported and thus best for dating, but these were extremely scarce. The smallest sample size required for AMS ^{14}C dating is 10 mg of carbonate, so the sample had to consist of single juvenile shells of at least 10 mg. Whenever appropriate shells were lacking from an interval, shells of less favourable quality were used, to ensure full coverage of the shoreface to beach interval.

Dating

The selected shell samples were AMS-dated at Utrecht University (for a description of the method see Van der Borg *et al.*, 1987). The ages were normalised to their $\delta^{13}\text{C}$ values with respect to the PDB standard (age BP). The ages have been corrected for the marine reservoir effect by subtracting 402 years (Stuiver *et al.*, 1986, Stuiver and F., 1993, age (m) BP, marine corrected in Appendix A). A calendar age has been obtained by calibrating the marine-corrected age (Calib4 Stuiver and Reimer, 1993, cal BP, calibrated age in Appendix A). Throughout the text we use the denotation BP for $\delta^{13}\text{C}$ corrected ages, (m)BP for marine-reservoir-effect corrected ages and cal BP for calibrated ages. Please notice that the ages presented by Van der Valk (1992, 1996a) have not been corrected for $\delta^{13}\text{C}$ and marine reservoir effects on the assumption that the two effects even out (Mook, 1991). These ages should be comparable to our marine-reservoir-corrected ages.

4.4 Dates

The dates are presented in Appendix A. In addition to the newly obtained AMS dates (Van der Spek *et al.*, 1999, and unpublished), previously published dates are presented (Van der Valk, 1992, 1996a), as well as a number of unpublished dates that were made available by the Free University (Amsterdam, The Netherlands, Van der Valk, 1995). For each dating, the shell species is given, as well as a short description of shell size and condition. Unless indicated otherwise ('doublet'), the shells were not articulated.

The large number of AMS dates per core enables a check on the consistency of the dates: the dates should young in upward in the core. The rationale is simple: an older shell can be reworked and mixed with younger material, but there are hardly any natural processes that bring younger shell material from above into the sediments. In other words, the youngest shell material gives the best estimate of the age of final deposition (Goodfriend and Stanley, 1996). Shells that are older than underlying shells, but within the error range, are included in the dates. The check on the consistency of the dates shows that only a limited number of dates need to be removed for further analyses (Appendix Chapter 4). The largest numbers of out-of-sequence dates are found in the cores with the lowest sedimentation rates (table 4.1). When the sedimentation rates are low the reworking of older shell material is largest (Roy, 1991), and the chances of selecting a re-deposited older shell increase. Within cores MDI, GD, LD and ZR a large number of the dates fall within the error margins of succeeding samples. The intervals in these cores have very high sedimentation rates (> 1 cm/year). In these cases the sedimentation rate exceeds the resolution of the dating method.

Figure 4.1: Haarlem cross section, lines indicate cores, dots represent sample locations for ^{14}C dates, including dates of Van der Valk (1992; 1996). The topography of the land surface, i.e., the high dune cover, has been omitted. The samples of equal age have been used to construct isochrons (solid lines with age indications, all ages are in (m) BP). See figure 4.3 for a clear indication of hiatuses, and notice that the x-axis of the Wheeler diagram corresponds to that of the cross section. The three units are indicated in the figure in different shading. Hatched and stippled lines indicate extrapolations of isochrons and Unit boundaries.

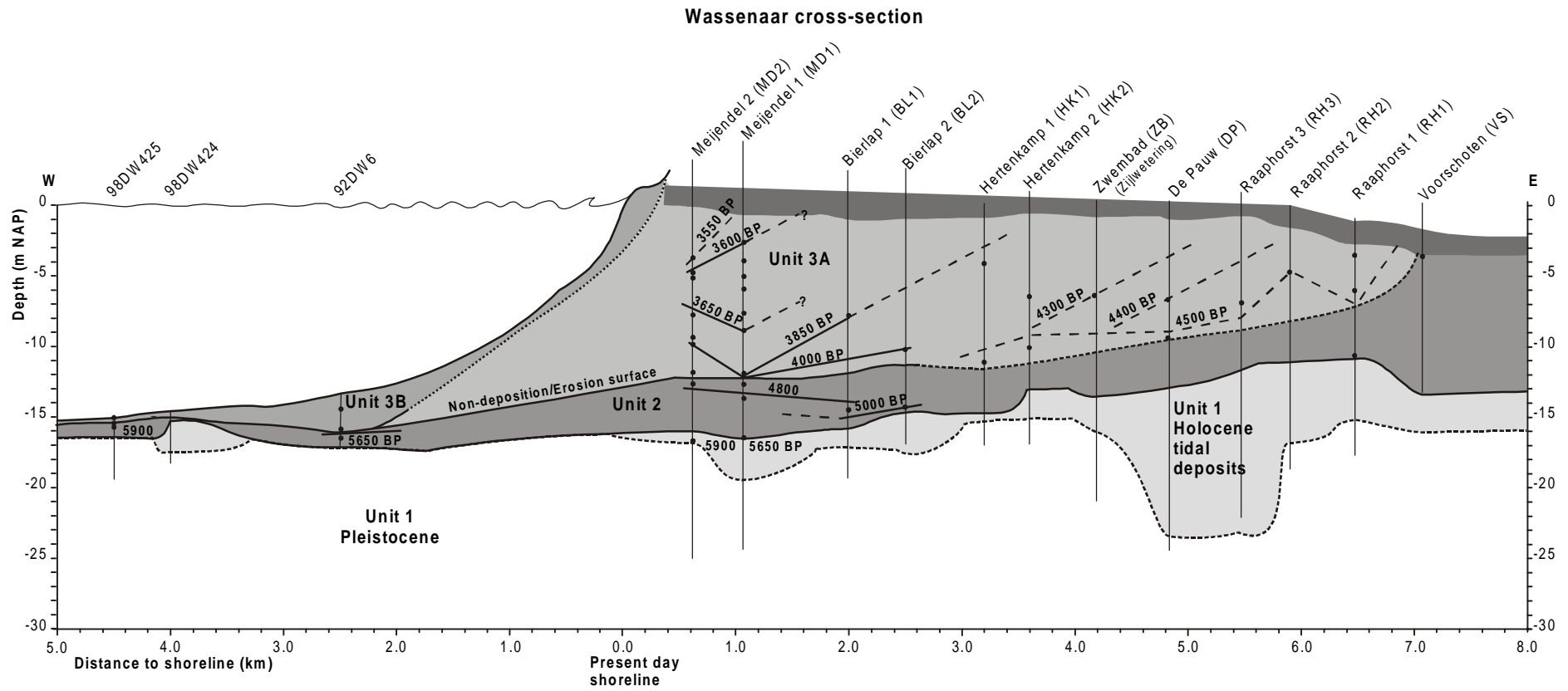


Figure 4.2: Caption on following page.

Comparison of the new AMS ^{14}C dates with the conventional ^{14}C dates in the Haarlem section indicates in most cases (13 out of 17) little difference between the ages (including errors). Older conventional ages are related to mixing of older shell material due to reworking and re-deposition. Younger conventional dates are related to the admixture of younger shell material from higher up in the borehole during the drilling. The use of bailer samples does not permit to distinguish between in-situ material and contaminations. In the analysis of the Haarlem cross section we only use the AMS ^{14}C dates. In the Wassenaar section the absence of AMS dates for the major part of the cores forces us to use the conventional ^{14}C dates.

The results of dating of single shells are good, especially given the fact that all dated material was reworked prior to deposition. The dates compare well with earlier obtained conventional ^{14}C dates and the internal consistency of the dates is usually good. Only a limited number of dates is older than underlying dates and had to be excluded from the analyses. This means that by selecting small, fragile shells with as little signs of transportation as possible, we have indeed excluded the major part of older reworked shell material from our sampling.

The out-of-sequence dates in core RSP may be related to the precipitation of 'old' carbonate from the groundwater on the shells. The out-of sequence dates originate from an interval with distinct red and black stains on shells and sand. The base of the red interval lies around -5 m NAP and the colouring increases and intensifies towards the top of the interval at -3 m NAP. At -3 m NAP the red colours give way to black, which continues to -2 m NAP. The overlying 4 m do not show colouring. The colouring most likely represents an oxygenation front, where iron-oxides followed by manganese-oxides precipitated. Distinct red and brownish colours of shells have been observed on the modern sea floor and in Holocene deposits and have been attributed to emerging groundwater at the sea-floor (Van Straaten, 1965). Associated with the emerging ground water carbonate precipitation occurs at the sea-floor, which is evident from the presence of pieces of recent sandstone with carbonate cement and mixed iron-oxide-carbonate cement on North Sea beaches (Van Straaten, 1957c, 1965). Oxygenation of emerging groundwater from the older dune and beach deposits just below the beach surface is a likely candidate for the formation of the red and black colouring in core RSP. It is not unlikely that under such conditions dissolved carbonate from older beach and dune deposits precipitated from the groundwater.

4.5 Cross sections

Throughout the text we use the subdivision in units 1, 2 and 3 that we have introduced in the previous chapter (Chapter 3), based on sedimentary characteristics, depositional environment and age. Unit 1 consists of Pleistocene sands, Holocene basal peat and clay and Holocene tidal deposits (Figure 3.10 and 3.11). The tidal deposits have a characteristic shell assemblage dominated by *Cerastoderma edule* and *C. glaucum*. The Holocene deposits of Unit 1 originate from transgressive tidal back-barrier basins.

Figure 4.2: Wassenaar cross section, lines indicate cores, dots represent sample locations for ^{14}C dates, including dates of Van der Valk (1992; 1996). Cores east of MD1 have a limited number of ^{14}C samples. The topography of the land surface, i.e., the high dune cover, has been omitted. The three units have been indicated and samples of equal age have been used to construct isochrons. Hatched and stippled lines indicate extrapolations of isochrons and Unit boundaries.

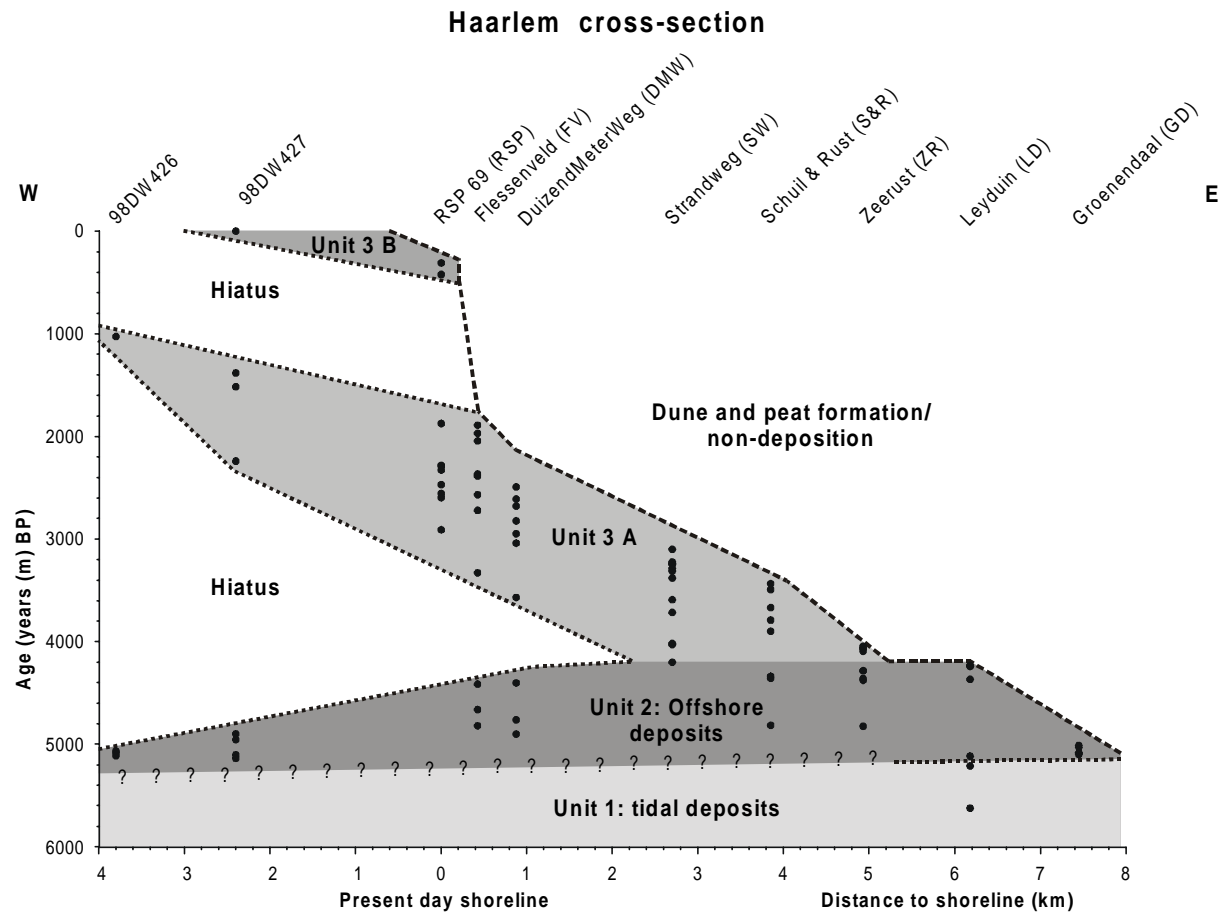


Figure 4.3: Wheeler diagram for the Haarlem cross section. The distance to the shoreline is plotted against the age of the samples. The interpreted units are indicated, see text for discussion. Deposits of Unit 3 consists of shoreface and beach deposits. Boundaries of hiatuses are stippled, boundary with overlying peat and dune deposits is hatched.

Unit 2 overlies Unit 1 and consists of shoreface, beach, and coarse-grained offshore deposits and sand-mud laminations (Figure 3.10 and 3.11). The deposits of Unit 2 originate from offshore depositional environments of the transgressive coastal system. Unit 3 consists of shoreface, beach and beach-plain deposits (Figure 3.10 and 3.11). These deposits were part of the prograded coastal system. *Spisula subtruncata* and *S. elliptica* dominate the shell assemblage of Unit 2 and 3. In the offshore cores modern North Sea sand overlies the deposits, while in the land-based cores peat and dune sand caps the prograded deposits.

The facies transition of Unit 2 to Unit 3 is well defined in the westward land-based cores of the Haarlem and Wassenaar cross sections, where shoreface sands disconformably overlie coarse-grained offshore deposits and sand-mud laminations (Chapter 3, figure 3.10 and 3.11). In the coast-parallel cross section a facies transition between Unit 2 and 3 is absent, as both units consist of shoreface sands. However, the hiatus between Unit 2 and 3 in the offshore covers a large time interval. At the landward sides of the coast-perpendicular cross sections a facies transition between Unit 2 and 3 is also absent. In these cores the boundary between the units was extrapolated from the hiatus (Figure 4.1 and 4.2).

Below we use the age of the samples to construct isochrons in the cross sections, to construct Wheeler diagrams (Wheeler, 1958, figure 4.3 and 4.4) and to estimate sedimentation and progradation rates. We only use the in-sequence dates, on the assumptions that out-of-sequence dates consist of reworked older material. In the Wheeler diagrams the locations of

the cores is plotted against the age of the samples (Wheeler, 1958). Where a small height interval between samples in a cross section is associated with a large time interval in the Wheeler diagram, non-deposition or erosion has taken place (compare figure 4.1 and 4.3, compare and figure 4.4 with 4.6). In other words, combined with a cross section the Wheeler diagram reveals hiatuses.

Table 4.1: Sedimentation rates of the analysed cores of the Haarlem cross section and of cores MD1 and MD2 from the Wassenaar cross section. The sedimentation rates are based on a best fit through age-versus-depth plots of the in-sequence dates from Unit 3 (see figure 4.5). The sedimentation rates of core GD are from Unit 2. The maximum and minimum age indicate the time interval for which the sedimentation rates were determined. Ages are given in cal BP, i.e., real years.

Core	Interval	n	maximum age (cal BP)	minimum age (cal BP)	sedimentation rate (cm/year)	R ²
RSP	0,5 - -9,0 m	5	2707 - 2613 BP	398 - 295 BP	0,39	0,994
FV	-1,5 - -11,5 m	5	3685 - 3578 BP	1928 - 1838 BP	0,50	0,923
DMW	-3,0 - -12,5 m	5	3989 - 3879 BP	2718 - 2666 BP	0,71	0,907
SW	-3,5 - -13,0 m	6	4837 - 4798 BP	3406 - 3333 BP	0,50	0,837
S&R	-1,0 - -11,5 m	6	5029 - 4876 BP	3909 - 3813 BP	0,59	0,878
ZR	-2,5 - -12,0 m	6	5110 - 5107 BP	4683 - 4528 BP	1,78	0,801
LD	-2,5 - -10,0 m	4	5048 - 4953 BP	4864 - 4811 BP	3,47	0,785
GD	-6,0 - -12,0 m	5	5913 - 5853 BP	5905 - 5839 BP	3,90	0,641
MD I	-2,5 - -12,0 m	7	4387 - 4270 BP	4056 - 3930 BP	2,17	0,585
MD II	-3,5 - -10,0 m	5	4381 - 4432 BP	3979 - 3830 BP	1,24	0,868

4.5.1 Haarlem cross section

Cross section and Wheeler diagram

The tidal deposits of Unit 1 are older than the overlying deposits of Unit 2, i.e., older than 5100 (m) BP. In core LD there is no hiatus between Unit 1 and Unit 2 (Figure 4.3), but this is not necessarily so in the other cores. The age of Unit 2 ranges from 5100 (m) BP to 4200 (m) BP. The isochrons in the offshore and shoreface deposits of Unit 2 are more or less horizontal (Figure 4.1). The one isochron in Unit 2 that runs up from shoreface into beach deposits in core GD is near vertical (Figure 4.1), because the age of the samples is almost identical (maximum difference of 77 years). The ages from the coarse-grained offshore deposits (Chapter 3) in Unit 2 are higher than 4660 ± 44 (m) BP and overlying deposits are invariably younger than 4412 ± 47 (m) BP. The top of the coarse-grained offshore deposits is therefore regarded as a condensed horizon of 4700 to 4400 (m) BP. The condensed horizon is interpolated through the intermediate SW core, in which the coarse-grained offshore deposits are absent. Within the shoreface and offshore deposits of Unit 2 the age of the seaward samples is slightly higher than the age of the landward samples.

In the seaward half of the cross section a large hiatus is present, which is clearly visible in the Wheeler diagram (Figure 4.3). The hiatus separates shoreface deposits of around 5000 (m) BP of Unit 2 from shoreface deposits with ages around 2000 to 1000 (m) BP of Unit 3. The hiatus between Unit 2 and Unit 3 in the western half of the cross section has a near horizontal orientation. The hiatus that splits Unit 2 from Unit 3 diminishes eastward (Figure 4.3). The landward-correlative conformity of the hiatus lies around 4200 (m) BP (Figure 4.1).

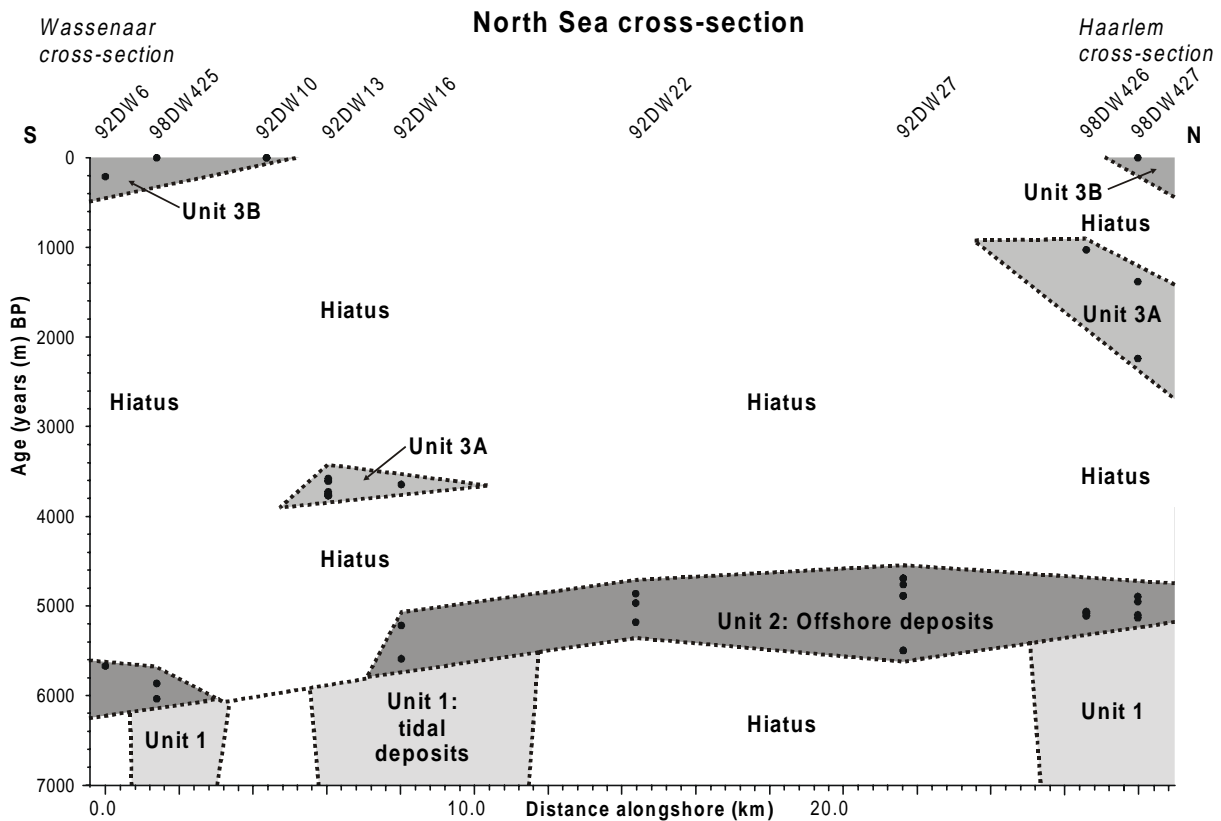


Figure 4.4: Wheeler diagram of the North Sea cross section, with the distance from the shoreline versus the age of the samples. The interpreted units are indicated, Unit 3 consists of shoreface deposits. Boundaries of hiatuses are stippled and the boundary with overlying peat and dune sand is hatched. Hiatuses make up a major part of the sequence in the North Sea cores.

The age of the shoreface and beach deposits of Unit 3 decreases seaward, from 4200 BP to 400 BP. The isochrons in Unit 3 dip seaward and the youngest isochrons in Unit 3 have a steeper slope than the older ones (Figure 4.1). In cores RSP and 98DW427 a hiatus of about 1000 years is present in the deposits of Unit 3 (Figure 4.3). Unit 3 is subdivided into Unit 3A with deposits up to 1000 (m) BP and Unit 3B with all deposits in between 1000 (m)BP and recent.

Sedimentation & progradation rates

In figure 4.5 A and B the age (in calendar years, cal BP) of the samples from cores RSP and LD are plotted against their depth. The best-fit through the in-sequence samples gives the net sedimentation rate for that time interval. Net sedimentation rates encompass sedimentation, non-deposition and erosion. The large jump in age from about 6000 to 5000 cal BP in core LD is accompanied by limited difference in height (Figure 4.1) and represents an interval of non-deposition or erosion. The sedimentation rates from the intervals without the hiatus have been estimated by a best fit through the in-sequence dates. The sedimentation rates for all Haarlem cores are presented in table 4.1. Sedimentation rates are highest at 3.90 cm/year in the easternmost core GD and decrease westward. The sedimentation rates increase again in core DMW but decrease even further west down to 0.39 cm/year in RSP. The absence of in-sequence dates from -6.0 to -0.5 m in core RSP makes the sedimentation rate less reliable than suggested (table 4.1).

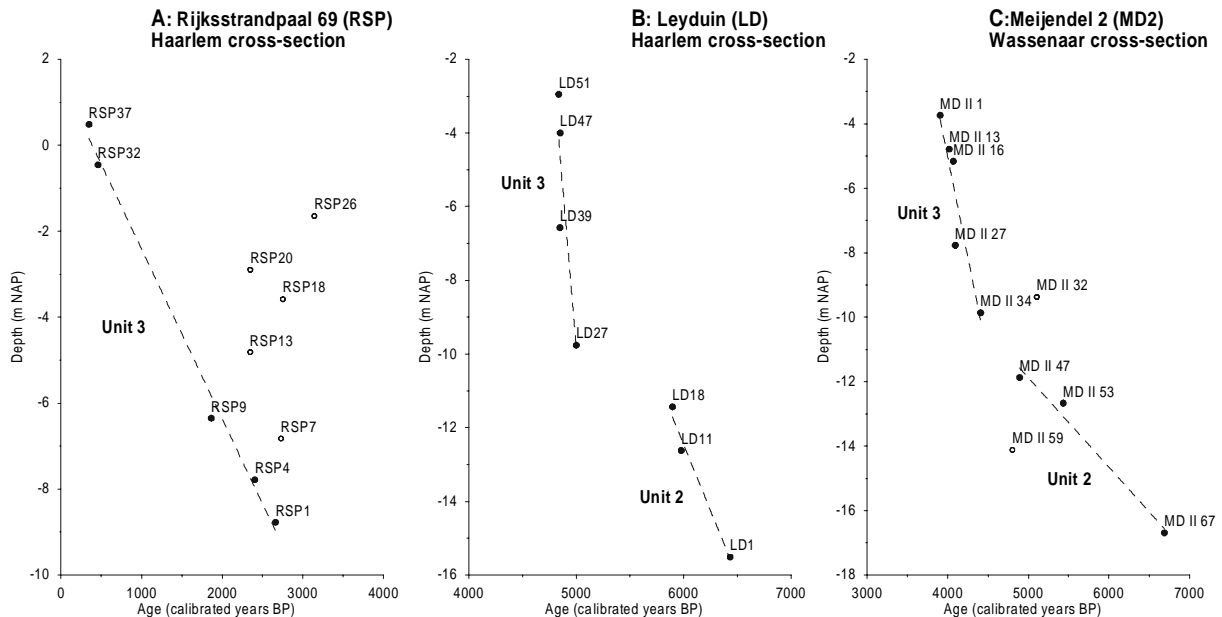


Figure 4.5: Graphs of the depth versus the age of the samples of two cores from the Haarlem cross section and one from the Wassenaar cross section. The closed dots represent dates that are younger than the underlying dates (in-sequences dates), and the open dots represent dates that are older than underlying dates (out-of-sequence dates). The hatched lines are best fits through the in-sequence dates that render sedimentation rates of the deposits. A steep line represents a high sedimentation rate. The sedimentation rates have been calculated separately for units 2 and 3. The sedimentation rates from Unit 3 are given in table 4.1. Ages are given in cal BP, i.e., real years.

The age of samples at similar heights in the different cores gives an estimate of the horizontal sedimentation rate or progradation rate. The advantage of this method instead of using the isochrons is that all samples are used and the accuracy of method can be determined. The highest and lowest ages used for the estimate limit the age range for which the progradation rate is valid. We have used samples from Unit 3A and used height intervals of 2.5 m. The results are presented in table 4.2, including the standard deviations of the fits. Progradation rates are highest for sample intervals with the oldest age range (5000 to 3600 cal BP: 2.53 m/year); younger age ranges give progressively lower progradation rates (down to 1.08 m/year for 3850-350 cal BP).

4.5.2 North Sea cross section

Cross section and Wheeler diagram

In the construction of the along-shore cross section (Figure 4.6) we have used cores from more or less similar water depths. Cores 92DW10 and 98DW427 that are used in the Wheeler diagram (Figure 4.4) have been omitted from the cross section (Figure 4.6) because they originate from deviating water depths. In the Wheeler diagram of the North Sea cross section (Figure 4.4) three groups of dates can be recognised in the shoreface deposits of units 2 and 3. These groups are separated by large hiatuses.

The Holocene tidal deposits of Unit 1 occur locally, and have ages over 6100 to 5200 (m) BP. The boundary between tidal deposits and Pleistocene deposits within Unit 1 varies, it lies around -16.5 m NAP near the Wassenaar cross section, and around -19 m NAP in the Haarlem cross section. The boundary between the shoreface deposits of Unit 2 and the underlying tidal deposits and Pleistocene of Unit 1 lies around -17 m NAP. Unit 2 displays a

clear trend from older in the southern part (6100 to 5600 (m)BP) to younger in the northern part (5200 to 4700 (m)BP).

The boundary between the old shoreface deposits of Unit 2 and the young shoreface deposits of Unit 3 or modern North Sea sand varies around –16 m. In the middle part of the cross section shoreface deposits of Unit 3 with ages from 3800 to 3600 (m)BP are found. Another group is formed by relatively young shoreface deposits that range in age from 2300 (m)BP to recent, which are restricted to the southern and northern edges of the cross section. The limited number of samples with an equal age and the thin intervals hinder the construction of isochrons. The thickness of the overlying recent North Sea sand varies from 0.75 to 0 m.

Table 4.2: Progradation rates of a number of 2.5 m thick intervals from the Haarlem cross section. The progradation rates are based on a best fit through the age-versus-distance from the shoreline plots of the in-sequences dates. The maximum and minimum age indicate the time interval for which the progradation rates are valid. Ages are given in cal BP, i.e., real years.

Interval	n	maximum age (cal BP)	minimum age (cal BP)	progradation rate (m/year)	R ²
0.5 - -2.0 m	4	3909 - 3813 BP	398 - 295 BP	1,08	0,893
-2.0 - -4.5 m	8	4895 - 4809 BP	2718 - 2666 BP	2,15	0,945
-4.5 - -7.0 m	7	4890 - 4808 BP	1900 - 1828 BP	2,05	0,941
-7.0 - -9.5 m	9	5046 - 4937 BP	2471 - 2335 BP	2,13	0,973
-9.5 - -12.0 m	9	5063 - 4957 BP	3685 - 3578 BP	2,53	0,787
-12.0 - -14.5 m	7	5075 - 4966 BP	0 BP	1,43	0,829

4.5.3 Wassenaar cross section

Cross section

For the construction of the Wassenaar cross section (Figure 4.2) conventional ¹⁴C dates were used for the eastern half of the cross section. The limited number of dates in the Wassenaar cores hinders the construction of a useful Wheeler diagram.

Unit 1 has an age over 5900 (m) BP. Basal Peat is found around –15 m NAP. When we relate the formation of the Basal Peat to the Holocene rise in sea level (Jelgersma, 1979) this correlates to an age of 7400 BP. The one dated sample from the tidal deposits (RHI10A: 6745 ± 105) is noticeably older than 5900 (m) BP. The age of Unit 2 ranges from 5900 (m) BP to 4500 BP. Ages of 5900 (m)BP and 5650(m) BP in shoreface deposits of Unit 2 are found at comparable heights, and have been indicated in the cross section (Figure 4.2). Furthermore, two near-horizontal isochrons can be constructed with ages of 5000(m)BP and of 4800 (m) BP.

The subdivision of offshore and shoreface deposits in Unit 2 and 3 is straightforward in cores MD 1 and MD2, where the sharp break in the facies, from coarse-grained offshore deposits to shoreface deposits, is associated with a shift in age from 5900 to 4600 (m)BP to 4300 to 3500 (m)BP. The sharp facies transition is also visible in cores BL1 and BL2. East of core BL2 the boundary between Unit 2 and Unit 3 is not well constrained, due to a lack of dates and the absence of sharp facies transitions. The boundary has been drawn below the dates of 4500 BP, and runs smoothly up to –4 m NAP in between cores RH1 and VS. In the offshore cores old shoreface deposits of Unit 2 are found, overlain by very young shoreface

deposits of Unit 3. Shoreface deposits of Unit 3 with an age that corresponds to the age of shoreface deposits in the land-based cores are absent in the offshore cores.

The age of Unit 3 ranges from 4500 BP to 3550 BP. In the beach and shoreface deposits of Unit 3 two seaward-dipping isochrons have been drawn through samples with ages of 4300 and 4400 BP, and an isochron has been constructed through several samples with ages around 4500 BP. The isochron of 4500 BP displays a bump in core RH2, which coincides with the occurrence of cross-bedded shoreface deposits. Given the limited number of dates, the reliability of these isochrons is very limited. Within the shoreface and beach deposits of cores MD1 and MD2 a larger number of isochrons can be constructed with more confidence. Most of the isochrons dip seaward, apart from isochrons of 3650 and 3850 (m) BP in the cross-bedded shoreface deposits, which dip landward.

Progradation rates & sedimentation rates

Due to the limited amount of dates in the cores landward of MD 1 the progradation rates can not be estimated by a best fit from a depth-versus-distance plot. However, tentative progradation rates were determined from the isochron spacing. Progradation rates in the Wassenaar cross section range around 5 m/year (an age of about 4500 (m)BP for RH2 and an age of about 3500 (m)BP for MD2, over 5.2 km). The large number of dates on the Meijendel cores does permit an estimate of the sedimentation rate (Figure 4.5 C, MD2, and table 4.1). The Meijendel cores have different sedimentation rates in units 2 and 3. Unit 2 has relatively low sedimentation rates (0.27 and 0.33 cm/year); Unit 3 has high sedimentation rates of 2.17 and 1.24 cm/year.

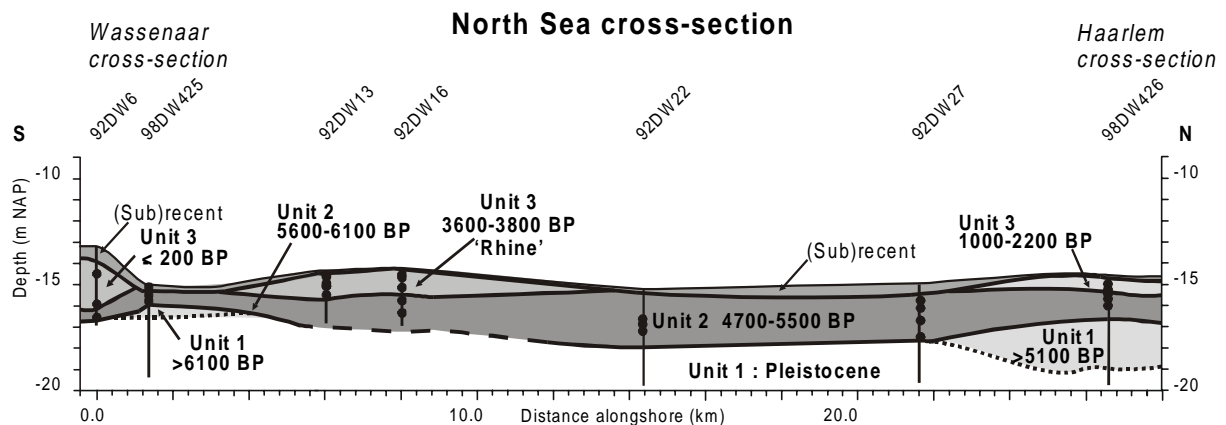


Figure 4.6: North Sea cross section from a depth of -15 m NAP on the modern shoreface (figure 2.1 for location of cores). The lines indicate cores, dots represent sample locations for ^{14}C dates. Two of the cores that are plotted in the Wheeler diagram of the North Sea (figure 4.4) have not been included in the cross section, because their depths deviate from the cross section. Three units have been distinguished, based on facies characteristics and hiatuses. See figure 4.4 for a clear indication of hiatuses. Hatched and stippled lines indicate extrapolations of Unit boundaries.

4.5.4 Previous work.

The reconstructed large-scale evolution is similar to that of prior investigations of these deposits (Van Straaten, 1965, Van der Valk, 1992, 1996a, Chapter 3), i.e., the deposits originate from a transgressive coastal system and a succeeding prograding coastal system. The The Hague cross section is located some 6 kilometres south of the Wassenaar cross section. Van Straaten (1965) based his reconstructions on lithological and palynological (Zagwijn, 1965) correlations, as ^{14}C dates from the cross section were not available. The entire sequence in the The Hague cross section is similar to the sequence in the Wassenaar cross section. The correlations and sedimentological reasoning lead to a reconstructed coastal evolution deposition well comparable to ours (Van Straaten, 1965, his figure 26). The tidal deposits originate from the transgressive coastal system, these are overlain by coarse-grained offshore deposits of the transgressive shoreface, which in turn are overlain by prograded deposits. Given the similarity of the Wassenaar and the The Hague cross sections, the similarities in reconstructed coastal evolution are no surprise. However, the improved chronostratigraphy gives a much more rigid support of these interpretations.

A previous isochron chart of the Haarlem cross section was presented by Van der Valk (1992, 1996a). The number of (conventional) ^{14}C dates was limited to 24. Most ages of the deposits obtained with the AMS ^{14}C dating are comparable to the ages obtained with conventional ^{14}C dating by Van der Valk (1992, 1996a, see section on dates). Van der Valk (1992, 1996a) used the assumption that the geometry of the isochrons was roughly similar to the modern shoreface profile to interpolate isochrons with an interval of 200 years in between the ^{14}C dates. Van der Valk (1992, 1996a) ascribed deposits interpreted here as transgressive offshore deposits, to coastal progradation. He recognised two truncations of isochrons, from 3800 to 3600 BP and from 2800 to 2600 BP. These truncations were not recognised in our cross section (Figure 4.1). The inferred truncations likely resulted from the interpolation of the very limited number of dates. The steepening of the isochrons from old to young, observed in the cross section of Van der Valk (1992, 1996a) and in our cross section (Figure 4.1) is discussed below.

4.5.5 Holocene coastal evolution

The basal part of the Holocene deposits in the Haarlem and Wassenaar cross sections originates from the period of transgression, and the overlying deposits originate from the phase of progradation (Chapter 3). The Holocene coastal evolution is sketched in figure 4.7 B to F. The tidal deposits of Unit 1 originate from a back-barrier setting and from the tidal inlet (Figure 4.7 A). The offshore deposits of Unit 2 originate seaward of the coastal barrier (shoreface and shelf in figure 4.7 A). The overall succession of Unit 1 overlain by Unit 2 is transgressive and from Unit 1 to Unit 2 the shoreline has traversed the location of the cross section (Figure 4.7 B and C). The succession of offshore deposits from Unit 2, overlain by shoreface and beach deposits of Unit 3 represents the shift to coastal progradation (Figure 4.7 E and F). The detailed timeframe presented above increases the detail in the timing of deposition of Unit 2 and 3.

The mechanism for the shift of transgression to progradation during the Holocene coastal evolution has been presented by Beets *et al.* (Beets *et al.*, 1992, 1994) and Beets and Van der Spek (2000). These authors suggest that the imbalance between the accommodation space in the back-barrier basins, controlled by sea-level rise, and the sediment supply to the basins controlled the coastal retreat (see Chapter 1 for a more elaborate summary). Transgression ended when the back-barrier basins were filled-in and hence sediment demand from the offshore diminished. The decrease in demand resulted in a surplus of sediment supply to the beach and shoreface and hence resulted in the start of progradation. As the back-

barrier basins silted up and their tidal volume decreased, the size and extent of the tidal inlets and tidal channels diminished. Eventually the tidal inlets closed completely. In other words, the shift from transgression to progradation is associated with the closure of tidal inlets. The closure of the tidal inlet of the Haarlem area was reconstructed by Van der Valk (1992, 1996a). An example of inlet closure prior to coastal progradation in the Alkmaar Bergen region, North of Haarlem, was presented by Westerhoff *et al.* (1987) and Beets *et al.* (Beets *et al.*, 1996b), and the closure of the tidal inlet in the Ypenburg area (Chapter 2) presents another example.

Unit 2

All deposits in Unit 2, apart from those in cores GD and VS represent deposition in deeper water, and all show distinct wave influences. The offshore deposits of Unit 2 represent a transgressive evolution over the underlying tidal deposits of Unit 3. The distribution of dates in Unit 2 does not display a distinct trend, as, for instance, samples with an age of 5100 (m) BP are found at both ends of the Haarlem cross section. In the Haarlem cross section the deposits of Unit 2 fill in the bumps that were left on the sea floor by the transgressive coastal system (Figure 4.7 D). This is especially clear in the landward dipping isochron of 4850 (m) BP, which is overlain by younger horizontal isochrons.

In cores GD and VS a gradual transition of tidal deposits of Unit 1 into shoreface and beach deposits of Unit 2 was observed (Chapter 3). The transition of tidal deposits to shoreface and beach deposits was related to the closure of tidal inlets. The deposits of Unit 2 can be considered to be the first prograded coastal deposits, dating from after the deposition of Unit 1 and originating seaward from the shoreline. Alternatively, the deposits can be regarded as the transition stage from Unit 1 to Unit 2. The closure of the tidal inlets did not occur synchronous alongshore (see for instance the closure of the Ypenburg tidal channel, in Chapter 2). The gradual transition from tidal-channel to shoreface deposits observed in cores GD and VS resulted from an alongshore shift of the position of the inlet and from the decrease of the cross section of the tidal inlet. In other words, locally the transgression of the tidal inlet system halted and transition to shoreface and beach deposition occurred, but further alongshore the inlet was still present and transgression continued. We therefore suggest that the shoreface and beach deposits in Unit 2 do not yet represent a full scale alongshore transition to coastal progradation, but rather represent a stage of transition.

Unit 3

Unit 3 contains seaward-dipping isochrons of increasingly younger age from land to sea and was deposited by the prograding coastal system (Figure 4.7 E and F). Associated with the progradation, erosion or non-deposition occurred at the transition of the lower shoreface to North Sea shelf (Figure 4.7 E). The likely cause for the erosion was the tidal reworking of the North Sea floor and the lowermost shoreface (Van Straaten, 1965). The erosion or non-deposition resulted in the formation of the large hiatus between units 2 and 3. The landward decrease of the hiatus represents the time between the last deposition of the transgressive coastal system and the first deposition of the prograded coastal system. An estimate of the amount of erosion at the location of the hiatus is difficult to give; however, the volume that was eroded has never been so large that it hindered wave action more landward, and its height must have been restricted.

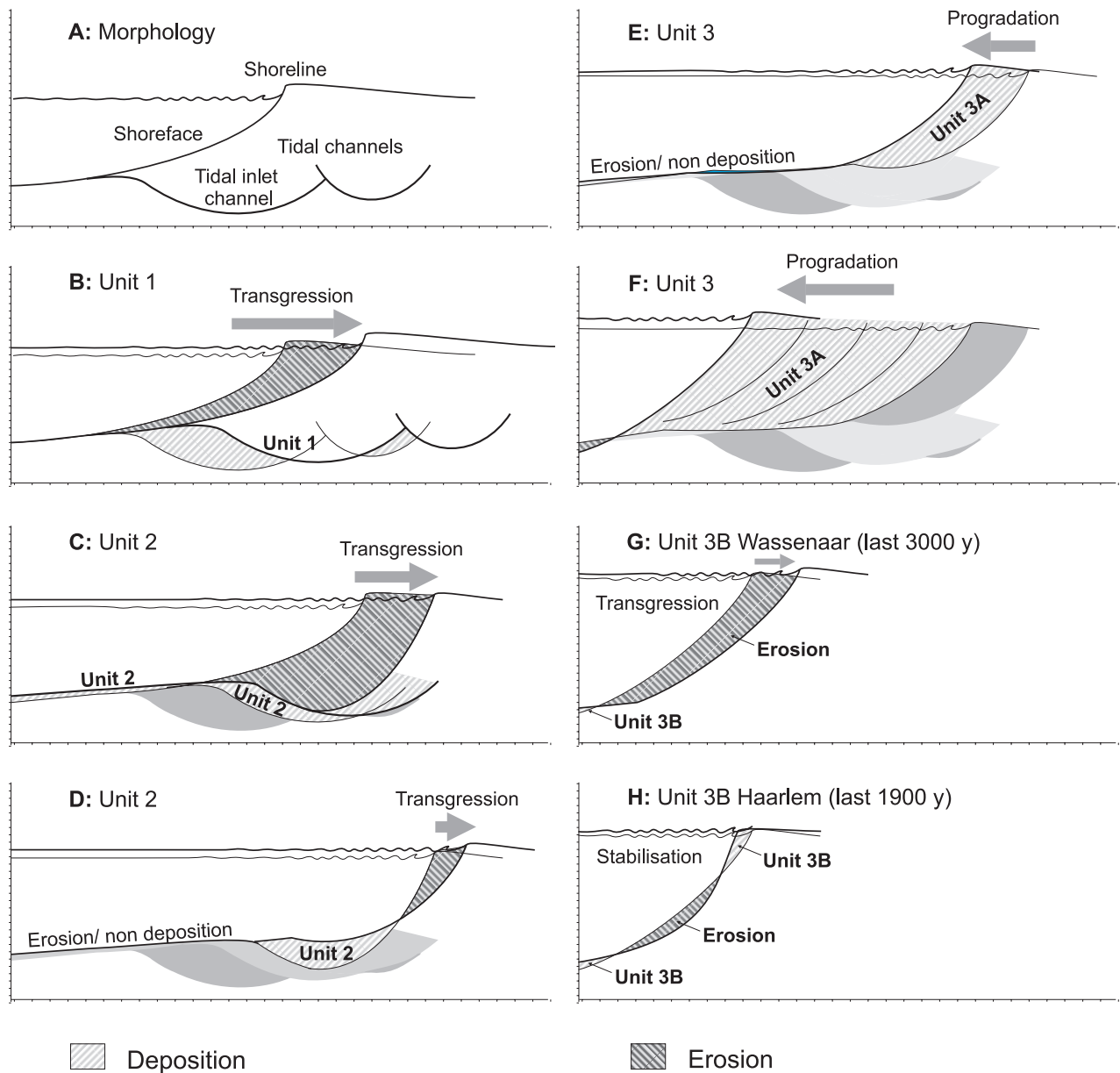


Figure 4.7: Cartoon with the interpreted large-scale coastal evolution of the Western Netherlands. A) Indication of the depicted morphology; tidal deposition is envisaged in incised channels. B) Transgression with deposition of tidal channels of Unit 1. All deposits from the shoreface were eroded during ongoing coastal retreat. C) Decrease in the rate of coastal retreat. Tidal deposition of Unit 1 has ended in the area of the cross section, and shoreface deposits are preserved on the lower shoreface. D) Limited coastal decrease and deposition of shoreface sediments in the remainder of the incised tidal channel. E) Onset of progradation, i.e., the start of deposition of Unit 3A. In the left half of the cross section only limited deposition takes place and a large hiatus develops. F) Continuous progradation and the deposition of Unit 3A. The area of non-deposition or erosion on the lower shoreface and shelf is gradually buried under prograded deposits. G) Coastal evolution of the last 3000 years of the Wassenaar area, where erosion has removed part of the prograded deposits. Only on the shoreface some younger deposits are preserved. H) Possible scenario of the coastal evolution in the Haarlem region, with ongoing deposition on the beach, breaker bar and lower shoreface, and erosion on the middle shoreface. See the text for a discussion of the genesis of Unit 3B.

Offshore

In the coast-parallel cross section (Figure 4.6) the deposits are similar to the offshore stretches of the coast-perpendicular cross sections: Tidal deposits of Unit 1 are overlain by shoreface sands of Unit 2, which in turn are overlain by shoreface deposits of Unit 3, with a large hiatus in between. The presence of Unit 1 is very localised, which is related to the local incision by tidal channels and tidal inlets from which these deposits originate (Beets *et al.*, 1995). The transgressive shoreface deposits of Unit 2 become progressively younger from south to north (Beets *et al.*, 1992). Transgression ended earlier in the south, which is reflected in the age of the transgressive shoreface deposits.

Within Unit 3 marked age differences occur. In the seaward part of the Wassaenaar cross section deposits of Unit 3 with a similar age as Unit 3 in the land-based part are absent. Unit 3 on the modern shoreface consists of recently deposited material. This reflects either that limited further seaward progradation of Unit 3 occurred, or that erosion effectively removed all traces of progradation. A combination of limited progradation and effective erosion is also possible (Figure 4.7G). In the Haarlem cross section deposits of Unit 3 have partly similar ages as Unit 3 in the land-based cores, i.e., the shoreface deposits of the prograded coastal system extend down below the modern shoreface. In addition recently deposited shoreface sands are present. In between the Wassaenaar and Haarlem cross sections recently deposited shoreface sands are absent in the cross section (Figure 4.4 and 4.6).

In two cores north of the Wassaenaar cross section, fronting Katwijk, deposits of Unit 3 with an age around 3700 (m) BP are present. The location lies seaward of the former Rhine outlet at Katwijk, where the outward curving and truncated beach-plain and beach-ridge pattern suggests that a wave-dominated delta has been present. Unit 3 in these cores likely originates from the progradation of the wave-dominated delta into the area. The associated middle-shoreface, upper-shoreface, beach and beach-plain deposits have been eroded.

4.6 Discussion

4.6.1 Sediment transport

Beets *et al.* (1992) estimated the volume of shoreface and beach deposits to be $9 \cdot 10^9 \text{ m}^3$. The authors did not distinguish between the transgressive deposits of Unit 2 and prograded deposits of Unit 3. However, when regarding sediment sinks in order to deduce sediment sources for coastal evolution, the distinction between Unit 2 and Unit 3 is important. We will not try to estimate the volumes in Unit 2 and 3, given uncertainties and alongshore differences in the boundaries between Unit 2 and 3. It is sufficient to conclude that the volume of prograded shoreface and beach sediments is less than $9 \cdot 10^9 \text{ m}^3$.

The deposits in Unit 2 represent the offshore parts of the transgressive coastal system. In the transgressive coastal system a major part of the sediment was transported onshore through the tidal inlets (Beets *et al.*, 1992). Coarse-grained offshore deposits are an important part of Unit 2. Following Van Straaten (1965) we have suggested that the coarse-grained offshore deposits were deposited on shoreface-connected ridges (see previous chapter), and it is likely that their formation was facilitated by the onshore-directed sediment transport. In other words, it is likely that the coarse-grained offshore deposits originate from cross-shore sediment transport.

According to Beets *et al.* (1992) the sediment for coastal progradation was supplied by longshore sediment transport from erosive promontories, by cross-shore sediment transport from the North sea floor and from relic offshore ebb-tidal delta sand bodies of the former transgressive coastal system. The presence of shoreface deposits in Unit 2 below the modern shoreface, suggests that wave action was severe enough to form storm beds. This implies that

the North Sea was by that time already devoid of remnants of the transgressive system, down to a depth of about -15 m NAP, which in turn suggests that the contribution of offshore erosion of transgressive ebb-tidal delta sand bodies has been limited. The only ebb-tidal deposits recognised in the subsurface are found in the vicinity of a former tidal inlet near Castricum (Westerhoff *et al.*, 1987, Beets *et al.*, 1996b). These deposits have been buried under prograded shoreface deposits and thus can not have contributed to progradation.

Based on the above arguments relic ebb-tidal delta deposits have not contributed to coastal progradation. The sediment balance for coastal progradation is now reduced to the contributions of the cross-shore and long-shore sediment transport. An important observation on the prograded shoreface and beach deposits is the presence of a fine-grained middle shoreface zone, which does not contain traces of grains larger than $150\ \mu\text{m}$ (see Chapter 5 for an extensive discussion). This zone is present in the westernmost stretch of the Haarlem cross section, and is even more pronounced in the eastern half of the Haarlem cross section and in the entire Wassenaar cross section (Chapter 3). Van Straaten (1965) also observed a fine-grained zone in the prograded deposits of The Hague cross section. The implication of the fine-grained middle shoreface zone is that it is unlikely that coarse-grains ($> 150\ \mu\text{m}$) have traversed the shoreface (Van Straaten, 1965). Coarse grains from the North Sea floor have thus not contributed to coastal progradation, or in other words, all coarse grains in the prograded upper shoreface and beach deposits must have originated from longshore sediment transport.

The deposition that resulted from gradients in the longshore sediment transport imposed by the curvature of the shoreline, has been calculated by Zitman (1987). These calculations have been used by Beets *et al.* (1992) and Van der Spek (1995) to derive an upper limit for the contribution of longshore sediment transport to progradation. Their estimates suggest that up to 35 to 40 % of the prograded deposits have been contributed by longshore sediment transport. Zitman modelled the longshore sediment transport along a slope of 1:100 and 1:200, while shoreface slopes of 1:300 or more gentle may be more realistic for initial progradation (see Chapter 6). The applied transport formulation is also the intermediate of three formulations, and it is unclear which one would be better applicable. So, the modelled longshore sediment transport does not present an upper threshold, and we suggest that the contribution of the longshore sediment transport may have been larger than the estimates presented by Beets *et al.* (1992) and Van der Spek (1995).

During a major part of the phase of progradation, the lowermost parts of the shoreface in the Haarlem and Wassenaar cross sections have been dominated by non-deposition or erosion (Figure 4.1 and 4.2). An estimate of the volume of eroded sediments cannot be given. There is no reason to assume that the sediment that has been eroded at the lowermost parts of the shoreface has contributed directly to progradation of the upper shoreface and beach through cross-shore sediment transport.

4.6.2 Sediment sources for progradation

Based on the above arguments, longshore sediment transport is thought to be the dominating contributor to coastal progradation. Offshore transgressive ebb-tidal delta sand bodies have not contributed to progradation. In the prograding coastal system the erosion of soft-sediment promontories north and south of the coastal stretch became the dominating source of sediments. In the south deposits in the incised Rhine/Meuse valley formed a soft promontory. This promontory protruded at least until 3500 BP, as is evident from the truncation of seaward curving beach ridges south of The Hague (Beets *et al.*, 1992). In the north the glacial deposits in the Texel headland formed a soft rock promontory. The beach ridges that extend from the former Texel headland indicate that some sediment was transported from the headland to the

south. Most of this material was probably funnelled directly in the Alkmaar Bergen tidal inlet (Beets *et al.*, 1992, Beets *et al.*, 1996b). During the last stages of progradation (some time after 3500 BP) the protrusion formed by the Rhine outlet near Katwijk was eroded.

Deposition of the prograding coastal stretch was controlled by imbalances in the longshore sediment transport, which were imposed by the curvature of the shoreline (Zitman, 1987). Initially the soft-sediment promontories and the transgressed stretch in between formed a strong imbalance in the longshore sediment transport, which resulted in high rates of deposition. With the ongoing erosion of the promontories and the progradation in between, the imbalance in the longshore sediment transport decreased and consequently, the rate of progradation decreased (Beets *et al.*, 1992).

Two factors complicate this simple pattern. First, the transition from transgression to progradation did not occur simultaneously alongshore. This implies that tidal inlets still acted as major sediment sinks in the transgressive parts, while other parts already prograded (Beets *et al.*, 1992). Part of the alongshore-transported sediment was funnelled into the transgressive back-barrier basins and did not contribute to progradation. Secondly, the activity of the Rhine outlet near Katwijk interacted with the longshore sediment transport on the coastal stretch and influenced progradation.

The seaward curvature of the beach ridges and beach plains around the Rhine outlet shows its importance for the regional progradation. Coastal progradation near the outlet has continued several kilometres west of the modern day coastline. The pattern of beach ridges and beach plains around Katwijk has the appearance of a wave-influenced delta (Galloway, 1975). The phase of major activity of the Old Rhine branch started around 4600 BP (Törnqvist, 1993). Major activity in the Old Rhine branch continued until around 2900 to 2600 BP, when the Vecht system became a major Rhine branch (Törnqvist, 1993). Part of the fluvial influence may have consisted of the direct supply of sediment to the area. The Rhine outflow also acted as a hydraulic barrier in the longshore sediment transport. The resulting imbalance in the longshore sediment-transport lead to high rates of deposition. The importance of this mechanism was demonstrated in the calculations of the contributions of longshore sediment transport to coastal progradation by Zitman (1987).

Progradation in the Wassenaar area started somewhere before 4500 BP. In the Wassenaar cross section the progradation rates were high. This can be attributed to the initially strong curvature of the shoreline and the resulting large imbalance in the longshore sediment transport, the vicinity of the sediment source and the influence of the Old Rhine. The major source of the sediments, the protrusion in the former Rhine/Meuse fluvial valley, was located about 15 km south of Wassenaar.

After the activity of the Old Rhine branch ceased around 2900 to 2600 BP (Törnqvist, 1993), the driving mechanism behind the protrusion of the wave-dominated delta ended. The strong imbalance in the longshore sediment transport imposed by the protrusion resulted in coastal erosion. Longshore sediment transport smoothed the coast. The abrupt seaward end of the Wassenaar cross section, without signs of a decrease in progradation rates, results from the erosion of the Old Rhine protrusion. The eroded sediment contributed to coastal progradation north of the Old Rhine outlet.

Progradation in the Haarlem area started around 4200 BP, with high progradation and sedimentation rates. Similar to the Wassenaar cross section we attribute the initial high rates to large imbalances in the longshore sediment transport. Notice that the initial progradation rate in the Haarlem cross section is lower than that in the Wassenaar cross section. This difference results from the large distance between the Haarlem cross section and the protrusion in the former Rhine/Meuse fluvial valley, and the limited influence of the Old Rhine outlet. The decrease in the progradation and sedimentation rates in the Haarlem cross

section resulted from the decrease in the imbalance in the longshore sediment transport. The slight increase in sedimentation rate in core DMW may be related to the erosion of the former Old Rhine protrusion. The end of coastal retreat in the Haarlem cross section is discussed below, in relation to the deposition of Unit 3B.

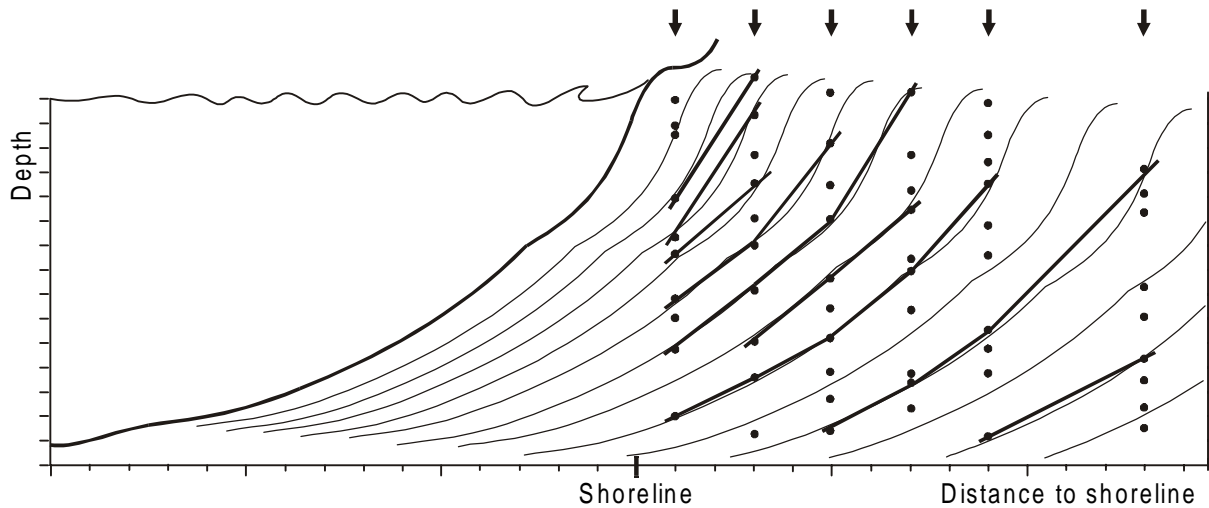


Figure 4.8: Hypothetical coast-perpendicular cross section through a prograded coastal system. The thin lines indicate the coastal profile at different time steps. The coastal profile is kept similar for all time steps. The spacing of the profile decreases, which can be regarded as a decrease in the rate of coastal progradation. A number of cores (arrows) with randomly distributed samples (dots) is indicated. The dots from different cores that are found on the same coastal profile are of equal age. The dots of equal age are connected to form isochrons (the thick lines). The isochrons display a clear steepening trend in the seaward direction. As the geometry of the coastal profiles does not change, the trend in the isochrons is an ‘apparent steepening’.

4.6.3 Apparent steepening

The isochrons in the westernmost half of the Haarlem cross sections have a steeper slope than those more to the west (Figure 4.1). This steepening of isochrons was also observed by Van der Valk (1992, 1996a), and was related to an increase in the slope of the shoreface profile during progradation. There is indeed a change from gentler to steeper slopes during deposition of Unit 3. This is due to the similar base of the lower shoreface (the erosion or non-deposition surface that separates Unit 2 and 3) and the rise of sea level during progradation (see also Chapter 6). However, the steepening in the western part of the Haarlem cross section may be an artefact of the method, as will be demonstrated below.

The distribution of the sample points and ages may result in apparent changes of the coastal profile. Figure 4.8 shows a hypothetical example of a coast with a decreasing rate of progradation, but without changes in the geometry of the coastal profile. The prograded coastal profiles are penetrated by a number of cores with randomly spaced samples. Samples from similar coastal profiles, i.e., of equal age, are connected to form isochrons. The most distinct trend in the isochrons is coastward steepening (Figure 4.8). The apparent change of the isochron steepness is related to the lack of cores seaward of the shoreline, which hinders the continuation of the youngest isochrons seaward. So, the youngest isochrons are only based on samples from the steep upper shoreface, and the more gentle middle and lower shoreface do not contribute to the reconstructions. Secondly, the trend is enhanced by the denser spaced coastal profiles that result from the decrease in the rate of progradation.

The fact that the steepening of the isochrons is an artefact of the method, rather than a natural trend, is supported by ground-penetrating radar images from the vicinity of the Haarlem cross section (Van der Spek *et al.*, 1999). The reflectors in the ground-penetrating radar images are mainly seaward dipping, occasionally with short landward dipping reflectors. The seaward-dipping reflectors represent beach and upper shoreface profiles, and the landward-dipping reflectors represent superimposed breaker bars and inter-tidal bars. The dips of the seaward reflectors are about 4° for the entire area westward from core ZR, which is similar to the slope of the modern upper shoreface and beach. Seaward changes in the slope of the reflectors are absent (Van der Spek *et al.*, 1999).

4.6.4 Youngest developments: Unit 3B

In the Haarlem cross section the distribution of ages in the westernmost shoreface deposits is complex. In the Wheeler diagram we have distinguished Unit 3A and 3B on basis of an intermediate hiatus. The cluster of dates around 1000 (m) BP in the marine cores (Figure 4.1 and 4.3) is a continuation of Unit 3A, and thus a continuation of progradation, which shows that at least on the lower shoreface progradation continued to 1000 (m) BP. The absence of in-sequence dates from that time interval in core RSP hinders the recognition of such a trend in the upper shoreface and beach deposits. Continuous deposition in core RSP (as depicted in figure 4.5) implies that progradation continued to about 400 (m) BP (Figure 4.7 H). Discontinuous sedimentation, where the absence of in-sequence dates in the -6.5 to -0.5 m NAP interval represents erosion, suggest some coastal retreat after 1000 cal BP, followed by limited deposition after 400 cal BP. The erosive event prior to 400 cal BP may be a large flood event in the 16th century, with the 'Allerheiligenvloed' of 1570 (All Saints flood: see Jelgersma *et al.*, 1995) as a likely candidate.

Erosion of the prograded shoreface and beach deposits has been related to the formation of the high dunes with abundant fine shell fragments that cap the beach-ridge and beach-plain deposits (Umbgrove, 1947, 1950, Zagwijn, 1969). During progradation low dunes formed on the beach ridges. Not until Roman times deposition of the high, Younger Dunes started (Tesch, 1921, Zagwijn, 1984). In the opinion of these authors the sand in the Younger Dunes originated from the shoreface and beach, based on the abundance of fine shell fragments in the dune sands. Estimates of the sand volume in the dunes have been used to reconstruct the original coastline position after progradation. Pool (1989, 1993a) estimates 2.1 to 3 km of erosion following progradation. The reconstructions of Pool (1989, 1993a) are based on the assumption that all eroded sand was transported cross-shore into the dune area. The isochrons and progradation and sedimentation rates in the Haarlem cross section all show a gradual decrease of progradation (Figure 4.1 and table 4.1 and 4.2). Extrapolation of these trends suggests that progradation did not continue much further offshore. Therefore the reconstructed progradation of several kilometres (Pool, 1989, 1993a) seems unlikely.

In the Wassenaar cross section Unit 3B is found only on the modern shoreface. The lack of a core from the modern beach (similar to core RSP in the Haarlem cross section) hinders recognition of Unit 3B below the modern beach. The large hiatus between Unit 3A and 3B in the Wassenaar cross section shows that after deposition of Unit 3A erosion dominated the local coastal evolution (Figure 4.7 G). The deposits of Unit 3B likely represent the ongoing erosion and deposition that characterise the shoreface environment.

4.7 Conclusions

Selection of pristine single juvenile shells effectively excludes most reworked shell material and allows detailed AMS ^{14}C dating of coastal deposits

Two groups of offshore, shoreface and beach deposits with a *Spisula* shell assemblage can be distinguished. The oldest group represents the offshore environment of the transgressive coastal system and shoreface and beach deposition of the transitional stage from transgression to progradation. The youngest group represents shoreface and beach deposits of the prograded coastal system. At the seaward side a hiatus separates the groups. The time represented in the hiatus decreases landward, while in the landward half a gradual transition between the units exists.

The transgressive offshore deposits are relatively old in the south and relatively young in the north. This trend is in harmony with the ages of the beach-ridge and beach-plain deposits. The presence of shoreface deposits of Unit 2 below the modern shoreface shows that the North Sea was already devoid of transgressive remnants down to -15m NAP. The contribution of transgressive remnants, for instance ebb-tidal deltas, to coastal progradation has therefore been limited.

The high sedimentation rates in the Wassenaar cross section result from the vicinity to the sediment source in the former Rhine/Meuse fluvial valley. The proximity of the Old Rhine outlet may have further aided high sedimentation rates in the Wassenaar cross section. After the rapid progradation near Wassenaar, erosion occurred when the activity of the Old Rhine ceased and erosion of the protrusion commenced.

Progradation rates near Haarlem were lower than near Wassenaar, because of its position further away from the major sediment source and further away from the Old Rhine outlet. The decrease in progradation and sedimentation rates in the Haarlem cross section is related to the decrease of the curvature of the shoreline and the related decrease of the imbalance in the alongshore sediment transport. A slight increase in the sedimentation rates is related to the erosion of the Old Rhine protrusion. The gradual decrease of sedimentation and progradation rates in the Haarlem cross section suggests that the prograded shoreline has not extended much further seaward.

The steepening of subsequent seaward isochrons in the western half of the Haarlem cross section is an artefact of the method. Ground-penetrating radar images show that the geometry of the upper shoreface and beach profiles was identical during progradation.

Appendix 4 (Following pages): Carbon dates from the Haarlem, Wassenaar and North Sea cross sections, including carbon dates presented by Van der Valk (1992; 1996), and previously unpublished dates from the Free University, Amsterdam (Van der Valk, 1995).

Core	number	X coord	Y coord	depth	species	size	characteristics	Age	Age (marine corrected)	Calibrated age	C 14 lab.
								Carbon years, BP	Carbon years, BP	Solar years	sample no.
		Dutch Ordnance (RD)	m NAP								
RijksStrandPaal 69											
24H-594	RSP37	95.100	484.890	0,49	Spisula	juvenile		712 ± 34 BP	310 ± 34 BP	398 - 295 BP	UtC 7969
24H-594	RSP32	95.100	484.890	-0,46	Spisula	juvenile	chemical & mechanical weathering	825 ± 43 BP	423 ± 43 BP	488 - 429 BP	UtC 7968
24H-594	RSP26	95.100	484.890	-1,65	Spisula	juvenile	some periostracum	3311 ± 45 BP	2909 ± 45 BP	3208 - 3074 BP	UtC 7967
24H-594	RSP20	95.100	484.890	-2,90	Spisula	juvenile	black Mn spots, red Fe spots	2684 ± 44 BP	2282 ± 44 BP	2378 - 2316 BP	UtC 7966
24H-594	RSP18	95.100	484.890	-3,58	Spisula	juvenile		2998 ± 41 BP	2596 ± 41 BP	2777 - 2728 BP	UtC 7965
24H-594	RSP13	95.100	484.890	-4,81	Spisula	juvenile	red Fe spots	2687 ± 38 BP	2285 ± 38 BP	2373 - 2320 BP	UtC 7964
24H-594	RSP9	95.100	484.890	-6,35	Spisula	juvenile	some periostracum, little blue stains	2275 ± 33 BP	1873 ± 33 BP	1900 - 1828 BP	UtC 7963
24H-594	RSP7	95.100	484.890	-6,82	Spisula	juvenile	some periostracum, little blue stains	2958 ± 31 BP	2556 ± 31 BP	2746 - 2713 BP	UtC 7962
24H-594	RSP4	95.100	484.890	-7,79	Spisula	juvenile	some periostracum	2728 ± 49 BP	2326 ± 49 BP	2471 - 2335 BP	UtC 7914
24H-594	RSP1	95.100	484.890	-8,77	Spisula	juvenile	some periostracum	2871 ± 39 BP	2469 ± 39 BP	2707 - 2613 BP	UtC 7913
Flessenveld											
24H-599	FV72	95.450	484.850	-0,40	Spisula	juvenile	slight chemical weathering	2371 ± 36 BP	1969 ± 36 BP	2015 - 1931 BP	UtC 7970
24H-599	FV58	95.450	484.850	-1,81	Spisula	juvenile	slight mechanical weathering	2291 ± 39 BP	1889 ± 39 BP	1928 - 1838 BP	UtC 7904
24H-599	FV51	95.450	484.850	-2,72	Spisula	juvenile		2788 ± 34 BP	2386 ± 34 BP	2590 - 2436 BP	UtC 7903
24H-599	FV47	95.450	484.850	-3,41	Spisula	juvenile	slightly damaged	2767 ± 42 BP	2365 ± 42 BP	2532 - 2367 BP	UtC 7902
24H-599	FV41	95.450	484.850	-4,81	Spisula	juvenile	red Fe spots	2446 ± 38 BP	2044 ± 38 BP	2119 - 2013 BP	UtC 7901
24H-599	FV35,5	95.450	484.850	-6,32	Spisula	juvenile, doublet	periostracum present	2969 ± 40 BP	2567 ± 40 BP	2756 - 2714 BP	UtC 7920
24H-599	FV28	95.450	484.850	-8,95	Spisula	doublet	periostracum present	3122 ± 43 BP	2720 ± 43 BP	2934 - 2826 BP	UtC 7900
24H-599	FV22	95.450	484.850	-11,30	Spisula	doublet	periostracum present	3729 ± 44 BP	3327 ± 44 BP	3685 - 3578 BP	UtC 7899
24H-599	FV17	95.450	484.850	-12,72	Spisula	juvenile	slightly damaged	4814 ± 47 BP	4412 ± 47 BP	5202 - 4987 BP	UtC 7898
24H-599	FV9,5	95.450	484.850	-13,85	Spisula	juvenile	damaged, periostracum present	5062 ± 44 BP	4660 ± 44 BP	5458 - 5317 BP	UtC 7919
24H-599	FV2	95.450	484.850	-16,62	Spisula	juvenile, doublet	periostracum, little blue stains	5218 ± 43 BP	4816 ± 43 BP	5608 - 5555 BP	UtC 7897
24H599	FV5A	95.450	484.850	-0,59	Spisula				2230 ± 80		GrN 14196
24H599	FV7B	95.450	484.850	-3,09	Spisula				2410 ± 50		GrN 14197
24H599	FV14B	95.450	484.850	-9,34	Spisula				2810 ± 50		GrN 14198
24H599	FV18B	95.450	484.850	-13,22	Spisula				3750 ± 60		GrN 14199
24H599	FV23B	95.450	484.850	-17,92	Spisula, Mactra & Macoma				5150 ± 90		GrN 14224
DuizendMeterWeg											
24H-594	DMW7a	96.080	484.710	0,16	Spisula	juvenile	mechanical weathering	3079 ± 41 BP	2677 ± 41 BP	2869 - 2773 BP	UtC 7896
24H-594	DMW11b	96.080	484.710	-3,21	Spisula	juvenile	stains	2893 ± 38 BP	2491 ± 38 BP	2718 - 2666 BP	UtC 7918
24H-594	DMW13b	96.080	484.710	-4,85	Spisula	juvenile		3012 ± 35 BP	2610 ± 35 BP	2785 - 2739 BP	UtC 7895
24H-594	DMW15b	96.080	484.710	-6,40	Spisula	juvenile		3349 ± 40 BP	2947 ± 40 BP	3249 - 3141 BP	UtC 7917
24H-594	DMW17c	96.080	484.710	-7,91	Spisula	juvenile	periostracum present	3223 ± 42 BP	2821 ± 42 BP	3077 - 2948 BP	UtC 7894

Core	number	X coord Dutch Ordnance (RD)	Y coord m NAP	depth m NAP	species	size	characteristics	Age Carbon years, BP	Age (m. corr.) Carbon years, BP	Calibrated age Solar years	C 14 lab. sample no.
DuizendMeterWeg											
24H-594	DMW7	96.080	484.710	-10,09	Macoma	juvenile	slightly damaged	3441 ± 42 BP	3039 ± 42 BP	3351 - 3254 BP	UtC 7893
24H-594	DMW17	96.080	484.710	-12,47	Spisula		periostracum present	3968 ± 42 BP	3566 ± 42 BP	3989 - 3879 BP	UtC 7892
24H-594	DMW20	96.080	484.710	-12,98	Spisula	juvenile		4801 ± 42 BP	4399 ± 42 BP	5121 - 4977 BP	UtC 7891
24H-594	DMW28	96.080	484.710	-15,41	Spisula		periostracum present	5161 ± 44 BP	4759 ± 44 BP	5573 - 5463 BP	UtC 7890
24H-594	DMW44	96.080	484.710	-19,58	Spisula	juvenile	damaged	5300 ± 50 BP	4898 ± 50 BP	5706 - 5597 BP	UtC 7916
24H594	DMW8B	96.080	484.710	0,13	Mactra				2320 ± 80		GrN 14225
24H594	DMW14C	96.080	484.710	-5,64	Spisula & Mactra				2540 ± 60		GrN 14226
24H594	DMW30	96.080	484.710	-18,67	Spisula				4910 ± 100		GrN 14195
Strandweg											
24H-598	SW69	97.640	483.990	-1,20	Spisula	juvenile, doublet	fragment, mechanically weathered	3625 ± 33 BP	3223 ± 33 BP	3553 - 3458 BP	UtC 7961
24H-598		97.640	483.990	-1,20	Spisula	juvenile, doublet	fragment, mechanically weathered	3687 ± 57 BP	3285 ± 57 BP	3648 - 3500 BP	UtC 7960
24H-598	SW63	97.640	483.990	-3,49	Spisula	juvenile	little periostracum	3501 ± 40 BP	3099 ± 40 BP	3406 - 3333 BP	UtC 7912
24H-598	SW60	97.640	483.990	-4,08	Spisula	juvenile	periostracum present	3713 ± 41 BP	3311 ± 41 BP	3665 - 3564 BP	UtC 7911
24H-598	SW57	97.640	483.990	-5,17	Macoma	juvenile	slightly damaged, periostracum present	3640 ± 37 BP	3238 ± 37 BP	3573 - 3466 BP	UtC 7910
24H-598	SW52	97.640	483.990	-6,31	Spisula	juvenile		3992 ± 37 BP	3590 ± 37 BP	4060 - 3903 BP	UtC 7909
24H-598	SW47	97.640	483.990	-8,25	Spisula	juvenile	periostracum present	3647 ± 35 BP	3245 ± 35 BP	3579 - 3472 BP	UtC 7908
24H-598		97.640	483.990	-8,25	Spisula	juvenile	periostracum present	3781 ± 39 BP	3379 ± 39 BP	3737 - 3638 BP	UtC 7907
24H-598	SW42	97.640	483.990	-10,04	Spisula	juvenile	some periostracum	4116 ± 39 BP	3714 ± 39 BP	4219 - 4088 BP	UtC 7906
24H-598	SW36	97.640	483.990	-11,09	Spisula	juvenile	damaged, some periostracum	4429 ± 45 BP	4027 ± 45 BP	4626 - 4508 BP	UtC 7959
24H-598		97.640	483.990	-11,09	Spisula	juvenile	damaged, some periostracum	4417 ± 123 BP	4015 ± 123 BP	4788 - 4402 BP	UtC 7958
24H-598	SW32	97.640	483.990	-12,66	Spisula	juvenile	periostracum present	4601 ± 41 BP	4199 ± 41 BP	4837 - 4798 BP	UtC 9705
24H598	SW18B	97.640	483.990	-9,26	Spisula				3740 ± 60		GrN 15125
24H598	SW21A	97.640	483.990	-11,58	Spisula				4210 ± 60 & 4250 ± 60 & 4260 ± 60		GrN 14202
24H598	SW21A	97.640	483.990	-11,58	Spisula				4250 ± 60		GrN 14201
24H598	SW21A	97.640	483.990	-11,58	Spisula				4260 ± 60		GrN 14200
24H598	SW31A	97.640	483.990	-20,88	Cerastoderma				7010 ± 120		GrN 14206
Zeerust											
24H-599	ZR13	99.910	484.300	-14,22	Spisula	juvenile	some periostracum	5224 ± 49 BP	4822 ± 49 BP	5614 - 5562 BP	UtC 9785
24H-599	ZR21	99.910	484.300	-12,01	Spisula	juvenile	some periostracum	4684 ± 40 BP	4282 ± 40 BP	5110 - 5107 BP	UtC 9761
24H-599		99.910	484.300	-12,01	Spisula	juvenile	some periostracum	4684 ± 40 BP	4282 ± 40 BP	5075 - 4966 BP	UtC 9761
24H-599	ZR28	99.910	484.300	-10,89	Spisula	juvenile	some periostracum	4775 ± 42 BP	4373 ± 42 BP	5063 - 4957 BP	UtC 9762
24H-599	ZR40	99.910	484.300	-8,68	Spisula	juvenile	some periostracum	4760 ± 44 BP	4358 ± 44 BP	5046 - 4937 BP	UtC 9763
24H-599	ZR52	99.910	484.300	-7,04	Spisula	juvenile	some periostracum	4493 ± 44 BP	4091 ± 44 BP	4786 - 4603 BP	UtC 9764
24H-599	ZR73	99.910	484.300	-4,23	Spisula	juvenile	some periostracum	4445 ± 42 BP	4043 ± 42 BP	4683 - 4528 BP	UtC 9765

Core	number	X coord Dutch Ordnance (RD)	Y coord	depth m NAP	species	size	characteristics	Age Carbon years, BP	Age (m. corr.) Carbon years, BP	Calibrated age Solar years	C 14 lab. sample no.
Zeerust											
24H-599	ZR82	99.910	484.300	-2,74	Spisula	juvenile	some periostracum	4466 ± 49 BP	4064 ± 49 BP	4770 - 4753 BP	UtC 9766
24H-599		99.910	484.300	-2,74	Spisula	juvenile	some periostracum	4466 ± 49 BP	4064 ± 49 BP	4728 - 4548 BP	UtC 9766
24H596	ZR12B	99.910	484.300	-7,06	Spisula				4070 ± 70		GrN 14227
24H596	ZR20A	99.910	484.300	-14,06	Spisula				4820 ± 90		GrN 14228
Schuil & Rust											
24H-595	SR6	98.800	484.225	-1,21	Spisula	juvenile	some periostracum, chemically weathered	3893 ± 44 BP	3491 ± 44 BP	3909 - 3813 BP	UtC 9753
24H-595	SR17	98.800	484.225	-4,02	Spisula	juvenile	some periostracum	3836 ± 49 BP	3434 ± 49 BP	3842 - 3701 BP	UtC 9754
24H-595	SR26	98.800	484.225	-5,19	Spisula	juvenile	some periostracum	4190 ± 41 BP	3788 ± 41 BP	4344 - 4216 BP	UtC 9755
24H-595	SR36	98.800	484.225	-6,90	Spisula	juvenile	some periostracum	4069 ± 47 BP	3667 ± 47 BP	4151 - 4048 BP	UtC 9756
24H-595	SR43	98.800	484.225	-8,65	Spisula	juvenile	some periostracum	4299 ± 50 BP	3897 ± 50 BP	4485 - 4363 BP	UtC 9757
24H-595	SR51	98.800	484.225	-9,96	Spisula	juvenile	some periostracum	4757 ± 47 BP	4355 ± 47 BP	5046 - 4914 BP	UtC 9758
24H-595	SR54	98.800	484.225	-11,04	Spisula	juvenile	some periostracum, slightly damaged	4738 ± 42 BP	4336 ± 42 BP	5029 - 4876 BP	UtC 9759
24H-595	SR67	98.800	484.225	-13,58	Spisula	juvenile	some periostracum, slightly blue	5214 ± 43 BP	4812 ± 43 BP	5601 - 5560 BP	UtC 9760
24H595	SR13	98.800	484.225	-2,10	Macoma				3620 ± 60		GrN 14193
24H595	SR19	98.800	484.225	-6,90	Spisula				3780 ± 50		GrN 14194
Leyduin											
24H-599	LD1	101.120	484.340	-15,51	Cerastoderma	fullgrown, doublet		6021 ± 44 BP	5619 ± 44 BP	6477 - 6388 BP	UtC 9767
24H-599	LD11	101.120	484.340	-12,62	Spisula	juvenile	some periostracum	5610 ± 45 BP	5208 ± 45 BP	6029 - 5925 BP	UtC 9768
24H-599	LD18	101.120	484.340	-11,44	Spisula	juvenile	some periostracum	5515 ± 42 BP	5113 ± 42 BP	5921 - 5871 BP	UtC 9769
24H-599	LD27	101.120	484.340	-9,76	Spisula	juvenile	some periostracum	4767 ± 39 BP	4365 ± 39 BP	5048 - 4953 BP	UtC 9770
24H-599	LD39	101.120	484.340	-6,57	Spisula	juvenile (two)	some periostracum	4639 ± 37 BP	4237 ± 37 BP	4890 - 4808 BP	UtC 9786
24H-599	LD47	101.120	484.340	-4,00	Spisula	juvenile	some periostracum	4640 ± 60 BP	4238 ± 60 BP	4895 - 4809 BP	UtC 9787
24H-599	LD51	101.120	484.340	-2,95	Spisula	juvenile	some periostracum	4632 ± 47 BP	4230 ± 47 BP	4864 - 4811 BP	UtC 9771
25C343	LDI/4	101.120	484.340	-2,70	Cerastoderma				4270 ± 60		GrN 14203
25C343	LDII,III/3	101.120	484.340	-11,30	Spisula				5080 ± 50		GrN 14204
Groenendaal											
25C-347	GD14	101.280	484.820	-11,92	Macoma	juvenile		5485 ± 48 BP	5083 ± 48 BP	5907 - 5838 BP	UtC 9772
25C-347	GD26	101.280	484.820	-9,87	Spisula	juvenile	some periostracum, little blue	5483 ± 45 BP	5081 ± 45 BP	5905 - 5839 BP	UtC 9773
25C-347	GD34	101.280	484.820	-8,93	Spisula		some periostracum	5498 ± 45 BP	5096 ± 45 BP	5913 - 5853 BP	UtC 9774
25C-347	GD40	101.280	484.820	-8,04	Spisula	juvenile	some periostracum, stained	5430 ± 50 BP	5028 ± 50 BP	5878 - 5729 BP	UtC 9775
25C-347	GD56	101.280	484.820	-6,05	Spisula	juvenile	some periostracum, damaged	5411 ± 47 BP	5009 ± 47 BP	5860 - 5715 BP	UtC 9776
25C347	GD15A	102.280	483.820	-12,85	Macoma				5330 ± 280		GrN 14231
Cruquis											
25C346	CQ11A	103.220	483.090	-13,50	Macoma				5620 ± 60		GrN 14209

Core	number	X coord Dutch Ordnance (RD)	Y coord m NAP	depth m NAP	species	size	characteristics	Age Carbon years, BP	Age (m. corr.) Carbon years, BP	Calibrated age Solar years	C 14 lab. sample no.
Meijndel 2											
30E-302	MD II 1	83.970	463.520	-3,74	Spisula	juvenile	slightly weathered	3940 ± 60 BP	3538 ± 60 BP	3979 - 3830 BP	UtC 8204
30E-302	MD II 13	83.970	463.520	-4,79	Spisula	juvenile	periostracum	4021 ± 41 BP	3619 ± 41 BP	4079 - 3955 BP	UtC 8205
30E-302	MD II 16	83.970	463.520	-5,16	Spisula	juvenile	some periostracum	4065 ± 45 BP	3663 ± 45 BP	4138 - 3997 BP	UtC 8206
30E-302	MD II 27	83.970	463.520	-7,77	Spisula	juvenile	periostracum	4071 ± 35 BP	3669 ± 35 BP	4134 - 4051 BP	UtC 8207
30E-302	MD II 32	83.970	463.520	-9,37	Spisula	juvenile	elliptica some periostracum, slightly blue	4823 ± 46 BP	4421 ± 46 BP	5211 - 4999 BP	UtC 8208
30E-302	MD II 34	83.970	463.520	-9,86	Spisula	juvenile	some periostracum	4381 ± 44 BP	3979 ± 44 BP	4381 - 4432 BP	UtC 8209
30E-302	MD II 47	83.970	463.520	-11,87	Spisula	juvenile	periostracum	4682 ± 45 BP	4280 ± 45 BP	4948 - 4832 BP	UtC 8210
30E-302	MD II 53	83.970	463.520	-12,67	Spisula	juvenile	slightly damaged	5090 ± 70 BP	4688 ± 70 BP	5545 - 5320 BP	UtC 8211
30E-302	MD II 67	83.970	463.520	-16,69	Macoma	fully grown		6245 ± 42 BP	5843 ± 42 BP	6883 - 6654 BP	UtC 8213
Meijndel 1											
30E-301	MD I 4	84.190	463.040	-2,64	Spisula	juvenile		4001 ± 34 BP	3599 ± 34 BP	4056 - 3930 BP	UtC 8194
30E-301	MD I 14	84.190	463.040	-3,95	Spisula	juveniles (two)	periostracum	4074 ± 43 BP	3672 ± 43 BP	5561 - 5449 BP	UtC 8195
30E-301	MD I 20	84.190	463.040	-5,06	Spisula	juvenile	periostracum	4022 ± 37 BP	3620 ± 37 BP	4076 - 3962 BP	UtC 8196
30E-301	MD I 23	84.190	463.040	-5,94	Spisula	juvenile		4074 ± 43 BP	3672 ± 43 BP	4146 - 4045 BP	UtC 8197
30E-301	MD I 33	84.190	463.040	-7,66	Spisula	juvenile	blue, some periostracum	4078 ± 47 BP	3676 ± 47 BP	4155 - 4046 BP	UtC 8198
30E-301	MD I 38	84.190	463.040	-8,88	Spisula	juvenile	slightly blue, periostracum	4035 ± 37 BP	3633 ± 37 BP	4088 - 3974 BP	UtC 8199
30E-301	MD I 51	84.190	463.040	-11,93	Spisula	juveniles (two)	blue, some periostracum	4237 ± 37 BP	3835 ± 37 BP	4387 - 4270 BP	UtC 8200
30E-301	MD I 58	84.190	463.040	-12,70	Spisula	juveniles (three)		4995 ± 42 BP	4593 ± 42 BP	5372 - 5344 BP	UtC 8201
30E-301		84.190	463.040	-12,70	Spisula	juveniles (three)		4995 ± 42 BP	4593 ± 42 BP	5338 - 5282 BP	UtC 8201
30E-301	MD I 63	84.190	463.040	-13,71	Spisula	juvenile	periostracum	5251 ± 40 BP	4849 ± 40 BP	5639 - 5574 BP	UtC 8202
30E-301	MD I 78	84.190	463.040	-16,49	Spisula	juvenile	blue, periostracum	6048 ± 44 BP	5646 ± 44 BP	6498 - 6404 BP	UtC 8203
Bierlap 1											
30G812	<i>BLI17B</i>	84.810	462.130	-7,82					3840 ± 105		GrN 11982/1243
30G812	<i>BLI26,1</i>	84.810	462.130	-14,52					4830 ± 60		GrN 15121
30G812	<i>BLI26,2</i>	84.810	462.130	-14,52					5265 ± 110		GrN 11983/1244
Bierlap 2											
30G813	<i>BLII5</i>	85.140	461.840	-10,24					4000 ± 110		GrN 11984/1245
30G813	<i>BLII6A</i>	85.140	461.840	-14,32					4985 ± 105		GrN 11985/1246
30G813	<i>BLII6C</i>	85.140	461.840	-14,32					5025 ± 110		GrN 11986/1247
Hertenkamp 1											
30G814	<i>HKI6A</i>	85.980	461.850	-4,14					3920 ± 100		GrN 11987/1248
30G814	<i>HKI14B</i>	85.980	461.850	-11,14					4525 ± 90		GrN 11988/1249

Core	number	X coord Dutch Ordnance (RD)	Y coord	depth m NAP	species	size	characteristics	Age Carbon years, BP	Age (m. corr.) Carbon years, BP	Calibrated age Solar years	C 14 lab. sample no.
Hertenkamp 2											
30G815	HKII8B	86.410	461.785	-6,48					4490 ± 105		GrN 11989/1250
30G815	HKII12B	86.410	461.785	-10,10					4730 ± 105		GrN 11990/1251
Zijlwetering											
30G816	ZW8A	86.780	461.370	-6,40					4300 ± 110		GrN 11991/1252
De Pauw											
30G817	DP8B	87.370	461.070	-6,69					4410 ± 105		GrN 11992/1253
30G817	DP11B	87.370	461.070	-9,39					4520 ± 110		GrN 11993/1254
Raaphorst 3											
30G818	RHIII?	87.390	460.500	-6,92					4630 ± 100		GrN 15120
Raaphorst 2											
30G819	RHII5B	88.450	460.770	-4,75					4500 ± 100		GrN 11994/1255
Raaphorst 1											
30G820	RHI3A	88.850	460.325	-3,56					4765 ± 100		GrN 11995/1256
30G820	RHI5B	88.850	460.325	-6,06					4455 ± 105		GrN 11996/1257
30G820	RHI10A	88.850	460.325	-10,68					6745 ± 105		GrN 11997/1258
92DW10	10DW2			-18,23	Spisula	juvenile, doublet		-992 ± 36 BP	Modern	Modern	UtC 7995
92DW10	10DW4			-18,45	Spisula	juvenile		4288 ± 44 BP	3886 ± 44 BP	4430 - 4345 BP	UtC 7996
92DW10	10DW6			-18,52	Spisula	juvenile, doublet		-1068 ± 32 BP	Modern	Modern	UtC 7997
92DW16	16DW4			-14,67	Tellinus	juvenile, doublet		4100 ± 60 BP	3698 ± 60 BP	4224 - 4058 BP	UtC 7984
92DW16	16DW14			-15,75	Spisula	juvenile some periostracum		5620 ± 50 BP	5218 ± 50 BP	6071 - 5930 BP	UtC 7985
92DW16	16DW16			-16,34	Spisula	some periostracum		5992 ± 42 BP	5590 ± 42 BP	6435 - 6345 BP	UtC 7986
92DW16	16DW2			-14,53	Macoma	juvenile, doublet		4232 ± 41 BP	3830 ± 41 BP	4386 - 4257 BP	UtC 7987
92DW16	16DW9			-15,14	Spisula	juvenile, doublet		4047 ± 45 BP	3645 ± 45 BP	4121 - 3978 BP	UtC 7988
92DW22	22DW5			-16,79	Spisula	juvenile some periostracum		5370 ± 41 BP	4968 ± 41 BP	5754 - 5673 BP	UtC 8004
92DW22	22DW7			-17,12	Spisula	periostracum		5584 ± 42 BP	5182 ± 42 BP	5995 - 5910 BP	UtC 8005
92DW22	22DW2			-16,55	Spisula	juvenile some weathering		5265 ± 39 BP	4863 ± 39 BP	5749 - 5581 BP	UtC 8006
92DW27	27DW5/Cal 1			-15,67	Spisula	juvenile slight mechanical weathering		5094 ± 44 BP	4692 ± 44 BP	5910 - 5853 BP	UtC 8030
92DW27	27DW5/Cal 2			-15,67	Spisula	juvenile slight mechanical weathering		5094 ± 44 BP	4692 ± 44 BP	5830 - 5752 BP	UtC 8030
92DW27	27DW7			-16,03	Spisula	juvenile periostracum		5164 ± 41 BP	4762 ± 41 BP	5936 - 5902 BP	UtC 8031
92DW27	27DW10/Cal 1			-16,61	Spisula	juvenile periostracum		5289 ± 36 BP	4887 ± 36 BP	6170 - 6143 BP	UtC 8032
92DW27	27DW10/Cal 2			-16,61	Spisula	juvenile periostracum		5289 ± 36 BP	4887 ± 36 BP	6104 - 5988 BP	UtC 8032
92DW27	27DW10/Cal 3			-16,61	Spisula	juvenile periostracum		5289 ± 36 BP	4887 ± 36 BP	5961 - 5958 BP	UtC 8032
92DW27	27DW14/Cal 1			-17,38	Macoma	juvenile periostracum		5900 ± 50 BP	5498 ± 50 BP	6783 - 6700 BP	UtC 8033
92DW27	27DW14/Cal 2			-17,38	Macoma	juvenile periostracum		5900 ± 50 BP	5498 ± 50 BP	6700 - 6672 BP	UtC 8033

Core	number	X coord Dutch Ordnance (RD)	Y coord m NAP	depth	species	size	characteristics	Age	Age (m. corr.)	Calibrated age	C 14 lab.
								Carbon years, BP	Carbon years, BP	Solar years	sample no.
92GW13	13GW1			-14,55	Spisula	juvenile, doublet		3981 ± 48 BP	3579 ± 48 BP	4047 - 3888 BP	UtC 7998
92GW13	13GW2			-14,62	Spisula	juvenile, doublet		4154 ± 41 BP	3752 ± 41 BP	4256 - 4130 BP	UtC 7999
92GW13	13GW5			-14,93	Spisula	juvenile, doublet		4129 ± 42 BP	3727 ± 42 BP	4234 - 4099 BP	UtC 8000
92GW13	13GW8			-15,48	Macoma	juvenile, doublet		4171 ± 45 BP	3769 ± 45 BP	4297 - 4153 BP	UtC 8001
92GW13	13GW6A/1			-15,06	Spisula	juvenile, doublet		4010 ± 49 BP	3608 ± 49 BP	4076 - 3922 BP	UtC 8002
92GW13	13GW6A/2			-15,06	Spisula	juvenile, doublet		4173 ± 38 BP	3771 ± 38 BP	4290 - 4172 BP	UtC 8003
92GW6	6GW1			-14,49	Spisula	juvenile	some weathering	1515 ± 38 BP	1113 ± 38 BP	1089 - 996 BP	UtC 7992
92GW6	6GW4			-15,91	Spisula	juvenile	some weathering	611 ± 34 BP	209 ± 34 BP	278 - 244 BP	UtC 7993
92GW6	6GW7			-16,54	Spisula	juvenile	periostracum	6072 ± 46 BP	5670 ± 46 BP	6535 - 6418 BP	UtC 7994
98DW425	425DW5			-15,77	Spisula	juvenile	chemical and mechanical weathering	6439 ± 45 BP	6037 ± 45 BP	6955 - 6850 BP	UtC 7989
98DW425	425DW7			-15,50	Spisula		chemical and mechanical weathering	6266 ± 44 BP	5864 ± 44 BP	6753 - 6663 BP	UtC 7990
98DW425	425DW9			-15,10	Spisula	juvenile	some periostracum	-906 ± 45 BP	-1308 ± 45 BP	0 - 0 BP	UtC 7991
98DW426	426DW7			-15,97	Spisula	juvenile		5483 ± 41 BP	5081 ± 41 BP	5901 - 5839 BP	UtC 7979
98DW426	426DW9			-15,64	Spisula	juvenile	some periostracum	5466 ± 43 BP	5064 ± 43 BP	5904 - 5840 BP	UtC 7980
98DW426	426DW12			-15,41	Spisula	juvenile		5512 ± 45 BP	5110 ± 45 BP	5921 - 5862 BP	UtC 7981
98DW426	426DW14			-15,20	Spisula		little blue stains, periostracum	1429 ± 35 BP	1027 ± 35 BP	984 - 926 BP	UtC 7982
98DW426	426DW16			-14,94	Spisula	juvenile	little blue stains, periostracum	1798 ± 37 BP	1396 ± 37 BP	1353 - 1288 BP	UtC 7983
98DW427	427DW1			-15,59	Spisula	juvenile	periostracum	5536 ± 45 BP	5134 ± 45 BP	5939 - 5880 BP	UtC 7971
98DW427	427DW4			-15,27	Spisula	juvenile	periostracum	5502 ± 48 BP	5100 ± 48 BP	5916 - 5851 BP	UtC 7972
98DW427	427DW6			-14,92	Spisula	juvenile	some periostracum	5298 ± 44 BP	4896 ± 44 BP	5697 - 5598 BP	UtC 7973
98DW427	427DW9			-14,51	Spisula	juvenile	some periostracum	5354 ± 41 BP	4952 ± 41 BP	5740 - 5653 BP	UtC 7974
98DW427	427DW10			-14,42	Spisula	juvenile	little blue stains, some periostracum	2642 ± 31 BP	2240 ± 31 BP	2334 - 2299 BP	UtC 7975
98DW427	427DW12			-14,02	Spisula	juvenile	some periostracum	1784 ± 30 BP	1382 ± 30 BP	1333 - 1284 BP	UtC 7976
98DW427	427DW14			-13,52	Spisula	juvenile		1918 ± 31 BP	1516 ± 31 BP	1500 - 1403 BP	UtC 7977
98DW427	427DW17			-12,93	Spisula	juvenile	damaged, some periostracum	-2819 ± 25 BP	Modern	0 - 0 BP	UtC 7978

Chapter 5: A model for shoreface deposition of Holocene prograded coastal deposits (Haarlem, The Netherlands), based on grain-size distributions and sedimentary structures.

Abstract

Comparison of Holocene prograded shoreface deposits with deposits from the modern shoreface of the Western Netherlands suggests that sheet-flow conditions dominate deposition on the shoreface during storms in the past and present. The grain-size distributions and sedimentary structures from four undisturbed cores from the seaward edge of prograded coastal deposits have been analysed.

In all cores a comparable sequence is found. All shoreface deposits are characterised by the occurrence of thick storm beds. Lower shoreface deposits from the basal part of the sequence have been intensely bioturbated. The storm beds of the overlying middle shoreface deposits are characterised by distinct grading and fine-grained tops of silt and mud. Storm beds from the upper shoreface deposits are amalgamated. In the overlying breaker-bar zone cross-bedding and thick chaotic shell beds occur. The finest sediment, without coarse sand grains, is found in the middle shoreface deposits. The entire sequence is fining upward from lower to middle shoreface and coarsening upward from middle shoreface to the breaker bar and beach. The sequence deviates from the sequence found in older prograded shoreface deposits, that displays a fining upward, and contains distal storm-sand layers at its base.

The basal fining-upward sequence reflects the decrease of tide influences from the North Sea floor up to the shoreface. The coarsening-upward trend in the upper part of the sequence is the result of the increase in wave attack from deep to shallow water. The fine-grained middle shoreface demonstrates that coarse grains do not traverse this zone, i.e., coarse-sand grains are only transported alongshore, on the lower shoreface and from the upper shoreface to the beach. The fine-grained sediment can be transported in long- and cross-shore directions over the entire shoreface. The grading of the individual storm beds and the coarse-fine-coarse sequence on the shoreface are best explained by oscillatory sheet-flow conditions during storms.

5.1 Introduction

The shoreface stretches from the beach down to the shelf (Niedoroda, 1985). Erosion, sediment transport and deposition on deeper parts of the shoreface are only partly understood (Wright, 1995). Most changes on the shoreface occur under storm conditions. During storms the shoreface is a rough environment, which makes accessibility and measurements of any kind difficult. The shoreface is too shallow for sea-going research vessels, too rough for small beach-operated boats, and too deep for access from the beach. Conceptual and numerical models of shoreface dynamics are therefore only in part constrained by measurements (Cowell *et al.*, 1999a). This hinders predictions of shoreface development under changing conditions, as for instance induced by large infrastructures and by changes in sea level.

All composite sequences of shoreface deposits based on box cores from modern coasts display a coarsening in grain size from the lower shoreface to the beach (Reading and Collinson, 1996, their figure 6.85 for overview). The coarsening is associated with a decrease of preserved bioturbation traces and an increase in the number and the thickness of parallel-laminated storm beds. The span of the wave-controlled features is controlled by the wave climate (Howard and Reineck, 1981). Shipp (1984) presented observations from Long Island (NY) that show coarse-grained patches in between fine deposits on the lower shoreface, and incorporated these in his composite sequence. This seems to be the only sequence in which coarser-grained deposits from the lower shoreface are reported.

Sequences from the shelf up to the lower shoreface profiles do generally show a fining in grain size (Swift, 1976a, Liu and Zarillo, 1989, Guillen and Hoekstra, 1996). The coarse-grained shelf deposits are regarded as relic or palimpsest sand sheets, remoulded and winnowed by geostrophic and tidal currents on deeper water (Swift, 1976a). In a composite sequence this would be represented by a basal erosion surface with an erosive lag (Nummedal and Swift, 1987). In general, the sequence of deposits in sediment-supply dominated (allochthonous) shoreface-to-shelf systems (Swift, 1976b, Swift and Thorne, 1991) consists of shelf mud, with an upward increase in abundance and thickness of storm-sand beds. The sequence of deposits in accommodation-dominated (autochthonous) shoreface-to-shelf systems (Swift, 1976b, Swift and Thorne, 1991) consists of a coarse basal lag deposit and erosion surface, which represents the shelf, overlain by coarsening shoreface deposits.

The coarsening upward sequence on modern shelf-to-shoreface systems consists of mud with intermittent storm-sand layers from the shelf up to the middle shoreface, a cross-bedded interval from the foreshore and upper shoreface, and a parallel-laminated top interval from beach processes (figure 7.11 in Elliot, 1986). Facies models of barred (Davidson-Arnott and Greenwood, 1976, Greenwood and Mittler, 1985) and non-barred coasts (Clifton *et al.*, 1971) have lunate megaripples on a major part of the shoreface and breaker-bar zone. Davidson-Arnott and Greenwood (1976) suggest that lunate megaripples occur under asymmetric-oscillatory flow, while plane bedding is stable under symmetric-oscillatory flow. Grain size also affects the stability field, lunate megaripples do not develop in fine grains (Clifton, 1976). Steep, short period waves may also hinder the development of lunate megaripples (Davidson-Arnott and Greenwood, 1976).

Modern storm-sand layers typically consist of an erosive base, occasionally with a coarse lag, horizontal to low-angle lamination overlain by an interval with wave-ripple lamination and a burrowed interval (Kumar and Sanders, 1976, Aigner and Reineck, 1982). Most storm-sand layers are graded (Aigner, 1985). From proximal upper-shoreface settings down to distal shelf setting the thickness and the grain size of the sand layers decreases and the thickness of intermittent mud layers increases, along with an increase in the intensity of bioturbation (Aigner and Reineck, 1982, Aigner, 1985).

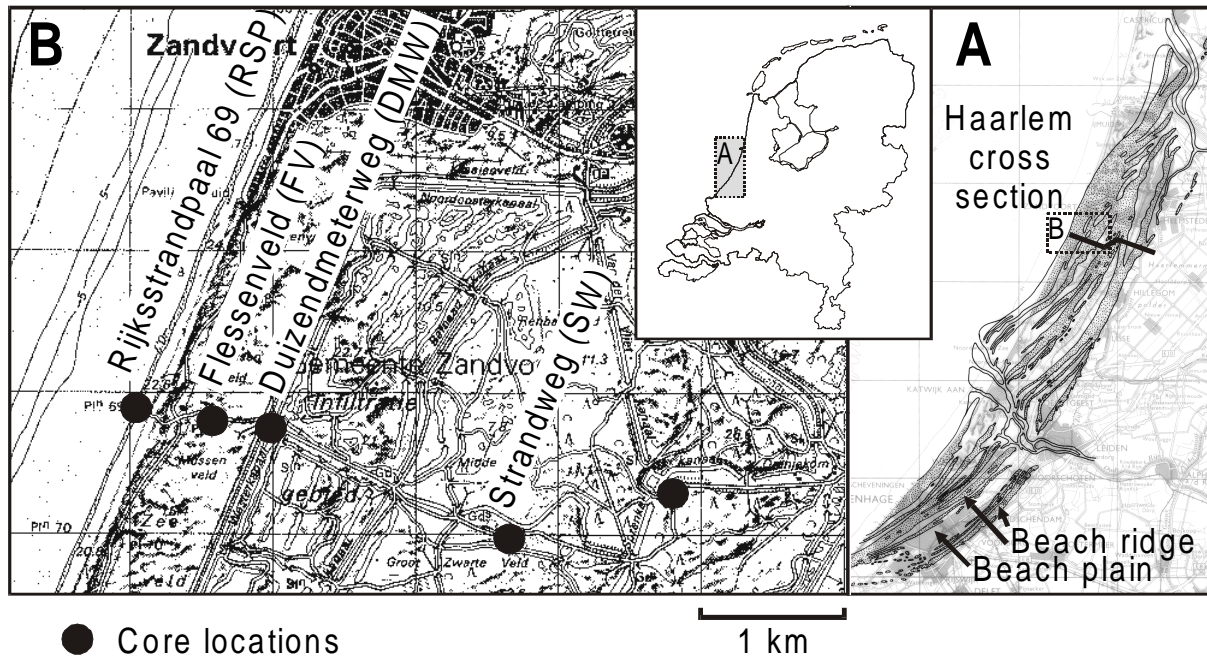


Figure 5.1 A: Map of the beach-ridge and beach-plain morphology of the Western Netherlands, with the location of the Haarlem cross section. Inset shows position of the map within the Netherlands.

Figure 5.1B: Detailed map with location of cores.

The mechanisms that result in the deposition of storm-sand layers are not well understood (Johnson and Baldwin, 1996). Processes at the seabed include storm waves and various types of currents, including wind-driven currents, storm-surge ebb currents, and density currents. Distinction must be made between the processes that result in the erosion and entrainment of the sediments and the processes that result in transport and deposition of the sediments. Wave action at the sea floor is usually regarded as the principle agent of erosion and sediment entrainment, while the various types of currents result in sediment transport. The type of currents on the shoreface and shelf during storms depends on the setting of the shelf and the regional climate conditions.

Landward of the modern coast in the western Netherlands, from Monster to Bergen aan Zee (Figure 1.1), shoreface and beach deposits with ages of 5500 to 400 BP are found at depths from +2 m to -15 m NAP (Unit 3, figure 1.3). In map view the deposits are represented by a series of beach ridges and beach plains (Figure 1.2 and figure 5.1). The shoreface and beach deposits are increasingly younger seaward and represent a phase of coastal progradation. For information on the large-scale evolution of the Holland coast and governing controls we refer to Beets *et al.* (1992, 2000) and Chapter 4. Distribution and characteristics of the deposits are well known from cores and other subsurface information sources. These deposits are comparable with modern shoreface sediments.

The aim of this chapter is to reconstruct the depositional conditions on the shoreface during Holocene coastal progradation and to present a model for shoreface deposition during coastal progradation and a slow rise of sea level. The Holocene shoreface deposits near Haarlem in the western Netherlands are compared to modern shoreface sediments, to validate the depositional model for modern shoreface conditions. The age of the prograded shoreface deposits ranges from 4000 to 400 BP (Chapter 3 and 4). Sea level was lower during that period and the coastal configuration was slightly different (Beets *et al.*, 1992, Beets and Van der Spek, 2000). The offshore-wave conditions and the tides were well comparable to modern

conditions (tides: Franken, 1987, waves: Stive, 1987, Gerritsen and Berentsen, 1998). A comparison with modern shoreface characteristics and dynamics is therefore feasible. The main difference between the fossil and modern shoreface is their prograding (Van Straaten, 1965, Van der Valk, 1996a) versus erosional /stable behaviour (Van Vessem and Stolk, 1990, De Ruig and Louisse, 1991).

5.1.1 Coastal Dynamics of the Western Netherlands

Along the Holland coast and in the adjacent North Sea, waves and tidal action govern the hydrodynamic conditions. The North Sea floor is dominated by semi-diurnal tidal action and the upper shoreface is dominated by wave action and wave-driven currents (Van Straaten, 1961, Roelvink and Stive, 1990, Stive *et al.*, 1990). This separation is similar to that between the zone of friction-dominated flow/geostrophic flow and the zone of wave-driven flow of Swift (1976a, 1976b). During storms the North Sea floor experiences severe wave action as well (Van der Meene, 1994, 1996). Wind-driven currents alter the current pattern in the North Sea (Dronkers *et al.*, 1990, Van der Giessen *et al.*, 1990, De Ruijter *et al.*, 1992), as does the buoyant plume of the Rhine River (Visser *et al.*, 1991). Tidal-current speeds at the North Sea floor regularly exceed 0.7 m/s (Rijkswaterstaat, 1994), and result in the formation of mega-ripple and sand-wave fields in coarse sand (Van Alphen, 1989).

Grain-size distributions of modern sediments from the Holland coast were presented by Van Straaten (1961, 1965), Terwindt (1962), and Van Alphen (1987). The grain-size distribution over the shoreface has a strong along-shore persistence, with coarse sand below depths of -10 to -12 m, 2.5 to 3 km seaward of the shoreline, fine sand and mud layers in a zone parallel to the coast at depths of -8 to -5 m, and again coarse sand up to the beach. Van Alphen (1987) shows that the alongshore variability in grain-size and mud layer distribution is partly related to breaker-bar distribution and partly to geological relics (notably the former Old Rhine delta at Katwijk). The occurrence of mud layers is restricted to fair-weather periods (Van Alphen, 1987). Terwindt (1962) has compared the grain-size distributions along several profiles during storm and fair weather conditions. His results reveal that the largest variations in grain size occur on the beach and the shoreface during storms. Bathymetric changes in the coarse-grained zone below -11 m are very small. The fine-grained material that is found during fair weather up to -4 m NAP, is eroded during storms. This fine-grained material is not found on the post-storm profile, and must have been transported out of the area in cross-shore or longshore direction.

Van der Valk (1992) investigated box cores from the modern shoreface at Egmond (south of Bergen aan Zee, figure 1.1). He demonstrated that the modern shoreface consists of graded beds with parallel lamination and large cross-bedding. Bioturbation and mud layers are abundant in deep water, as well as in the top layer of all box cores down from -4.5 m NAP. The structures and lithology at the base of the box cores reflect higher-energy conditions than those at the top. The lower-energy deposits in the top parts of the box cores are due to the collection of the box cores during the summer, with quiet-weather conditions prior to collection. Most of the fair-weather characteristics are eroded during subsequent storms and are not preserved in the geological record (cf. Van den Berg, 1977).

5.2 Methods

The cores used in this study were collected by Van der Valk (1992, 1996a). Abbreviations of core names are used throughout the text: Rijkstrandpaal 69: RSP, Flessenveld: FV, Duizendmeterweg: DMW, Strandweg: SW (fig 5.1B for locations). The borings consist of 1 m long undisturbed cores made with a hammer corer operated within a casing. Sediment samples for grain-size analysis were selected on basis of lacquer peels and photographs, to incorporate most grain-size variations. On average 4 samples were collected per metre,

sample thickness varied from 2 to 10 cm. The sample thickness of core DMW was about 30 cm, and one sample was collected per metre. The samples were sieved over a 2 mm mesh sieve to separate shells from the sediment. The coarse and fine fractions were weighed and the weight percentage of the fraction larger than 2 mm was calculated. The grain-size distribution of the fraction smaller than 2 mm was determined with a Malvern laser-particle sizer. The laser-particle analysis gives volume-based grain-size distributions. For core DMW, the grain sizes of the intervals in between the laser-particle-sized samples were determined visually at 10 cm intervals with a grain-size comparator (Eijkelkamp, standard soil type). The pattern of the Malvern grain sizes and the pattern of the visually determined grain sizes are well comparable (fig 5.2), but the absolute values of the visual method tend to be larger (see table 5.1). The sedimentary and burrowing structures were studied in the photographs and lacquer peels.

Table 5.1: Average grain sizes of the deposits in the four cores. The top depths of the intervals, the average grain sizes, number of samples and standard deviation of the grain sizes are indicated. Average grain sizes of DMW (in italics) are based on visual comparison that tend to be larger than laser particle sizes.

Core	interval	depth of base (m NAP)	average grain size (micron)	standard deviation	n
RSP					
	Lower shoreface	-8,01	168	7	3
	Middle shoreface	-6,57	124	62	5
	Upper shoreface	-4,35	224	40	6
	Breaker bar	-0,47	341	79	20
	Beach	1,99	325	68	9
FV					
	Lower shoreface	-7,4	194	47	29
	Middle shoreface	-6,31	140	49	7
	Upper shoreface	-2,21	174	25	29
	Breaker bar	-0,71	285	101	8
	Beach	1,3	211	53	15
DMW					
	Lower shoreface	-8,53	<i>176</i>	97	33
	Middle shoreface	-6,72	<i>165</i>	70	13
	Upper shoreface	-4,09	<i>333</i>	133	15
	Breaker bar	-1,38	<i>455</i>	124	20
	Beach	0,36	<i>312</i>	54	13
SW					
	Lower shoreface	-9,3	180	53	9
	Middle shoreface	-7,9	117	28	15
	Upper shoreface	-5,31	207	24	8
	Breaker bar	-3,5	248	48	8
	Beach	-0,83	254	59	9

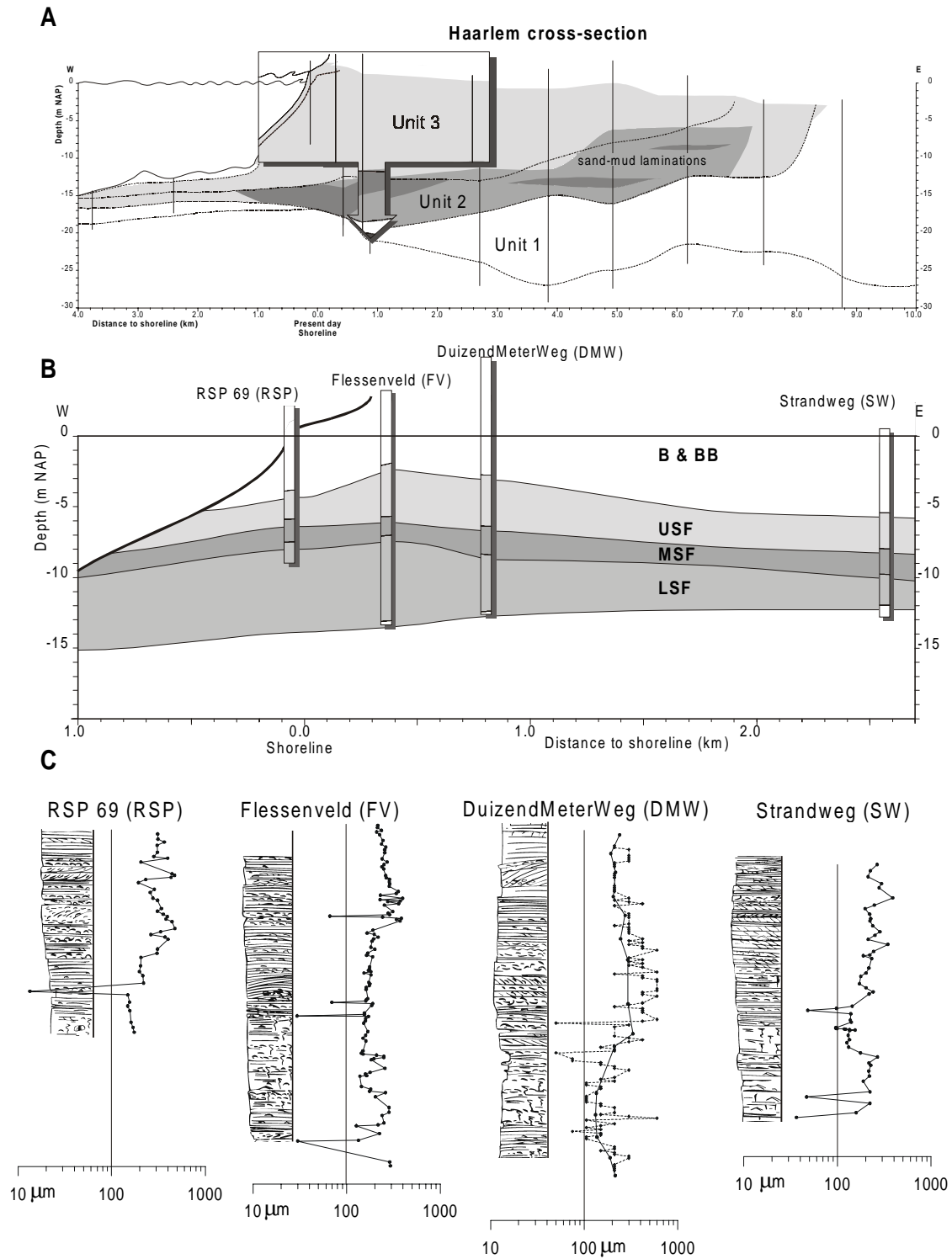


Figure 5.2: Seaward part (B) of coast perpendicular Haarlem cross section (A) with logs and median grain sizes of cores (C). See text for detailed description of lithology and structures.

5.3 Description

The prograded shoreface deposits of unit 3 (Chapter 3 and 4) consist of amalgamated storm-sand beds with parallel lamination. The shoreface deposits are overlain by breaker-bar and beach deposits of similar age, which in turn are overlain by aeolian dunes. In the three westernmost cores the base of unit 3 is formed by a sharp break in depositional characteristics, which is associated by a hiatus (Chapter 4). The lithology and structures of the shoreface and breaker-bar deposits and interpretations of the depositional processes are presented below. The boundaries and average grain sizes of the intervals are presented in table 5.1. The subdivision of the shoreface deposits further details the division presented in Chapter 4. The subdivision and interpretation elaborates on the work of Van der Valk (1996a). For a detailed description of other deposits and their distribution in the Haarlem cross section we refer to Chapter 4.

The subdivision presented here only holds for the four seaward cores of the Haarlem cross section. East of these four cores, in the cores in the older prograded deposits, the lower shoreface deposits are absent and the basal part of the sequence is formed by sand-mud laminations (Figure 5.2), i.e., thin storm-sand layers, occasionally with wave-ripple lamination in a mud matrix. In core SW the basal part of the prograded shoreface deposits of unit 3 also consists of sand mud laminations.

5.3.1 Lower shoreface deposits

The diagnostic criterion for the recognition of lower shoreface deposits is the bioturbation of beds. The interval starts around -13 m NAP and the transition with the overlying middle shoreface deposits starts around -8 m. The deposit are middle sand (176μ) and have been bioturbated. Remnants of mud layers of several cm thick are visible in parts of the interval. Grading of the beds is obscured by bioturbation. In most parts remnants of the original bedding have remained (Figure 5.3A), but some parts have been completely bioturbated. The common structure is horizontal parallel lamination. Slightly (up to 5°) inclined parallel lamination and slightly fanning laminae are observed as well. Laminae have a thickness of 1 mm or less; fining or coarsening trends in lamina thickness were not observed. The thickness of the individual beds is 10 to 20 cm, but some of the boundaries have been blurred by bioturbation. Slightly inclined erosion surfaces separate these beds. In core SW the thickness of the beds increases gradually, from several cm in the underlying sand-mud laminated interval to decimetres in the lower shoreface deposits. Shells and shell fragments are common in the interval. Shells are usually small juveniles, but larger specimens occur in the more shell-rich cores. Beds of shell-fragment beds (up to 5 cm thick), with a chaotic distribution of the fragments, occur in the basal parts of the interval (Figure 5.3B). Convex-up shells on laminae are found throughout the interval and their abundance increases towards the top. Convex-up shells are usually restricted to the basal laminae of the storm beds. Combinations of a thin chaotic layer overlain by a layer with convex-up shells are observed as well (Figure 5.3C).

The abundance of bioturbation traces is the most important characteristic of the lower shoreface deposits. Bioturbation is attributed to burrowing by marine animals, for instance infaunal shells, such as *Spisula subtruncata*, *Donnax vittatus* and others, heart urchins (*Echinocardium cordatum*), and several species of worms, which inhabit the entire shoreface and the breaker bar zone (Eisma, 1966, De Bruyne and Van der Valk, 1991). The individual beds are considered to represent single storm events (cf. Van Straaten, 1965, Van der Valk, 1996a). The horizontal-parallel lamination indicates upper stage bed conditions during deposition. The occurrence of slightly inclined lamination, fanning of laminae and inclined erosion surfaces may all be attributed to hummocky-cross stratification (HCS). The limited

width of the cores with respect to the wavelength of large-scale cross stratification hinders a definite interpretation. The occurrence of thick beds of shell fragments is restricted to this interval. The shell-fragment beds probably originate from selective transport of fragments to the area, or by selective transport of complete shells out of the area. The concentration of the shell fragments in beds results from the winnowing of all other sediment during storms. The deposition of shells in thin chaotic layers and in convex-up position will be discussed in relation to storm-layer deposition.

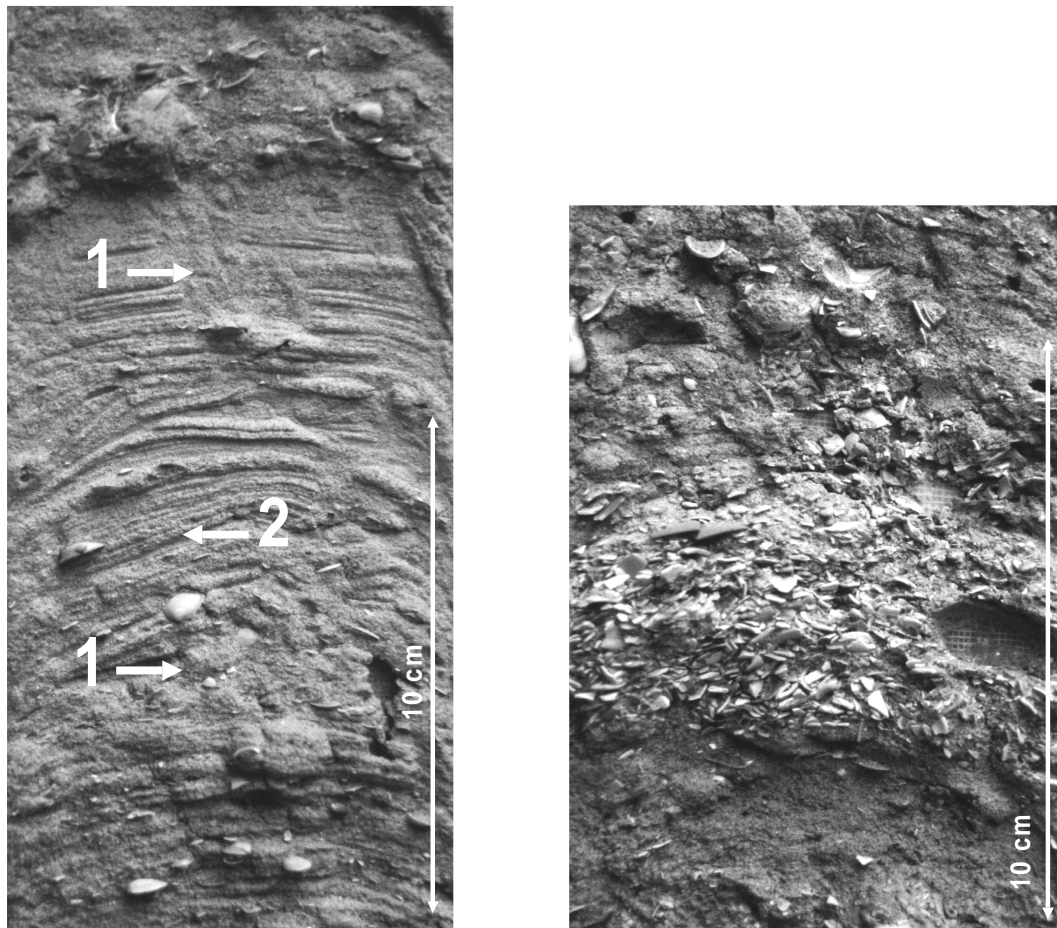


Figure 5.3: Photographs of lacquer peels from cores with representative structures of the facies.

Figure 5.3 A (left): Lower shoreface deposits with remnants of parallel lamination (2), blurred by bioturbation (1). The laminae are slightly inclined and show some fanning. Core FV (-11.05 to -11.16 m NAP).

Figure 5.3 B (right): Lower shoreface deposits with shell bed (arrow), which mainly consists of shell fragments. Fragments are chaotically distributed through the bed and show no preferred orientation. Core FV (-11.31 to -11.36 m NAP).

Figure 5.3 C (following page): Lower to middle shoreface deposits with a shell bed that consists of a chaotic basal layer without preferred orientations (1), overlain by a layer with predominantly convex-up shells (2). The bed consists of horizontal parallel lamination. Core DMW (-8.54 to -8.58 m NAP).

5.3.2 Middle shoreface deposits

The diagnostic criterion for the recognition of middle shoreface deposits is the presence of fine-sandy graded beds with silt and mud tops. The base of the interval lies around -8 m NAP and the top around -6.5 m NAP. The thickness of the interval is around 1.5 m. Although its thickness is limited, the interval can be recognised in all cores. The interval invariably separates the coarse-grained bioturbated lower-shoreface deposits from the coarse-grained upper-shoreface deposits. The graded beds have an average grain size of 124μ . The grain-size distribution of a graded bed of the interval in core SW is shown in figure 5.3D. The top of the bed consists of a transition from fine sand to silt. Notice that coarse sand grains are missing in the interval, even in the base of the graded beds. The mud layers on top of the beds often contain 1 to 2 cm thick sand layers with wave-ripple lamination. The beds have a distinct horizontal-parallel lamination. The transition to silt at the top is often accompanied by a 1 to 2 cm thick wave-ripple-laminated bed. Traces of bioturbation are completely absent. Shells and shell fragments are less common than in the underlying lower-shoreface deposits and are invariably small juvenile specimens. Shells are found chaotically distributed in thick layers (5 cm thick) and in thin layers, but also convex-up in layers at the base of beds and distributed convex-up over the laminae.

The graded beds represent single storm events. Horizontal-parallel lamination indicates upper stage plane bed conditions during deposition, while the thin wave-ripple laminated intervals at the top indicate a decrease of wave-orbital velocities. The fine-grained intervals at the top of the beds result from waning-storm and fair-weather conditions. The absence of bioturbation cannot be related to the absence of burrowing animals from this zone, because the (modern) middle shoreface is rich in life (Eisma, 1966, De Bruyne and Van der Valk, 1991). Hence the absence of bioturbation must be related to the erosion of bioturbated top sections of the beds during storms. The limited amount of shells, as compared to the lower shoreface, is attributed to the higher sedimentation rates, and therefore limited influence of winnowing. The absence of coarse-sand grains suggests that these were not transported to or through this zone.

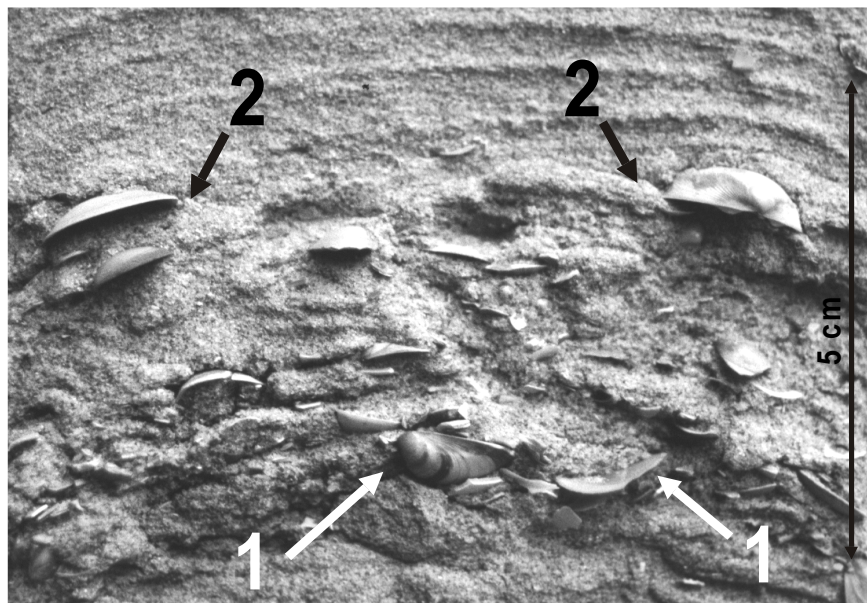


Figure 5.3 C: Caption on previous page.

5.3.3 Upper shoreface deposits

The upper shoreface deposits consist of graded beds without fine-grained tops and with convex-up shells on the laminae. The diagnostic criterion to distinguish upper- from middle-shoreface deposits is the absence of silt and mud layers. The base of the interval lies around – 6.5 m NAP and the top of the interval varies from –5 m NAP in RSP and DMW to –2.2 m NAP in FV. The thickness of the interval varies accordingly. The grain size of the deposits has an average of 202 μ and increases from base to top. Horizontal-parallel lamination is the most common structure of the beds, although slightly inclined-parallel lamination with fanning of laminae is found as well. The tops of the beds have been truncated, in some cases with a slight inclination of the erosion surface. The beds have a thickness of 20 to 30 cm. Towards the top of the interval the grading of the beds is less pronounced. Traces of burrowing are absent, apart from one bed in SW. Shells are common throughout the interval, and specimens are generally coarser than in the underlying middle-shoreface deposits. Shells are found in convex-up position at the base of beds, as well as in convex up position on the laminae (Figure 5.3E) Occasionally shells are found chaotically dispersed in thin layers (up to 1 cm) at the base of the storm beds.

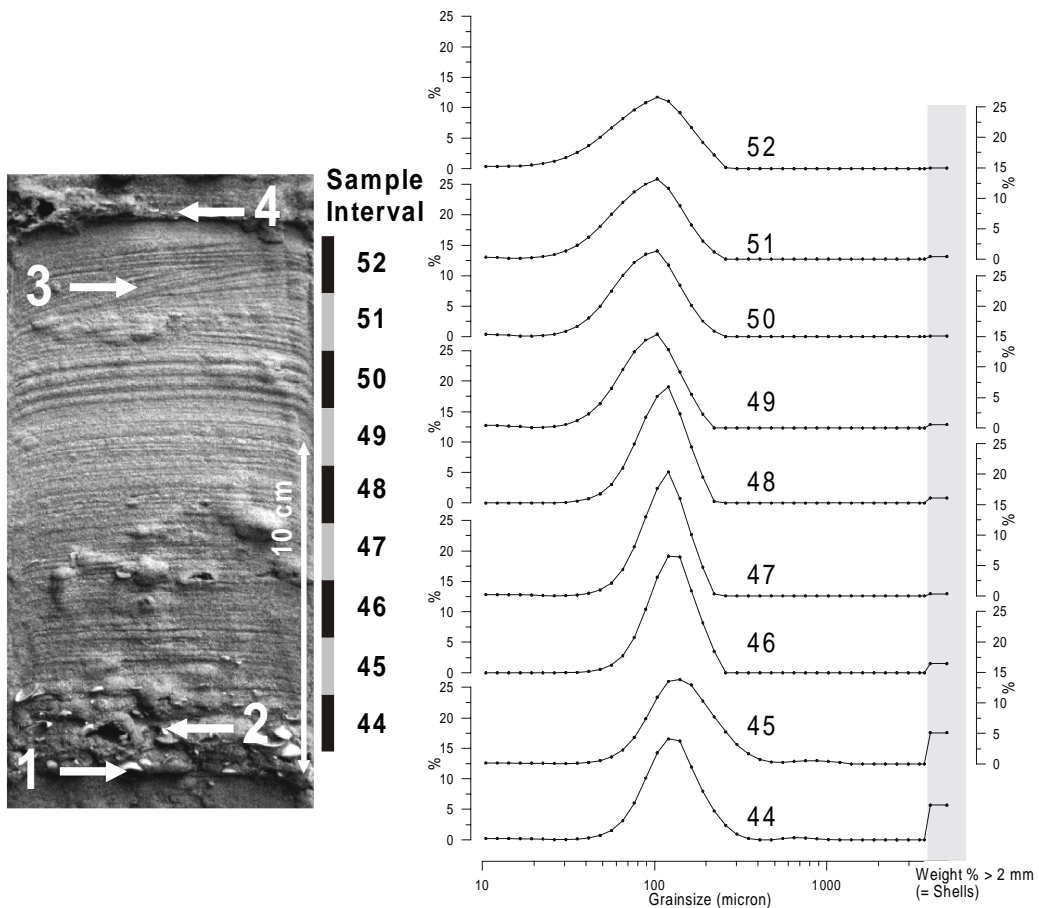


Figure 5.3 D: Graded bed from the middle shoreface deposits, with basal erosion surface (1), basal shell layer (2), thin wave-ripple-laminated bed (3) and mud layer. Top of the bed has been truncated, and is covered by a storm bed (4). The grain-size distributions of the samples from this bed are plotted to the right and display a clear fining upward. Core SW (-9.13 to –9.30 m NAP).

As in lower and middle shoreface deposits the graded beds represent single storm events. The absence of fine-grained tops of beds and the absence of bioturbation are both attributed to erosion during subsequent storms. Horizontal-parallel lamination indicates upper-stage plane bed conditions during deposition. The inclined and fanning laminae may well represent hummocky-cross stratification.

5.3.4 Breaker-bar deposits

Breaker bar deposits are characterised by cross-bedding and the occurrence of thick (up to 30 cm) chaotic shell beds, often overlain by an interval with shells convex-up on laminae (Figure 5.3G). The occurrence of the cross-bedding and the thick chaotic shell layers are the diagnostic criteria to distinguish breaker bar deposits from the underlying upper shoreface deposits. The base of the deposits varies from -5 to -2.2 m NAP, and the top ranges from -2 to 0 m NAP. The transition from upper shoreface deposits to breaker-bar deposits is accompanied by a sharp increase in grain size in FV and RSP. The average grain size is 290μ . On top of the breaker-bar deposits parallel-laminated beach deposits are found, with occasionally thin shell layers and ripple-laminated intervals.

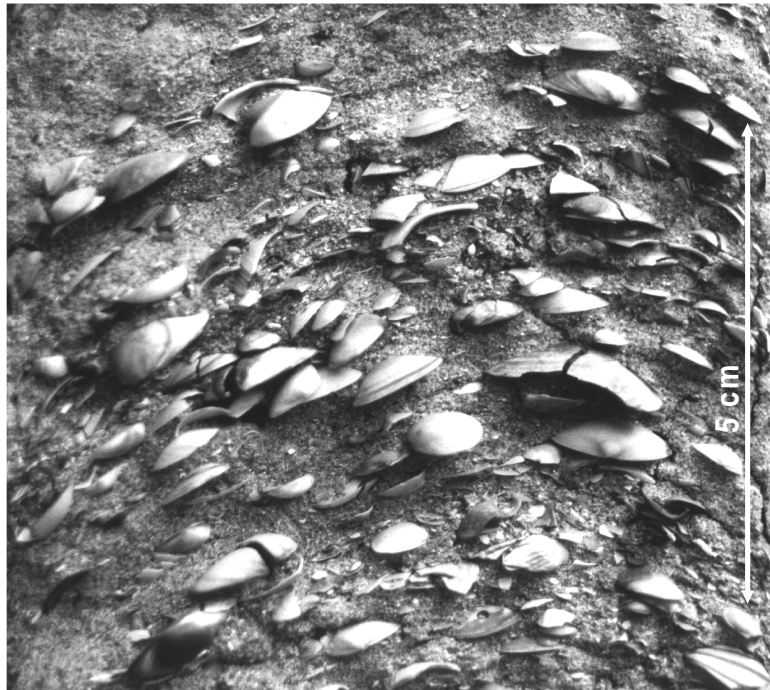


Figure 5.3 E: Storm bed from upper shoreface deposits with horizontal parallel lamination and abundant shells in stable (convex-up) position on the laminae. Core FV (-6.06 to -6.20 m NAP).

5.3.5 Shoreface sequence

The results have been summarised in a composite log with structures, grain sizes, grains-size trends, storm-bed characteristics, and bioturbation (Figure 5.4). All shoreface deposits are characterised by storm beds with horizontal-parallel lamination. Differences between the shoreface deposits are the presence of bioturbation (characteristic for the lower-shoreface interval), the presence of fine-grained tops of storm beds (characteristic for the middle-shoreface interval) and the absence of fine-grained tops of storm beds (characteristic for the upper-shoreface interval). The breaker-bar interval is dominated by cross-bedding, while storm beds are absent. The lower- to middle-shoreface intervals form a fining-upward sequence. The middle- to upper-shoreface to breaker-bar intervals form a coarsening-upward sequence. The breaker-bar interval and the overlying beach and dune deposits form another fining-upward sequence. The characteristics of the beach and dune deposits can be found in Chapter 4.

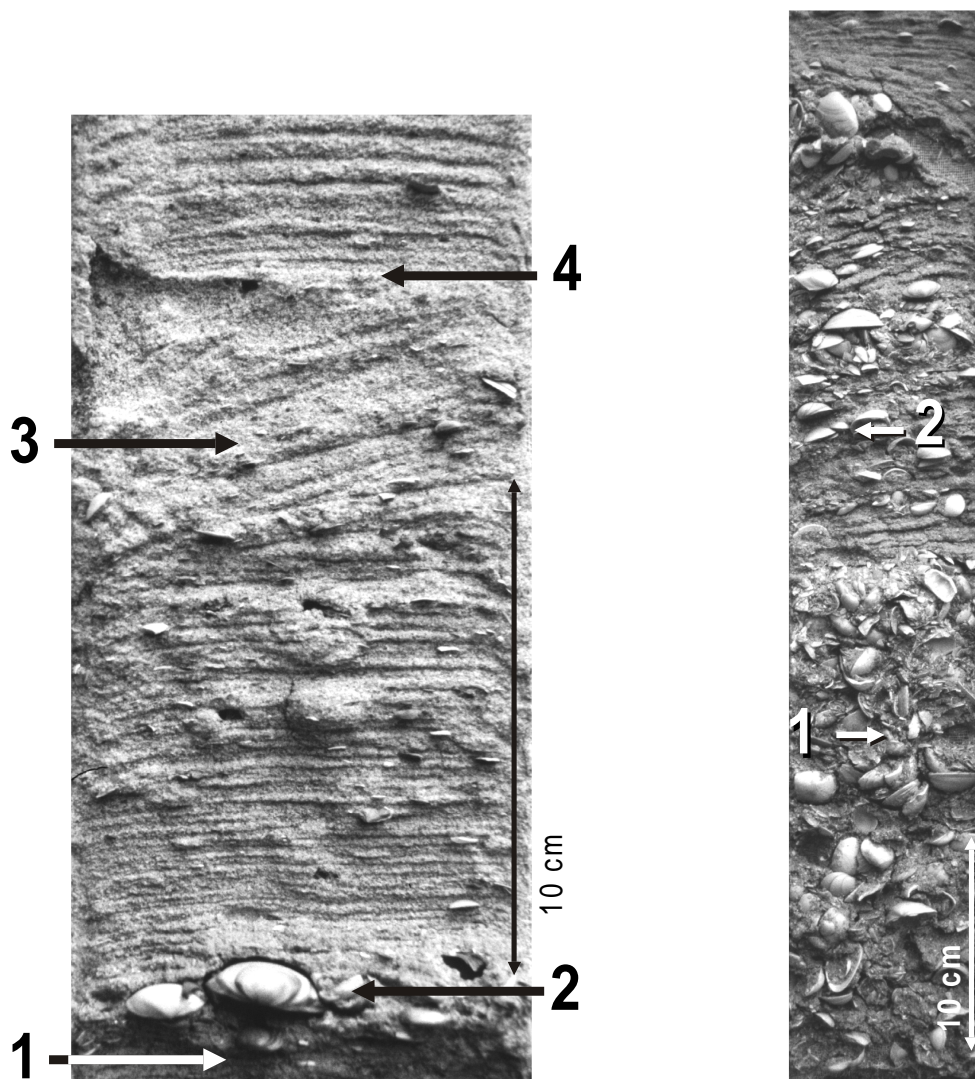


Figure 5.3 F (left): Sandy storm bed from the upper shoreface. Basal erosion surface (1), basal shell layer with convex-up shells (2), clear horizontal parallel lamination at the base of the bed (from 2 to 3), gradually grading into fanning cross bed (3). The top laminae have been truncated by the overlying storm bed (4). Core DMW, (-6.21 to -6.37 m NAP)

Figure 5.3 G (right): Breaker-bar deposits with characteristic thick-chaotic shell bed (1) and overlying cross bedding with convex-up shells (2). Core DMW (-3.65 to -4.09 m NAP)

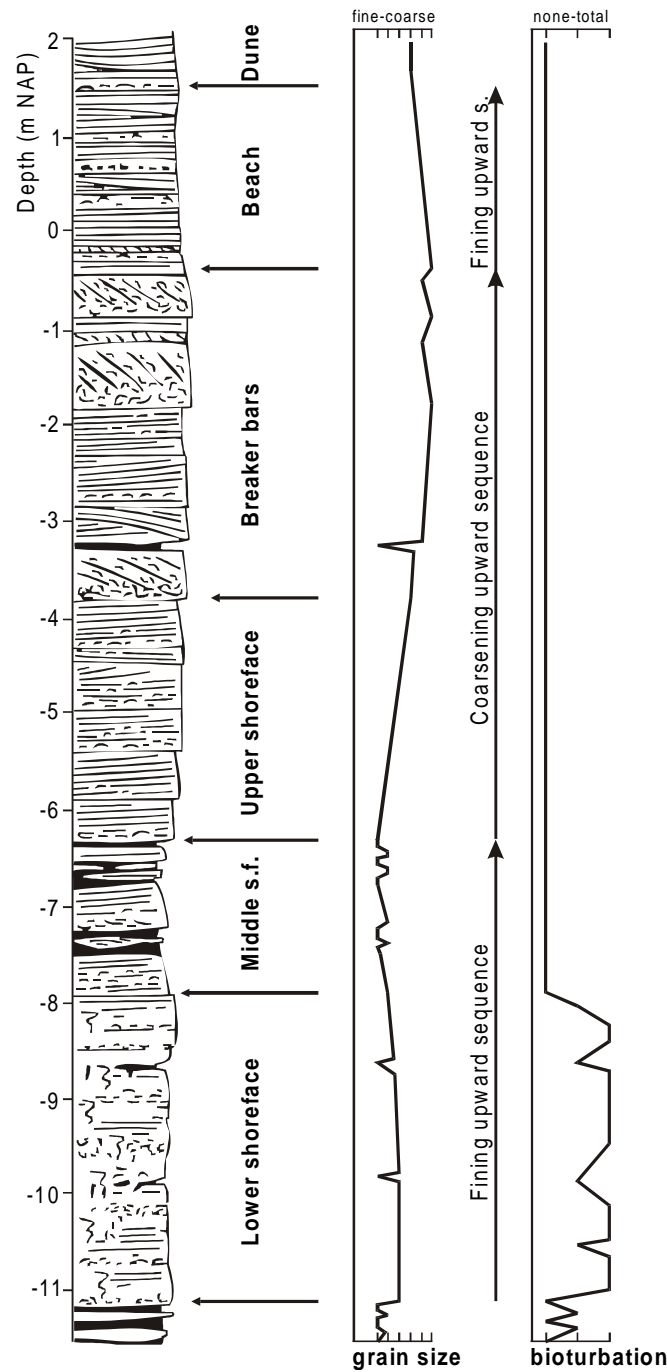


Figure 5.4: Composite log with the characteristics of the shoreface, breaker bar and beach deposits based on the cores from the Haarlem cross section (figure 5.2). Grain size, and bioturbation are indicated.

5.4 Interpretation and discussion

In the discussion we focus on the shoreface deposits and the conditions during their deposition. For an extensive discussion of breaker bar and beach deposits see Chapter 3. The differences in the depth of the intervals that are clearly visible in figure 5.2, are related to large-scale changes in coastal evolution (Chapter 3 and 4). The sequence of the prograded deposits in the Haarlem cross section is compared with the previously described sequence from the western Netherlands and with other coastal sequences. The characteristics of the

storm beds are discussed in relation with the mechanisms of storm-bed formation. The difference in bioturbation, distribution of fine-grained sediment layers and the overall grain-size distribution is related to the occurrence of storms and the intensity of tidal currents. The storm-bed characteristics and the overall sequence of the deposits are used to reconstruct the influence of tides and waves on deposition. The likelihood of deposition by oscillatory sheet-flow versus offshore-directed currents and the consequences for the sediment transport on and to the shoreface are discussed.

5.4.1 Facies models

Van der Valk (1992, 1996a, his figure 34) presented a depositional model for shoreface sands and distal storm sands in the Haarlem cross section, based on the work of Aigner and Reineck (1982). Thin sandy storm sand layers in a mud matrix were deposited as distal storm beds, while the shoreface sands represent proximal amalgamated storm beds. The resulting sequence is coarsening upward (Van der Valk, 1992, 1996a, his figure 37). This model is valid for the cores with sand-mud laminations below the middle shoreface deposits, i.e., for all cores landward of core SW (Figure 5.2). However, this model can not account for the deposition of coarse-grained lower shoreface deposits, found in the seaward cores of the cross section.

Van Straaten (1965) presented an extensive description of a coast-perpendicular cross section near The Hague. The lithology, grain sizes and structures in the cross section are comparable to those presented here; mud layers (middle-shoreface deposits) are more extensive in the The Hague cross section. The coarse-grained lower shoreface deposits were interpreted as an extension of the coarse-grained shelf (Van Straaten, 1965). Based on the extensive middle shoreface, without coarse sand, Van Straaten (1965) suggested that the cross-shore exchange of the coarse sand grains was very limited.

In comparison to shoreface sequences at other locations around the world (Elliot, 1986), the evidence for lunate megaripples is restricted in our sequence. The absence of lunate megaripples may be due to the relatively small grain size on the shoreface, that hinders the development of lunate megaripples (Clifton, 1976). In addition, the waves on the North Sea have a relatively short period (Van Straaten, 1961, Hokke and Roskam, 1987) and such wave conditions hamper the development of lunate megaripples (Davidson-Arnott and Greenwood, 1976). Most shoreface-to-beach sequences from modern coasts are coarsening upward, with shelf mud at their base (Reading and Collinson, 1996, their figure 6.85). In contrast, the sequence from the Haarlem cross section (Figure 5.4), starts with a fining upward, followed by a coarsening upward. Shelf mud and distal thin storm-sand layers are absent in the seaward half of the Haarlem cross section (Figure 5.4). It is important to notice that the coarse-grained lower-shoreface deposits at the base of the sequence have built up as part of the progradational sequence (chapter 3 and 4). The deposits do not represent a coarse erosional lag (Nummedal and Swift, 1987), which is a normal part of accommodation-dominated (autochthonous) shoreface-to-shelf systems (Swift, 1976b, Swift and Thorne, 1991).

The grain-size distribution in the cores is comparable to that on the modern shoreface, with a coarse-fine-coarse trend from lower shoreface to beach (Van Straaten, 1961, 1965). At present the depths of the grain-size transitions are found slightly deeper. The presence of fine-grained deposits and mud layers halfway between the North Sea floor and the beach on the modern shoreface (Van Straaten, 1965, Van Alphen, 1987), is comparable to the middle shoreface deposits in the prograded sequence. The structures in the basal parts of the box cores from the modern shoreface (Van der Valk, 1992) are also similar to the structures found in the prograded shoreface deposits. The structures at the top of the box cores reflect fair-weather structures, and these have not been preserved in the prograded deposits.

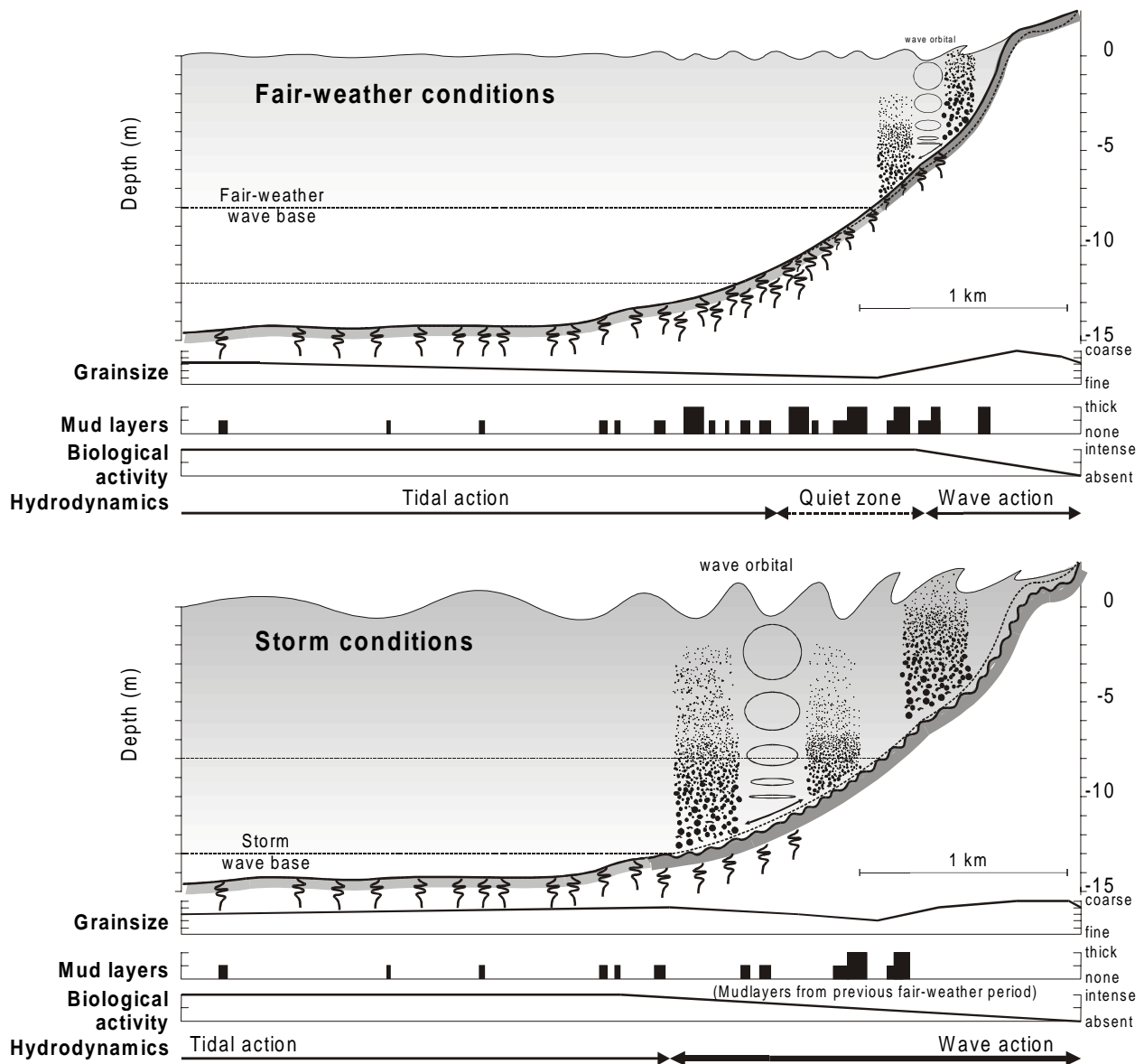


Figure 5.5: Cartoon of shoreface processes during fair-weather conditions and during storm conditions. **Upper halve:** Under fair-weather conditions coarse-grained sediments are found on the beach, breaker bar and the highest part of the upper shoreface. The mobility of the coarse-grained material is limited due to limited wave action. The wave-asymmetry effect may result in a net transport of coarse-grained sediments in the direction of the long-shore current (dependent on wave incidence). On the lower shoreface tidal currents may transport some coarse-grained sediment. Fine-grained sediment can accumulate from the middle to the upper shoreface. Tidal currents hinder abundant deposition of fine-grained sediments on the lower shoreface. Fine-grained sediments may originate from the lower shoreface and lower shelf and get trapped on the quiet middle shoreface. The quiet conditions on the upper, middle and lower shoreface permit all types of marine life, which results in extensive bioturbation. **Lower halve:** During severe storms the entire shoreface and shelf are subject to wave action and coarse sediment can be eroded and entrained, where it is available. The coarse grains remain in the basal layer of the water column. Transport of the coarse grains results from wave-asymmetry effects and from the currents that the basal layer experiences. On the upper shoreface more wave energy is available and coarse grains can be entrained higher in the water column. Transport of coarse grains is more pronounced there. Fine sediment is suspended high up in the water column over the entire shoreface and shelf. The fine-grained sediment can be transported virtually anywhere with the currents that are superimposed on the oscillatory flow. Deposition of fine grains is restricted to the waning of the storm on the shoreface. Tidal currents on the North Sea floor hinder abundant deposition of fine grains.

5.4.2 Storm beds and shoreface sequence

The common denominator of the shoreface deposits is the presence of amalgamated storm beds. The erosion surface at the base of the storm bed shows that erosion preceded their deposition. The erosion was sufficient to remove any sediments with traces of bioturbation in the top few centimetres of the shoreface profile down to the lower shoreface. On the other hand, the erosion was not sufficient to remove all fine-grained sediment from the middle shoreface. The conditions during erosion and the thickness of the eroded material can only be guessed at. In the breaker bar zone the erosion and truncation of beds resulted from bedform migration. This was accompanied by the continuous winnowing of fine sand from these deposits.

The deposition of the beds occurred during the waning of the storm, due to decreasing flow conditions and a dramatic reduction in flow capacity. The grading of the individual beds (Figure 5.3D) represents sorting within the flow and decreasing flow conditions (this is comparable to the deposition of a graded turbidite bed, see for instance: Stow and Bowen, 1980). The sorting within the suspension is due to differences in fall velocity of sand of different grain sizes. In high-density suspensions grain-grain interactions may add to the sorting (Bagnold, 1954). Coarse grains concentrate at the base of the flow and settle first, while fine grains remain higher in the flow and take longer to settle (Cook and Gorsline, 1972, their fig.15). Eventually silt and mud will settle and deposit at places where post-storm fair-weather conditions permit.

Most beds show distinct horizontal-parallel lamination (Figure 5.3D, base of figure 5.3F), indicative of upper-stage plane-bed conditions. The upper-stage plane-bed conditions can result from oscillatory flow (the near-bottom wave-orbital velocities), from unidirectional currents or from combinations of the two (combined flow: Arnott and Southard, 1990, Myrow and Southard, 1991).

Shells differ in hydrodynamic response from sand due to differences in density and geometry. The distribution of shells can be used as an additional marker for depositional conditions. Thick chaotic shell beds at the base of storm beds (Figure 5.3B) are likely the result of winnowing of fine sediment; sand and silt are eroded by the currents, but the coarse shells cannot be entrained and are left at the sea floor. As soon as currents affect the shells, they will be turned into a stable, convex-up position. The transition from chaotic-distributed shells to convex-up shells is found within several beds (Figure 5.3C) and reflects an increase in current velocities. If the current velocities increase even further, the shells can be entrained in the flow and will be found convex-up on the laminae (Figure 5.3C). High current velocities of longer duration may have a similar effect. The increase of the amount of shells on the laminae from lower to upper shoreface probably results from higher energy conditions on the upper shoreface. Deposition of chaotic shell beds can also occur by settling from suspension of shells (Middleton, 1967). The settling of shells would be accompanied by the deposition of sand (Allen, 1984) and the resulting bed would consist of a shell-sand mixture. Hence, settling from a suspension does not result in the deposition of a chaotic shell bed with little matrix overlain by a sandy storm bed. It is therefore less likely that the settling from a suspension is responsible for the formation of the chaotically distributed shells in beds in these deposits.

The distribution of bioturbation traces is inversely related to the wave energy acting on the shoreface, i.e., restricted at the highest parts and abundant on the lower shoreface. This distribution results from the influence of storms and fair weather periods at different depths. Under fair-weather conditions the top layer of the entire shoreface is being bioturbated (Howard and Reineck, 1972, Van der Valk, 1992). During storms the top layer of the

sediment is eroded and bioturbation traces are thus removed. The severity of the storm determines to which water depth erosion occurs. Severe storms will destroy the burrowing traces over the entire shoreface, while moderate storms destroy burrowing traces down to lesser depths. Because moderate storms occur more frequently than severe storms, erosion on the middle shoreface is more frequent than on the lower shoreface.

Van Straaten (1961, 1965) argued that the Holocene fine-grained middle-shoreface deposits (lithologic zone II, table II, Van Straaten, 1965) result from the rapid burial of fine-grained sediments by storm sands and is evidence of high sedimentation rates. In his view mud is deposited during slack tides, and buried by sand during periods with stronger currents. This may be stimulated by the predominance of fine-grained sediment supply to the shoreface zone and by the production of faecal pellets on the shoreface (Van Straaten, 1961). Indeed a high sedimentation rate improves the preservation, as is evident from the thick middle-shoreface interval in the Wassenaar cross section, that has experienced rates of progradation twice as fast as those at Haarlem (Van der Spek *et al.*, 1999, Chapter 3 and 4). However, the abundance of middle shoreface deposits within the Haarlem section does not differ between the different cores although the rate of progradation decreased from SW to RSP (Chapter 3). Therefore, we suggest that deposition and preservation of fine-grained sediment on the middle shoreface is a normal part of the shoreface sequence in the Western Netherlands. High sedimentation rates enhance the thickness of middle shoreface zone.

5.4.3 Depositional model

The coarse sand in the breaker bar and beach zone is related to wave reworking. Offshore wave heights and the shoreface profile determine the wave activity along the profile and account for the seaward fining. The coarse sand on the North Sea floor resulted from ongoing tidal reworking and the winnowing of fine-grained components (Van Straaten, 1961, 1965). It is essentially an erosional sand sheet (Swift, 1976b, Roy *et al.*, 1994). The coarse-grained lower shoreface lies directly adjacent to the coarse-grained North Sea floor and received coarse-sand grains from that area. The fine-grained zone in between the North Sea floor and the breaker bar and beach is the transition between the tide-dominated North Sea shelf and the wave-dominated beach and upper shoreface. Tidal currents in deeper parts of the North Sea are well capable of eroding mud and fine sand particles (Van der Meene *et al.*, 1996). On the present-day coast, the presence of mud layers in the transition zone during fair weather (Van Alphen, 1987) is evidence for the limited strength of tidal currents in this zone. The presence of mud layers also demonstrates that during fair weather wave action is equally restricted in this zone. The middle shoreface is thus a tranquil zone with limited current and wave action at the bottom during fair weather, and this was similar during progradation. During storm periods severe wave action resulted in reworking of deeper parts of the profile, and real big storms affected the North Sea floor as well. The coastal sequence (Figure 5.4) can be seen as the combination of a fining-upward tidal sequence with a coarsening-upward wave sequence.

The model for storm-bed emplacement needs to incorporate the abundance of horizontal parallel-laminated deposits and the trends in bioturbation, abundance of fine-grained layers and grain size over the entire shoreface. From the abundance of horizontal parallel-laminated storm beds we have inferred that oscillatory-sheet flow or unidirectional currents are the mechanisms for sediment erosion and deposition. The principle driving force of oscillatory-sheet flow is intense wave reworking, while the driving force for unidirectional currents is any type of flow, i.e., suspension-driven flows: storm-induced turbidity currents; and circulation-driven flows: rip-current flows, downwelling, etc.

Oscillatory-sheet flow can account for the coarse-grained lower shoreface deposits. During severe storms oscillatory sheet-flow conditions can extend down to the North Sea

floor and erode and entrain the coarse-grained material and redeposit it as storm beds. The instantaneous wave-orbital velocities observed on the North Sea floor by Van der Meene (1994) are well within the upper-stage plane-bed field, and are well capable of entraining coarse grains. The coarsening upward from the middle shoreface to the beach results when, during the waning of a storm, wave action on the lower part of the shoreface ceases and fine grains settle out of suspension. As the storm declines even further this also becomes possible on the middle shoreface. On the upper shoreface such conditions are only reached under very tranquil conditions.

Offshore-directed currents can explain the offshore fining from the beach to the middle shoreface, which results from the decay of the flow as it moves down the shoreface slope. The coarse-grains are deposited once the flow loses any strength and eventually only fine-grained deposits are found. Down-stream fining is observed in turbidites (Kuenen and Migliorini, 1950), in proximal-to-distal storm-sand layers and tempestites (Aigner and Reineck, 1982, Nelson, 1982, Aigner, 1985) and in deposits from rip currents (Gruszczynski *et al.*, 1993). However, offshore-directed currents can not explain the coarse-grained storm beds at the lower shoreface.

So, on basis of the overall grain-size distribution from shoreface to beach we favour oscillatory sheet-flow as the prime agent for deposition of storm beds. Other arguments against shoreface deposition by offshore-directed currents are the total absence of current-related structures and the convex-up position of shells on the laminae. No current ripples occur below the fine-grained tops of the storm beds (the Bouma C interval), there is no cross-bedding as commonly observed in rip-current channels (Gruszczynski *et al.*, 1993), and there are no large asymmetric cross beds from the flow-dominated stability field (Myrow and Southard, 1991). The common presence of shells in stable convex-up position on the laminae reflects continuous reworking and is thus an additional argument for oscillatory-sheet flow.

5.4.4 Sources of sediments

In relation to the processes on the shoreface we have to discuss the sources of sediment for coastal progradation. We distinguish a fine transport component ($< 150 \mu$) and a coarse transport component ($> 150 \mu$) (cf. Van Straaten, 1965, Van der Valk, 1996a). The fine transport component comprises all grain sizes that are found in the middle shoreface deposits and that thus can be transported over the entire shoreface. The coarse transport component incorporates all sediment coarser than found in the middle shoreface deposits, and is constrained to the lower and the upper shoreface deposits.

Under fair-weather conditions (Figure 5.5A) fine grains will be subject to wave-induced long-shore currents and to wave-induced up- or downwelling in the upper shoreface and breaker zone, and to tidal currents on the lower shoreface and shelf. Accumulation of fines occurs on the middle and upper shoreface during fair weather (Terwindt, 1962). Coarse grains are more difficult to transport and are subject to onshore-directed wave-asymmetry effects in the zone of wave breaking (see for instance Allen, 1970), and may be transported (in traction) by tidal action on the lower shoreface and shelf. Bed-form migration winnows fine-grained sediment from the breaker-bar zone.

During storm conditions (Figure 5.5B) coarse grains can be eroded and entrained in the flow as well, and currents may add to wave asymmetry effects. Bypassing of coarse grains through the middle shoreface can be ruled out as an important process as this is not recorded in the bases of middle-shoreface storm beds (Van Straaten, 1965). Wave-asymmetry effects on shelf and lower shoreface are not present or not capable of such transport, while wave-asymmetry effects on the upper shoreface result in onshore transport of coarse grains (Wright

et al., 1991). Coarse grains in the upper shoreface, breaker bar and beach will thus be contained in this zone (Allen, 1970, Swift and Thorne, 1991).

As a consequence, the coarse grains in the upper shoreface, breaker bars and beach must have been supplied by longshore transport. There are no restrictions on the transport of the fine-grained fraction, and both cross-shore and longshore transport of the fine-grained material may have added to coastal sedimentation. This implies that the North Sea shelf may have acted as a source of fine-grain sediment for coastal progradation. The source of coarse-grained sediments for coastal progradation must be sought alongshore in eroding coastal stretches (The Belgium and South-Netherlands coast and former Rhine and Meuse delta in the South, and the Texel Headland in the North, cf. Beets *et al.*, 1992, see discussion in Chapter 4). The similarity in the grain-size distribution over the modern shoreface and in the fossil sequence suggests that similar processes acted in the past as do nowadays. The similarity in sedimentary structures supports this notion.

5.5 Conclusions

The four most seaward cores of the coast-perpendicular Haarlem cross section can be subdivided in three shoreface intervals, overlain by a breaker-bar and beach interval. The shoreface intervals all consist of graded storm beds with basal erosion surfaces. The lower shoreface interval can be distinguished on basis of bioturbation traces, the middle shoreface interval contains fine-grained deposits at the top of graded beds, the upper shoreface interval is not bioturbated and does not contain fine-grained beds. The overlying breaker bar deposits contain thick shell beds and cross-bedding. The grain-size trend from lower shoreface to beach is fining upward overlain by coarsening upward.

The sedimentation on the shoreface reflects the increase in wave action up along the shoreface profile. The increase in wave action is a combination of the daily wave action that increases upward along the profile and the recurrence of severe storms that have an impact on deeper water too. The limited recurrence of large storms that affect the entire shoreface is reflected in the abundance of bioturbation traces in the lower shoreface interval. In the other intervals bioturbation traces, formed under fair-weather conditions are erased during subsequent storms. The presence of silt and mud on top of the graded storm beds of the middle shoreface results from restricted re-suspension by tidal currents and wave action. On the upper shoreface continuous wave action prohibits deposition of mud.

The North Sea shelf and lower shoreface was controlled by tidal action, the upper shoreface to beach was dominated by wave action. The zone in between was relative quiet under fair-weather conditions, while during severe storms the entire shoreface and shelf were influenced by wave action. The storm beds have been deposited by wave-driven oscillatory-sheet flow. The fine-grained middle shoreface indicates that cross-shore transport of coarse grains did not occur. The coarse-grained material in the lower shoreface deposits was derived from the adjacent North Sea floor, while the coarse material in the upper shoreface is derived from long-shore transport. Fine grains can be transported in cross-shore and long-shore direction over the shoreface.

The grain-size distribution of the sequence mimics the grain-size distribution on the modern shoreface after storms. The conclusion that long-shore sediment transport was responsible for the deposition of coarse grains in the upper shoreface to beach, and that fine-grained sediments are delivered by cross-shore and longshore sediment transport, is valid for modern shoreface dynamics too.

Chapter 6: Modelling the decrease in wave height over the shoreface due to slope-induced changes in bottom friction.

Abstract

Wave height-reduction on the shoreface is partly induced by friction at the bottom. The bottom friction depends on the slope of the shoreface and on the seabed grain size and morphology. The slope of the shoreface profile from prograded shoreface deposits in a coast-perpendicular cross section is determined from isochrons. The slope of the shoreface increased from 0.15° during initial progradation to 0.59° during final progradation. The wave-height reduction from -10 to -5 m below palaeo-mean sea level on the reconstructed shoreface profiles has been calculated. The calculations show that high, long-period waves are more dampened than low short period waves. On the gentle initial-prograded shoreface slope about 35% of the high waves remain, on the steep slope of the modern shoreface 60% of the high waves remain.

The difference in wave-height reduction induced by differences in travel length over the shoreface slope can well explain observed variation in the shoreface deposits. Shoreface deposits from the initial prograded coast consist predominantly of mud with thin wave-laminated storm sand and silt layers. The shoreface deposits indicate relatively quiet depositional conditions during initial progradation. Shoreface deposits of the final prograded coast consist of dm parallel-laminated thick storm beds of sand. The shoreface deposits indicate high-energy depositional conditions during final progradation.

6.1 Introduction

Holocene coastal deposits in the Western Netherlands consist of transgressive coastal deposits overlain by prograded wave-dominated deposits (Chapter 1). The deposits of the prograded wave-dominated coastal system consist of shoreface, breaker bar and beach deposits (Chapter 4). Deposition prograded over tidal deposits of the transgressive coastal system. The Haarlem cross section runs perpendicular to the coast from the initial prograded deposits to the modern shoreline (Figure 3.2). In the cross section a marked change in the distribution and character of the shoreface deposits from initial to final progradation is visible. The initial prograded shoreface deposits consist of mud with thin storm sand layers of fine sand and silt. The storm layers usually contain wave-ripple lamination. The shoreface deposits from the end of progradation consist of thick storm beds of middle to fine sand, with scarce thin mud layers. The storm sand beds usually contain horizontal parallel lamination. The transition from predominantly mud with thin storm sands to predominately sand is gradual. The depth up to which mud and thin storm sands are found increases in the direction of progradation and is associated with an increase in the thickness and abundance of storm sand beds. Van Straaten (1965) observed that the depth at which mud layers were found in prograded shoreface deposits increase seaward, similar to the trend in the Haarlem cross section (figure 3.11). This trend was also observed in the Wassenaar cross section (Van Someren, 1988, and Chapter 3, figure 3.10).

The change in the character of the deposits during coastal progradation can be regarded as the result of an increase in wave energy during progradation. Initially mud was deposited under relatively quiet conditions, while thin storm sand layers were deposited during higher energetic events. During progradation the deposition of mud continued to occur under relatively quiet conditions, but most of the mud was during storm events. During the storm events more and more sand was reworked into thick storm sand layers.

Changes in the overall wave-climate of the North Sea during the Holocene have been modelled by Stive (1987). The model outcome showed that the wave climate changed little during the last 6000 years. Changes in the overall wave climate can thus be ruled out as a possible cause of change in the character of shoreface deposits. Van Straaten (1965) envisaged a bar on the lower shoreface during initial coastal progradation, that sheltered the middle and upper shoreface from intense wave action. There is indeed evidence for the presence of such bars during the earlier stages of coastal evolution (Van Someren, 1988, and Chapter 3). Other possible mechanisms for the lower wave-energy during initial progradation are changes induced by the shoreface profile itself, i.e., reduction of wave height due to bottom friction. Two factors play a role in the reduction of wave height on the shoreface profile: the slope of the shoreface and the friction factor, which is a combination of seabed morphology (rippled versus plane bed) and grain-size (Nielsen, 1983, Van Rijn and Houwman, 1999).

In this chapter we test the assumption that the low-energy character of shoreface deposits from the initial stage of progradation has resulted from wave-height reduction due to the relatively large travel length imposed by a gentle shoreface slope. We do this by calculating the loss in wave height over shorefaces with different slopes using Nielsen's explicit wave formulae (Nielsen, 1982, 1983). We use geological data to estimate the slopes of the shoreface from the start to the end of progradation. In addition we discuss the role of the friction factor, the influence of wave refraction, the shoreface-slope development, the consequences for sediment transport and deposition. Previous explanations for the low-energy shoreface deposits are briefly discussed.

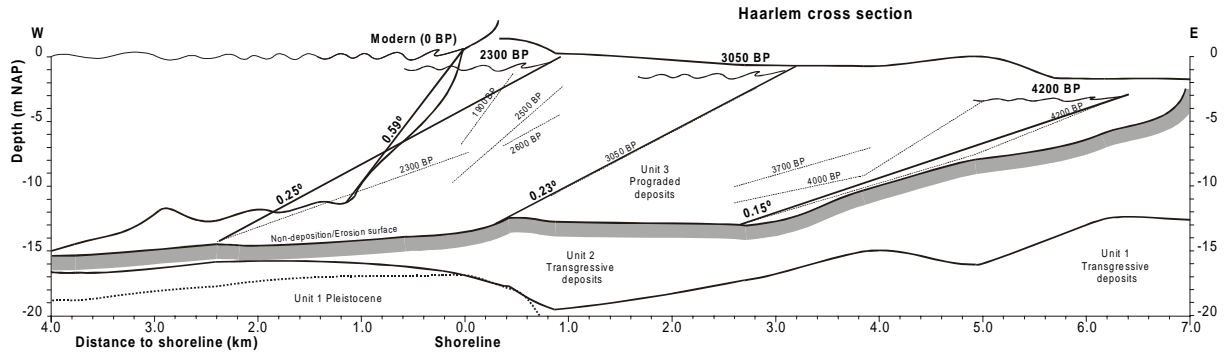


Figure 6.1: The Haarlem cross section with schematic stratigraphy; shaded grey marks the pre-progradation deposits that form the substrate for progradation. For information on the stratigraphic units 1 to 3 see Chapter 3 and 4. In the prograded shoreface deposits the isochrons, based on AMS ^{14}C dates on single shells are indicated in grey (see Chapter 3, figure 3). The black lines indicate the reconstructed shoreface profiles. The slopes of the profiles are indicated as well, as is the sea level from that period. The isochron of 3050 coincides with the reconstructed shoreface profile.

6.1.1 Hypothesis

The transition from low-energy shoreface deposition of thin sandy storm layers in mud to high-energy shoreface deposition of thick sandy storm beds without mud results from an increase in wave-energy during coastal progradation. We assume that the increase in wave action during progradation of the coastal system is related to the observed increase in slope of the lower shoreface during progradation. A gentle slope of the shoreface means that the distance over which waves ‘feel’ the influence of the bottom is larger and thus that the reduction of wave height due to friction at the seafloor is large. On a steep slope the distance over which the influence of the bottom is felt is much smaller and hence, the reduction of the wave height is more limited. The change in the shoreface slope is induced by the nearly level substrate for progradation, by the rise of sea-level, and by the progradation itself.

6.2 Methods

6.2.1 Profile reconstruction

The Haarlem cross section (Chapter 3 and 4, figure 3.11 and 4.1) is used to reconstruct the shoreface profiles during progradation. We reconstruct the shoreface profile during initial progradation over the top of transgressive coastal deposits (Figure 6.1). The transition of transgression to progradation occurred around 4700 to 4400 BP. The age of the prograded deposits has been determined with AMS ^{14}C dating of single shells and was used to construct isochrons (Chapter 3). We have used the isochrons from the prograded shoreface, breaker bar and beach deposits to reconstruct the slope of the shoreface.

The upper boundary of the shoreface profile is delimited by the sea level of that time (from Jelgersma, 1979). The lower boundary is given by the top of the underlying transgressive deposits. In the westernmost half of the cross section this is a non-depositional/erosional surface. The shoreface profiles with their slopes, which were used for the calculations are indicated in figure 6.1. We have used the isochrons of 4200 and 3050 BP that stretch from the lower to the upper boundary. The small nick in the 4200 BP isochron was smoothed. The 2300 BP timeline was constructed slightly different, because the actual isochron only covers the lowest part of the cross section. For the upper boundary of the 2300

BP cross section a position between the isochrons of 1900 and 2500 BP was interpolated. The modern shoreface profile was averaged over its steepest part, from –11 to 0 m NAP. The shoreface profiles were used to calculate the slope of the shoreface. The wave-height reduction over the interval of –10 to –5 m below palaeo-mean sea level was calculated

6.2.2 Wave climate

We use modern wave statistics at –10 m waterdepth in the North Sea as starting conditions for the calculations of the loss of wave height. The wave statistics are an average over the 10 year period 1975-1986 from Meetpost Noordwijk (Hokke and Roskam, 1987) as presented by Stive and De Vriend (1995). Kohsiek (1988) gives an average (50%) wave for the Dutch coast of 1.1 m with a wave period of 3.7 s. Model calculations of Stive (1987) indicate that the wave climate of the North Sea around 5000 BP was much similar to the modern wave climate. Despite the increase in waterdepth due to the rise in sea level the average wave height and wave period were only slightly less (below 5%) at 5000 BP. Only the wave skewness changed considerably, but this parameter is not considered in the calculations.

Table 6.1: Average wave height, wave period and occurrence frequency of waves at –10 m below mean sea level over a 10 year period, from 1975 to 1986 from the platform Meetpost Noordwijk, which is representative for the coast of the Western Netherlands (Hokke and Roskam, 1987; cited by Stive and De Vriend, 1995).

H (m)	T (s)	Frequency (%)
0.25	4.0	20.778
0.75	4.5	36.462
1.25	5.0	20.805
1.75	5.3	11.741
2.25	5.5	5.4
2.75	6.0	2.7
3.25	6.5	1.1
3.75	7.0	0.6
4.25	7.5	0.3
4.75	8.0	0.1
5.25	8.5	0.1
5.75	9.0	0

6.2.3 Wave height reduction

The loss of wave height over a gently sloping shoreface profile was calculated with Nielsen's (1983) explicit wave formulae. X axis is positive in the direction of wave propagation (landward) and depth is positive (so beach slope is negative)

$$H_2 = H_1 \sqrt{\frac{c_{g1} \cos \alpha_1}{c_{g2} \cos \alpha_2}} \left/ \left[1 + \beta H_1 \sqrt{\frac{c_{g1} \cos \alpha_1}{c_0}} I \right] \right. \quad (6.1)$$

$$\beta = \frac{k_0 f_e}{3\pi} \frac{dh}{dx} \quad (6.2)$$

$$k_0 h = \frac{4 \pi^2}{g T^2} h \quad (6.3)$$

with $\alpha=0^\circ$ the analytical solution of I becomes

$$I = \frac{4}{5} (k_0 h_1)^{-1.25} \left[1 - \left(\frac{h_1}{h_2} \right)^{1.25} \right] + (k_0 h_1)^{-0.25} \left[\left(\frac{h_1}{h_2} \right)^{0.25} - 1 \right] - \frac{61}{360} (k_0 h_1)^{0.75} \left[\left(\frac{h_1}{h_2} \right)^{0.75} - 1 \right] \quad (6.4)$$

following Nielsen (1982) we approximate c_g/c_0 with the intermediate water depth ($h/L_0 < 0.2$) equation

$$\frac{c_g}{c_0} = \sqrt{2 \pi \frac{h}{L_0}} e^{-\pi \frac{h}{L_0}} \quad (6.5)$$

If we consider c_{g1} and c_{g2} constant, equation 1 becomes for $\alpha=0^\circ$:

$$H_2 = H_1 / \left[1 + H_1 \frac{k_0 f_e}{3 \pi \frac{dh}{dx}} \sqrt{\sqrt{2 \pi \frac{h}{L_0}} e^{-\pi \frac{h}{L_0}} I} \right] \quad (6.6)$$

6.3 Results

6.3.1 Wave height

The loss in wave height on the shoreface slopes of 0.15° , 0.25° and 0.59° is calculated for all types of waves in table 6.1. For all simulations an identical value of 0.15 is taken for the friction factor (f_e). The results are presented in figure 6.2. The original wave height at -10 m, the remaining wave height at -5 m and the remaining percentage of the waves is given for all waves. The reduction of the wave height is larger on the gentle slopes. The wave-height reduction is much more effective for the long-period high waves than for the short-period low waves. On the most gentle slope only 25% of the highest long-period waves remains, against 57% on the steepest slopes.

In other words, the gentle shoreface from the period of initial progradation resulted in altogether lower waves and dampened out all the large waves. The results of the simulations are also expressed in figure 6.3, where the wave-height distribution after their reduction over the lower shoreface is plotted. The pattern in the modern wave distribution at -5 m is comparable to that of the original wave-height distribution at -10 m. The distribution after wave-height reduction on the gentle slope shoreface from 4200 BP shows no waves over 2 m at -5 m. The distribution after wave-height reduction on the intermediate slopes holds an intermediate position.

6.4 Discussion

The outcome of the calculations shows that the slope of the shoreface has a marked influence on the wave-height reduction due to the changes in travel length over the seafloor. The gentle lower-shoreface slope of the initial prograding coast reduced the impact of wave on the shoreface and beach much more than the steep slope of today.

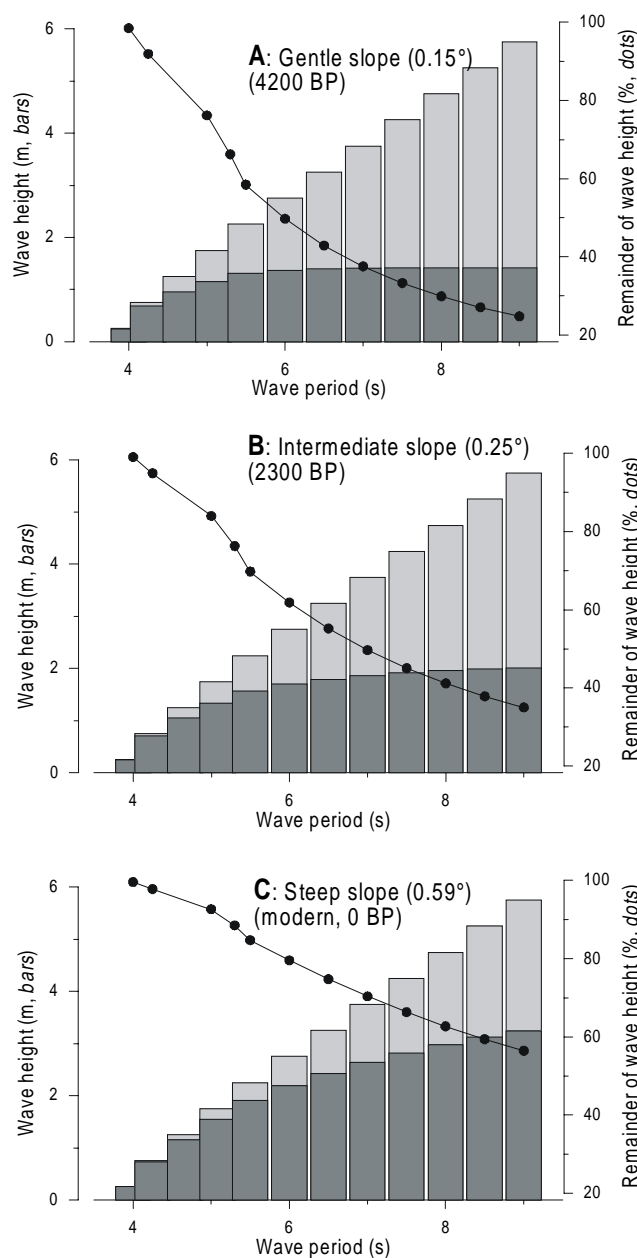


Figure 6.2: Graph of the decrease in wave height from -10 m to -5 m palaeo-mean sea level on shoreface profiles with different slopes. The friction factor is constant at 0.15 for all calculations. The light bars indicate the wave height at -10 m that is used as input for all three graphs. The dark bars represent the wave-height at -5 m, after wave-height reduction due to bottom friction. The dotted line indicates the remaining wave-heights as a percentage of the original wave height, i.e., it represents the differences between the light bars and the dark bars. Figure 6.2A represents the situation at 4200 BP, with a gentle shoreface slope of 15° . In figure 6.2 B the situation at 2300 BP is represented, with a shoreface of slope of 0.25° . This situation is roughly similar to the situation of 3050 BP. In 6.2 C the modern situation is shown, with a relatively steep shoreface slope of 0.59° .

6.4.1 Shoreface slope

We have used a simplification of the C^{14} -based isochrons to estimate the slope of the shoreface. The actual slopes of the lower and middle shoreface may deviate in detail from the slopes we reconstructed, but the trend, from gentle to steep during progradation, is clearly present. We calculated the wave-height decrease over the deeper water depths (-10 to -5 m

palaeo-mean sea level), because in the upper part of the shoreface profile other processes (wave-breaking, breaker-bar formation, swash, etc.) start to dominate the dynamics.

The lack of isochrons in the deeper part of the western half of the cross section makes it difficult to reconstruct the evolution of the shoreface slope between 3050 and 0 BP. The reconstructed 2300 BP shoreface profile is relatively gentle, compared to the 2500 and 1900 BP isochrons. The actual 2300 BP profile may well have been steeper than the reconstructed profile, giving a more gradual shift from the gentle 3050 profile to the steep modern profile. It is also worth to notice that considerable alongshore variation occurs in the modern shoreface slope (Postma and Kroon, 1986). The Haarlem cross section has a relatively steep cross section (compare the modern shoreface of the Haarlem and the Wassenaar cross section in figure 3.3 and 3.7, and notice that the modern Wassenaar shoreface is relatively gentle (slope down to -11 m is 0.40°))

6.4.2 Friction factor (f_e)

The friction factor or energy-dissipation factor is an important component in the calculation of the wave-height reduction (Nielsen, 1983, Van Rijn and Houwman, 1999). In the friction factor the bottom friction due to grain and form roughness are combined. In the calculations above we have used a constant friction factor, because we concentrate on the influence of shoreface slope alone. However, from the lithology and the sedimentary characteristics we can infer that the grain size and the morphology of the seabed have changed considerably in during progradation. The initial prograded deposits contain mainly mud with some thin fine-sand layers with wave-ripple lamination. The final prograded shoreface deposits consist of dm thick parallel-laminated storm-sand beds, likely deposited under sheetflow conditions (Chapter 5). In other words, the grain-size has increased during progradation and the seabed morphology has shifted from wave ripple bedding to plane bedding. It is likely that the friction factor has changed along with these changes.

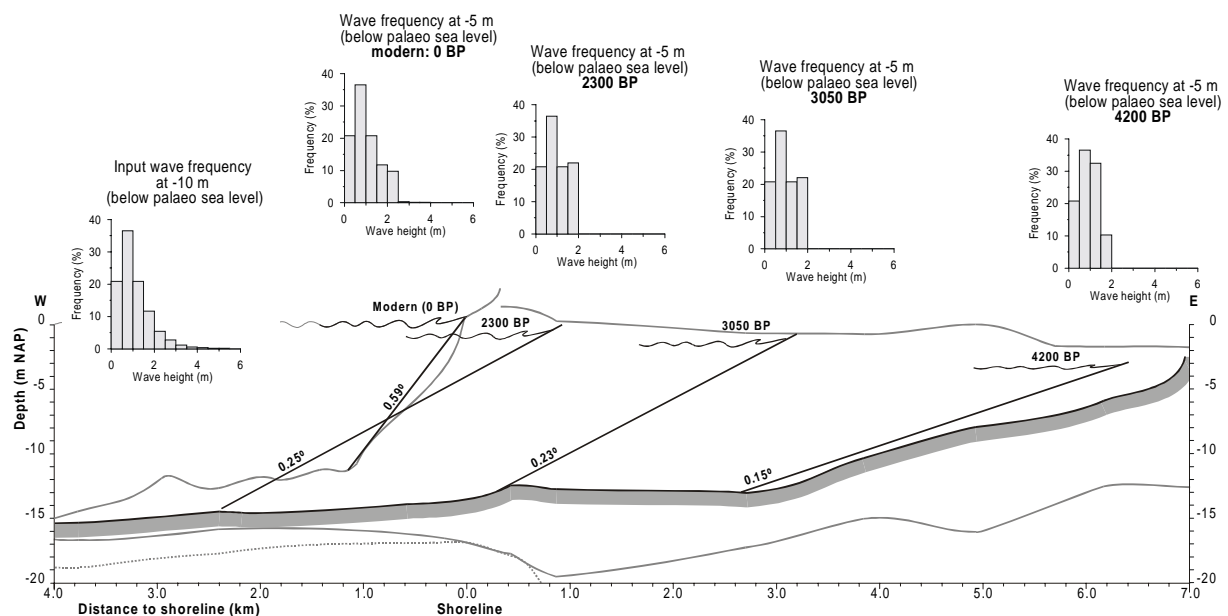


Figure 6.3: The Haarlem cross section with the reconstructed lower shoreface profiles and with the frequency of the wave heights of different classes at the -5 m palaeo-mean sea level. The input distribution at -10 m palaeo-mean sea level is shown as well. On the modern shoreface the large waves are reduced, but the distribution of waves still resembles the pattern at the -10 m. On the 4200 BP shoreface profile all large waves have been reduced and only waves smaller than -2 m remain at -5 m.

There is no shared opinion on the best method for the determination and calculation of the friction factor and several approaches may be applied to calculate grain and form roughness (Van Rijn, 1993, Van Rijn and Houwman, 1999). The form roughness depends on the wave-ripple height and length. Usually the relation consists of the square of the ripple height, divided by the ripple length and multiplied by a factor. The factor can vary from 8 (Nielsen, 1983) to 28 (Grant and Madsen, 1982). The grain roughness is always expressed as a function of the grain size (expressed as d_{50} or d_{90}), in some cases combined with the skin friction Shield's parameter θ' (Van Rijn, 1993). In the sheetflow regime the form roughness is not of importance, the bottom roughness and friction factor under sheetflow conditions is related to sediment-concentration gradients and the sheet-flow layer. According to Van Rijn (1989, 1993), the grain roughness of the sheetflow bed is in the order of the sheetflow layer thickness or the boundary layer thickness. The friction factor does not exceed a certain threshold value, that is usually considered to be 0.3 (Nielsen, 1983, Van Rijn, 1993). Research of Van Rijn and Houwman (1999) demonstrated that a constant bed-roughness factor lead to improved predictions of current velocities in a 1-DV flow model over friction factors calculated with the methods outlined above. The value of 0.15 used in the calculations is high compared to the value of 0.1 obtained by Van Rijn and Houwman (1999), and compared to values normally used in the shoreface zone (also around 0.1, Stive, personal communication).

Apart from knowledge of the grain size and the seabed morphology, the calculation of the friction factor requires knowledge of the water semi-excursion and the horizontal orbital velocity at the bottom. To keep out of circular reasoning, either a rigid relation between friction factor, the hydraulic roughness and the grainsize is introduced that is based on laboratory observations (Nielsen, 1983), or the grain roughness is solved by iteration (Van Rijn, 1993). Because the calculation of the friction factor is complicated and because the multitude of methods gives several possible outcomes for similar situations we refrain from calculating the friction factor.

To demonstrate the influence of the friction factor on the wave height reduction four different scenarios are presented in the Appendix. We have used equation 6.6, but now with arbitrary values of 0.3 and of 0.05 for the friction factor for the steepest and gentlest shoreface slope from the reconstructions. The extreme differences in the friction factor lead to differences of up to 40% in the wave-height reduction. Changes in the energy-dissipation may thus have influences on the wave-height reduction in the same order of magnitude as the changes in shoreface slope.

6.4.3 Quantitative?

The outcome of the calculations should be considered as an indication of the influence of the shoreface slope on the shallow-water wave climate, but may not be regarded as the absolute palaeo-wave climate at -5 m below palaeo-sea level. The influence of the friction factor f_c has been discussed above. The direction at which the waves reach the coast and refraction on irregular substrates affects the wave-climate too. All calculations have been done for waves that approach the coast with wave crests aligned to the shoreline. For waves with different angles to the coast the reduction of wave height will be larger, because the path over which the waves travel is longer and the bottom friction larger (Nielsen, 1983). This is the case for the modern wave climate, where moderate storm waves and fair-weather waves predominantly arrive from the west, and high storm waves predominantly arrive from the northwest (Van Straaten, 1961). We have no estimates of the directions of the palaeo-wave climate.

Locally-generated wind waves are not incorporated in the calculations. Such waves may have a considerable effect on the shallow-water wave climate. The effect of locally-generated waves was larger for the gentle shoreface slope, because the length over which the wind affects the waves increases.

The transgressive coastal evolution prior to coastal progradation has led to the development of humps and bumps on the lower shoreface surface (see for instance the 4850 BP isochron in the Haarlem cross section, figure 4.1). Wave refraction on the irregularities result in differences in the wave-height at the shoreline. The wave refraction leads to local changes in the wave height. The importance of wave refraction decreases with progradation, because the humps silt up and the bumps are eroded, leading to an overall smoother lower shoreface.

For a quantitative estimate of the wave-height reduction on the different shoreface configurations during progradation, more sophisticated spatial calculations of the wave-height reduction and refraction are required. The direction of the wave climate, locally generated wind waves and the complex morphology of the shoreface should be included in these calculations. This is not a straightforward exercise, because it requires knowledge of the palaeo-wind climate and of the subsurface morphology in 3-dimensions.

6.4.4 Other explanations

Van Straaten (1965) suggested that the relatively quiet conditions during initial coastal progradation resulted from sheltering of the shoreface and beach by an offshore submarine bar (his figure 26). The bars acted as offshore breakwaters that reduced wave action on the coast. Evidence for submarine bars were coarse-grained deposits that originated from an offshore environment seaward of the shoreface. This bar was present during initial progradation. During later stages of progradation Van Straaten envisaged a bar more seaward. All direct evidence for the second bar would have been erased during later coastal erosion. Despite improved offshore coring techniques and an increased knowledge of the deposits below the modern shoreface remains of such a bar have never been found (Beets *et al.*, 1995). The absence of remains of these bars makes this explanation less likely.

An overall quieter wave climate could explain the low energetic conditions during initial progradation. However, the model calculations of Stive (1987) do not show a large influence of a lower sea level on the wave climate. A different wind intensity and direction may have tampered the wave climate, but indications for such climatic changes are absent. The main argument against changes in wave climate is found in the prograded deposits themselves. The shift from low energetic to high energetic deposits is found in all prograded deposits. The timing of progradation differs along the coastal stretch (Beets *et al.*, 1992) and hence the timing of the shift from high- to low-energetic deposition has differed along the coast. This is a strong argument against a changing wave climate because this would affect the whole coastal stretch simultaneously.

Changes in the shoreface slope are favoured over other explanations for the change in the energy character of the shoreface deposits, because the change in slope is inherent to the progradation and the rise of sea level.

6.4.5 Sediment transport and sedimentation rates

The indications of a change in wave climate induce speculations about the influence of the lower shoreface slope on sediment transport and deposition. The low wave heights on the gentle shoreface profile result in low near bottom velocities. If near-bottom velocities are

sufficiently low mud can be deposited and preserved on the shoreface. The deposition of mud increases the sedimentation rate on the shoreface.

Accretion or erosion of beaches is related to fair-weather versus storm conditions (Van den Berg, 1977). The decrease of the wave height due to the gentle lower shoreface slope during the start of progradation may have led to a greater proportion of fair-weather conditions on the beach and thus have increased accretion. The modern wave climate shows a relation between the wave height and the angle of incidence on deep water. High storm waves approach the coast on average from the northwest, while moderate storm waves and fair-weather waves on average approach the coast from the west (Van Straaten, 1961). Because the gentle lower shoreface slope reduced the higher waves more effectively than the lower waves, the average direction of the longshore transport may have been different. Assuming a similar relation between wave height and wave incidence for 5000 BP this means reduced wave influences from the northwest and therefore less longshore transport to the south.

The most important effect of the shoreface slope on sediment transport and deposition is that the place where most wave energy is dissipated changes. On a steep shoreface slope most wave energy is dissipated on the upper shoreface and beach, while on a gentle shoreface slope much energy is dissipated further offshore. In other words, as sediment transport is directly related to the wave-energy dissipation, the sediment transport on a steep shoreface slope will be restricted to the upper shoreface and beach. On a gentle shoreface slope the sediment transport will be extended over a much larger part of the shoreface.

6.5 Conclusions

The gentle-sloped lower shoreface of the initial progradational coast reduced the wave height of the upper shoreface and beach more than today's shoreface, due to the increased bottom friction. On steep shoreface slopes, like the modern shoreface, the decrease of the wave height due to bottom friction is limited. Observed differences in shoreface deposition during progradation, relatively fine-grained deposition with wave ripple lamination during initial progradation and relatively coarse-grained plane-bed storm sands during final progradation, are explained by the change in slope of the shoreface profile during progradation.

List of symbols

c	Wave-phase velocity
c_g	Wave-group velocity
f_e	Friction factor or Energy dissipation factor
g	Acceleration of gravity
H	Wave height
h	Water depth
k	Wave number ($2\pi/L$)
L	Wave length
T	Wave period
α	Angle between wave crests and bottom contours
β	see equation 6.2
subscript "0"	means deep water value
subscript "1"	at starting depth h_1
subscript "2"	at final depth h_2

Appendix 6 Bottom friction factor

We have calculated the contribution of f_e to the loss in wave height. We have calculated the wave height reduction of the waves in table 6.1 for two values of f_e , on steep slopes and gentle slopes, using equation 6.6. The results are presented in fig 6.A.

The reduction of the wave-height on the gentle slope with the low friction factor ranges up to 35% for the highest long-period waves. On the steep slope the reduction of the high long-period waves is up to 20%. For the high friction factor the reduction is up to 90% on the gentle slope and up to 70% on the steep slope. In other words, on the gentle slope and on the steep slope an increase in the friction factor from 0.05 to 0.3 leads to an extra reduction of the wave height of about 55 to 30 %.

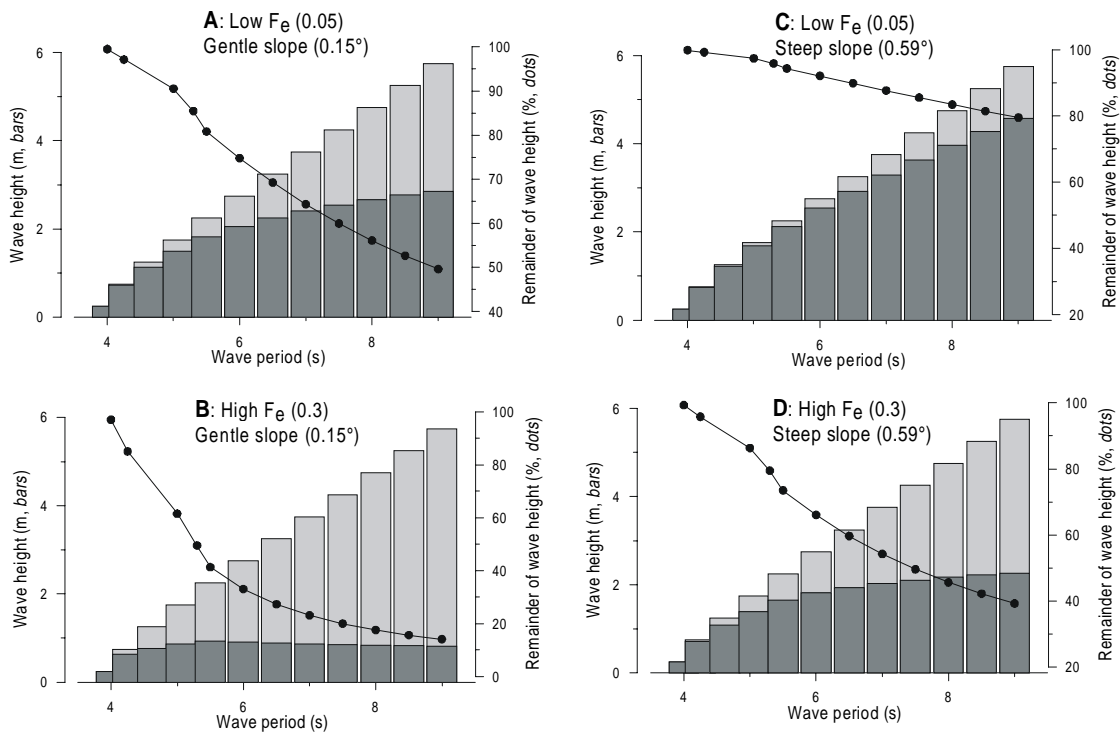


Figure 6.A: Graph of the decrease in wave height from -10 m to -5 m palaeo-mean sea level on shoreface profiles with different slopes and with different friction factors. The graphs have a similar construction as in figure 6.2; the light bars indicate the wave height at -10 m that is used as input for all three graphs, while the dark bars represent the wave height at -5 m, after wave-height reduction due to bottom friction. The dotted line indicates the remaining wave heights as a percentage of the original wave height, i.e., it represents the differences between the light bars and the dark bars. In figure 6.A.1 A and B the wave-height reduction on a gentle slope (0.15°) is depicted, with a low friction factor (0.05 in A) and a large friction factor (0.3 in B). The difference in wave-height reduction of the largest waves is about 50 %. Similar differences in friction factor are depicted in figure 6.A.1 B and C on a steep slope (0.59°). The high friction factor in D (0.3) leads to about 30% more reduction of the wave height than the low friction factor in C (0.05).

Chapter 7: Simulations of Holocene coastal stratigraphy from the western Netherlands with the Shoreface Translation Model.

Abstract

Numerical stratigraphic models can be used to simulate the geometry of deposits, to check geological models and to reveal patterns and mechanisms of deposition and erosion that otherwise remain unnoticed. The Shoreface Translation Model (STM) computes the response of the coastal system to changes in external variables and to changes in the geometry of the coastal system. Here the STM is used to investigate the role of substrate slope, sea-level rise, sediment supply and changes in the width of the coastal system in the Holocene coastal evolution of the western Netherlands. An important aspect of the transgressive coastal system in the western Netherlands is the import of sediment from the offshore into back-barrier basins by cross-shore sediment transport via tidal inlets and tidal channels.

Simulated transgressive coastal systems develop under conditions of a fast rise of sea level and limited sediment supply. Such transgressive coastal systems leave a trail of deposits on the shelf floor: the trailing-edge sand sheet. Substrate slope and net sediment supply control the thickness of this trailing-edge sand sheet. Tidal-channel incision and reworking on the shelf also influence the thickness of the sand sheet. In the simulations a decrease in the rate of sea-level rise leads to a decrease in the rate of coastal retreat. Combined, the sea-level rise and the width of the coastal system determine the accommodation space, which in turn determines the sediment demand from offshore and hence the coastal retreat. A decrease of coastal retreat drives the simulated coastal system into a stage of aggradation. Eventually coastal retreat ceases completely and progradation starts.

The stratigraphies produced by the STM are well comparable to the stratigraphies from the Holocene of the western Netherlands. Despite the fact that the geology of the western Netherlands is well constrained, the model simulations show some previously unrecognised patterns. The model simulations point to a stage of coastal aggradation, prior to progradation, and suggest that transgressive shoreface deposits can be preserved when coastal retreat diminishes. The simulations of coastal evolution thus increase our understanding of coastal evolution.

7.1 Introduction

Numerical stratigraphic models can be used to simulate the geometry of depositional systems in time (Cross and Harbaugh, 1990, Watney *et al.*, 1999). Numerical stratigraphic models are based on mathematical rules, which are either tentatively scaled-up from ‘first principles’ (physical laws) of sedimentation and erosion or are rules that are distilled from our understanding of geological processes (Cross and Harbaugh, 1990). Numerical stratigraphic models can be used to check assumptions based on geological arguments (Oreskes *et al.*, 1994). If, for instance, one observes a stacking pattern of delta lobes and assumes a rise in sea level to be the cause, this assumption can be investigated with a stratigraphic model. Numerical stratigraphic models can also be used to reveal interdependencies and feedback mechanisms that were previously unnoticed (Cross and Harbaugh, 1990). Nevertheless, mathematical geological models are gross simplifications of the natural processes. Model simulations will therefore at best represent a simplified image of what went on. Model simulations do never represent the ‘true’ course of events (Oreskes *et al.*, 1994). The responsibility of the geologist is to check whether model simulations represent valid geological information or numerical flaws, and thus to corroborate or improve underlying assumptions and mathematical rules.

An outline of the geology of the western Netherlands and of the controlling factors has been presented in Chapter 1. The substrate for the Holocene coastal evolution is formed by gently seaward dipping Pleistocene deposits, with slopes of 0.015° to 0.020° (Figure 1.4). Sea-level rise during the Holocene was initially fast and decreased around 6000 BP (Jelgersma, 1979, figure 1.5). The rapid rise of sea level in the beginning of the Holocene resulted in rapid coastal transgression. The transgressive coastal system consisted of wide back-barrier basins, with formation of peat on the landward side and deposition of tide-influenced sediments on the seaward side (Pons *et al.*, 1963, Zagwijn, 1986). The size of the tidal back-barrier basins varied alongshore (Beets *et al.*, 1992). The greater part of the sediment in the back-barrier basins originated from the Pleistocene substrate offshore and from erosion of offshore transgressive remnants (Beets and Van der Spek, 2000). Direct fluvial input into the coastal system played a minor role (Beets and Van der Spek, 2000). In response to the deceleration of the rise in sea level the tidal basins silted up (Beets *et al.*, 1992, 1994, Beets and Van der Spek, 2000). This resulted in a decrease of the sediment demand from offshore and hence in diminishing coastal retreat. Eventually, coastal retreat ended completely and progradation of the coastal system started (Van Straaten, 1965, Beets *et al.*, 1992, 1994). The prograded coastal system consists of shoreface and beach deposits (Chapter 3 and 4 and references cited therein). The start of coastal progradation occurred first in the south and about 1000 years later in the north of the western Netherlands.

In this chapter we use the Shoreface Translation Model (STM) of Cowell *et al.* (1992, 1995, 1999b) to simulate coastal stratigraphy under conditions of sea-level rise and net sediment supply. In the model the substrate slope, the sediment supply, the rate of sea-level rise and the width of the coastal system are varied to reveal their influences on the stratigraphy. The simulations of the model will be compared to geological observations described in Chapters 2, 3 and 4. The comparison of model simulations and geological observations demonstrates some limitations of the model in representing certain geometries.

The Shoreface Translation Model holds an intermediate position between stratigraphic models that mimic shoreline evolution over geological time scales (10 ka to 100 Ma) and large-scale coastal-evolution models that reconstruct coastal evolution over political to historical time scales (10 years to 100 years). In general, stratigraphic models predict the coastline position as a function of sea level, tectonic subsidence and sediment input (Cross

and Harbaugh, 1990, Watney *et al.*, 1999). The resolution in the coastal environment is limited. Some recently developed models take shoreline and shelf behaviour into account to increase the detail in the simulation (e.g. Carey *et al.*, 1999). However, this approach is still not applicable to simulate the detail needed in the Holocene record. Large-scale coastal evolution models are usually restricted to specific environments. For instance, the Panel model (Stive and De Vriend, 1995) and the PonTos model (Steetzel and De Vroeg, 1999) have been specifically designed for shoreface evolution. The ASMITA model (Stive *et al.*, 1998) mimics the behaviour of tidal basins and adjacent shoreface stretches that show limited transgression. The need to simulate transgressive barriers with large tidal basins and to include local sediment budgets and changing cross-shore geometries left the STM as the most appropriate choice for model simulations of the Holocene coastal deposits of the western Netherlands. The STM has been used with success to model coastal evolution and morphologies in southeast Australia (Roy *et al.*, 1994, Cowell *et al.*, 1995, 1999b), and the US East Coast (Cowell *et al.*, 1999b) over Holocene time spans. A preliminary STM simulation of the Holocene transgressive evolution of the Dutch coast has demonstrated the applicability of the STM for this setting (Cowell *et al.*, 1999b).

7.2 The Shoreface Translation Model

The Shoreface Translation Model (STM) is a geometric morphological-behaviour model (Cowell *et al.*, 1995, Stive and De Vriend, 1995), that simulates the response of a coastal barrier to changes in sea level, substrate, sediment input and coastal morphology. The underlying principles are sediment conservation and the generalised Bruun rule (Dean and Maurmeyer, 1983). The generalised Bruun rule predicts the lateral translation of a coastal barrier in response to sea-level change as a function of the accommodation space created in the coastal system (Dean and Maurmeyer, 1983). The assumption in the Bruun rule is that the morphology of the coastal system is in equilibrium with the local hydrodynamic and substrate conditions, and remains in equilibrium as sea level changes. The coastal system's surface, i.e., the coastal barrier, the back barrier, and the shoreface profile adjust directly (within a timestep) to the change of sea level (Figure 7.1).

Essentially, the STM keeps track of the volume of sediment in the coastal system. An incremental rise in sea level (during one timestep) results in an increase of the accommodation space in the coastal system (Figure 7.1B). Sediment from outside the coastal system, i.e., from deltaic or neritic sources, will fill part or all of the accommodation space. The remainder of the accommodation space will be filled with sediment that is eroded from the shoreface. This volume of eroded sediments determines the amount of coastal retreat. Any changes in the morphology of the coastal system (a change in width of the coastal system, a deepening of the shoreface, etc.) will be accounted for, as these change the sediment budget and will affect coastal retreat. If the accommodation space that is created by sea-level rise is smaller than the sediment input from outside the coastal system, the remainder of the sediment will be distributed over the shoreface and the coastal system will prograde.

The STM is a cross section model, i.e., it is 2-dimensional. The cross section may be regarded as the representation of a 3-dimensional situation, i.e., the laterally variable characteristics are projected on the cross section. The choice of the area that is represented in the cross section is arbitrary. However, choosing an area with limited alongshore variability means that the outcome of the model can be compared with the stratigraphy. The representation of the coastal system in the STM does not per se represent the morphology of the coastal barrier and back-barrier basins. It is the volume in the coastal system that counts. So, rather than viewing the back-barrier area as an extension of the coastal barrier, it may be regarded a flood delta, bay-head delta, sub-tidal flat or a combination of these, as long as the sediment volume remains similar.

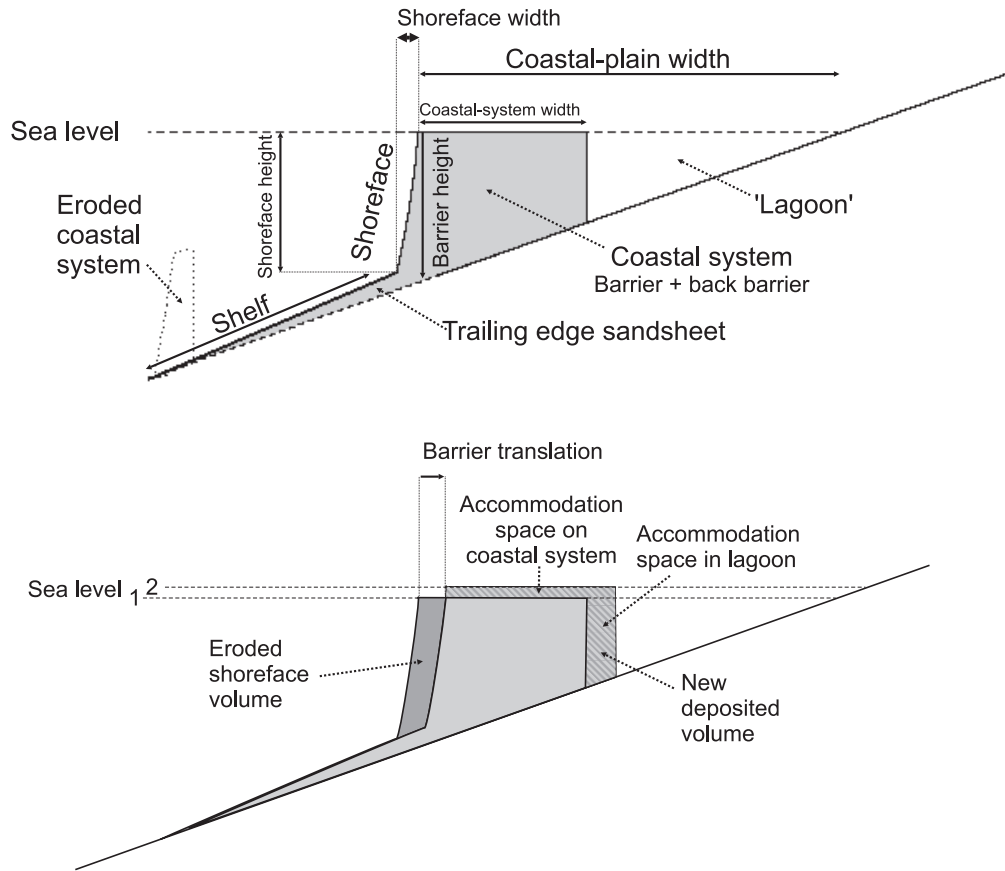
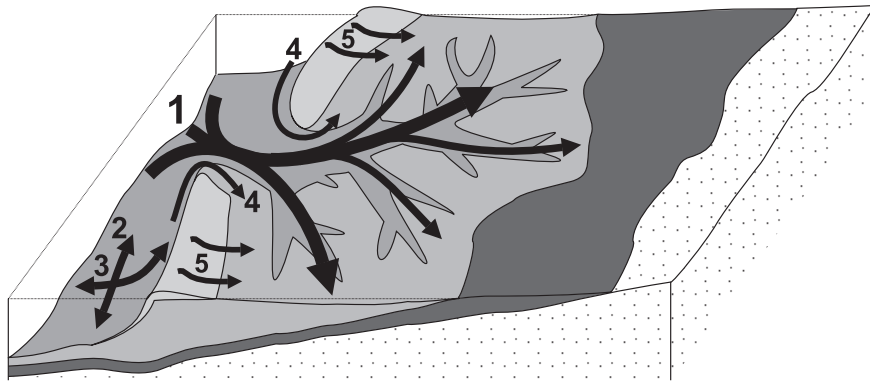


Figure 7.1 A: Definition sketch of the basic profile-geometry parameters used in STM simulations. Apart from the geometry parameters, the rate of sea-level rise and the sediment input into the coastal system are important in the simulations. Notice that the representation of the back-barrier basin is schematic.

Figure 7.1 B: Response of the model coastal system to a rise in sea level. Accommodation space is created by the rise of sea level on top of the coastal system and by the progradation of the coastal system into the lagoon. The accommodation space is filled with the sediment supply to the coastal system. The remainder of accommodation space is filled with eroded shoreface sediments, and this volume determines the retreat of the coastal system.

Figure 7.2 (Following page): Sketch of transgressive (A) and prograding (B) coastal systems and the pathways for the sediment transport. The transgressive coastal system consists of a barrier and back-barrier. The back-barrier is a tidal basin, with a tidal channel system and a tidal inlet. Peat is formed at the landward side of the basin. Cross-shore sediment transport occurs through the tidal inlet (1), and by cross-shore transport processes on the shelf-shoreface-beach system (3), while overwash (5) may form an additional cross-shore sediment-transport pathway. In addition longshore sediment transport on the shoreface and shelf may occur (2), and sediment may be delivered to the tidal basin by longshore sediment transport (4). The prograding coastal system has no connection to the back-barrier basin, where peat formation expands. In the prograding coastal system sediment transport is restricted to longshore and cross-shore sediment transport on the shoreface and shelf.

A: Transgressive coastal system



B: Prograding coastal system

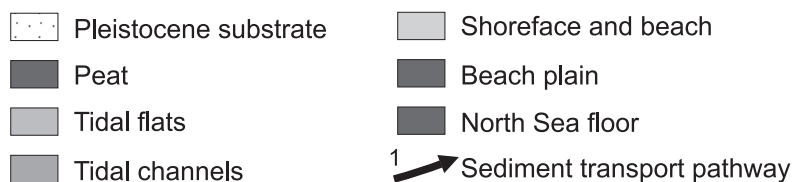
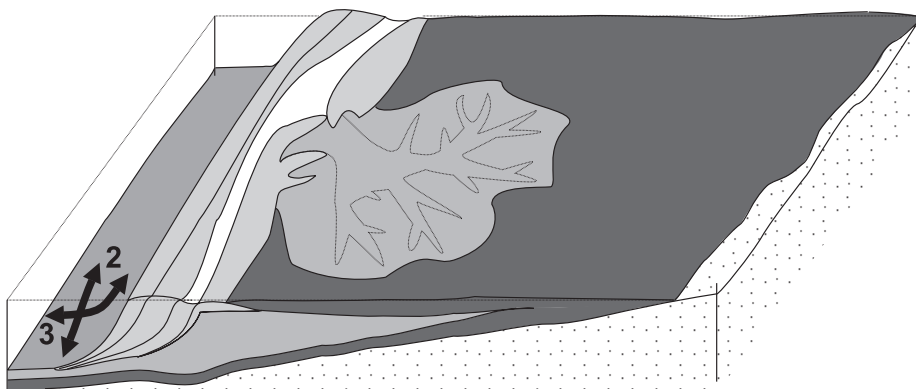


Figure 7.2: Caption on previous page

We apply the STM to situations with gentle substrate slopes ($< 0.5^\circ$). In these situations the coastal system consists of a shoreface, with a designated depth, length and curvature, and a coastal barrier and back-barrier (Figure 7.1). The dimensions of the coastal barrier and back barrier are incorporated in the width of the coastal system. The coastal system has a maximum width. The maximum width represents the maximum size of the tidal back-barrier basin. The maximum size of tidal back-barrier basins can be controlled by tidal dynamics of the basin (Van der Spek, 1994), or by the influence of other types of sedimentation (fluvial) and peat formation in part of the accommodation space on the coastal plain. The intersection of sea level with the substrate is the landward end of the coastal plain. The distance from the landward end of the coastal plain to the seaward end of the coastal barrier is the width of the coastal plain. If the width of the coastal system is smaller than the

width of the coastal plain a lagoon¹ is present in the model. In reality, this lagoon can be filled with peat or fluvial clay, although the deposition of fluvial mud and the formation of peat are not incorporated in the model simulations used here.

The coastal morphology represented in our STM model experiments is depicted in figure 7.2A, and consists of a tide-influenced coast with tidal inlets and extensive tidal-channel systems. The width of the coastal system in the model represents the width of the tidal back-barrier basin, i.e., the basin length to which sediment can be transported by the tides. We assume that the bulk of the sediment delivery to the coastal system occurs from the marine realm, either through longshore transport or by cross-shore sediment supply from the shelf. The sediment is imported and redistributed via tidal-channel systems. Washover into the back-barrier basins may contribute as well. Some of the sediment may be delivered directly into the basin by rivers. When coastal progradation occurs, we assume that the prograding coastal system lacks tidal inlets and tidal channel systems (Figure 7.2B). No sediment is transported into the back-barrier basin in that case. Hence, the width of the coastal system of the prograding coast is smaller than that of the transgressive coast. The sediment supply to the coastal system is the net sediment supply. The increase in accommodation space outside the modelled coastal system (dunes, new tidal back-barrier basins) must be subtracted of the bulk sediment supply to calculate the net sediment supply.

Tidal channels and inlets are not represented in the model output, but do form an important part of the Holocene stratigraphy. The extent of tidal-channel incision and tidal-channel deposits can be addressed semi-quantitatively. If the lateral translation of the coastal system is limited (translation \ll coastal-system width) the accommodation space on the barrier per timestep (which equals deposition on the coastal system) is given by the width of the coastal system multiplied by the increase of the sea level. We relate the accommodation space to the tidal prism, i.e., a large accommodation space means a large tidal prism. The tidal prism in turn is related to the extent and volume of the tidal-channel system (O'Brien, 1931, 1969, FitzGerald *et al.*, 1984). Thus, we relate the abundance and incision depth of tidal channels to the amount of accommodation space.

Table 7.1: Variables used in the experiments.

		Sea level	Substrate slope	Sediment supply	Coastal-system width
Experiment 1	Trailing-edge sand sheet	constant	varying	varying	constant
Experiment 2	Transgression-progradation	decelerating	constant	varying	constant
Experiment 3	End-of-transgression	decelerating	varying	constant	varying
Experiment 4	Transgressive shoreface	decelerating	constant	constant	constant

¹ In this chapter we use the term ‘lagoon’ for simulated stratigraphies, where it represents the area in between the landward end of the coastal system and the end of the coastal plain. The phrases back-barrier basin and tidal back-barrier basin are used for simulated stratigraphies and the real stratigraphy. In the simulations the back-barrier basin is part of the coastal system (Figure 7.1). Lagoon and (tidal) back-barrier basin are thus not interchangeable in this text.

7.3 Numerical Experiments

The parameters that were varied in the experiments are shown in table 7.1. Previous experiments (Roy *et al.*, 1994, their figure 4.9, Cowell *et al.*, 1999b, their figure 8A) have demonstrated that on relatively gentle substrate slopes a layer of back-barrier deposits escapes transgressive-shoreface erosion if there is a net sediment supply and if the sea level rises relatively fast. The layer of back-barrier deposits on the shelf is referred to as the trailing edge-sand sheet (Swift, 1976a, Roy *et al.*, 1994). Experiment 1 is designed to investigate the influence of the substrate slope and the sediment supply on the thickness of a trailing-edge sand sheet.

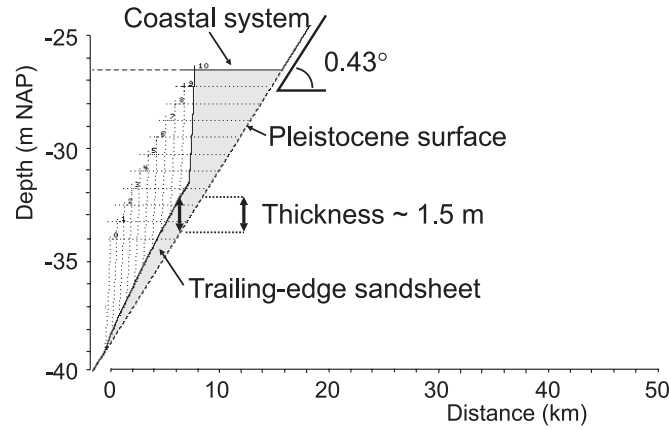
The rate of sea-level rise is the dominating control on Holocene coastal evolution (Curry, 1964). The influence of the decrease in the rate of sea level is investigated in experiment 2. The applied sea-level rise follows the Holocene sea level of the western Netherlands, with an initial fast rise, followed by a gradual deceleration (Jelgersma, 1979). There is a constant sediment supply to the coastal system, and coastal-system width, substrate slope and shoreface geometry are kept constant. Experiment 3 is a follow-up of experiment 2, in which the influence of the coastal-system width, sediment supply and substrate slope on a transgressive coast with a decelerating sea-level rise are investigated. In experiment 3A the maximum width of the coastal system is reduced per timestep. The rationale behind this reduction is that the accommodation space on the coastal system is reduced because of sediment input from other sources (fluvial sediments and peat formation). In experiment 4 the shoreface of the transgressive coast under decelerating sea-level rise is shown in detail.

7.3.1 Experiment 1

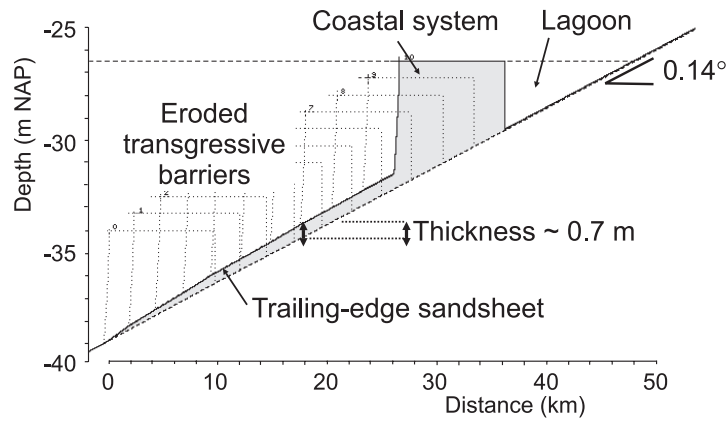
The results of the simulations with a constant rise of sea level and variation of the substrate slope and sediments supply are shown in figure 7.3. The substrate slope is 0.014° (0.25 m over 1 km) in experiments 1B and 1C, and 0.043° (0.75 m over 1 km) in experiment 1A. The sediment supply is 2000 m^3 per metre coastline in 100 year in experiments 1A and 1B, and is 4000 m^3 per metre coastline in 100 year in experiment 1C. The shoreface depth is constant at -5 m and the maximum width of the coastal system is constant at 10 km. The geometry of the coastal system stays identical during experiment 1. The effect of a net sediment supply during a fast rise of sea level is the formation of trailing-edge sand sheet. The thickness of the trailing-edge sand sheet varies. The initial thickening of the trailing-edge sand sheet that can be observed in all simulations results from the evolution towards an equilibrium situation. The thickness remains constant after several timesteps.

The difference between experiments 1A and 1B is the substrate slope that is three times as steep in experiment 1A. As a result, the trailing-edge sand sheet of experiment 1A is about twice as thick as that of experiment 1B. The rate of coastal retreat in experiment 1A is half of that in 1B. The difference in thickness is best explained in terms of accommodation space: the gentle slope of experiment 1B means that the sediment has to be smeared out over a greater distance and hence the sediment layer is thinner. Experiment 1A lacks a lagoon behind the coastal system, because there is no space to develop such a basin on the steep slope. The sediment input in experiment 1C is twice as large as the sediment input in experiment 1B, and as a result the trailing-edge sand sheet of experiment 1C is about twice as thick as that of experiment 1B. The surplus of sediment in experiment 1C with respect to 1B is deposited in the trailing-edge sand sheet.

A: steep substrate slope



B



C: double supply

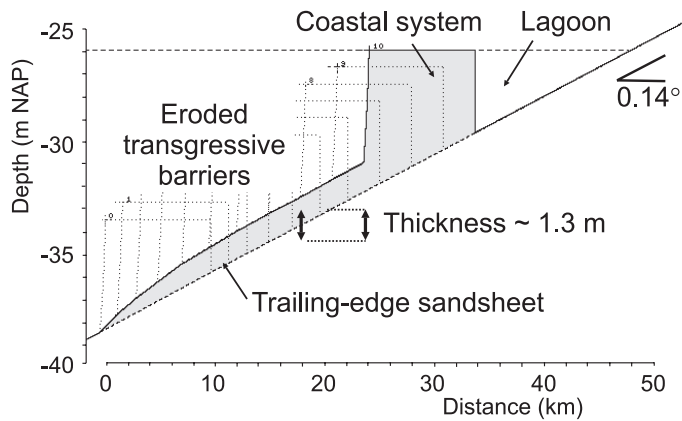


Figure 7.3: Model simulation of the trailing-edge sand sheet formation. Sea level rises at a constant rate, the variables are substrate slope and sediment input. A) Steep slope (0.043°) and limited sediment supply (2000 m^3 per metre coastline in 100 year) result in a relatively thick trailing-edge sand sheet. B) Gentle slope (0.014°) and limited sediment supply (2000 m^3 per metre coastline in 100 year) result in a thin trailing-edge sand sheet. C) Gentle (0.014°) slope and large sediment supply (4000 m^3 per metre coastline in 100 year) result in a thick trailing-edge sand sheet.

7.3.2 Experiment 2

The simulation is presented in figure 7.4A; the sea-level curve and the coastline positions during the simulation are shown in figure 7.4B. The experiment starts with sea level at -20.25 m, corresponding to about 7500 BP. The substrate in the simulation has a slope of 0.014° , the maximum width of the coastal system is 24 km during transgression, and the net sediment supply to the coastal system is 8000 m^3 per metre coastline in 100 year. As in all simulations in this chapter, the shoreface geometry does not change during the simulation. Initially, the coastal system stretches from the shoreline to the substrate and there is no lagoon landward of the coastal system. The width of the coastal system increases until the maximum width is reached, and a lagoon develops behind the coastal system. Initially, the sea level rises fast, creating lots of accommodation space on the coastal system. In combination with the increase in width of the coastal system, the sediment demand from the shoreface is large. This results in large coastal retreat during the first 1600 years.

Around 6000 BP the rise of sea level decreases and as a result the amount of accommodation space that is created per time step on the coastal system decreases (Figure 7.4B). For a large part the accommodation space is filled in with the net sediment supply to the system. The sediment demand from the shoreface is therefore strongly reduced. Hence the rate of coastal retreat is strongly reduced, and aggradation, induced by the ongoing rise in sea level, starts to dominate the coastal evolution. During the stage of aggradation the coastal system develops as a stationary barrier (Roy and Thom, 1981, Roy *et al.*, 1994).

As soon as the sediment input into the coastal system exceeds the creation of accommodation space by the rise of sea level, retreat of the coast ends. At that moment, all sediment supply is available for progradation of the coastal system. In the model simulation the width of the coastal system is reduced from that moment on. This is based on the geological observation that the end of coastal retreat is associated with the closure of tidal inlets and the end of back-barrier deposition. In other words, the back-barrier basin ceases to act as a sink for sediment. The rise of sea level hardly has an effect on the formation of accommodation space on the shoreface. Hence, the rate of progradation is barely influenced by the rate of sea-level rise.

The stratigraphy of the simulation consists of an offshore trailing-edge sand sheet of limited thickness, an landward-thinning wedge of transgressive deposits and a seaward-thickening wedge of prograded deposits. The prograded deposits overly the trailing-edge sand sheet.

7.3.3 Experiment 3

Experiment 3 is aimed to explore the parameters that influence the rate of transgression and aggradation and the timing of progradation. The simulations are extensions of experiment 2 with an identical rise of sea level. The sediment input into the coastal system is constant at 8000 m^3 per metre coastline in 100 year, and is similar in all experiments. The slope of the substrate is 0.014° (0.25 m in 1 km) in experiments 3A, 3C and 3D, the substrate slope in experiment B is 0.017° (0.29 m in 1 km). The maximum width of the coastal system decreases with 0.5 km per 100 years from 20 to 16 km in experiment 3A, and it is constant at 20 km in experiments 3B and 3C, and constant at 30 km in experiment 3D. All simulations are terminated at the onset of coastal progradation.

The overall outcome of the simulations is comparable. In response to the deceleration of the sea-level rise the rate of coastal retreat decreases, until the coastal system aggrades, and eventually ceases. The overall stratigraphy produced by the simulations is therefore comparable, with a trailing-edge sand sheet on the shelf and thick transgressive deposits of

the coastal system (Figure 7.5). The timing of the decrease of coastal retreat, the aggradation and the end of the experiments, i.e., the start of progradation, vary between the experiments. This is illustrated in figure 7.6, where the sea-level signal, the width of the coastal-system and the accommodation space of the experiments are shown.

The steeper substrate slope of experiment 3B relative to 3C leads to a slightly thicker trailing-edge sand sheet. The decrease of the coastal retreat and the end of transgression do not differ in simulations 3B and 3C. The end of transgression is thus independent of the substrate slope. Once the coastal system starts to aggrade rather than to retreat, the major part of the accommodation space is created on top of the coastal system, and thus depends on the coastal-system width and the sea-level rise. The amount of accommodation space that is created at the landward end of the barrier is of relatively minor importance, and this is the only part that is influenced by the substrate slope. Notice that this is only so if the coastal-system width is limited, otherwise accommodation space will be added continuously at the landward side of the coastal system.

With respect to simulation 3C, simulation 3A has an initially smaller coastal system, and the width decreases during the simulation. The decrease of the system represents the fill of the coastal plain with other than tidal back-barrier deposits, which limits the extent of the tidal basin. Due to the decrease of the system width, the increase in accommodation space during sea-level rise is more reduced than in simulation 3C. Thus the threshold, at which the net supply of sediment surpasses the accommodation space and coastal retreat ends, is reached earlier in simulation 3A than in simulation 3C. Relative to simulation 3C, the coastal system of simulation 3D is much wider, which generates the opposite effect of that in simulation 3A. It takes much longer to reach the threshold at which the net sediment supply surpasses the accommodation space, and therefore transgression continues much longer in simulation 3D.

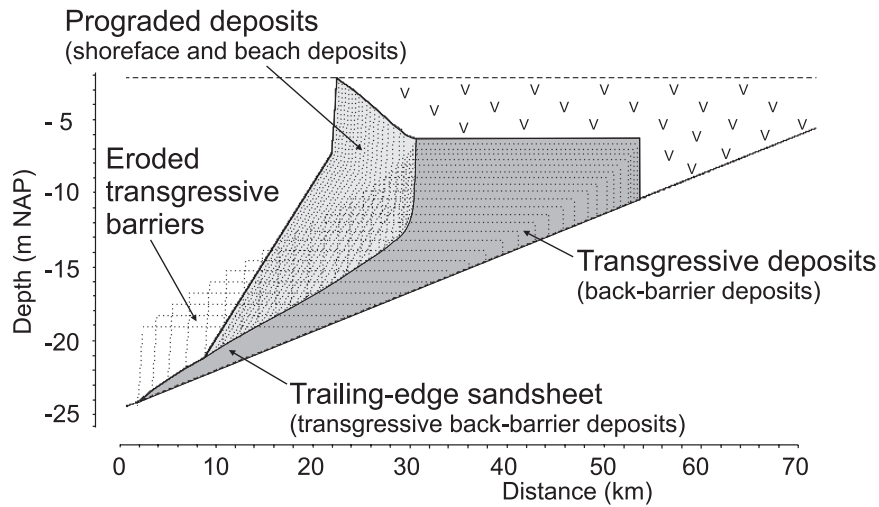
Also note that the aggradation of the coastal system only lasts until progradation starts. This means that the duration of aggradation is longer for the experiment with the widest coastal system. In other words, the thickness of the coastal system is largest for coastal systems with a large width.

7.3.4 Experiment 4

The set-up of the experiment is similar to experiment 2 and 3C, with the exception of the shoreface length, that has been extended to 3 km. The rate of sea-level rise decreases gradually during the experiment. We focus on the shoreface during the final stages of transgression.

The overall response is similar to the response in experiment 2. The retreat of the coastal system gradually decreases in response to the deceleration of the rise in sea level, and the coastal system enters a stage of aggradation. The response of the shoreface consists of two parts: upward translation due to sea-level rise and landward translation, due to coastal retreat. When the landward translation is limited during the stage of aggradation, the upward translation may result in the preservation of the lower part of the shoreface profile. Meanwhile the upper part of the shoreface profile still recedes and is erosive. The difference in behaviour of the lower and upper part of the shoreface profile results from the gentle lower shoreface slope versus steep upper shoreface slope. The preservation of lower shoreface deposits is enhanced by the gentle shoreface profile in the simulation.

A



B

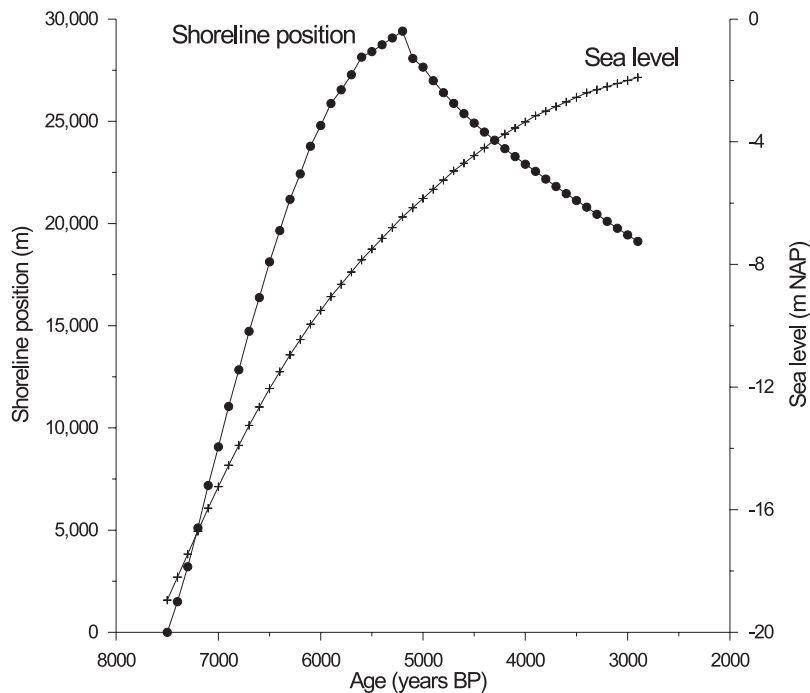
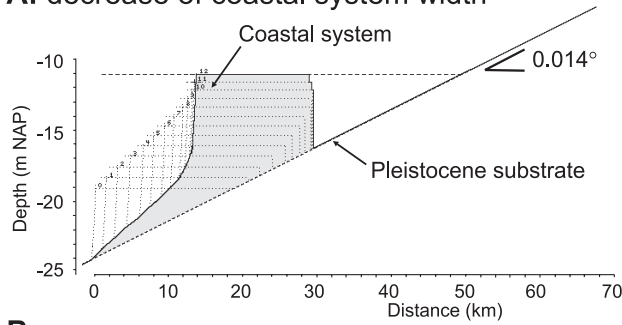
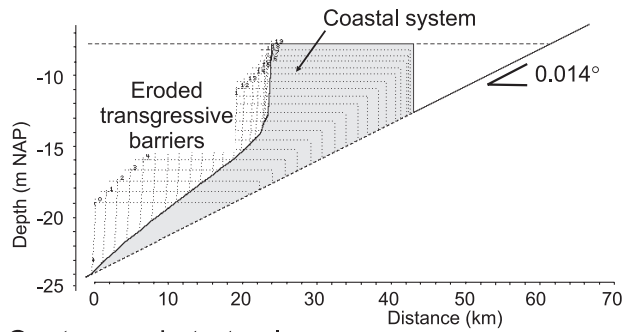


Figure 7.4: Model simulation of transgression followed by progradation. The single variable in the experiment is the rise of sea level. The maximum coastal-system width was reduced from 24 km down to 100 m after the shift to coastal progradation. The slope of the subsurface is (0.014°) , the sediment supply is constant (8000 m^3 per metre coastline in 100 year). A) Model output of the experiment, with an initial retreating coast, followed by a gradual decrease of the retreat and aggradation of the barrier. Eventually transgression ends and the barrier starts prograding. B: graph with the sea-level height (crosses, right axis) and the shoreline position (dots, left axis).

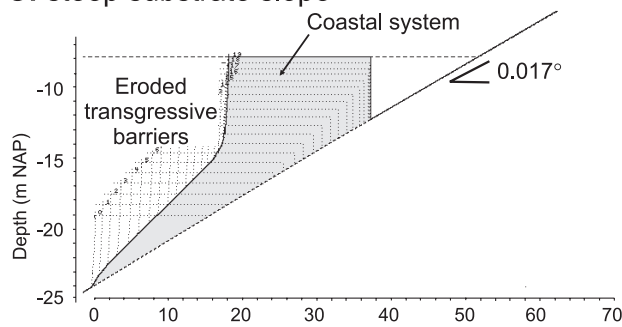
A: decrease of coastal system width



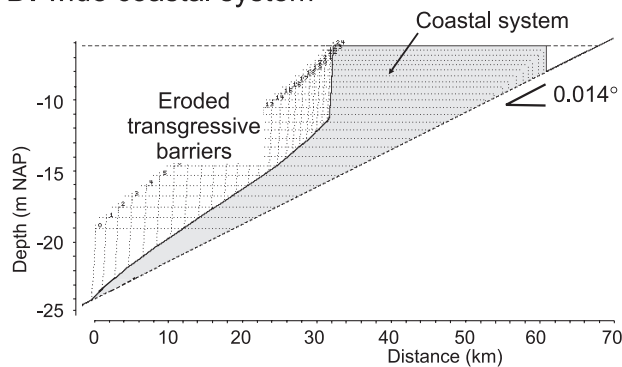
B



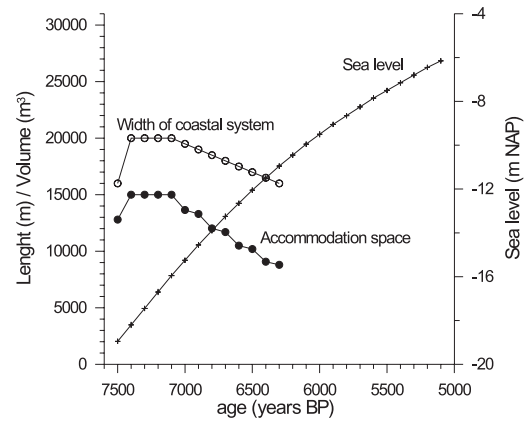
C: steep substrate slope



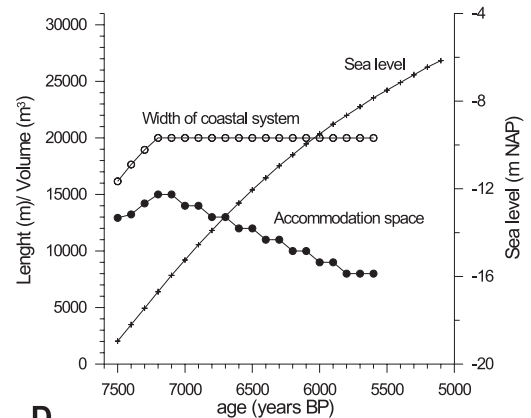
D: wide coastal system



A



B & C



D

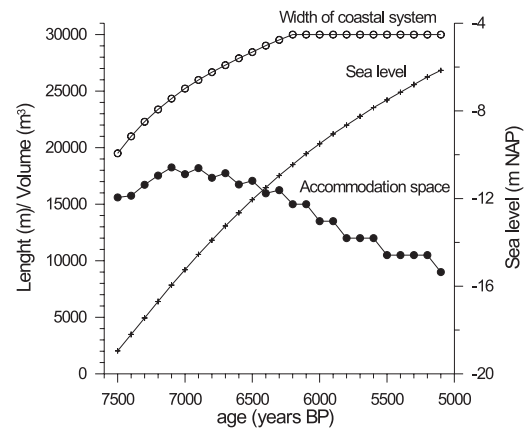


Figure 7.5 (left): Model simulation of the diminishing of transgression and start of barrier aggradation as a function of decreasing sea-level rise. The main variable is the rate of sea-level rise; other variables are the substrate slope and the coastal-system width. Sediment supply is constant at 8000 m^3 per metre coastline in 100 year. A) Gentle slope (0.014°) and the width of the coastal system decreases from 20 km to 16 km (at 0.5 km per 100 year). B) Slightly steeper slope (0.019°) and constant maximum coastal system width (20 km); Compare B) to C) with gentle slope (0.014°) but further similar characteristics. D) Identical to C) (slope is 0.014°), apart from the larger maximum coastal-system width (30 km).

7.4 Discussion

The simulated stratigraphies of the experiments look roughly similar to the stratigraphy of the Holocene coastal deposits in the western Netherlands (compare the outcome of experiment 2 in figure 7.4A with figure 1.3 in the Introduction). The landward-thinning wedge of transgressive deposits and the seaward thickening wedge of shoreface deposits up to the shoreline are observed in the stratigraphy of the western Netherlands and in the model simulation. The resemblance suggests that the model experiments do represent the Holocene large-scale coastal evolution. This supports earlier observations on STM simulations of other coasts (Roy *et al.*, 1994, Cowell *et al.*, 1995, 1999b), where the STM was capable of simulating various types of coastal morphologies.

Comparing the simulated stratigraphy with an arbitrary cross section is valid if alongshore variability is limited, but must be regarded with caution if localised phenomena (tidal inlets, fluvial deltas) are incorporated. Irregularities in the subsurface may result in local thicker or thinner deposits that are absent in the simulations (see for example for instance figure 6 in Cowell *et al.*, 1995). When the model stratigraphies are compared to cross sections, the irregularities in surfaces and local phenomena should be averaged over the area of consideration.

7.4.1 Controls on large-scale coastal; evolution

Sea-level rise

The influence of the rate of sea-level rise is expressed most distinctly in experiments 2, 3 and 4. The deceleration of the rate of sea-level rise leads to a decrease of the rate of coastal retreat and eventually to coastal progradation (Figure 7.4). The control by the rate of sea-level rise is exerted through the accommodation space on the coastal system. It is the combination of system width and incremental sea-level rise that controls the accommodation space and hence controls shoreface-sediment demand and coastal retreat. Such a control of the rate of sea-level rise on the coastal evolution has been determined for the Holocene coastal evolution of the western Netherlands (Beets *et al.*, 1992, 1994, Beets and Van der Spek, 2000) and for a number of other Holocene coastal sequences (amongst others, Curray, 1964, for the Costa Nayarit, Mexico, Thom, 1983, for several examples from south-eastern Australia, Roy *et al.*, 1994, 1997, for examples from New South Wales, Australia). Compared to the width of the coastal system of the transgressive coast, which incorporates large back-barrier basins, the width of the prograding system is limited (Figure 7.2). Hence, the control of sea-level rise on coastal progradation is restricted, because the accommodation space that results from sea-level rise is relatively small for the prograding system.

Figure 7.6 (previous page, right): Graphs with the results of the simulations depicted in figure 7.5 (A, B & C and D denote the experiments). Crosses represent sea level (right-hand axis), open dots give the width of the coastal system (left-hand axis), closed dots represent the back-barrier accommodation space (sea-level change-coastal-system width, left hand axis).

Substrate slope

A steep substrate slope leads to a lower rate of coastal retreat and the development of a relatively thick trailing-edge sand sheet (Figure 7.3A). The role of the substrate slope is very limited in timing of the end of transgression (Figure 7.5C and 7.6C). When the transgression of the coastal system halts and aggradation starts, the substrate slope does not influence the coastal system anymore. However, the substrate slope in the model is a 2-dimensional representation of the 3-dimensional topography. The topography of the Pleistocene substrate has controlled the geometry and size of the tidal back-barrier basins (Beets *et al.*, 1992, 1994, Beets and Van der Spek, 2000). In other words, in reality the substrate topography does influence the large-scale coastal evolution. In the model this is incorporated in the width of the coastal system, which indeed does influence the end of retreat.

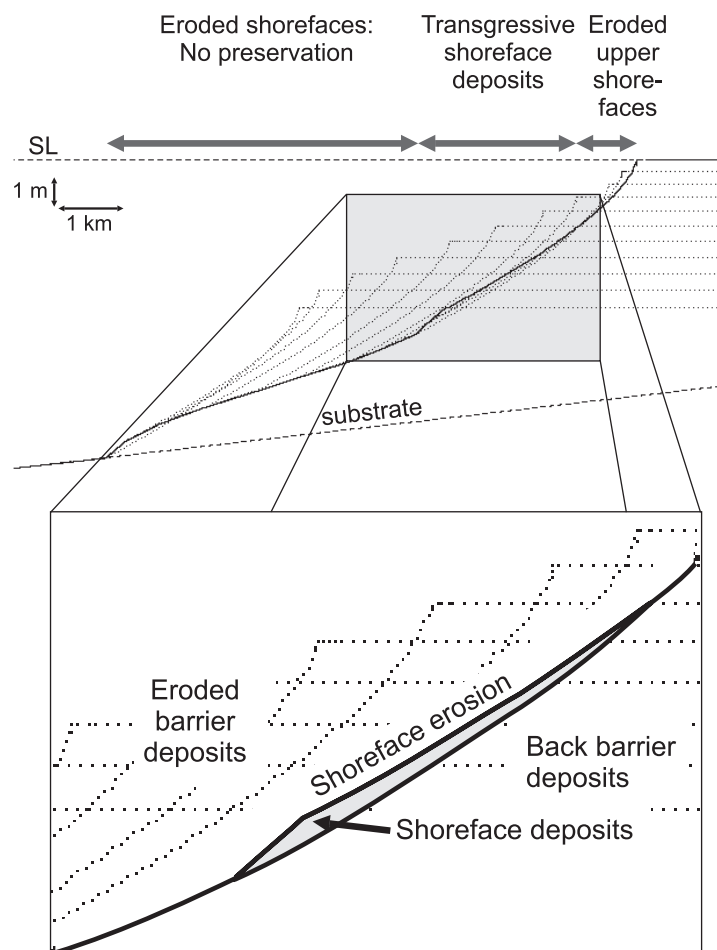


Figure 7.7: Experiment to demonstrate the preservation of shoreface deposits of the transgressive coast. Variables are similar to those in the experiments 2 and 3C (figure 7.4 and 7.5), apart from the shoreface length that has been increased to 3000 m.

Sediment supply

A larger sediment supply leads to a greater thickness of the trailing-edge sand sheet (Figure 7.3C). The influence of sediment supply on the rate of coastal retreat and the timing of the end of transgression has not been shown in the experiments, as it is simple and straightforward. When the rise of sea level decelerates, a relatively large sediment supply leads to a relatively fast decrease of the rate of coastal retreat and a relatively early start of progradation. This occurs because a larger part of the sediment demand on the coastal system is filled in by the net sediment supply, and less sediment is needed from shoreface erosion. Sediment supply is the major control on coastal progradation. We have not modelled the influence of sediment supply on progradation, but it can simply be deduced that twice as much sediment during the phase of coastal progradation in experiment 2 leads to twice as much progradation.

Coastal-system width

A wide coastal system continues to retreat for a long time, while a narrow coastal system stops to retreat relatively early under similar decelerating sea-level rise and constant sediment supply (Figure 7.5). The coastal system width defines the accommodation space during sea-level rise; a wide system has a large accommodation space. A wide coastal system can be regarded as a coastal system with a large tidal back-barrier basin. The size of the tidal back-barrier is related to the substrate slope and morphology, and to the influence of other sedimentation and peat formation in the coastal plain.

7.4.2 Trailing-edge sand sheet

In experiment 1 the formation of the trailing-edge sand sheet is simulated (Figure 7.3). A trailing-edge sand sheet forms on all gentle slope substrates if the coastal system has a positive sediment budget. Trailing-edge sand sheets have been recognised on a number of shelf systems (Swift, 1976b, Roy *et al.*, 1994). In the North Sea back-barrier deposits from transgressive Holocene coastal system are found in varying abundance. Holocene deposits are particularly abundant along the modern shoreline (Beets *et al.*, 1995). Comparison of the transgressive back-barrier deposits from the North Sea with the trailing-edge sand sheets from the simulation is not straightforward for several reasons.

The knowledge of the distribution of Holocene sediments in the North Sea is limited, and a comparison of the simulated trailing-edge sand sheets with North Sea sequences is therefore not feasible. The transgressive remnants buried under the prograded shoreface deposits are better known (left half of figure 7.10), and can be compared to the model outcomes. In two areas, south of The Hague and around Velzen and IJmuiden, the transgressive deposits consist of basal peat and back-barrier clay (Figure 7.10A and C). In all other places the transgressive deposits consist of sediments from tidal-channels (Figure 7.10B and D). The maximum thickness of the transgressive tidal-channel deposits is larger than that of the other transgressive deposits. The reworking of the transgressive back-barrier deposits by tidal channels seems to be of prime importance in the stratigraphy of the North Sea trailing-edge sand sheet.

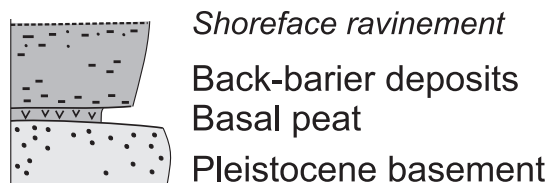
In the simulation the trailing-edge sand sheet consists of back-barrier deposits from the landward edge of the coastal system (Figure 7.8A). Tidal channel incisions and tidal channel deposition were not represented in the simulations. The Holocene transgressive deposits consist of back-barrier deposits overlain by tidal channel deposits. Where channel incision is deep, the transgressive deposits consist solely of tidal-channel deposits (Figure 7.8 B).

After deposition of the trailing-edge sand sheet in the model simulations they are not subject to further reworking. In reality tidal and storm-driven currents and storm-wave reworking cause ongoing erosion and deposition in the North Sea (Houbolt, 1968). The

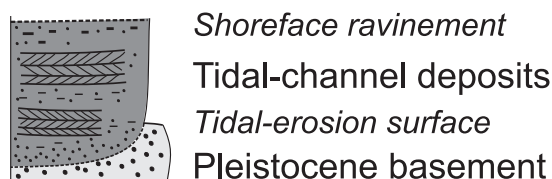
transgressive coastal deposits on the North Sea floor have been subject to severe reworking, leading to the formation of an ‘inner-shelf sand sheet’ (cf. Roy *et al.*, 1994). Depending on the amount of reworking, all or part of the transgressive deposits have been eroded or remoulded (Figure 7.8 C).

An irregular substrate leads to an enhanced preservation potential in depressions, while humps are more easily eroded. This has been demonstrated in several model simulations (Roy *et al.*, 1994, Cowell *et al.*, 1995, Cowell *et al.*, 1999b). In the simulation of experiment 1 we have assumed a constant shoreface depth, but in reality the depth and geometry of the shoreface varied. An increase in the shoreface depth leads to the erosion of most back-barrier deposits, as demonstrated by an earlier simulation of the North Sea stratigraphy by Cowell *et al.* (1999b). In their simulation the increase of the shoreface depth of the transgressive coast effectively eroded all Holocene material from the North Sea floor.

A: trailing-edge sandsheet



B : tidal channel erosion and deposition



C: North Sea reworking

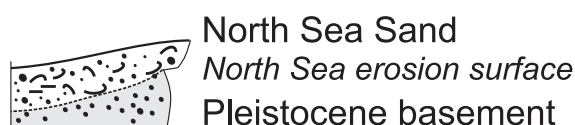


Figure 7.8: Stratigraphy of the trailing-edge sand sheet in the North Sea. Pl.: Pleistocene substrate. A) Without reworking by tidal channel and North Sea processes. B) With tidal-channel incision and tidal-channel deposition, but without North Sea processes. C) With reworking and deposition in the North Sea .

7.4.3 End of transgression

In the simulations of the end of transgression (experiment 3, Figure 7.5 and 7.6) we have seen that under conditions of decelerating sea-level rise the width of the coastal system is of major importance in determining the rate of coastal retreat. The sediment supply plays an important role as well, the coast retreats faster with a large sediment supply. During transgression tidal-channel incision and deposition in the seaward part of the transgressive coast has occurred (Pons *et al.*, 1963, Van Straaten, 1965). The stratigraphy depends on the depth and extent of tidal-channel incisions. The size and extent of the tidal channels can be coupled qualitatively to the accommodation space of the coastal system (Figure 7.9).

The modelled stratigraphy with tidal channel incision (Figure 7.9) can be compared to the observed stratigraphy from the western Netherlands (Figure 7.10). Simulation 3A (Figure 7.9A), with the decrease in the width of the coastal system is comparable to the situation in the former Rhine Meuse valley (Figure 7.10A). The decrease in the width of the coastal system, i.e., in the size of the tidal basins, is induced by the large fluvial input into the area. The small tidal basin leads to tidal channel incisions with a limited depth, and hence some of the transgressive deposits from the landward side of the basin are preserved. Simulation 3C (Figure 7.9C) is well comparable to the situation near Haarlem (Figure 7.10C), with a wide back-barrier basin and thus relatively deep tidal-channel incisions. No transgressive deposits from the landward side of the basin are preserved here. Simulation 3D (Figure 7.9D) is well comparable to the situation near Alkmaar/Bergen (Figure 7.10D), with an even wider back-barrier basin, and deeper tidal-channel incisions. The aggradation of coastal deposits prior to coastal progradation has been observed in the washover deposits at Ypenburg (Chapter 2).

Simulation 3C (Figure 7.9C) has a comparable substrate slope as the area near IJmuiden/Velzen (Figure 7.10C). However, the simulated and actual stratigraphies deviate; the tidal-channel incisions in the simulations are deep relative to those in the stratigraphy. This deviation follows from the fact that the tidal inlet and tidal channels of the back-barrier basins were located north and south of the cross section. This demonstrates that the 2-dimensional model results and the complex spatial distribution of natural systems have to be compared with care.

In the experiments the timing of the end of transgression varies from 6300 BP for simulation 3A to 5100 BP for simulation 3D (Figure 7.6). In reality the transition to progradation occurs around 5500 BP in the south and around 4500 in the north of Holland (Beets *et al.*, 1992, see also Chapter 1, 2, 3 and 4). The difference in timing of the transition in the simulations is of the same order. The difference has been attributed to differences in the size of the tidal basins (Beets *et al.*, 1992), which is represented in the model by differences in the width of the coastal system. Hence, the mechanism that results in the difference in timing in the real world and in the model simulations is comparable.

Based on simulations 3B and 3C (Figure 7.5C, 7.5B and 7.6B, 7.6C) we have inferred that the influence of the substrate on the end of transgression and the beginning of progradation has been limited. Indirectly, the role of the substrate is very important, because it controls the size and geometry of the tidal back-barrier basins. The best example is the development of the large tidal basin (the Alkmaar Bergen tidal basin) in the wide funnel-shaped incised Vecht valley

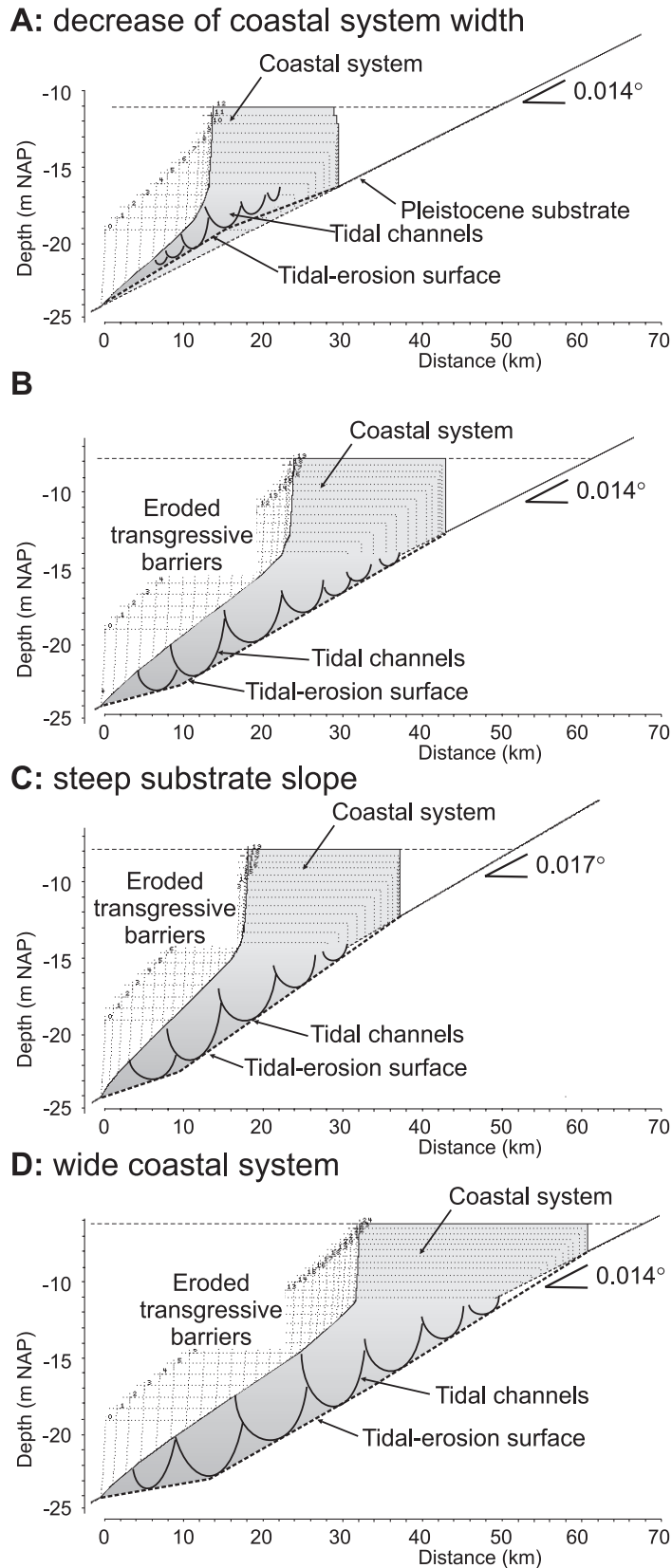


Figure 7.9: Simulated stratigraphies of simulation 3 (figure 7.5), with an indication of the effect of tidal-channel incision and tidal-channel deposition on the stratigraphy. The depth of the tidal channels is related qualitatively to the accommodation space in the coastal system, shown in figure 7.6. A large accommodation space leads to deep tidal-channel incisions. See caption of figure 7.5 for description of the variables in the four simulations.

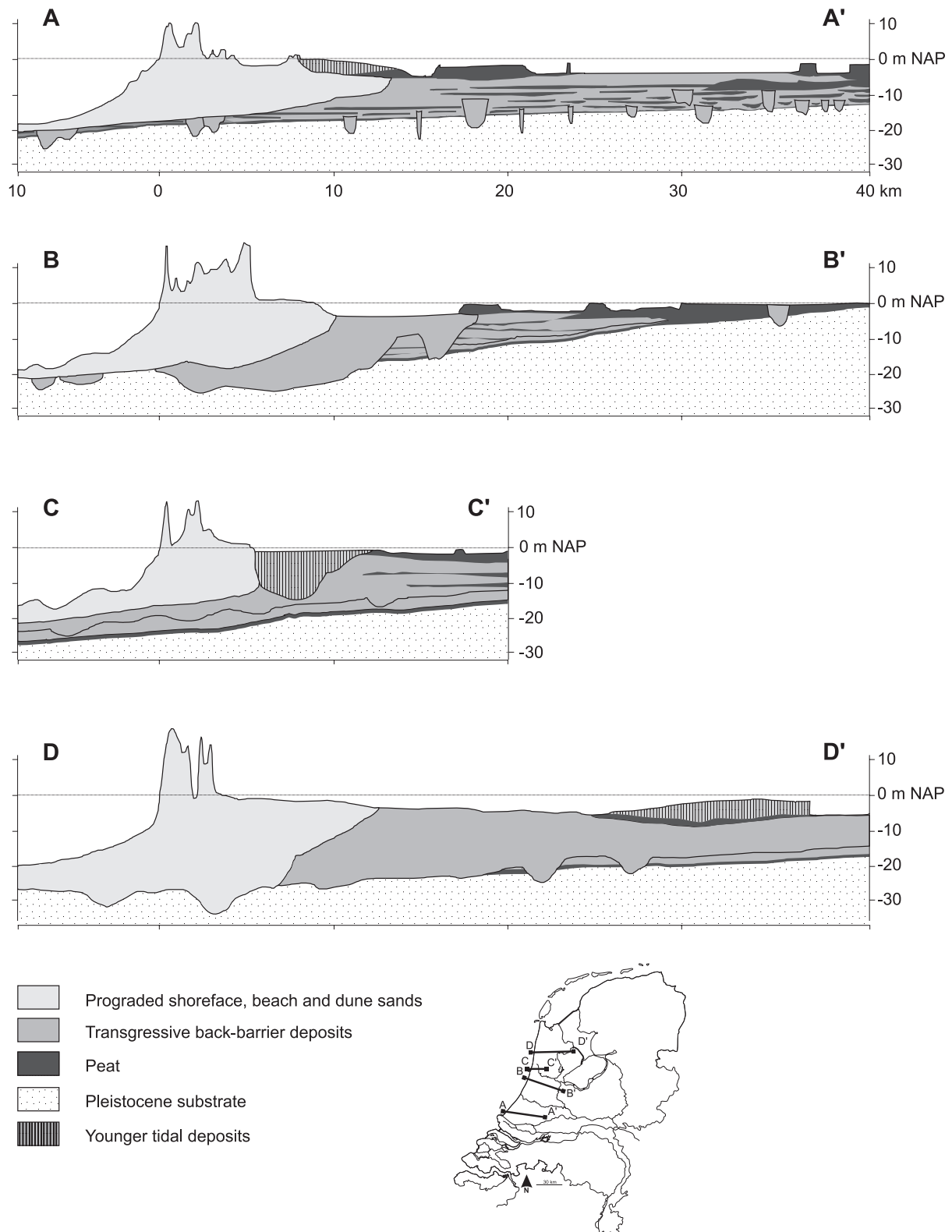


Figure 7.10: Stratigraphy of a number of cross sections from the western Netherlands. Locations are indicated in the map. Captions continue on following page.

Figure 7.10 A: The southern cross section (A-A', figure 1.2) extends from Monster, just south of The Hague, to Gouda (figure 1.1). The cross section is based on Van Straaten (1965), Verbraeck (1970), De Mulder et al. (1983), Van der Meene et al. (1988) and De Gans et al. (1998). The base of the Holocene deposits is formed by the westward dipping Pleistocene substrate. On top of the Pleistocene basal peat, organic rich clays are found. Locally small channels with fluvial deposits (Van der Meene

et al., 1988; De Groot and De Gans, 1996) and estuarine deposits (in the western half De Wolf, 1986; Törnqvist *et al.*, in press) are found incised into the top of the Pleistocene deposits. On top of the basal peat intercalations of organic-rich mud and peat are found. Westward and upward in the sequence the organic-rich mud has a more marine character. Towards the top the deposits become more sandy. Locally sandy channel deposits are found (Verbraeck, 1970; Van der Meene *et al.*, 1988). In the eastern half of the cross section the top 5 m of the deposits consist of peat. In the western half of the cross section deep incisions with sandy tidal-channel deposits are found (Van Straaten, 1965). In the western eight km of the cross section only a thin interval of mud and peat is found, which is overlain by shoreface, beach and dune deposits. Just east of the dunes a thin cover of young tidal deposits is present.

Figure 7.10 B: Cross section B-B' stretches from Zandvoort, southwest of Haarlem, in the direction of Hilversum (figure 1.1). The cross section is based on Riezebos and du Saar (1969), Van der Valk (1992; 1996) and Blokzijl *et al.* (1995). The Pleistocene substrate dips gently towards the west. The basal deposits on top of the Holocene consist of peat. Peat is absent in the western 15 km of the cross section. In the eastern part of the cross section the Holocene consist entirely of peat. On top of the basal peat brackish mud is found. Several peat layers intercalate with the mud. The thickness and abundance of the peat layers increases to the east. The brackish mud gradually grades into marine mud from tidal environments and gradually becomes sandier. Locally sandy tidal-channel deposits are found. Towards the top the sand gives way to peat. The base of the Holocene deposits in the western fifteen kilometres of the cross section consists of sandy tidal-channel deposits. Shoreface, beach and dune sands overlies the sandy tidal-channel deposits in the western ten kilometres of the cross section. The main difference between cross sections B-B' and C-C' is the presence of basal peat and mud below the prograded shoreface, beach and dune sands in cross section C-C', and the presence of sandy tidal channel deposits, with an incised base, at that position in cross section B-B'.

Figure 7.10 C: Cross section C-C' stretches from IJmuiden and Velzen, north of Haarlem to Amsterdam (figure 1.1). The cross section is simplified from Westerhoff *et al.* (1987). Only the western half of the cross section is displayed, the eastern half of the cross section is roughly similar to the eastern half of cross section B-B'. In the western half of the cross section the Pleistocene substrate is overlain by basal peat. There is a gradual transition of the basal peat into mud, which in turn shows a gradual increase in marine characteristics. The mud is the 'Velzen' or 'Hydrobia' clay of Van Straaten (1957). Sandy tidal-channel deposits erosively overlie the muddy tidal deposits. In the westernmost ten km of the cross section the thickness of the tidal-channel deposits is limited. The tidal-channel deposits are overlain by shoreface, beach and dune deposits. More to the east the sandy tidal channel deposits continue up to - 5 m NAP. The sandy tidal-channel deposits are overlain by peat and younger tidal deposits. Directly east of the dunes a channel fill of young tidal deposits is found. These young tidal deposits originate from the Oer-IJ, a former fluvial outlet of the Rhine.

Figure 7.10 D: The northern cross section (D-D', figure 1.2) stretches from Bergen aan Zee to the direction of Enkhuizen (figure 1.1). The cross section is simplified from cross sections in Westerhoff *et al.* (Westerhoff *et al.*, 1987) and Beets *et al.* (1996). The Pleistocene substrate dips to the west. Basal peat is restricted to the eastern half of the cross section. The basal peat is overlain by marine mud, the 'Velzen' or 'Hydrobia' clay (Van Straaten, 1957). Overlying the marine mud sandy and muddy tidal deposits are found. In the western half of the cross section sandy and muddy tidal deposits erosively overlie the Pleistocene substrate. Peat intercalations are absent in the tidal deposits. On top of the tidal deposits a peat layer is found, while in the easternmost part a thin cover of young tidal deposits is found. In the westernmost twelve kilometres of the cross section, shoreface, beach and dune deposits erosively overlie the Pleistocene substrate. The basal part of the shoreface, beach and dune deposits consists of mud with thin storm-sand layers, the 'Bergen Clay'. The Bergen clay locally reaches a thickness of 20 m, and its base locally lies as deep as -35 m NAP.

7.4.4 Transgressive shoreface

In experiment 4 it is shown that preservation of transgressive shoreface deposits can occur when the rate of coastal decreases, but is not yet zero (Figure 7.7). The preservation on the lower part of the shoreface may be regarded as Bruun-type behaviour, i.e., coastal retreat on the upper shoreface, compensated by aggradation on the lower shoreface (Bruun, 1962).

Shoreface deposits from the transgressive coastal system are present below all prograded shoreface deposits from The Hague to Haarlem. Bearing in mind the simplifications in the simulation, the mechanisms presented in this simulation (Figure 7.7) may have accounted for the preservation of these transgressive shoreface deposits. The appeal of this type of preservation lies in the fact that it is an integral part of the transition from transgression to progradation. No other changes in the coastal system have to be invoked to explain the preservation of these deposits.

7.4.5 Transition

In experiment 2 the shift from transgressive to prograding coastal evolution is preceded by a decrease of the rate of retreat, but the transition is still quite sudden (Figure 7.4). The sudden character of the shift is wholly dependent on the assumption that the sediment input is governed by external factors. The sediment sources can be longshore transport from the south or north or cross-shore transport from deeper parts of the North Sea. It is likely that the coastal system itself exerts control on the sediment input, for example because large tidal channels are more effective in importing sediments than small tidal channels. In that case the shift has been more gradual. Such a gradual shift is very likely, considering reconstructions of the gradual closure of tidal inlets in Ypenburg (Chapter 2) and near Alkmaar/Bergen (Westerhoff *et al.*, 1987, Beets *et al.*, 1996b).

7.4.6 Mud and Peat

The STM experiments have all been run without distinction between mud and sand deposition. This is not realistic because coastal deposits contain a fair percentage of mud, especially in the back-barrier deposits. According to Van der Spek (1995, in Beets and Van der Spek, 2000) the percentage of mud is around 36 % in the western Netherlands. If the percentage of mud in the back-barrier deposits decreases during transgression, mud is lost from the system. This may imply that more sediment was eroded from the shoreface to account for the loss of mud (causing a larger coastal retreat), or that more sediment had to be imported from other sources (larger longshore or cross-shore sediment contribution). Inversely, if tidal channels have incised into Pleistocene sand, and the tidal-channel deposits consist partly of mud, the incision of tidal channels has contributed extra sand. Some tidal-channel fills, for instance in the former Bergen/Alkmaar inlet are characterised by high percentages of mud (Westerhoff *et al.*, 1987, Beets *et al.*, 1996b). These tidal-channel incisions thus have acted as a source of sand and should be considered in sediment-budget calculations.

In the model we have only considered deposition of sand and clay. In the back-barrier basins peat is also formed. Peat forms only a limited part of the coastal deposits (5 %, according to Van der Spek, 1995, in Beets and Van der Spek, 2000). The role of peat may have been more pronounced than its abundance indicates, because the compaction of peat can reduce it to 25 to 15 % of its original volume (Bennema, 1954). In the initial transgressive coastal system peat formed at the landward side of the back-barrier basins. Prior to compaction the peat has filled part of the accommodation space in the basins. Hence, it reduced the sediment demand. The formation of peat at the landward side of the tidal basins continued during the transgression and may have continuously reduced the accommodation space in the back-barrier basins.

7.4.7 A model world

Modelling the evolution of the coastal system is only possible with *a priori* knowledge of the depositional system, or more specifically, of the sediment-transport pathways and transport capacities of the coastal system. The wide coastal system that we use in the above simulations

is only feasible if we know that there is a mechanism for the deliverance of sediments from offshore to inshore. In addition we have to know that sediment is available. In the Holocene coastal system the two prerequisites are met: there are plenty of tidal inlets and tidal channels that form an efficient cross-shore sediment-transport pathway (Beets *et al.*, 1992), and there is plenty of Pleistocene sand in the substrate. Other coasts lack either the tidal-import mechanisms, because of the relatively limited tidal influences (for instance because the wave climate is much more energetic like on the New South Wales coast, Australia, Roy and Boyd, 1996), or they lack sufficient sand sources (also on the New South Wales coast, Australia, Roy and Boyd, 1996).

The assumption of equilibrium between the rise of sea level and the sedimentation in the back-barrier is a simplification of all types of processes that enhance sedimentation on tidal flats in back-barrier (tidal asymmetry, the settling lag effect, and biological factors). The assumption is certainly not justified for all situations. For instance, the sedimentation rate in the Bergen/Alkmaar Basin lagged behind the rate of sea-level rise (Westerhoff *et al.*, 1987, Van der Spek and Beets, 1992, Beets *et al.*, 1996b). This does not alter the validity of the model for such conditions: a sedimentation rate lower than the rate of sea-level rise does result in an increase in accommodation space. This may be represented by a larger width of the coastal system. In other words, deviations from the equilibrium in the real world do not necessarily affect the model results, if properly accounted for.

The above discussion clearly demonstrates the value of modelling large-scale coastal behaviour. The model is not a tool one can use to reconstruct the Holocene evolution from scratch. A thorough understanding of the deposits and of underlying mechanisms is needed before a simulation can be run. This works in several ways: knowledge of the input variables is needed to run the model, the stratigraphy of the real world and its variation must be known to be compared to the model outcome, and transport processes must be understood to justify the model approach. 'A thorough understanding' does not mean that we do know all about the system. There are still parts and periods of which the understanding can grow through model simulations. Of course, new aspects that are revealed by the model (transgressive shoreface preservation, coastal aggradation at the end of transgression) should be checked in the real world.

7.5 Conclusions

The simulations of the Holocene coastal evolution with the STM demonstrate the influence of the rate of sea-level rise, the sediment supply, substrate slope, and coastal-system width. The substrate slope and the sediment supply control the thickness of the trailing-edge sand sheet on the North Sea floor. The rate of coastal retreat is controlled by the rate of sea-level rise, by the width of the coastal system and by the net sediment supply. The influence of the substrate slope is exerted through the width of the coastal system. The width of the coastal system represents the size of the tidal back-barrier basins. The modelled stratigraphies of the transgressive coastal systems resemble the observed real-world stratigraphies. The simulations support geological observations that show that the balance between the accommodation space in the back-barrier basins, controlled by the rate of sea-level rise, and the sediment supply determine the rate of coastal retreat and the onset of coastal progradation. The simulations point to two previously unnoticed patterns. Firstly, prior to progradation, at the end of transgression, the coastal system enters a stage of aggradation, with only limited coastal retreat. The stage of aggradation has been observed in the field at Ypenburg (Chapter 2). During the last stages of transgression shoreface deposits may be preserved on the lower shoreface. Transgressive shoreface deposits have been found alongshore in the Holocene sequence of the western Netherlands (Chapter 3 and 4).

Chapter 8: Summary and Conclusions.

Large-scale coastal evolution in the western Netherlands during the Holocene was characterised by an initial stage of transgression followed by a stage of coastal progradation. The last 2000 years the position of coastline of the western Netherlands was relatively stable, with local retreat and advance. Coastal deposits from the western Netherlands have been studied in detail in the Ypenburg area, in cores from coast-perpendicular cross sections near Haarlem and Wassenaar and in cores from the modern shoreface. The age of deposition has been determined with AMS ^{14}C dating of single shells. A model has been used to reconstruct the wave-height reduction on the palaeo-shoreface profiles and model simulations have been used to reveal previously unobserved patterns in the large-scale coastal evolution. The combination of traditional sedimentological research with tools like cone-penetration tests (CPT), ground-penetrating radar (GPR), AMS ^{14}C dating, and modelling of palaeo-conditions and stratigraphic modelling used in this thesis, presents a powerful means to unravel the geological past.

Ypenburg: transgression to progradation

The deposits at Ypenburg originate from the final stages of coastal retreat and the initial stages of progradation in the western Netherlands. The depositional sequence in the area is unique, because it contains deposits from the transgressive shoreline. As yet, such deposits have not been described from the Netherlands. The deposits from the Ypenburg area also give insight into the development of a coastal sedimentary system during the transition from transgression to progradation.

The first signs of the approach of the shoreline to the location are an increase in sand content and marine shells in fine-grained back-barrier deposits. The transgressive coastal deposits in the area originate from wave-influenced subtidal flats, small-tidal channels, intertidal flats and marshes. The transgressive shoreline was dominated by erosion in small tidal channels. Evidence for the presence of a transgressive wave-build barrier -of some kind- are absent in the area. The transgression was followed by a stage of aggradation, dominated by the deposition of a stack of washovers. The washovers display a clear proximal-to-distal trend to the southeast. Progradation started with the formation of a beach ridge and beach plain, marshes and small dunes. The closure of the tidal inlet in the northeastern half of the area started after coastal progradation had commenced. The closure of the tidal inlet was dominated by the deposition of elongated spit-like sand bodies.

This study shows that the transition from transgression to progradation was dominated by a stage of aggradation. Model simulations of the response of the coastal system to a decrease in the rate of sea-level rise also show that the end of coastal retreat is characterised by a stage of aggradation. The transgressive and transitional deposits deviate from deposits from later stages of progradation. The transgressive shoreline was dominated by small-tidal channels and wave-influenced subtidal flats, and the transitional shoreline was characterised by the deposition of washovers. This study also indicates that in this area the closure of the tidal inlet followed after the onset of progradation.

AMS ^{14}C dating of single shells

The results of the AMS ^{14}C dating of slightly reworked single shells demonstrate the feasibility of this method to determine the age of shoreface and beach deposits. Juvenile shells, with as little signs of reworking as possible, were selected from undisturbed cores. The shells were AMS ^{14}C dated. The consistency of the dates was checked, i.e., shells from higher up in the sequence should be younger than shells from underlying deposits. The consistency

of the dates was good. Only when sedimentation rates are very low, 'too old' shells become abundant. The fact that all shell material from these deposits has been reworked prior to deposition means that the actual age of deposition is slightly younger than the age of the shells.

Haarlem and Wassenaar: transgression and progradation

The Holocene deposits in coast-perpendicular cross sections near Haarlem and Wassenaar consist of transgressive tidal back-barrier deposits, overlain by transgressive offshore deposits, in turn overlain by prograded shoreface, breaker-bar and beach deposits. In chapter 3 and 4 a comprehensive facies description and facies model of these deposits is presented, along with a more detailed timeframe for deposition and erosion. The facies model and timeframe are used to refine the model for large-scale coastal evolution and the implications in terms of sources of sediment and sediment transport processes are discussed.

Transgressive tidal-channel deposits form the base of the Holocene sequence in most cores. Basal Peat and clay, i.e., deposits from the landward side of the transgressive tidal back-barrier basin, were found in two cores only. The tidal channels from the seaward parts of the transgressive back-barrier basins have incised into the Pleistocene substrate and eroded most of the Basal Peat and clay. Transgressive offshore and shoreface deposits overlie the transgressive back-barrier deposits. These deposits consist of shoreface sands, of mud with thin storm-sand layers, and of coarse-grained offshore deposits. The mud with thin storm-sand layers was in particular deposited in depressions on the sea floor that resulted from earlier formed incisions by tidal channels. The coarse-grained offshore deposits probably originated from the formation of shoreface-connected ridges. The gradual transition of tidal deposits into shoreface sands and beach deposits at the landward side of the Haarlem cross section marks the transition to progradation. The transgressive offshore deposits are not small isolated remnants, but they form a persistent and continuous part of the coastal sequence, also underneath the modern shoreface. Model simulations show that during the final stages of coastal retreat deposits may be preserved on the lower shoreface, during limited coastal retreat and ongoing sea-level rise. This study shows that the preservation of transgressive offshore deposits is a normal part of the large-scale evolution from transgressive to prograding. The presence of shoreface storm beds around depths of -16 m NAP indicates that wave action on the shoreface was already severe during transgression. The presence of protruding transgressive remnants on the North Sea floor would have hindered wave action, and their presence can thus be excluded.

The overlying deposits of the prograded coastal system consist of shoreface, beach and beach-plain deposits. In the seaward half of the cross section a hiatus is present between the transgressive and the prograded deposits. The hiatus has evolved due to limited erosion and non-deposition on the lower shoreface and shelf during progradation. In the middle part of the cross section a marked change in facies is associated with the hiatus. The duration of the period of non-deposition and erosion represented by the hiatus increases seaward. At the landward side there is a gradual transition from transgressive to prograded deposits.

Isochrons in the prograded shoreface deposits near Haarlem become progressively steeper during the final stages of progradation. This steepening trend is an artefact that results from the absence of seaward cores with dates of lower shoreface deposits, and from the decrease of the rate of progradation. Ground-penetrating-radar images of reflectors that represent profiles from the upper shoreface, breaker-bar and beach have a slope similar to their recent equivalents and indeed do not display changes in slope (Van der Spek *et al.*, 1999). The overall slope from the lowermost shoreface, dominated by erosion and non-deposition to the upper shoreface does become steeper during progradation.

Progradation near Wassenaar has continued at high rates. The shoreface deposits near Wassenaar contain more mud and silt than shoreface deposits near Haarlem. The high rates of progradation enhanced the preservation of mud in the shoreface deposits. The high rates of progradation also favoured the development of beach plains and the preservation of cross-bedded shoreface deposits. The rapid progradation near Wassenaar was followed by severe coastal erosion. Near Haarlem the progradation rates were altogether lower and decreased in time. Extrapolation of the progradation rates in the Haarlem cross section indicates that the shoreline has not advanced much further seaward. Coastal erosion after the stage of progradation thus was limited.

The shoreface sequence

In Chapter 5 the Holocene prograded shoreface deposits from the seaward part of the Haarlem cross section are studied in detail, to infer the depositional conditions during storms and to infer the contributions of longshore relative to cross-shore sediment transport to progradation. The entire prograded shoreface sequence is dominated by the presence of thick storm beds with erosive bases. Distal thin-storm-sand layers are absent in the sequence. The lower-shoreface deposits are bioturbated; the storm beds of the middle-shoreface deposits have preserved silt and mud tops. The transition from lower- to middle-shoreface deposits is fining upward, and the transition from middle- to upper-shoreface deposits and further to breaker-bar and beach is coarsening upward.

The preservation of bioturbation structures in the lower shoreface deposits is related to the limited recurrence of heavy storms that affected the lower shoreface and could erode its bioturbated layer of sediments. The presence of the coarse sand fraction in the lower shoreface deposits probably resulted from the import of coarse sand from the adjacent North Sea floor during severe storms and by tidal currents. The deposition of silt and mud layers on the middle shoreface reflects quiet conditions during fair weather. This also implies that tidal currents, that dominate the North Sea floor, had a limited influence on the middle shoreface. The coarsening upward in grain size from the middle shoreface via the upper shoreface and breaker bar to the beach is the result of the increase in wave influences from deep to shallow water.

Following Van Straaten (1965), we suggest that the grain-size distribution over the shoreface demonstrates that limited cross-shore exchange of coarse sand (over 150 μm) from the North Sea floor to the upper shoreface and beach occurred. It is therefore concluded that longshore-sediment transport dominated the deposition of sand coarser than 150 μm on the upper shoreface, breaker bar and beach. The transport of sand finer than 150 μm can have occurred in the cross-shore as well as the longshore directions. The horizontal-parallel bedding that dominates most storm beds originates from deposition under upper stage-plane bed conditions. The coarse-fine-coarse pattern from lower to upper shoreface and the stable (convex-up) position of shells within the storm beds points to wave-driven oscillatory sheet-flow conditions during deposition of storm sand beds.

The grain-size distributions of the Holocene sequence and that of the modern shoreface are well comparable. The storm beds in the sequence also resemble modern storm-sedimentary structures. These similarities suggest that storm deposition on the modern shoreface is reminiscent of storm deposition on the Holocene prograded shoreface.

Wave-height reduction on the shoreface

The deposits from the initial prograding shoreface reflect quiet depositional conditions, especially in the abundance of thin storm-sand layers high up the palaeo-shoreface. The amalgamated storm beds from the final stages of progradation reflect high-energy depositional conditions over the entire shoreface. During progradation the overall slope from

lowermost shoreface to the upper shoreface profile increased. The increase of the entire shoreface slope has influenced the wave heights on the shoreface and beach. The influence of the slope of the entire shoreface on shallow-water wave heights was calculated with the analytical model of Nielsen (1983). The reduction of the wave-height varies with the slope of the shoreface profile.

The isochrons in the prograded shoreface deposits (Chapter 4) are used to infer the shoreface slope from the lowermost part of the shoreface to the upper shoreface during progradation. Although the slope of the upper shoreface, breaker-bar and beach does not seem to have changed during progradation (Chapter 4), the extension of the shoreface down to its lowermost parts does become steeper. This steepening resulted from the progradation over a relatively flat substrate, while sea level rose. The slope of the entire shoreface showed an increase from 0.15° to 0.59° during progradation. The wave-height reduction of high, long-period waves is about 65 % on the gentle slope, versus 40 % on the steep one. The effect is less pronounced for low, short-period waves. A gentle shoreface profile is an effective filter that removes most high, long-period waves. So, the wave conditions on the coast were relatively quiet during initial progradation due to this effect.

The influence of the shoreface slope on the wave-height reduction is sufficient to explain differences in the character of the shoreface deposits. The zone over which wave action was dissipated was more extended during initial progradation and confined to a narrow band during final stages of progradation.

Modelling coastal evolution

The influence of the rate of sea-level rise, the substrate slope, the input of sediment, and the width of the coastal system on the large-scale coastal evolution of the western Netherlands was simulated with the Shoreface Translation Model (Cowell *et al.*, 1995). The model outcome supports that the imbalance between the sediments supply and the accommodation space in the back-barrier basin is the main control on large-scale coastal evolution (Beets *et al.*, 1992, 1994, Beets and Van der Spek, 2000). The rate of sea-level rise and the size of the tidal back-barrier basins determine the accommodation space. The simulations also reveal some patterns in the coastal evolution that previously have not been noticed.

In the model simulations the thickness of the trailing-edge sand sheet on the North Sea floor is determined by the rate of sea-level rise, the substrate slope and the overall sediment input. In reality, other factors, like depressions and elevations in the substrate, the incision depth of tidal channels and the extent of subsequent reworking on the North Sea floor determine the actual thickness of transgressive remnants on the North Sea floor.

The rate of sea-level rise in combination with the sediment input and the width of the coastal system determine the rate of transgression and the end of transgression in the simulations. The substrate slope has little influence on the end of transgression. During the initial fast rise of sea level the increase in accommodation space in the coastal system is large, and hence coastal retreat is large. With the deceleration of the rise of sea level, the increase in accommodation space decreases, and hence the rate of coastal retreat decreases. This results in a stage of limited coastal retreat and coastal aggradation. Eventually coastal retreat stops completely and progradation starts. The extent and depth of tidal-channel incisions and deposits can be qualitatively linked to the model results, via the width of the coastal system and the sea-level rise.

The model simulations point to a period of limited coastal retreat and aggradation prior to the start of progradation. Observations from Ypenburg demonstrate that indeed a stage of aggradation occurred prior to progradation. Radiocarbon dates from the shoreface deposits demonstrate that transgressive shoreface deposits have been preserved in the coastal

system. The model simulations confirm that during the final stages of transgression shoreface deposits may be preserved

Cross-shore versus longshore sediment transport

A number of aspects of the transgressive and prograded shoreface deposits allows to assess the relative contributions of longshore and cross-shore sediment transport to coastal progradation. The presence of shoreface deposits indicates that wave action on the shoreface during transgression was well capable of the erosion of older deposits. The presence of protruding transgressive remnants on the North Sea floor would have hindered wave action, and their presence can thus be excluded. Such transgressive remnants, for instance ebb-tidal delta deposits, thus have contributed little sediment to coastal progradation. The omnipresent transgressive offshore deposits below prograded shoreface deposits and below the modern shoreface demonstrate that erosion of the lowermost parts of the shoreface and the North Sea floor has been limited after transgression. This also demonstrates that this erosion has contributed little sediment to coastal progradation. The fine-grained storm beds of the prograded middle shoreface deposits, without traces of the coarse sand fraction, demonstrate that little cross-shore transport of coarse sand occurred during progradation. The coarse sand in the prograded upper-shoreface, breaker-bar and beach deposits thus must have been contributed by longshore-sediment transport. The absence of sediment sources that could contribute to coastal progradation by cross-shore sediment transport, combined with the indications that indeed no cross-shore sediment transport of coarse grains has taken place, points to the importance of longshore sediment transport for coastal progradation.

The differences in progradation rates near Haarlem and Wassenaar are best explained by the dominance of longshore sediment transport over cross-shore sediment transport. The high rate of progradation near Wassenaar was due to the influence of the Old Rhine delta north of Wassenaar and to the proximity of the longshore sediment source, the former protruding Rhine Meuse area south of The Hague. In essence, the area near Leiden, including Wassenaar, developed as a wave-dominated delta. The decrease of the progradation rate near Haarlem was due to exhaustion of the sediment source in the south. Furthermore, the progradation resulted in a smooth coastline with a limited curvature, and much of the longshore-sediment transport continued further north. The seaward truncation of the Wassenaar cross section resulted from coastal erosion that smoothed the coastline once the fluvial activity in the delta of the Old Rhine ended.

Samenvatting

Nederland dankt zijn huidige vorm aan veranderingen van de kust in de laatste 9000 à 8000 jaar van het Holoceen. In dit proefschrift wordt het onderzoek aan bepaalde aspecten van de kustontwikkeling in West-Nederland (figuur 1.1) toegelicht en worden de verkregen resultaten besproken. Aan de hand van gegevens over de opbouw van de ondergrond, die in de afgelopen 150 jaar beschikbaar zijn gekomen, zijn verschillende stadia van die kustontwikkeling gereconstrueerd. Hieronder worden eerst de grootschalige ontwikkelingen, zoals opgemerkt en verwoord door Beets e.a. (1992) en Beets en van der Spek (2000), beschreven. Daarna volgt een samenvatting van de verschillende onderwerpen, die in dit proefschrift aan de orde komen.

Alle grootschalige ontwikkelingen van de kust zijn in de eerste plaats gekoppeld aan de zeespiegel, die aan het begin van het Holoceen snel steeg (figuur 1.5). Het toen nog droge Noordzegebied liep relatief snel vol water en de kustlijn verplaatste zich van wat nu Het Kanaal is richting Nederland. Al spoedig begon de getijdenwerking in de Noordzee een belangrijke rol te spelen in het Nederlandse kustgebied. Er ontstonden grote getjebekkens, enigszins vergelijkbaar met de huidige Waddenzee. Het resultaat was een door een aantal zeegaten onderbroken kust. Via die zeegaten werd in de getjebekkens volop zand en klei afgezet. Dit materiaal was afkomstig van de Noordzee zelf; de rivieren brachten relatief weinig zand en klei naar het kustgebied. Het sediment werd aan de kuststrook onttrokken, wat er toe leidde, dat de kustlijn zich steeds verder landwaarts verplaatste. Doordat de zeespiegel tot ongeveer 6000 jaar geleden snel bleef stijgen, was er in de getjebekkens volop ruimte voor het afzetten van zand en klei.

Samenvattend: vanaf ongeveer 8000 tot 6000 jaar geleden bestond de Nederlandse kust uit “wadden”, die zich steeds verder landwaarts verplaatsten.

Rond 6000 jaar geleden begon de snelheid, waarmee de zeespiegel steeg, af te nemen (figuur 1.5). Hierdoor werd de ruimte voor het afzetten van zand en klei in de getjebekkens beperkt. Er werd minder materiaal van de kuststrook landwaarts verplaatst en de terugschrijding van de kust werd geringer. De getjebekkens werden kleiner en slibden uiteindelijk dicht. De zeegaten, die de kustlijn onderbraken, raakten afgesloten.

Met het vol raken van de getjebekkens en het afsluiten van de zeegaten bestond er geen mogelijkheid meer om zand en klei in de getjebekkens te laten “verdwijnen”. Al het materiaal, dat naar de kust werd aangevoerd, parallel aan of dwars op de kust, werd nu opgeslagen bij de kustlijn zelf. Hierdoor begon de kust uit te bouwen. De vorm van deze kustlijn leek veel op de huidige: uitgebreid aaneengesloten strand, met lage duintjes en zonder zeegaten.

Samenvattend: na 6000 jaar geleden stagneerde de terugschrijding van de kust en stopte uiteindelijk volledig, waarna al het naar de kust aangevoerde materiaal ten goede kwam aan de uitbouw.

De aanvoer van materiaal naar de kust en de daarmee gepaard gaande uitbouw ervan ging door tot ongeveer 3000 jaar geleden in het zuiden (Den Haag-Leiden) en tot ongeveer 1000 jaar geleden in het noorden (Haarlem). Delen van de kust, met name ten zuiden van Den Haag en rond Katwijk, erodeerden weer na het eindigen van de uitbouw. Het zand, dat hierbij vrijkwam, kwam terecht bij de nog steeds uitbouwende kust verder in het noorden, in duinen en in de Waddenzee.

De grootschalige ontwikkeling van de West-Nederlandse kust bestaat dus uit een periode met kustterugschrijding, gevolgd door een periode van uitbouw en uiteindelijk stabilisatie van de kustlijn in de laatste 2000 jaar. De stratigrafie, die dit heeft opgeleverd, is schematisch weergegeven in figuur 1.3. In dit proefschrift wordt het onderzoek aan een aantal aspecten van deze ontwikkeling beschreven.

Bij het onderzoek is gebruik gemaakt van traditioneel sedimentologisch onderzoek in ontsluitingen en aan boringen (analyses van de samenstelling, het bekijken en interpreteren van structuren in het sediment en van andere karakteristieken van het sediment, zoals de schelpenfauna), van technieken om de ondergrond te karakteriseren (sonderingen en grondradar) en van moderne (AMS-) koolstofdateringen van zeeschelpjes. Verder zijn computermodellen gebruikt om de golfcondities in het eerste stadium van de uitbouwende kust na te bootsen en de grootschalige kustontwikkelingen te simuleren.

De vorm van de terugschrijdende kust is beschreven aan de hand van de resultaten van veldonderzoek en van de uit boringen verkregen gegevens. Hierbij is ook in detail gekeken naar de omslagfase, toen de kust na terugschrijding ging uitbouwen. Van deze omslagfase zijn ook de afzettingen van de toenmalige vooroever bestudeerd. De snelheid van uitbouw kon met behulp van schelpdateringen worden bepaald. Daarbij is een onderscheid gemaakt tussen de bijdragen van respectievelijk het langtransport en het kustdwarse transport van zand. Hieronder volgt een samenvatting van de onderwerpen, die voor een beter begrip van de grootschalige kustontwikkeling zijn bestudeerd.

Ypenburg

Ypenburg, ten oosten van Rijswijk en Voorburg, ligt op de grens van de getijbekkens van de terugschrijdende kust en de oudste delen van de uitbouwende kust. In dit gebied is de laatste fase van de terugschrijdende kust bewaard gebleven en kan de omslag naar uitbouw bestudeerd worden. In figuur 2.13 is de gereconstrueerde kustontwikkeling bij Ypenburg geschetst.

Een toename van zand en dunne zandlaagjes in de klei van de getijbekkens is het eerste teken, dat de kustlijn richting onderzoeksgebied opschuift. Ook komen steeds meer schelpjes uit waddenmilieus in de klei voor. De terugschrijdende kustlijn zelf, dus de grens tussen de getijbekkens en buitengaats, bestond uit getijdenplaten waarop de golven invloed hadden, heel kleine getijdengeultjes, getijdenplaten zonder golfinvloed en kwelders. In Ypenburg is de terugschrijding op de meeste plaatsen gekenmerkt door een erosievlak, met de bijbehorende scherpe overgang van kleiig naar zandig materiaal, veroorzaakt door erosie in kleine getijdengeultjes. In het gebied zijn geen aanwijzingen gevonden voor het voorkomen van een door golven opgebouwde strandwal.

Na het laatste beetje terugschrijding bleef de positie van de kustlijn enige tijd stabiel. Tijdens deze fase werd een dikke stapel overslagzanden (“washovers”) afgezet. In het westelijke deel van het gebied bestaan de overslagzanden uit lobben, die vrij direct achter de bron zijn opgebouwd. Meer naar het oosten, verder van de bron, werd het zand tijdens stormen in dunne plaatvormige lagen afgezet. Hierna begon de eerste, beperkte uitbouw van de kust. De vorm van de kustlijn begon steeds meer te lijken op die, welke we ook van de latere uitbouw kennen: aan de zeezijde een lage strandwal, die de achtergelegen intergetijdeplaat, de strandvlakte, afschermd van directe golfwerking. Op verhogingen in de strandvlakte, overgeërfd van de er ondergelegen overslagzanden, werden kleine duintjes gevormd, met daarachter een kweldergebied. Het hele gebied werd doorsneden door kleine geultjes, die voornamelijk tijdens stormen actief waren. Op de kleine duintjes zijn sporen van menselijke

activiteit en bewoning aangetroffen, van waterkuilen tot een grafveld met goed geconserveerde menselijk skeletten.

Tijdens het begin van de uitbouw werd het restant van een klein zeegat in het noordelijk deel van Ypenburg afgesloten. In het zuidwesten zorgden een aantal strandhaken voor een steeds verdere afscherming van het zeegat. Uiteindelijk raakte het helemaal afgesloten en ontwikkelde zich ten westen van Ypenburg de strandwal van Rijswijk en Voorburg.

In de modelsimulaties van de grootschalige kustontwikkeling (figuur 7.4 en 7.5) is de fase van opbouw (aggradatie), die in Ypenburg plaatsvond op de overgang van terugschrijding naar uitbouw, heel duidelijk zichtbaar.

Koolstofdateringen van individuele schelpjes

In alle strand- en vooroeverafzettingen bevinden zich schelpjes; deze worden gebruikt om de ouderdom van de afzettingen te bepalen met koolstofdatering. De schelpjes bevinden zich nooit in levenspositie: ze zijn, voordat ze definitief werden begraven, omgewerkt tijdens één of meerdere stormen. Dit betekent dus ook, dat de schelpen altijd iets ouder zijn dan het moment van afzetting. Naarmate schelpen vaker zijn omgewerkt voordat ze definitief begraven raken, wordt de mogelijkheid om de afzetting, waarin ze worden aangetroffen, te dateren steeds kleiner. Het is dus zaak om schelpjes te dateren, die zo min mogelijk zijn omgewerkt. Daarom zijn kleine, juveniele schelpjes met zo weinig mogelijk tekenen van vertering -bij voorkeur met een min of meer intacte organische opperhuid (*periostracum*)- uitgezocht, die per stuk met de AMS-methode zijn gedateerd. Eén mooi exemplaar is voldoende voor het bepalen van de ouderdom van de afzetting waarin het voorkomt. Daardoor is het mogelijk gebruik te maken van exemplaren uit ongestoorde boorkernen, waarin ook de samenstelling en structuren van de afzetting bekeken kunnen worden.

De methode om individuele schelpjes, met zo min mogelijk tekenen van transport, te dateren is zeer goed bruikbaar voor het onderzoek aan de kustafzettingen in West Nederland. Vrijwel alle schelpjes hoger in de kernen zijn jonger dan de onderliggende schelpjes. Met andere woorden: de afzettingen worden netjes jonger naar boven toe. Alleen wanneer de snelheid, waarmee materiaal werd afgezet, zeer laag is geweest, kunnen schelpjes worden gevonden, die ouder zijn dan onderliggende exemplaren. De datering van de schelpjes geeft dus in de meeste gevallen de ouderdom van de afzettingen aan. Deze ouderdommen zijn gebruikt bij het reconstrueren van de kustontwikkelingen.

Haarlem en Wassenaar

De kustafzettingen in twee raaien boringen met een oriëntatie loodrecht op de kust zijn opnieuw bestudeerd (figuur 3.2). De raaien, bij Haarlem en Wassenaar, strekken zich uit van de meest landwaartse strandwal tot aan het huidige strand. Ze bestrijken het hele gebied van de uitgebouwde kust. Ook is een serie boringen van de huidige vooroever bekeken (figuur 3.2). Met de hierboven beschreven koolstofdateringsmethode aan de individuele schelpjes is de ouderdom van de afzettingen bepaald.

De basis van de boringen wordt gevormd door zand uit het Pleistoceen (de periode die vooraf ging aan het Holoceen). Op het Pleistocene zand bevindt zich in twee boringen basisveen, in de andere negentien liggen er getijdenafzettingen op. Het basisveen is waarschijnlijk wel overal gevormd, maar later opgeruimd door getijdengeulen, die horen bij de getijbekkens van de terugschrijdende kust en zich in het Pleistocene zand hebben ingesneden (figuur 4.7 B).

Op de afzettingen van de getjbeekkens, die landwaarts van de kustlijn zijn gevormd, bevinden zich afzettingen van de vooroever van de terugschrijdende kust. Deze afzettingen zijn zeewaarts van de kustlijn gevormd (figuur 3.12 A en B en 4.7 C) en bestaan uit stormzanden, klei met dunne stormzandlaagjes en grove vooroeverafzettingen. De klei met dunne stormzandlaagjes is vooral afgezet in diepe “kuilen”, restanten van eerder ingesneden getijdengeulen (figuur 4.7 D). De grove vooroeverafzettingen zijn waarschijnlijk gevormd als zandbanken op de Noordzeebodem, die doorliepen tot op de vooroever. Aan de meest landwaartse kant van de raaien is een geleidelijke overgang van getijdenafzettingen naar vooroever- en strandafzettingen zichtbaar. Deze overgang laat zien, dat de invloed van de getijdenwerking langzaam is afgenomen en uiteindelijk helemaal is verdwenen, op het moment dat de uitbouw van de kust begint.

De vooroeverafzettingen van de terugschrijdende kust zijn geen kleine plukjes, die toevallig bewaard zijn gebleven: ze zijn overal aanwezig onder de uitbouwende afzettingen. In simulaties met computermodellen is zichtbaar, dat vooroeverafzettingen bewaard kunnen blijven tijdens het laatste stadium van kustterugschrijding, wanneer de landwaartse verplaatsing nog maar zeer beperkt is en er nog steeds een duidelijk stijging van de zeespiegel plaatsvindt (figuur 7.7).

Een belangrijke observatie is het voorkomen van stormzandlagen op een diepte van 16 m onder NAP. Het betekent, dat op de toenmalige vooroever, rond een waterdiepte van ongeveer –11 m (dus gecorrigeerd voor de lagere stand van de zeespiegel), de golfwerking al heel behoorlijk was. Hieruit kan dan weer worden geconcludeerd, dat de golfwerking niet al te veel afgeremd kan zijn op de bodem van de Noordzee. Op de Noordzeebodem kunnen dus niet al te veel afzettingen van de terugschrijdende kust hebben gelegen.

Boven op de vooroeverafzettingen van de terugschrijdende kust bevinden zich vooroever- en strandafzettingen van de uitbouwende kust (figuur 4.7 E en F). In het landwaartse deel van de raaien is de overgang van afzettingen van de terugschrijdende kust naar die van de uitbouwende kust geleidelijk. In het zeewaartse deel is deze overgang gekenmerkt door een scherpe grens. Deze grens is te verklaren uit het feit dat op deze overgang gedurende lange tijd niets is afgezet; er heeft mogelijk zelfs (een beetje) erosie plaatsgevonden (figuur 3.12 C en D).

Tussen de vooroever- en de strandafzettingen in de Haarlemraai en die in de Wassenaarraai bestaan duidelijke verschillen, die samenhangen met de snelheid, waarmee op die plaatsen de kust uitbouwde. Bij Wassenaar was die snelheid veel hoger dan bij Haarlem. Hierdoor bleven bij Wassenaar structuren en klei bewaard, die bij Haarlem tijdens stormen zijn verdwenen. Ook het bewaard blijven van strandvlakte-afzettingen bij Wassenaar is te danken aan de snellere uitbouw.

Bij Wassenaar werd de snelle uitbouw gevolgd door een periode met erosie (figuur 4.7 G). Bij Haarlem nam de snelheid van uitbouw steeds verder af. Als deze trend van afnemende snelheid van uitbouw zeewaarts wordt doorgetrokken, kan worden geconcludeerd, dat de kust bij Haarlem niet veel verder uitgebouwd is geweest dan tegenwoordig. De latere erosie daar is waarschijnlijk gering geweest (figuur 4.7 H).

Aan de hand van de ouderdom van de afzettingen, bepaald met de eerdergenoemde koolstofdateringen van de schelpjes, kunnen vooroeverprofielen uit de fase van uitbouw van de kust worden gereconstrueerd. In de Haarlemraai levert dit profielen op van het bovenste deel van de vooroever, die zeewaarts steeds steiler worden (figuur 4.1). Deze versteiling is echter geen natuurlijke ontwikkeling, maar een artefact van de methode (figuur 4.8). De versteiling kan ontstaan, omdat er geen boorkernen zijn met dateringen van het diepere deel

van de vooroever, zodat het steile bovenste deel van het profiel steeds meer benadrukt wordt in de reconstructies.

Dat de versteiling een artefact is wordt bevestigd door grondradaropnames, waarin reflectoren zichtbaar zijn van de bovenste vooroever, de brekerbanken en het strand. Deze reflectoren hebben een helling, die overeenkomt met die van de vooroever, de brekerbanken en het strand van tegenwoordig. De helling van de reflectoren verandert niet zeewaarts. Overigens versteilt de helling van het complete vooroeverprofiel, van het diepste deel tot aan het strand, wel degelijk tijdens de uitbouw.

De vooroeverafzettingen van de laatste fase van uitbouw.

De afzettingen van de laatste fase van uitbouw in de Haarlemraai hebben een aantal opvallende kenmerken, die extra aandacht verdienen. De karakteristieken van de stormlagen maken het mogelijk de condities tijdens de afzetting te herleiden. Verder kunnen conclusies worden getrokken omtrent de bijdragen, die het zandtransport langs de kust en dwars op de kust aan de uitbouw heeft geleverd.

Het hele pakket vooroeverafzettingen, van de afzettingen van de diepste vooroever tot aan de onderkant van de brekerbankenafzettingen, wordt gekenmerkt door decimeters dikke stormlagen, waarbij de basis van ieder stormbed erosief is. Alle stormlagen hebben een duidelijke horizontale parallelle gelaagdheid, die wijst op hoge stroomsnelheden (“upper-stage plane-bed conditions”). Dunne stormlaagjes in klei, in de meeste literatuurvoorbeelden kenmerkend voor de diepste delen van de vooroever, ontbreken in de opeenvolging. Er zijn wel duidelijke verschillen tussen a) de afzettingen van de diepe vooroever, die sporen van doorgraving door beesten vertonen, b) de afzettingen van de middelste vooroever, waarin dikke kleilagen worden gevonden aan de bovenkant van iedere stormlaag, en c) de afzettingen van de bovenste vooroever, die noch sporen van doorgraving, noch kleilagen hebben. In het hele pakket vooroeverafzettingen is een duidelijke trend waarneembaar: grove afzettingen aan de basis, fijnere afzettingen in het middelste deel en opnieuw grovere afzettingen aan de bovenkant (figuur 5.4). De brekerbankenafzettingen, die boven op de vooroeverafzettingen worden gevonden, zijn nog weer iets grover.

De aanwezigheid van doorgravingsporen in de afzettingen van het onderste deel van de vooroever wordt verklaard door het beperkte voorkomen van stormen die hevig genoeg zijn om op het diepe deel van de vooroever materiaal te kunnen eroderen en zo de sporen van de doorgraving uit te wissen. Het grove zand in deze afzettingen is waarschijnlijk tijdens flinke stormen en door getijdenstromen aangevoerd van de aangrenzende Noordzeebodem (figuur 5.5 B). Het afzetten van de kleilagen op het middelste deel van de vooroever kan alleen plaatsvinden onder rustige omstandigheden, wat betekent, dat getijdenstromen weinig invloed hadden op dit deel van de vooroever. De toename van de korrelgrootte van achtereenvolgens de middelste vooroever, de bovenste vooroever en de brekerbanken is waarschijnlijk het gevolg van de invloed van golfwerking, die van diep naar ondiep water steeds sterker wordt.

Volgens Van Straaten (1965) verloopt op de vooroever het transport van fijn zand en klei (kleiner dan 150 μm) anders dan het transport van grover zand (groter dan 150 μm). De afwezigheid van grof sediment in de afzettingen van het middelste deel van de vooroever wijst erop, dat er geen grof zand uitgewisseld wordt tussen het diepste deel van de vooroever en het bovenste deel. Met ander woorden: waarschijnlijk kan het grove zand niet van de Noordzeebodem naar de bovenste vooroever getransporteerd worden, of vice versa. Al het grove zand in het bovenste deel van de vooroever, in de brekerbanken en op het strand moet dus langs de kust zijn aangevoerd. Deze beperking geldt niet voor het fijne zand en de klei,

die zowel dwars op als langs de kust kunnen worden getransporteerd. De horizontale parallelle gelaagdheden zijn waarschijnlijk gevormd door golfgedreven oscillerende stromingen van de waterlaag dicht bij de bodem, waarin een hoge concentratie zand in suspensie is ("sheet-flow" laag). Dit proces kan ook de grof-fijn-grof-verdeling van zand van de diepe vooroever naar het strand verklaren. Andere zandtransportmechanismen, zoals muistromen, zouden leiden tot een grof-fijn-verdeling van ondiep naar diep water.

De korrelgrootteverdeling van de vooroeverafzettingen van de uitbouwende kust zijn goed vergelijkbaar met die van sedimenten op de huidige vooroever. Ook de structuren en de korrelgrootteverdeling in de individuele stormlagen van de uitgebouwde vooroever en die van de moderne vooroever komen overeen. Deze overeenkomsten suggereren, dat de condities tijdens de vorming van de stormbedden toen en nu vergelijkbaar zijn.

Golfhoogte-afname op de vooroever.

In de Haarlemraai blijken de vooroeverafzettingen van de beginnende uitbouw nogal in karakter te verschillen van die van de laatste uitbouw. Met name het voorkomen van klei met dunne stormlaagjes in de vooroeverafzettingen van de beginnende uitbouw en het totaal ontbreken daarvan in de vooroeverafzettingen van de laatste uitbouw zijn opvallend (figuur 3.11). De klei met dunne stormlaagjes kwam tijdens het begin van de uitbouw voor tot hoog op het vooroeverprofiel. De omstandigheden, waaronder afzetting op de vooroever tijdens de beginnende uitbouw plaatsvond, waren veel rustiger dan de omstandigheden tijdens de laatste uitbouw. Tijdens de kustuitbouw werd de helling van de gehele vooroever, van de overgang naar de Noordzeebodem tot aan het strand, steeds steiler (figuur 6.1). De helling van het vooroeverprofiel beïnvloedt de golfhoogtes: wanneer golven over een vlak profiel de kust naderen verliezen ze meer energie door bodemwrijving dan wanneer het een steil profiel betreft. De invloed van de helling is berekend met het analytische model voor golfhoogte-reductie van Nielsen (1983).

De gereconstrueerde profielen in de uitgebouwde vooroeverafzettingen (uit Hoofdstuk 4, figuur 4.1 en 6.1) zijn gebruikt om de helling van de gehele vooroever te reconstrueren. De versteiling zeewaarts was het gevolg van het uitbouwen over een vrij vlak oppervlak, waarbij de zeespiegel nog steeds steeg. De helling van het gehele vooroeverprofiel nam tijdens de uitbouw toe van 0.15° tot 0.59° . De berekende afname van de golfhoogte over waterdieptes van -10 m tot -5 m op de vooroever is ongeveer 65% op de flauwe helling en 40% op de steile helling, voor hoge golven met een lange golfperiode. De afname van de golfhoogte is minder geprononceerd voor lage golven met een korte golfperiode. Met andere woorden: een flauw hellende vooroever werkt als een effectief filter tegen hoge golven (figuur 6.3). De golfcondities tijdens het begin van de uitbouw waren hierdoor relatief rustig.

In de modelberekeningen is het effect van een veranderde bodemwrijving (door verschillen in karakteristieken van de bodem, zoals de korrelgrootte en de aanwezigheid van ribbels) niet meegenomen. Een beperkte analyse laat zien, dat het effect van een andere bodemwrijving in dezelfde orde van grootte ligt als het effect van veranderingen in de helling van het profiel. Omdat het bepalen van de bodemwrijvingsfactor niet zonder meer mogelijk is, is dit verder buiten beschouwing gelaten.

De veranderingen in de afname van de golfhoogte door versteiling van de helling van het vooroeverprofiel geven een afdoende verklaring voor de verschillen tussen de startfase en de eindfase van de uitbouwende kust. Een bijkomend effect van het steilere vooroeverprofiel is, dat de zone, waar de golfenergie gedissipeerd wordt, steeds minder breed wordt. Dit heeft o.a. invloed op de golfbreking van scheef invallende golven en het resulterende sedimenttransport.

Het modelleren van grootschalige ontwikkelingen van de kust

De invloed van a) de zeespiegelstijging, b) de helling van het substraat, c) de toevoer van materiaal en d) de grootte van de getijbekkens op de lange termijn ontwikkelingen van de West-Nederlandse kust is gesimuleerd met het “Shoreface-Translation Model” (Cowell e.a., 1995). Het model steunt de geologische observaties, dat de wanverhouding tussen de toevoer van zand en klei enerzijds en de ruimte voor de afzetting van dit materiaal in getijbekkens anderzijds de kustontwikkeling bepaalt. De invloed van de snelheid van zeespiegelstijging komt het duidelijkst tot uiting in de getijbekkens. Wanneer de zeespiegel snel stijgt is er veel ruimte voor de afzetting van zand en klei en wordt er veel materiaal aan de kuststrook (het strand en de vooroever) onttrokken. De terugschrijding van de kust verloopt dan snel (figuur 7.4). Als de zeespiegel zó weinig stijgt en het getijbekken zó klein is, dat de ruimte voor zand en klei in het bekken kleiner is dan het aanbod vanuit de kuststrook, komt het sediment ten goede aan de kuststrook (figuur 7.4): de kust begint dan met uitbouwen.

In de modeluitkomsten is een aantal patronen te zien die eerder niet waren opgevallen. Allereerst blijkt de dikte van het sediment, dat na de terugschrijding van de kust achterblijft op de bodem van de Noordzee, afhankelijk van de snelheid waarmee de zeespiegel stijgt, van de toevoer van zand en klei en van de helling van het substraat (figuur 7.3). Veel toevoer van materiaal en/of een steilere helling leiden/leiden tot een dikker pakket afzettingen op de bodem van de Noordzee. In werkelijkheid speelt een aantal andere factoren, die niet in de modelsimulaties zijn meegenomen, ook een rol. Dit zijn o.a. de “kuilen” en “bulten” in het substraat, het insnijden van getijdengeulen en latere omwerking van de Noordzeebodem door getijdenstromingen en stormen (figuur 7.8).

Ten tweede blijkt uit de modelsimulaties, dat het einde van de kustterugschrijding wordt bepaald door de combinatie van de snelheid waarmee de zeespiegel stijgt, de grootte van de getijbekkens en de toevoer van zand en klei (figuur 7.5). De helling van het substraat is niet van belang voor de afname van de terugschrijding. Als de zeespiegel snel stijgt, is er veel ruimte in de getijbekkens en wordt zand en klei onttrokken aan de kustzone, wat leidt tot een snelle terugschrijding. De snelheid van terugschrijding neemt af, wanneer de zeespiegel minder snel stijgt. De kustlijn blijft nu door de beperkte terugschrijding min of meer stabiel, terwijl de doorgaande stijging van de zeespiegel resulteert in de opbouw van de kust. Uiteindelijk stagneert de achteruitgang helemaal en begint de uitbouw van de kust. Wanneer in de modelsimulaties de diepte en de verbreiding van de insnijdende getijdengeulen gekoppeld worden aan de grootte van de getijbekkens en de stijging van de zeespiegel, is de gereconstrueerde stratigrafie goed vergelijkbaar met die van de Hollandse kust (figuur 7.9 en 7.10).

In de modelsimulaties is verder een periode van beperkte kustterugschrijding zichtbaar, waarbij met name opbouw (aggradatie) plaatsvindt. De waarnemingen op Ypenburg onderschrijven deze modeluitkomst. In de modelsimulaties is de conservatie van deze afzettingen gedemonstreerd. De uitkomsten van de koolstofdateringen hebben het bestaan en het bewaard blijven van vooroeverafzettingen van de terugschrijdende kust bevestigd.

Langtransport versus kustdwarstransport van zand

Door bestudering van een aantal aspecten van de kustafzettingen is het mogelijk iets meer te zeggen over relatieve bijdragen van het langs- en het dwarstransport aan de uitbouw van de kust. De aanwezigheid van stormzanden van de terugschrijdende kust laat zien, dat er al veel golfwerking op de vooroever was en dus, dat er geen restanten van de terugschrijdende kust op de Noordzeebodem lagen. Dit betekent ook, dat dit soort resten niet kan hebben bijgedragen aan de uitbouw van de kust. Met andere woorden: deze veronderstelde bron voor

kustdwars transport van materiaal naar de kust (Beets e.a., 1992) heeft niet bestaan. Verder maakt de algemene aanwezigheid van stormzanden van de terugschrijdende kust ook duidelijk, dat er niet al te veel erosie op de diepere vooroever heeft plaatsgevonden: dit materiaal was anders al lang en breed verdwenen. Ook is op grond van de grof-fijn-grof-verdeling van de vooroeverafzettingen geconcludeerd, dat in ieder geval het grove zand niet dwars op de kust getransporteerd werd en dus, dat al het grove zand in het bovenste deel van het vooroeverprofiel, in de brekerbanken en op het strand l ngs de kust is aangevoerd.

De verschillen in de uitbouwsnelheden langs de kust, hoog bij Wassenaar en lager en afnemend bij Haarlem, zijn ook goed te verklaren uit de dominante rol van het langstransport van zand. De snelle uitbouw bij Wassenaar werd veroorzaakt door de monding van de Oude Rijn, iets noordelijker bij Katwijk. Verder bevond Wassenaar zich dicht bij de bron van het zand dat door langstransport werd aangevoerd, namelijk het uitstekende kustsegment, dat gevormd werd door de voormalige Rijn- en Maasmonding ten zuiden van Den Haag. Het hele gebied rond Leiden en Katwijk ontwikkelde zich als een door golven gedomineerde delta. De uitgebreide erosie van de kust bij Wassenaar is het gevolg van het rechttrekken van de kustlijn nadat de rivierinvloed van de Oude Rijn stopte.

De afname van de uitbouwsnelheid bij Haarlem was het gevolg van het uitgeput raken van de zuidelijke sedimentbron. Bovendien nam de kromming van de kustboog steeds verder af, waardoor een steeds groter deel van het sediment naar het noorden werd getransporteerd en dus niet ten goede kwam aan de uitbouw van de kust.

References

- Acker Stratingh, G. (1837) Kaart van de provincie Groningen met aanduidingen van de grondgesteldheid en de waterstaat, en vele, voor de geschiedenis van haren bodem belangrijke bijzonderheden, Groningen.
- Aigner, T. (1985) *Storm depositional systems*, 174 pp.
- Aigner, T. & Reineck, H. E. (1982) Proximality trends in modern storm sands from the Helgoland bight (North Sea) and their implications for basin analysis. *Senckenbergiana maritima*, **14**, 183-215.
- Allen, G. P. & Posamentier, H. W. (1993) Sequence stratigraphy and facies model of an incised valley fill: the Gironde Estuary, France. *Journal of Sedimentary Research*, **63**, 378-391.
- Allen, J. R. L. (1970) *Physical processes of sedimentation, an introduction*. Allen and Unwin, London, 248 pp.
- Allen, J. R. L. (1984) Experiments on the settling, overturning and entrainment of bivalve shells and related models. *Sedimentology*, **31**, 227-250.
- Amorosi, A. & Marchi, N. (1999) High-resolution sequence stratigraphy from peizocone tests: an example from the Late Quaternary deposits of the southeastern Po Plain. *Sedimentary Geology*, **128**, 67-81.
- Anonymous. (1954) Quaternary changes in level especially in The Netherlands. *Geologie en Mijnbouw*, **16**, 147.
- Anonymous. (1963) Foreword. *Verhandelingen van het K.N.G.M.G., Geologische serie*, **21-2**, 7.
- Antia, E. E. (1994) Vertical patterns of grain-size parameters of shoreface-connected ridges in the German Bight. *Geologie en Mijnbouw*, **73**, 13-22.
- Arnott, R. W. & Southard, J. B. (1990) Exploratory flow-duct experiments on combined flow bed configurations and some implications for interpreting storm-event stratification. *Journal of Sedimentary Research*, **60**(2), 211-219.
- Bagnold, R. A. (1954) Experiments on a gravity free dispersion of large solid spheres in a Newtonian fluid under shear. *Proceedings of the Royal Society of London, Series A Mathematical and Physical Sciences*, **225**, 49-63.
- Beets, D. J., Cleveringa, P., Laban, C. & Battagazore, P. (1995) Evolution of the lower shoreface of the coast of Holland between Monster and Noordwijk. *Mededelingen Rijks Geologische Dienst*, **52**, 235-247.
- Beets, D. J., Fischer, M. M. & De Gans, W. (1996a) Introduction: Ten papers on the coastal evolution of The Netherlands. *Mededelingen Rijks Geologische Dienst*, **57**, 5-8.
- Beets, D. J., Roep, T. B. & De Jong, J. (1981) Sedimentary sequences of the subrecent North Sea coast of the Western Netherlands near Alkmaar. *IAS Special Publication*, **5**, 133-145, International Association of Sedimentologists, Blackwell, Oxford.
- Beets, D. J., Roep, T. B. & Westerhoff, W. E. (1996b) The Holocene Bergen Inlet: closing history and related barrier progradation. *Mededelingen Rijks Geologische Dienst*, **57**, 97-131.
- Beets, D. J. & Van der Spek, A. J. F. (2000) The Holocene evolution of the barrier and the back-barrier basins of Belgium and the Netherlands as a function of late Weichselian morphology, relative sea-level rise and sediment supply. *Geologie en Mijnbouw / Netherlands Journal of Geosciences*, **79**, 3-16.
- Beets, D. J., Van der Spek, A. J. F. & Van der Valk, L. (1994) Holocene ontwikkeling van de Nederlandse kust., Report RGD rapport Rijks Geologische Dienst, Haarlem, 53 pp.
- Beets, D. J., Van der Valk, L. & Stive, M. J. F. (1992) Holocene evolution of the coast of Holland. *Marine Geology*, **103**, 423-443.
- Bennema, J. (1954) Holocene movements of land- and sea-level in the coastal area of the Netherlands. *Geologie en Mijnbouw*, **16**, 247-253.
- Bergman, K. M. & Snedden, J. W. (1999) Modern shelf sand ridges: from historical perspective to a unified hydrodynamic and evolutionary model. In: *Isolated shallow marine sand bodies: Sequence stratigraphic analysis and sedimentologic interpretation, SEPM special publication*, **64** (Ed. by R. W. Dalrymple), pp. 362. Society for Sedimentary Geology, Tulsa, OK.
- Bernard, H. A., Leblanc, R. J. & Major, C. F. (1962) Recent and Pleistocene geology of southwest Texas. In: *Geology of the Gulf Coast and Central Texas and guidebook of excursions*, pp. 175-225. Houston Geological Society, Houston.
- Blokzijl, J., Dubbelaar, W., De Gans, W., De Jong, J. & Metten, R. M. (1995) Vereenvoudigde geologische kaart van Haarlem en omgeving, scale 1 : 50.000. Rijks Geologische Dienst, Haarlem.
- Boersma, J. R. (1991) A large flood-tidal delta and its successive spill-over apron: detailed proximal-distal facies relationships (Miocene Lignite Suite, Lower Rhine Embayment, Germany). In: *Clastic Tidal Sedimentology, CSPG Memoir*, **16** (Ed. by D. G. Smith, G. E. Reinson, B. A. Zaitlin and R. A. Rahmani), pp. 227-254, Canadian Society of Petroleum Geologists, Calgary, Alberta.
- Boyd, R., Dalrymple, R. W. & Zaitlin, B. A. (1992) Classification of clastic coastal depositional environments. *Sedimentary Geology*, **80**, 139-150.
- Bruun, P. (1962) Sea-level rise as a cause of shore erosion. *Proceedings of the American Society of Civil Engineers, Journal for Water Harbors Division*, **88**, 117-130.

References

- Carey, J. S., Swift, D. J. P., Steckler, M., Reed, C. D. & Niedoroda, A. (1999) High-resolution sequence stratigraphic modeling 2: effects of sedimentation processes. In: *Numerical experiments in stratigraphy: recent advances in stratigraphic and sedimentologic computer simulations*, SEPM Special Publication, **62** (Ed. by J. W. Harbaugh, W. L. Watney, E. C. Rankey, R. Slingerland, R. H. Goldstein and E. K. Franseen), pp. 151-164. Society for Sedimentary Geology, Tulsa, OK.
- Clifton, H. E. (1976) Wave-formed sedimentary structures - A conceptual model. In: *Beach and nearshore sedimentation*, SEPM Special Publication, **24** (Ed. by R. A. Davis and R. L. Ethington), pp. 126-148. Society of Economic Paleontologists and Mineralogists, Tulsa, OK.
- Clifton, H. E. & Boggs, S. (1970) Concave-up pelecypod (Psephidia) shells in shallow marine sand, Elk river beds, Southwestern Oregon. *Journal of Sedimentary Petrology*, **40**(3), 888-897.
- Clifton, H. E., Hunter, R. E. & Phillips, R. L. (1971) Depositional structures and processes in the non-barred high-energy nearshore. *Journal of Sedimentary Petrology*, **41**(3), 651-670.
- Cook, D. O. & Gorsline, D. S. (1972) Field observations of sand transport by shoaling waves. *Marine Geology*, **13**, 31-55.
- Cowell, P. J., Hanslow, D. J. & Meleo, J. F. (1999a) The Shoreface. In: *Handbook of Beach and Shoreface Morphodynamics* (Ed. by A. D. Short), pp. 37-71. Wiley, Chichester.
- Cowell, P. J., Roy, P. S., Cleveringa, J. & De Boer, P. L. (1999b) Simulating coastal systems tracts using the shoreface translation model. In: *Numerical experiments in stratigraphy: recent advances in stratigraphic and sedimentologic computer simulations*, SEPM Special Publication, **62** (Ed. by J. W. Harbaugh, W. L. Watney, E. C. Rankey, R. Slingerland, R. H. Goldstein and E. K. Franseen), pp. 165-175. Society For Sedimentary Geology, Tulsa, OK.
- Cowell, P. J., Roy, P. S. & Jones, R. A. (1992) Shoreface Translation Model: Computer simulation of coastal-sand body response to sea-level rise. *Mathematical Computer Simulation*, **33**, 603-608.
- Cowell, P. J., Roy, P. S. & Jones, R. A. (1995) Simulation of large-scale coastal change using a morphological behaviour model. *Marine Geology*, **126**, 45-61.
- Cowell, P. J. & Thom, B. G. (1994) Morphodynamics of coastal evolution. In: *Coastal evolution, late Quaternary shoreline morphodynamics*. (Ed. by R. W. G. Carter and C. D. Woodroffe), pp. 33-86. University Press, Cambridge.
- Cross, T. A. & Harbaugh, J. W. (1990) Quantitative dynamic stratigraphy: A workshop, a philosophy, a methodology. In: *Quantitative Dynamic Stratigraphy* (Ed. by T. A. Cross), pp. 3-20. Prentice Hall, Englewood Cliffs.
- Curry, J. R. (1964) Transgressions and regressions. In: *Papers in Marine Geology, Shepard commemorative volume* (Ed. by R. L. Miller), pp. 175-203. MacMilland, New York.
- Curry, J. R., Emmel, F. J. & Crampton, P. J. S. (1969) Holocene history of a strand plain, lagoonal coast, Nayarit, Mexico. *Coastal Lagoons - a symposium*, Universidad Nacional Autonoma, Mexico, 63-100.
- Dalrymple, R. W., Boyd, R. & Zaitlin, B. A. (1994) History of research, types and internal organisation of incised valley systems: introduction to the volume. In: *Incised-valley systems: origin and sedimentary sequences*, SEPM Special Publication, **51** (Ed. by R. W. Dalrymple, R. Boyd and B. A. Zaitlin). Society of Economic Paleontologists and Mineralogists, Tulsa, OK.
- Davidson-Arnott, R. G. D. & Greenwood, B. (1974) Bedforms and structures associated with bar stratigraphy in the shallow water wave environment, Kouchibouguac Bay, New Brunswick, Canada. *Journal of Sedimentary Petrology*, **44**, 698-704.
- Davidson-Arnott, R. G. D. & Greenwood, B. (1976) Facies relationships on a barred coast, Kouchibouguac Bay, New Brunswick, Canada. In: *Beach and nearshore sedimentation*, SEPM Special Publication, **24** (Ed. by R. A. Davis and R. L. Ethington), pp. 149-168. Society of Economic Paleontologists and Mineralogists, Tulsa, OK.
- Davis, R. A. & Clifton, H. E. (1987) Sea-level change and the preservation potential of wave-dominated and tide-dominated coastal sequences. In: *Sea-level fluctuation and coastal evolution*, SEPM Special Publication, **41** (Ed. by N. D., O. H. Pilkey and J. D. Howard), pp. 167-178. Society of Economic Paleontologists and Mineralogists, Tulsa, OK.
- Davis, R. A. & Clifton, H. E. (1994) Sea-level change and the preservation potential of wave-dominated and tide-dominated coastal sequences. In: *Incised-valley systems: origin and sedimentary sequences*, SEPM Special Publication, **51** (Ed. by R. W. Dalrymple, R. Boyd and B. A. Zaitlin). Society of Economic Paleontologists and Mineralogists, Tulsa, OK.
- Davis, R. A., Fox, W. T., Hayes, M. O. & Boothroyd, J. C. (1972) Comparison of ridge and runnel systems in tidal and non-tidal environments. *Journal of Sedimentary Petrology*, **42**(2), 413-421.
- De Boer, P. L. (1979) Convolute lamination in modern sands of the estuary of the Oosterschelde, the Netherlands, formed as a result of entrapped air. *Sedimentology*, **26**, 283-294.
- De Bruyne, R. H. & Van der Valk, L. (1991) Schelpdieren in het Hollandse kustgebied: herkomst, aanspoelgedrag en transportmechanismen. (Voorstudie naar herkomst en betekenis voor zandtransport), Report RIVO, IJmuiden, 38 pp.

- De Gans, W., Kok, H., Zwaan, H. & Metten, R. M. (1998) Vereenvoudigde geologische kaart van Den Haag en omgeving, Nederlands Instituut voor Toegepaste Geowetenschappen TNO, Haarlem.
- De Gans, W., Laban, C. & Rijdsdijk, K. F. (1993) Overzichtskaart bovenkant pleistocene afzettingen in Nederland en in het Nederlandse deel van het Continentaal plat; schaal 1 : 250.000. Rijks Geologische Dienst, Haarlem.
- De Gans, W. & Van Gijssel, K. (1996) The Late Weichselian morphology of the Netherlands and its influence on the Holocene coastal development. *Mededelingen Rijks Geologische Dienst*, **57**, 11-25.
- De Groot, T. A. M. & De Gans, W. (1996) Facies variations and sea-level-rise response in the lower Rhine/Meuse area during the last 15.000 years (the Netherlands). *Mededelingen Rijks Geologische Dienst*, **57**, 229-250.
- De Mulder, E. J. F. & Bosch, J. H. A. (1982) Holocene stratigraphy, radiocarbon datings and palaeogeography of central and northern North-Holland (The Netherlands). In: *Mededelingen Rijks Geologische Dienst*, Vol. 36-3, pp. 111-160, Haarlem.
- De Mulder, E. J. F., Pruijssers, A. P. & Zwaan, H. (1983) Kwartairgeologie van 's Gravenhage en omgeving. In: *Mededelingen Rijks Geologische Dienst*, Vol. 37-1 (Ed. by H. W. J. Van Ameron and E. F. J. De Mulder), pp. 12-43, Haarlem.
- De Ruig, J. H. M. & Louisse, C. J. (1991) Sand budget trends and changes along the Holland coast. *Journal of Coastal Research*, **7**, 1013-1026.
- De Ruijter, W. P. M., Van der Giessen, A. & Groenendijk, F. C. (1992) Current and density structure in the Netherlands coastal zone. In: *Dynamics and exchange in estuaries and the coastal zone* (Ed. by D. Prandle), pp. 529-550. American Geophysical Union, Coastal and Estuarine Sciences.
- De Vries, H. & Barendsen, G. W. (1954) Measurements of age by the carbon-14 technique. *Nature*, **174**, 1138-1141.
- De Wolf, H. (1986a) Diatomeeënonderzoek van een boring bij Delft (Holoceen), Report Afdeling Diatomeeën Rijks Geologische Dienst, Haarlem, 5 pp.
- De Wolf, H. (1986b) Diatomeeënonderzoek van een boring Rijswijk 110, Report Afdeling Diatomeeën Rijks Geologische Dienst, Haarlem, 7 pp.
- Dean, R. G. (1991) Equilibrium beach profiles: characteristics and applications. *Journal of Coastal Research*, **7**(1), 53-84.
- Dean, R. G. & Maurmeyer, E. M. (1983) Models of beach-profile response. In: *CRC handbook of coastal processes and erosion* (Ed. by P. Komar and J. Moore), pp. 151-165. CRC press, Boca Raton.
- DeMowbray, T. & Visser, M. J. (1984) The genesis of lateral accretion deposits in sub-tidal channel deposits, Oosterschelde, southwest Netherlands. *Journal of Sedimentary Petrology*, **54**, 811-824.
- Doppert, J. W. C., Ruegg, G. H. J., Van Staaldin, C. J., Zagwijn, W. H. & Zandstra, J. G. (1975) Lithostratigrafie; Formaties van het Kwartair en Bover-Tertiair in Nederland. In: *Toelichting bij geologische overzichtskaarten van Nederland* (Ed. by W. H. Zagwijn and C. J. Van Staaldin), pp. 11-56. Rijks Geologische Dienst, Haarlem.
- Dronkers, J., Van Alphen, J. S. L. J. & Borst, J. C. (1990) Suspended sediment transport in the Southern North Sea. In: *Residual currents and long-term transport*, Vol. 38 (Ed. by R. T. Cheng), pp. 303-319. Springer, New York. *Coastal and Estuarine Studies*.
- Dubois, E. (1910) Over duinvalleien, den vorm van der Nederlandsche kustlijn en het ontstaan van laagveen in verband met bodembewegingen. *Tijdschrift van het Koninklijk Nederlands Aardrijkskundig Genootschap*, **27**, 395-402.
- Dubois, E. (1911) De Hollandse Duinen, grondwater en bodemdaling. *Tijdschrift van het Koninklijk Nederlands Aardrijkskundig Genootschap*, **28**, 395-415.
- Dubois, G. (1924) Classification du Quarternaire du Nord de la France et comparaison avec le Quarternaire danors. *Compte rendus des seances de l'académie des Sciences*, **tomé 179**, 475.
- Edelman, C. H. (1950) *Inleiding tot de bodemkunde van Nederland*. Noord Hollandse Uitgevers Maatschappij, Amsterdam, 178 pp.
- Eisma, D. (1966) The distribution of benthic marine molluscs off the main Dutch coast. *Netherlands Journal of Sea Research*, **3**, 107-163.
- Elliot, T. (1986) Siliciclastic shorelines. In: *Sedimentary environments and facies* (Ed. by H. G. Reading), pp. 155-188. Blackwell, Oxford.
- Eysink, W. D. (1979) Morfologie van de Waddenzee; Gevolgen van Zand en Schelpwinning, Report Waterloopkundig Laboratorium, Delft, 92 pp.
- Eysink, W. D. (1990) Morphologic response of tidal basins to changes. The Dutch coast: paper no. 8. 22 *International Conference on Coastal Engineering*, Delft, 1948-1961.
- Faber, F. J. (1942) *Nederlandse landschappen - bodem, gronden, geologische bouw*. Noorduijn en zoon, Gorinchem, 400 pp.
- Faber, F. J. (1947) *Geologie van Nederland, deel III, Nederlandse landschappen*. Noorduijn en zoon, Gorinchem, 537 pp.
- FitzGerald, D. M., Penland, S. & Nummedal, D. (1984) Changes in tidal inlet geometry due to back-barrier filling: East Frisian Islands, West Germany. *Shore and Beach*, **52**, 2-8.

References

- Flessa, K. W. (1998) Well-traveled cockles: Shell transport during the Holocene transgression of the southern North Sea. *Geology*, **26**(2), 187-190.
- Franken, A. F. (1987) Rekonstructie van het paleo-getijklimaat in de Noordzee, Report Delft Hydraulics Laboratory, Delft, 74 pp.
- Galloway, W. E. (1975) Process framework for describing the morphological and stratigraphic evolution of deltaic depositional systems. In: *Deltas; models for exploration* (Ed. by M. L. Broussard), pp. 87-98. Geological Society, Houston.
- Galloway, W. E. & Hobday, D. K. (1983) *Terrigenous Clastic Depositional Systems; Applications to petroleum, coal, and uranium exploitation*. Springer, New York, 423 pp.
- Gerritsen, H. & Berentsen, C. W. J. (1998) A modelling study of tidally induced equilibrium sand balances in the North Sea during the Holocene. *Continental Shelf Research*, **18**, 151-200.
- Goodfriend, G. A. & Stanley, D. J. (1996) Reworking and discontinuities in Holocene sedimentation in the Nile Delta: documentation from amino acid racemization and stable isotopes in mollusk shells. *Marine Geology*, **129**, 271-283.
- Grant, W. D. & Madsen, O. S. (1982) Movable bed-roughness in unsteady oscillatory flow. *Journal of Geophysical Research C*, **87**, 469-481.
- Greenwood, B. & Mittler, P. R. (1985) Vertical sequence and lateral transitions in the facies of a barred nearshore environment. *Journal of Sedimentary Petrology*, **55**(3), 366-375.
- Gruszczynski, M., Rudowski, S., Semil, J., Slominski, J. & Zrobek, J. (1993) Rip currents as a geological tool. *Sedimentology*, **40**, 217-236.
- Guillen, J. & Hoekstra, P. (1996) The "equilibrium" distribution of grain size fractions and its implications for cross-shore sediment transport: a conceptual model. *Marine Geology*, **135**, 15-33.
- Hine, A. C. (1979) Mechanisms of berm development and resulting beach growth along a barrier spit complex. *Sedimentology*, **26**, 333-351.
- Hokke, A. W. & Roskam, A. P. (1987) Gemeten golf klimaat in diep water, Report GWAO Rijkswaterstaat, Dienst Getijdewateren, The Hague.
- Houbolt, J. J. H. C. (1968) Recent sediments in the southern bight of the North Sea. *Geologie en Mijnbouw*, **47**, 245-273.
- Houman, K. T. & Van Rijn, L. C. (1999) Flow resistance in the coastal zone. *Coastal engineering*, **38**, 261-273.
- Howard, J. D., Frey, R. W. & Reineck, H. E. (1972) Georgia coastal region, Sapelo Island, U.S.A.: Sedimentology and Biology, I Introduction. *Senckenbergiana Maritima*, **4**, 3-14.
- Howard, J. D. & Reineck, H. A. (1981) Depositional facies of high-energy beach-to-shoreface sequence: comparison with low-energy sequence. *American Association of Petroleum Geologists Bulletin*, **65**, 807-830.
- Howard, J. D. & Reineck, H. E. (1972) Georgia coastal region, Sapelo Island, U.S.A.: Sedimentology and Biology. IV Physical and biogenic sedimentary structures of the nearshore shelf. *Senckenbergiana Maritima*, **4**, 81-123.
- Hoyt, J. H. & Henry, V. J. (1967) Influence of island migration on barrier sedimentation. *Bulletin of the Geological Society of America*, **78**, 77-86.
- Hulsen, L. J. M. (1994) Modelling paleo-getij in de Noordzee., Report Waterloopkundig Laboratorium, Delft, 101 pp.
- Hulsen, L. J. M. (1995) Modelling paleo-getij in de Noordzee; aanvullende berekeningen, niet uniforme MSL reductie., Report Waterloopkundig Laboratorium, Delft, 76 pp.
- Hunter, R. E., Clifton, H. E., Phillips, R. L. (1979) Depositional processes, sedimentary structures, and predicted vertical sequences in barred nearshore systems, Southern Oregon Coast. *Journal of Sedimentary Petrology*, **49**, 711-726.
- Jelgersma, S. (1961) Holocene sea-level changes in the Netherlands. *Mededelingen Geologische Stichting*, **7**, 101 pp.
- Jelgersma, S. (1979) Sea-level changes in the North Sea basin. In: *Acta Univ. Ups. Symp. Univ. Ups. Annum Quingentesimum Celebrantis, Vol. 2* (Ed. by E. Oele, R. T. E. Schüttenhelm and A. J. Wiggers), pp. 233-248, Uppsala.
- Jelgersma, S., De Jong, J., Zagwijn, H. W. & Van Regteren Altena, J. F. (1970) The coastal dunes of the Western Netherlands: Geology, vegetational history and archeology. In: *Mededelingen Rijks Geologische Dienst*, **21**, pp. 93-167. Rijks Geologische Dienst, Haarlem.
- Jelgersma, S. & Pannekoek, A. J. (1960) Post-glacial rise of sea-level in the Netherlands (a preliminary report). *Geologie en Mijnbouw*, **39**, 201-207.
- Jelgersma, S., Stive, M. J. F. & Van der Valk, L. (1995) Holocene storm surge signatures in the coastal dunes of the western Netherlands. *Marine Geology*, **125**, 95-110.
- Johnson, H. D. & Baldwin, C. T. (1996) Shallow siliciclastic seas. In: *Sedimentary environments, processes, facies and stratigraphy* (Ed. by H. G. Reading), pp. 232-280. Blackwell, Oxford.
- Kidwell, S. M. (1991a) The stratigraphy of shell concentrations. In: *Taphonomy: releasing the data locked in the fossil record* (Ed. by P. A. Allison and D. E. G. Briggs), pp. 212-290. Plenum Press, New York.

- Kidwell, S. M. (1991b) Taphonomy and time-averaging of marine shelly faunas. In: *Taphonomy: releasing the data locked in the fossil record* (Ed. by P. A. Allison and D. E. G. Briggs), pp. 115-209. Plenum Press, New York.
- Kohsiek, L. H. M. (1988) Reworking of former ebb-tidal delta's into large longshore bars following the artificial closure of tidal inlets in the southwest of the Netherlands. In: *Tide-influenced sedimentary environments and facies* (Ed. by P. L. De Boer, A. Van Gelder and S. D. Nio), pp. 113-122. Reidel, Dordrecht.
- Kraft, J. C. & John, C. J. (1979) Lateral and vertical facies relations of transgressive barriers. *American Association of Petroleum Geologist Bulletin*, **62**, 2145-2163.
- Kuenen, P. H. & Migliorini, C. I. (1950) Turbidity currents as a cause of graded bedding. *Journal of Geology*, **58**, 91-127.
- Kumar, N. & Sanders, J. E. (1974) Inlet sequence: a vertical succession of sedimentary structures and textures created by the lateral migration of tidal inlets. *Sedimentology*, **21**(1), 491-532.
- Kumar, N. & Sanders, J. E. (1976) Characteristics of shoreface storm deposits: modern and ancient examples. *Journal of Sedimentary Petrology*, **46**(1), 145-162.
- Liu, J. T. & Zarillo, G. A. (1989) Distribution of grain-sizes across a transgressive shoreface. *Marine Geology*, **87**, 121-136.
- Lorié, J. (1890) Contributions a la géologie des Pays-Bas V Les dunes intérieurs, les tourbières basses et les oscillations du sol. *Extrait des Archives Teyler, Serie II, tome III*, 87.
- Martini, I. P. (1991) Sedimentology of subarctic tidal flats of western James Bay and Hudson Bay, Ontario, Canada. In: *Clastic Tidal Sedimentology, CSPG Memoir*, **16** (Ed. by D. G. Smith, G. E. Reinson, B. A. Zaitlin and R. A. Rahmani), pp. 137-160, Canadian Society of Petroleum Geologists, Calgary, Alberta.
- Middleton, G. V. (1967) The orientation of concavo-convex particles deposited from experimental turbidity currents. *Journal of Sedimentary Petrology*, **37**, 229-232.
- Mook, W. G. (1991) Anorgansiche 14-C dateringen: van grondwater tot mariene afzettingen. In: *Dateringsmethoden in de kwartair geologie en archeologie* (Ed. by H. Heijnis and J. Van der Plicht), pp. 23-28. Centrum voor Isotopen Onderzoek, Groningen.
- Myrow, P. M. & Southard, J. B. (1991) Combined-flow model for vertical stratification sequences in shallow marine storm-deposited beds. *Journal of Sedimentary Research*, **61**(2), 202-210.
- Nelson, C. H. (1982) Modern shallow-water graded sand layers from storm surges, Bering Shelf: A mimic of Bouma sequence and turbidite systems. *Journal of Sedimentary Petrology*, **52**(2), 537-545.
- Nichols, M. M. (1989) Sediment accumulation rates and relative sea-level rise in lagoons. *Marine Geology*, **88**, 201-219.
- Niedoroda, A. W., Swift, D.J.P., Hopkins, T.S. (1985) The shoreface. In: *Coastal sedimentary environments* (Ed. by R. A. Davis), pp. 531-624. Springer, New York.
- Nielsen, P. (1982) Explicit formulae for practical wave calculations. *Coastal engineering*, **6**, 389-398.
- Nielsen, P. (1983) Analytical determination of nearshore wave height variation due to refraction, shoaling and friction. *Coastal engineering*, **7**, 233-251.
- Nummedal, D. & Swift, D. J. P. (1987) Transgressive stratigraphy at sequence-bounding unconformities: some principles derived from Holocene and Cretaceous examples. In: *Sea-level fluctuation and coastal evolution, SEPM Special Publication*, **41** (Ed. by N. D., O. H. Pilkey and J. D. Howard), pp. 129-143. Society of Economic Paleontologists and Mineralogists, Tulsa, OK.
- O'Brien, M. P. (1931) Estuary tidal prisms related to entrance areas. *Civil Engineering*, **1**, 738-739.
- O'Brien, M. P. (1969) Equilibrium flow areas in inlets on sandy coasts. *Journal of the American Society of Civil Engineers, Waterways and Harbours division*, **95**, 43-51.
- Oost, A. P. (1995) Dynamics and sedimentary development of the Dutch Wadden Sea with emphasis on the Frisian Inlet: a study of the barrier islands, ebb-tidal deltas, inlets and drainage basins. PhD Thesis, Utrecht University, Utrecht, 454 pp.
- Oreskes, N., Shrader-Frechette, K. & Belitz, K. (1994) Verification, validation, and confirmation of numerical models in the earth sciences. *Science*, **263**, 641-646.
- Pannekoek, A. J. (1956) Geologische geschiedenis van Nederland, toelichting bij de geologische overzichtskaart van Nederland op de schaal 1 : 200.000, pp. 147. Staatsdrukkerij, The Hague.
- Polak, B. (1929) Een onderzoek naar de botanische samenstelling van het Hollandsche veen. PhD Thesis, University of Amsterdam, Amsterdam, 187 pp.
- Pons, L. J. & Bennema, J. (1958) De morfologie van het pleistocene oppervlak in westelijk Midden Nederland, voorzover gelegen beneden gemiddeld zeeniveau (NAP). *Tijdschrift van het Koninklijk Nederlands Aardrijkskundig Genootschap*, **75**, 120-139.
- Pons, L. J., Jelgersma, S., Wiggers, A. J. & De Jong, J. D. (1963) Evolution of the Netherlands coastal area during the Holocene. *Verhandelingen van het K.N.G.M.G., Geologische serie*, **21-2**, 197-208.
- Pons, L. J. & Wiggers, A. J. (1958) De morfologie van het pleistocene oppervlak in Noord-Holland en het Zuiderzeegebied, voorzover gelegen beneden gemiddeld zeeniveau (NAP). *Tijdschrift van het Koninklijk Nederlands Aardrijkskundig Genootschap*, **75**, 140-152.

References

- Pool, M. A. (1989) Kustrekonstruktie: Een benadering met behulp van berekende volumina van het Hollandse Jonge Duinzand, Report Rijks Geologische Dienst, Haarlem, 20 pp.
- Pool, M. A. (1993a) Grootschalige kwantitatieve analyse van de ontwikkeling van de centraal Hollandse kust tussen Noordwijk en Scheveningen vanaf 4000 BP tot heden, Report Rijksuniversiteit Utrecht, Faculteit Aardwetenschappen, Utrecht, 34 pp.
- Pool, M. A. (1993b) Volumetric analyses of the Belgian and Dutch Late-Holocene coastal dunes and modelling of large scale coastal development in Central Holland. PhD Thesis, Belgium, Vrije Universiteit Brussel, 163 pp.
- Postma, R. & Kroon, A. (1986) Mathematische profielanalyse van de onderzeese oever en de aansluitende zeebodem voor de Nederlandse kust, Report GWAO Rijksuniversiteit Utrecht, vakgroep Fysische Geografie, Rijkswaterstaat, Dienst Getijdewateren, Utrecht, 37 pp.
- Reading, H. G. & Collinson, J. D. (1996) Clastic coasts. In: *Sedimentary environments, processes, facies and stratigraphy* (Ed. by H. G. Reading), pp. 154-231. Blackwell, Oxford.
- Reineck, H. E. & Singh, I. B. (1972) Genesis of laminated sand and graded rhythmities in storm-sand layers of shelf mud. *Sedimentology*, **18**, 123-128.
- Reineck, H. E. & Singh, I. B. (1975) *Depositional sedimentary environments*. Springer, Berlin, 439 pp.
- Reinson, G. E. (1984) Barrier-island and associated strand-plain systems. In: *Facies models* (Ed. by R. G. Walker), pp. 119-140. Geological Associations of Canada, Ontario.
- Reinson, G. E. (1992) Transgressive barrier islands and estuarine systems. In: *Facies models, response to sea level change* (Ed. by R. G. Walker and N. P. James), pp. 179-194. Geological Associations of Canada, Ontario.
- Riezebos, P. A. & du Saar, A. (1969) Een dwarsdoorsnede door de mariene Holocene afzettingen tussen Vijfhuizen en Vinkeveen. *Mededelingen Rijks Geologische Dienst*, **20**, 85-92.
- Rijkswaterstaat. (1994) Measured near-bed velocities in the coastal zone (in Dutch), Report Rijkswaterstaat RIKZ, The Hague, The Netherlands.
- Roelvink, J. A. & Stive, M. J. F. (1990) Sand transport on the shoreface of the Holland coast; The Dutch Coast: Paper no 5. *22 International Conference on Coastal Engineering*, Delft, 1909-1921.
- Roep, T. B. (1984) Progradation, erosion and changing coastal gradients in the coastal barrier deposits of the Western Netherlands. *Geologie en Mijnbouw*, **63**, 249-258.
- Roep, T. B. & Beets, D. J. (1988) Sea level rise and paleotidal levels from the sedimentary structures in the coastal barriers in the western Netherlands since 5600 BP. *Geologie en Mijnbouw*, **67**, 53-60.
- Roep, T. B., Van de Plassche, O., Van der Valk, L. & Ruegg, G. H. (1983) Sedimentologie van de strandwalafzettingen onder 's Gravenhage en Rijswijk. *Mededelingen Rijks Geologische Dienst*, **37**, 137-156.
- Roep, T. B., Van der Valk, L. & Beets, D. J. (1991) Strandwallen en Zeegaten langs de Hollandse kust. *Grondboor en Hamer*, 115-124.
- Roy, P. S. (1991) Shell hash dating and mixing models for palimpsest marine sediments. *Radiocarbon*, **33**, 283-289.
- Roy, P. S. (1994) Holocene estuary evolution-stratigraphic studies from Southeastern Australia. In: *Incised-valley systems: origin and sedimentary sequences*, **51** (Ed. by R. W. Dalrymple, R. Boyd and B. A. Zaitlin), Tulsa, OK.
- Roy, P. S. & Boyd, R. (1996) *Quaternary geology of Southeast Australia: a tectonically stable, wave-dominated, sediment-deficient margin*. IGCP project 367, *Field guide to the central New South Wales coast*. Geological Survey of New South Wales, Department of Mineral Resources, Sydney, 174 pp.
- Roy, P. S., Cowell, P., J., Ferland, M. A. & Thom, B. G. (1994) Wave-dominated coasts. In: *Coastal Evolution: Late Quaternary shoreline morphodynamics* (Ed. by R. W. G. Carter and C. D. Woodroffe), pp. 121-185. University Press, Cambridge.
- Roy, P. S. & Thom, B. G. (1981) Late Quaternary marine deposition in New South Wales and southern Queensland: an evolutionary model. *Journal of Geology Society of Australia*, **28**, 471-489.
- Roy, P. S., Zhuang, G. F., Birch, G. F., P.J., C. & Congxian, L. I. (1997) Quaternary geology of the Foster-Tuncurry coast and shelf, Southeast Australia, Report Geological Survey of New South Wales, Department of Mineral Resources, Sydney.
- Schwartz, R. K. (1982) Bedform and stratification characteristics of some modern small-scale washover sand bodies. *Sedimentology*, **29**, 835-849.
- Sha, L. P. (1990) Sedimentological studies of the ebb-tidal deltas along the West Frisian Islands, the Netherlands. PhD Thesis, Rijksuniversiteit Utrecht, Utrecht, 159 pp.
- Shipp, R. C. (1984) Bedforms and depositional sedimentary structures of a barred nearshore system, eastern Long Island, New York. *Marine Geology*, **60**, 235-259.
- Snedden, J. W. & Dalrymple, R. W. (1999) Modern shelf sand ridges: from historical perspective to a unified hydrodynamic and evolutionary model. In: *Isolated shallow marine sand bodies: Sequence stratigraphic analysis and sedimentologic interpretation*, **64** (Ed. by K. M. Bergman and J. W. Snedden), pp. 13-28. Society for Sedimentary Geology, Tulsa, OK.

- Snedden, J. W., Tillman, R. W., Kreisa, R. D., Schweller, W. J., Culver, S. J. & Winn, R. D. J. (1994) Stratigraphy and genesis of a modern shoreface-attached sand ridge, Peahala Ridge, New Jersey. *Journal of Sedimentary Research*, **B64**, 560-581.
- Stahl, L., Koczan, J. & Swift, D. J. P. (1974) Anatomy of a shoreface-connected sand ridge on the New Jersey Shelf: implications for the genesis of the shelf surficial sand sheet. *Geology*, **2**, 117-120.
- Staring, W. C. H. (1856) *De bodem van Nederland - De samenstelling en het ontstaan der gronden in Nederland*. Kruseman, Haarlem, 441 pp.
- Steenhuis, J. F. (1917) Beschouwingen over en in verband met de daling van den bodem van Nederland. Mededeelingen omtrent de geologie van Nederland, verzameld door de commissie voor het geologisch onderzoek. *Verhandelingen der Koninklijke Akademie der Wetenschappen, tweede sectie*, **19**.
- Steezel, H. J. & De Vroeg, J. H. (1999) Application of a multi-layer approach for morphological modelling. *Coastal Sediments 1999*, Long Island, New York, in press.
- Stive, M. J. F. (1987) Hoofdrapport kustgenese: Grootschalige vorming en ontwikkeling van de Nederlandse kust; Vorming en toetsing van hypothesen, Report Rijkswaterstaat, Dienst Getijdewateren, The Hague, 62 pp.
- Stive, M. J. F. & De Vriend, H. J. (1995) Modelling shoreface profile evolution. *Marine Geology*, **126**, 235-248.
- Stive, M. J. F., Roelvink, J. A. & De Vriend, H. J. (1990) Large-scale coastal evolution concept; The Dutch Coast: paper no 9. *22 International Conference on Coastal Engineering*, Delft, 1962-1974.
- Stive, M. J. F., Wang, Z. B., Capobianco, M., Ruol, P. & Buijsman, M. C. (1998) Morphodynamics of a tidal lagoon and the adjacent coast. In: *Physics of estuaries and coastal seas* (Ed. by J. Dronkers and M. Scheffers), pp. 397-407. Balkema, Rotterdam.
- Stow, D. A. V. & Bowen, A. J. (1980) A physical model for the transport and sorting of fine-grained sediment by turbidity currents. *Sedimentology*, **27**, 31-46.
- Stuiver, M. & F., B. T. (1993) Modeling atmospheric 14C influences and 14C ages of marine samples back to 10,000 BC. *Radiocarbon*, **35**, 137-189.
- Stuiver, M., Pearson, G. W. & Braziunas, T. F. (1986) Radiocarbon age calibration of marine samples back to 9000 cal yr BP. *Radiocarbon*, **28**, 980-1021.
- Stuiver, M. & Reimer, P. J. (1993) Extended 14C database and revised CALIB radiocarbon calibration program. *Radiocarbon*, **35**, 215-230.
- Swift, D. J. P. (1976a) Coastal sedimentation. In: *Marine sediment transport and environmental management* (Ed. by D. J. Stanley and D. J. P. Swift), pp. 255-310. Wiley, New York.
- Swift, D. J. P. (1976b) Continental shelf sedimentation. In: *Marine sediment transport and environmental management* (Ed. by D. J. Stanley and D. J. P. Swift), pp. 311-350. Wiley, New York.
- Swift, D. J. P. & Field, M. E. (1981) Evolution of a classic sand ridge field: Maryland sector, North American inner shelf. *Sedimentology*, **28**, 461-482.
- Swift, D. J. P., Parker, G., Lanfredi, N. W., Perillo, G. & Figge, K. (1978) Shoreface-connected sand ridges on American and European shelves: a comparison. *Estuarine and Coastal Marine Science*, **7**, 257-273.
- Swift, D. J. P. & Thorne, J. A. (1991) Sedimentation on continental margins, I: A general model for shelf sedimentation. In: *Shelf sand and sandstone bodies*, IAS Special Publication, **14** (Ed. by D. J. P. Swift, G. F. Oertel, R. W. Tillman and J. A. Thorne), pp. 3-31. International Association of Sedimentologists, Blackwell, Oxford.
- Terwindt, J. H. J. (1962) Studie naar korrelgrootte variaties aan de kust bij Katwijk, Report Rijkswaterstaat, The Hague, The Netherlands.
- Tesch, P. (1921) Duinstudies VI: De ouderdom van het Jonge duinlandschap. *Tijdschrift van het Koninklijk Nederlands Aardrijkskundig Genootschap*, **38**, 390-396.
- Tesch, P. (1922) Duinstudies VII: De positieve niveauperandering van de Nederlandsche kust in het Holocene tijdvak. *Tijdschrift van het Koninklijk Nederlands Aardrijkskundig Genootschap*, **39**, 66-76.
- Tesch, P. (1927) Duinstudies XI: De duinkust en de riviermondingen. *Tijdschrift van het Koninklijk Nederlands Aardrijkskundig Genootschap*, **44**, 1-11.
- Tesch, P. (1935) *De vorming van de Nederlandsche duinkust*. Wolters, Groningen, 86 pp.
- Tesch, P. & Van Veen, J. (1937) De jongste onderzoekingen in het nauw van Calais en langs de Nederlandsche kust; Naschrift, Repliek & Dupliek. *Tijdschrift van het Koninklijk Nederlands Aardrijkskundig Genootschap*, **54**, 364-377.
- Thom, B. G. (1983) Transgressive and regressive stratigraphies of coastal sand barriers in southeast Australia. *Marine Geology*, **56**, 137-158.
- Timmermans, P. D. (1935) Proeven over den invloed van golven op een strand. PhD Thesis, Rijksuniversiteit Leiden, Leiden, 156 pp.
- Timmermans, P. D. (1939) Over de eerste fasen van het ontstaan van de Nederlandsche duinkust. *Geologie en Mijnbouw*, **1**, 291-297.
- Törnqvist, T. E. (1993) Fluvial sedimentary geology and chronology of the Holocene Rhine-Meuse delta, The Netherlands. PhD Thesis, Utrecht University, Utrecht, 169 pp.

References

- Törnqvist, T. E., Wallinga, J., Murray, A. S., De Wolf, H., Cleveringa, P. & De Gans, W. (in press) Response of the Rhine-Meuse system (west-central Netherlands) to the Last Quaternary glacio-eustatic cycles: a first assesment. *Global and Planetary Change*.
- Umbgrove, J. H. F. (1947) Origin of the Dutch coast. *Koninklijke Nederlandse Akademie van Wetenschappen Proceedings, section of sciences*, **50**, 227-237.
- Umbgrove, J. H. F. (1950) *Symphony of the earth*. Nijhoff, The Hague, 220 pp.
- Van Alphen, J. (1987) De morfologie en lithologie van de brandingszone tussen Terheijde en Egmond aan Zee., Report Rijkswaterstaat, The Hague.
- Van Alphen, J. (1989) A geomorphological map of the Dutch shoreface and adjacent part of the continental shelf. *Geologie en Mijnbouw*, **68**, 433-444.
- Van de Plassche, O. (1982a) Sea-level change and water-level movements in The Netherlands during the Holocene. PhD Thesis, Free University, Amsterdam, 93 pp.
- Van de Plassche, O. (1982b) Significance of new basal peat dates for the trend of Holocene mean sea level rise in the Netherlands. *Geologie en Mijnbouw*, **61**, 397-399.
- Van de Plassche, O. (1986) Sea-level changes and waterlevel movements in The Netherlands during the Holocene. In: *Mededelingen Rijks Geologische Dienst, Vol. 36*, pp. 93. Rijks Geologische Dienst, Haarlem.
- Van de Plassche, O. & Roep, T. B. (1989) Sea-level changes in The Netherlands during the last 6500 years: Basal peat vs. barrier data. In: *Late Quaternary sea-level correlation and applications*. (Ed. by D. B. Scott, P. A. Pirazzoli and C. A. Honig), pp. 41-56. Kluwer Academic Publishers.
- Van den Berg, J. H. (1977) Morphodynamic development and preservation of physical sedimentary structures in two prograding recent ridge and runnel beaches along the Dutch coast. *Geologie en Mijnbouw*, **56**, 185-202.
- Van der Borg, K., Alderliesten, C., Houston, C. M., De Jong, A. F. M. & Van Zwol, N. A. (1987) Accelerator mass spectrometry with ¹⁴C and ¹⁰Be in Utrecht. *Nuclear instruments and methods in physics research*, **B29**, 143-145.
- Van der Giessen, A., De Ruijter, W. P. M. & Borst, J. C. (1990) Three-dimensional current structure in the Dutch coastal zone. *Netherlands Journal of Sea Research*, **25**, 45-55.
- Van der Meene, E. A., Van Meerkerk, M. & Staay, V. d. (1988) *Toelichting bij de Geologische Kaart van Nederland 1:50.000, Blad Utrecht Oost (31 O)*. Rijks Geologische Dienst, Haarlem.
- Van der Meene, J. W. H. (1994) The Shoreface-connected ridges along the central Dutch coast, PhD thesis. *Nederlands Geografische Studies*, **174**, 222.
- Van der Meene, J. W. H., Boersma, J. R. & Terwindt, J. H. J. (1996) Sedimentary structures of combined flow deposits from the shoreface-connected ridges along the central Dutch coast. *Marine Geology*, **131**, 151-175.
- Van der Molen, J. (Submitted) Holocene tidal conditions and tide-induced sand transport in the southern North Sea. *Journal of Geophysical Research*.
- Van der Spek, A. F. J. (1995) Holocene sediment influxes in the coastal zone of the Netherlands and the North Sea as a function of sea-level and tide-induced sand transport, Report Rijks Geologische Dienst, Haarlem, 13 pp.
- Van der Spek, A. J. F. (1994) Large-scale evolution of Holocene tidal basins in the Netherlands. PhD Thesis, Utrecht University, Utrecht, 191 pp.
- Van der Spek, A. J. F. & Beets, D. J. (1992) Mid-Holocene evolution of a tidal basin in the western Netherlands: a model for future changes in the northern Netherlands under conditions of accelerated sea-level rise ? *Sedimentary geology*, **80**, 185-197.
- Van der Spek, A. J. F., Cleveringa, J., Van Heteren, S., Van Dam, R. L. & Schrijver, B. (1999) Reconstructie van de ontwikkeling van de Hollandse Kust in de laatste 2500 jaar, Report NITG-TNO, Utrecht.
- Van der Valk, L. (1992) Mid- and Late- Holocene coastal evolution in the beach-barrier area of The Western Netherlands. PhD Thesis, Free University, Amsterdam, 235 pp.
- Van der Valk, L. (1995) Toelichting bij de Geologische Kaart van Nederland 1:50.000, Blad 's Gravenhage West (30W) en 's Gravenhage Oost (30O), Report Rijks Geologische Dienst, Haarlem, 54 pp.
- Van der Valk, L. (1996a) Coastal barrier deposits in the central Dutch coastal plain. *Mededelingen Rijks Geologische Dienst*, **57**, 133-200.
- Van der Valk, L. (1996b) Geology and sedimentology of Late Atlantic sandy, wave dominated deposits near The Hague (South-Holland, the Netherlands): a reconstruction of an early prograding coastal sequence. *Mededelingen Rijks Geologische Dienst*, **57**, 210-229.
- Van der Woud, A. (1998) *De Bataafse hut, denken over het oudste Nederland (1750-1850)*. Contact, Amsterdam, 222 pp.
- Van der Woude, J. D. (1981) Holocene paleoenvironmental evolution of a perimarine fluviatile area. PhD Thesis, Free University, Amsterdam, 118 pp.
- Van der Woude, J. D. (1984) The fluviolagoonal palaeoenvironment in the Rhine/Meuse deltaic plain. *Sedimentology*, **31**, 395-400.
- Van Rijn, L. C. (1989) Handbook of sediment transport by current and waves, Report Delft Hydraulics, Delft, 451 pp.
- Van Rijn, L. C. (1993) *Principles of sediment transport in rivers, estuaries, coastal seas and oceans*. Aqua Publishing, Amsterdam, 650 pp.

- Van Someren, M. (1988) Ontstaan der strandwallen van Wassenaar, Report Vrije Universiteit, Amsterdam, 47 pp.
- Van Staalduinen, C. J. (1979) *Toelichting bij de Geologische Kaart van Nederland 1:50.000, Blad Rotterdam West (37 W)*. Rijks Geologische Dienst, Haarlem, 227 pp.
- Van Staalduinen, C. J. & Van Veen, S. D. (1975) Geologische oversichtskaart van Nederland 1:60.000, behorende bij de Toelichting bij de Geologische oversichtskaart van Nederland. In: *Toelichting bij geologische overzichtskaarten van Nederland* (Ed. by W. H. Zagwijn and C. J. Van Staalduinen), pp. 77-87. Rijks Geologische Dienst, Haarlem.
- Van Straaten, L. M. J. U. (1954a) Composition and structure of Recent marine sediments in the Netherlands. *Leidse Geologische Mededelingen*, **19**, 1-110.
- Van Straaten, L. M. J. U. (1954b) Radiocarbon datings and changes of sea level at Velzen. *Geologie en Mijnbouw*, **16**, 247-253.
- Van Straaten, L. M. J. U. (1957a) The excavation at Velzen, general introduction. *Verhandelingen van het K.N.G.M.G., Geologische serie*, **17**, 93-99.
- Van Straaten, L. M. J. U. (1957b) The Holocene deposits. *Verhandelingen van het K.N.G.M.G., Geologische serie*, **17**, 158-183.
- Van Straaten, L. M. J. U. (1957c) Recent sandstones on the coasts of the Netherlands and of the Rhone delta. *Geologie en Mijnbouw*, **19**, 196-213.
- Van Straaten, L. M. J. U. (1961) Directional effects of winds, waves and currents along the Dutch North Sea Coast. *Geologie en Mijnbouw*, **40**, 333-346 & 363-391.
- Van Straaten, L. M. J. U. (1963) Aspects of Holocene sedimentation in The Netherlands. *Verhandelingen van het K.N.G.M.G., Geologische serie*, **21-2**, 149-172.
- Van Straaten, L. M. J. U. (1964) De bodem der Waddenzee. In: *Het Waddenboek* (Ed. by W. F. Anderson, J. Abrahamse, J. D. Buwalda and L. M. J. U. Van Straaten), pp. 75-151. Thieme, Zutphen.
- Van Straaten, L. M. J. U. (1965) Coastal barrier deposits in South- and North-Holland, in particular in the areas around Scheveningen and IJmuiden. *Mededelingen van de Geologische Stichting*, **17**, 41-76.
- Van Veen, J. (1937a) Korte beschrijving van de uitkomsten van onderzoekingen in de Hoofden en langs de Nederlandsche kust. *Tijdschrift van het Koninklijk Nederlands Aardrijkskundig Genootschap*, **54**, 155-195.
- Van Veen, J. (1937b) Onderzoekingen in de Hoofden in verband met de gesteldheid van de Nederlandse kust. PhD Thesis, Rijksuniversiteit Leiden, Leiden, 252 pp.
- Van Vessem, P. & Stolk, A. (1990) Sand budget of the Dutch coast; The Dutch Coast: Paper no 4. 22 *International Conference on Coastal Engineering*, Delft, 1895-1908.
- Venema, G. A. (1854) *Over het dalen van de noordelijke kuststreken van ons land*. J. Oomkens, Groningen, 80 pp.
- Verbraeck, A. (1970) *Toelichting bij de Geologische Kaart van Nederland 1:50.000, Blad Gorinchem (Gorkum) Oost (38 O)*. Rijks Geologische Dienst, Haarlem, 140 pp.
- Visser, M., De Ruyter, W. P. M. & Postma, L. (1991) The distribution of suspended matter in the Dutch coastal zone. *Netherlands Journal of Sea Research*, **27**, 127-143.
- Watney, W. L., Rankey, E. C. & Harbaugh, J. (1999) Perspectives on stratigraphic simulation models: current approaches and future opportunities. In: *Numerical experiments in stratigraphy: recent advances in stratigraphic and sedimentologic computer simulations*, *SEPM Special Publication*, **62** (Ed. by J. W. Harbaugh, W. L. Watney, E. C. Rankey, R. Slingerland, R. H. Goldstein and E. K. Franseen), pp. 3-21. Society for Sedimentary Geology, Tulsa, OK.
- Westerhoff, W. E. & Cleveringa, P. (1990) Sea-level rise and coastal sedimentation in Central Noord-Holland (The Netherlands) around 5000 BP: a case study of changes in sedimentation dynamics and sediment distribution. In: *Expected effects of climatic change on marine coastal ecosystems* (Ed. by J. J. Beukema and *et. al.*), pp. 133-138. Kluwer, Amsterdam.
- Westerhoff, W. E., De Mulder, E. F. J. & De Gans, W. (1987) *Toelichting bij de Geologische Kaart van Nederland 1:50.000, Blad Alkmaar West (19W) en Blad Alkmaar (19O)*. Rijks Geologische Dienst, Haarlem, 227 pp.
- Wheeler, H. E. (1958) Time stratigraphy. *American Association of Petroleum Geologist Bulletin*, **42**, 1047-1063.
- Wright, L. D. (1995) *Morphodynamics of inter continental shelves*. CRC press, Boca Raton, Fl., 241 pp.
- Wright, L. D., Boon, J. D., Kim, S. C. & List, J. H. (1991) Modes of cross-shore sediment transport on the shoreface of the Middle Atlantic Bight. *Marine Geology*, **96**, 19-51.
- Zagwijn, W. H. (1965) Pollen-analytic correlations in the coastal-barrier deposits near The Hague (The Netherlands). *Mededelingen van de Geologische Stichting*, **17**, 83-88.
- Zagwijn, W. H. (1969) Geologie en vegetatiegeschiedenis van de Nederlandse Kustduinen. In: *Jaarboek 1968/1969*, pp. 167-176. Koninklijke Maatschappij voor Natuurkunde "Diligentia", Den Haag.
- Zagwijn, W. H. (1984) The formation of the Younger Dunes on the west coast of The Netherlands (AD 1000-1600). *Geologie en Mijnbouw*, **63**, 259-268.
- Zagwijn, W. H. (1986) *Nederland in het Holoceen*. Rijks Geologische Dienst, Haarlem, 46 pp.
- Zitman, T. J. (1987) Analysis of the contribution of longshore sediment transport in the evolution of the Holland coast, Project Coastal Genesis, phase 1, Formulation and testing of hypotheses., Report Rijkswaterstaat, Dienst Getijdewateren, The Hague, 42 pp.

Dankwoord

Hierbij wil ik graag iedereen, die op de één of andere manier heeft bijgedragen aan het tot stand komen van dit proefschrift, heel hartelijk bedanken. Ook de mensen die ik niet met name noem, maar die wel degelijk iets hebben bijgedragen: Bedankt!

In de eerste plaats wil ik mijn promotor, Prof. Dr Poppe L. de Boer bedanken voor de mogelijkheid en de vrijheid om dit onderzoek te doen. De vraag naar manuscripten heeft de snelheid, waarmee het onderzoek is afgerond, flink opgevoerd en de nauwkeurige correcties van de stapels manuscripten hebben de leesbaarheid zeker verhoogd.

Mijn copromotor, Dr. Ad J. F. van der Spek, wordt bedankt voor zijn heldere kijk op zaken, zijn steun en de duidelijke, maar altijd opbouwende kritiek.

De faculteit Aardwetenschappen is altijd een interessante studie- en werkplek geweest. Kamergenoten Maarten Prins, Johan ten Veen, Bastian van Dijck, Quintijn Clevis en Rik Tjallingi wil ik bedanken voor hun tolerantie ten opzichte van mijn -vaak onrustige-aanwezigheid en de gezelligheid. De andere collega's en ex-collega's van de sedimentologiegroep, Paul Anten, Wessel van Kesteren, Xander Meijer, Albert Oost, George Postma, Marjan Reith, Jan-Berend Stuu, Marnella van der Tol, Gert-Jan Weltje, Marjolijn van Wijk en Sjoukje de Vries, ben ik ook zeer erkentelijk voor de plezierige samenwerking. Max van Heijst verdient door zijn vriendelijkheid, collegialiteit en steun een aparte vermelding: zonder onze cynergie was promoveren een zwaardere opgave geweest. De jaarlijks terugkerende excursies met Wout Nijman waren altijd een feest, waarbij ik steeds weer iets leerde. Ook de samenwerking met andere collega's, met name met de burens van Stratigrafie en Paleontologie, de structureel geologen en de mensen van het HPT laboratorium heb ik zeer op prijs gesteld. Bezoekjes over en weer bij Bart Bos en Fraukje Brouwer hebben regelmatig voor de broodnodige ontspanning gezorgd.

Bart Schrijver heeft tijdens zijn afstudeeronderzoek een enorme hoeveelheid data verzameld, is een grote hulp geweest bij het verzamelen van de schelpjes voor de koolstofdateringen en was ook nog eens gewoon gezellig om mee samen te werken.

Bij het TNO-NITG heb ik met veel plezier samengewerkt met de mensen van Geomariën en kust en District West en met verschillende personen van de laboratoria. Door het bekijken van kernen, monsters en gegevens heb ik veel meer geleerd over de ondergrond van Nederland dan is beschreven in dit boekje. André en Ben hebben de boringen op Ypenburg snel en netjes uitgevoerd.

Dirk Beets heeft op duidelijke wijze dit onderzoek ondersteund: bedankt voor vele verhelderende discussies.

Klaas van den Borg (R.J. van de Graaff laboratorium, Universiteit Utrecht) wordt bedankt voor de koolstofdateringen aan de vele schelpjes. Bert van der Valk en de Vrije Universiteit, Amsterdam, worden bedankt voor het beschikbaar stellen van de koolstofdateringen van de Wassenaar boringen.

Alle archeologen op Ypenburg, zowel van de AWR als van de steeds wisselende ploeg professionals, wil ik bedanken voor de koffie, de faciliteiten en de prettige samenwerking. Zonder Hans Koot, de gemeentearcheoloog van Rijswijk, had het onderzoek er heel anders uitgezien. De discussies in het veld met Chris Gutjahr en zijn vele goed gedocumenteerde rapporten over de geologie van Rijswijk en Ypenburg heb ik ook zeer op prijs gesteld.

Verschillende mensen hebben geholpen met het veldwerk op Ypenburg en bij het maken van een aantal lakprofielen. Ik wil met name Bastian van Dijck bedanken voor de twee weken handboren waarmee het onderzoek is begonnen.

Remke van Dam en Sytze van Heeteren, van de faculteit Aardwetenschappen van de Vrije Universiteit in Amsterdam, hebben op Ypenburg, op Texel en in de waterleidingduinen bij Haarlem grondradarprofielen verzameld. Hoewel de uitkomsten van dit onderzoek niet direct in dit proefschrift zijn terug te vinden, zijn zij wel van groot belang geweest voor een mijn begrip van de Hollandse kust. En ik had de ritjes met het trekkertje, door een paar van de mooiste landschappen van Nederland, ook niet willen missen.

Without the Pace project this research would not have been conducted. I would like to thank the leading scientist, Prof. Dr Huib de Vriend for the invitation of geologist in this coastal project and for his skilful and inspiring leadership. All the participants are thanked for their hospitality towards such a 'broekie'. The presentations and discussions have certainly broadened and enlightened my views on coastal research. Above all, the participants in topic 3 of the PACE project, Maarten Buijsman, Peter J. Cowell, Huib de Vriend, Alan W. Niedoroda, Chris W. Reed, Marcel Stive, are thanked for their discussions and contributions to this study.

During my short but pleasant and productive stay at the Geosciences department of Sydney University in Australia, the company of Peter J. Cowell, Peter S. Roy, Andy D. Short and roommate Aaron Coutts-Smith was greatly appreciated. All others at the Coastal Studies Unit and Geography are equally thanked for making this working trip a great experience. Sydney is certainly one of the best places in the world to study the coastal evolution of the western Netherlands.

In addition to Poppe and Ad a number of people has commented on earlier versions of the various chapters. The Introduction benefited from comments of Bart Bos and Piet Cleveringa. Comments from Dirk Beets and Chris Gutjahr have improved Chapter 2. Dirk Beets and Max van Heijst contributed to the contents and readability of chapter 3 and 4. Chapter 7 benefited from comments of Dirk Beets and Xander Meijer, and the Summary and Conclusions were carefully read by Bart Bos. The Acknowledgements and the Summary in Dutch were scrutinised by Meini Blom and Piet Cleveringa.

The members of the dissertation committee, Dr D.J. Beets, Dr P. J. Cowell, Prof. Dr H.J. de Vriend, Prof. Dr J.E. Meulenkamp, and Prof. Dr M.J.F. Stive are thanked for their interest and comments.

Verder wil ik natuurlijk mijn familie bedanken. Piet, dankjewel voor het wekken van de interesse in het vakgebied en in het doen van onderzoek en natuurlijk voor de vele discussies over het vak en de vakgenoten en je pogingen mijn interesse "breed" te houden. Meini, Nienke, Tjalling, Baukje, en aanhang, bedankt voor jullie gezelligheid en steun en voor de tolerante manier, waarop jullie de gesprekken over het vakgebied hebben ondergaan. Last but not least: Saskia, bedankt voor je communicatieve wenken, je aanwezigheid en vooral je liefde.

Curriculum Vitae

Jelmer Cleveringa is op 20 augustus 1972 in Coevorden geboren. Hij behaalde in 1990 aan het Fons Vitae Lyceum, te Amsterdam, het VWO diploma. In datzelfde jaar begon hij met de studie Geofysica aan de faculteit Aardwetenschappen van de Universiteit Utrecht. In het jaar daarop werd overgestapt naar de studie Geologie aan dezelfde faculteit. In 1992 behaalde hij propedeuse-examens in de Geofysica en de Geologie en in 1996 het doctoraalexamen in de Geologie. De afstudeeronderzoeken betroffen een sedimentologische studie naar afzettingen uit de Waddenzee, een onderzoek naar de patronen van getijdengeulen en een studie van de herkomst van sedimenten uit de Arabische Zee. Aansluitend begon in augustus 1996 het werk aan het promotieonderzoek aan de faculteit Aardwetenschappen van de Universiteit Utrecht. Het onderzoek werd, in nauwe samenwerking met het TNO-NITG -afdeling Geomariën en kust- uitgevoerd in het kader van het Europese Unie PACE project. Een deel van het onderzoek is verricht bij de Universiteit van Sydney, Australië, tijdens een werkbezoek in het voorjaar van 2000.



De auteur (links) werpt een vorsende blik op de kustlijn van Terschelling, onder begeleiding van zijn vader (december 1974).

